UNIVERSITÀ
DI TRENTO
Dipartimento di
Ingegneria e Scienza dell'Informazione

Department of Information
Engineering and Computer Science

Doctoral School in Information and Communication Technology

36th Cycle

Ground Vehicles and Ranging Sensors:

Structural Properties for Estimation and Control

Advisors

Prof. Luigi Palopoli

Prof. Daniele Fontanelli

Ph.D. Candidate

Francesco Riz

June 2024

Abstract

In this thesis we address the *constructibility* problem for a ground vehicle moving across an environment instrumented with ranging sensors. When the measurements collected by the vehicle along the trajectory are sufficiently informative, the *global* constructibility property is achieved and the vehicle is able to localise itself in the environment without relying on prior information on its state. When this condition is not met, the system can still achieve *local* (or *weak*) constructibility, where localising the robot requires some initial information on the state, such as a sufficiently small set containing the initial position of the robot, or some inaccessible areas of the Cartesian plane.

First, we address the *global* problem: we show that extending the well–known solutions for the *positioning* problem, e.g. trilateration, is not trivial and leads to unintuitive results where constructibility is not attained. By building an abstract trajectory, which contains all the relevant information to reconstruct the actual trajectory followed by the vehicle, we analyse how global constructibility properties are affected by the shape of the abstract trajectory, the number of sensors, their deployment in the environment, and the distribution of measurements among the beacons.

To describe *local* constructibility, we build the Constructibility Gramian for a robot described by the unicycle kinematic model. We rely on this tool for a twofold aim: (a) we build the same abstract trajectory presented for the global analysis and define necessary and sufficient conditions to attain local constructibility, and (b) in an environment instrumented with two beacons and for straight trajectories followed by the vehicle, we measure local constructibility by means of the smallest eigenvalue of the Constructibility Gramian, and we analyse how this metric is affected by the geometry of the scenario, e.g. the distance between anchors, and the distance between the trajectory and the line joining the anchors.

Lastly, we extend the devised results to multiagent systems, both for constructibility analysis and for trajectory planning algorithms. We build the Constructibility Gramian for the multiagent system with relative ranging measurements and assess local constructibility property. Then, we propose a trajectory planning algorithm where a pair of vehicles without *a priori* information achieve global constructibility with both absolute and relative measurements. Moreover, we propose a variation of the Constructibility Gramian, limited to the position variable and hence called *Position Gramian*, and use this tool in a Model Pre-

dictive Control framework to plan the trajectory of a tracker vehicle aiming at simultaneously localising itself and a collaborative target through ranging measurements.

Keywords

Range sensing; Ground robots; Constructibility; Observability for nonlinear systems; Sensor–based Control.

Contents

1 Introduction

Contents

Among many engineering disciplines, robotics is one of the fields that has attracted major interest and enthusiasm in recent times. The most iconic and known example of the rapid development in this field is given by the evolution of the products of Boston Dynamics, whose evolution originated with the first single–legged bouncing robots in 1984 [Raibert and Brown Jr, 1984], passing through the clumsy motion of the BigDog in 2005, to the famous legged robots Atlas and Spot[1]. While these evolutions have enjoyed great success in the industrial and in the research communities, concerns were also raised about their interactions with humans. In particular, a common concern is safety when the workspaces of the robots cross the workspaces of humans. Numerous researchers both in academia and industry have dealt with this problem, under the research field of *collaborative robots* [Vicentini, 2021], with main focus on industrial manipulators. Similarly, the same issue has been raised on autonomous mobile robots, travelling across an environment shared with humans, such as semi–automated warehouses where mobile robots are responsible for moving goods across the dynamic and possibly unknown environment represented by a factory, while humans execute some different tasks [Boldrer et al., 2022].

In such a scenario, common names and acronyms to refer to mobile robots are *Automated Guided Vehicles* (AGV) or *Unmanned Ground Vehicle* (UGV). These names focus on the main features of the robots, such as *automation*, i.e. there is no need for human operators constantly providing inputs to the robots, and *guidance*, highlighting that the main task performed by these robots is navigating across the environment. The navigation problem can be decomposed into different subtasks, such as *action planning*, where the robot (or robots) schedules the different locations to reach and duties to be executed, and *trajectory planning*, where the robots define the path from their current to their target location and determine the control inputs that ensure that the path is followed. The navigation tasks inevitably require the robots to be able to accurately estimate their current position and orientation (more precisely, their state vector), i.e. to *localise themselves in the environment*. To do so, the robots rely on two families of sensors: *proprioceptive* and *exteroceptive* sensors. Proprioceptive sensors, such as odometers, accelerometers and gyroscopes, yield information on the motion of the robot, e.g. instantaneous velocities or accelerations, which can be integrated over time to retrieve the relative displacement of the vehicle over a time interval. On the other hand, exteroceptive sensors perceive the environment around the vehicle and measure absolute quantities, such as distances, orientations and positions, referred to an external, possibly dynamic and unknown, reference frame. The family of exteroceptive sensors in-

[1] https://bostondynamics.com/legacy/

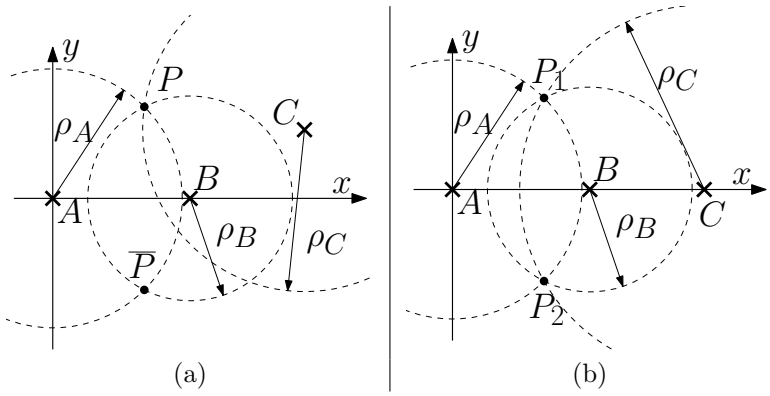

Figure 1.1: Two trilateration examples. (a) Noncollinear sensors, successful trilateration. (b) Collinear sensors, unsuccessful trilateration.

cludes many kinds of sensory systems, with different technologies, architectures and complexity. Common solutions for this family of sensors are represented by cameras, depth cameras and LiDAR– or RADAR–based systems, for unstructured indoor scenarios, the Global Positioning System (GPS) for large outdoor environments, and visual or ranging sensors, which usually rely on markers deployed beforehand in the environment. In this thesis, we will focus on ranging sensors, because of their simplicity, versatility, affordability, and low maintenance requirements. However, the listed advantages in the sensing system introduce some limitations. Because of the reduced amount of information that can be collected from a fixed ranging sensors, reconstructing the position (or the state) of a vehicle is not always possible. Intuitively, ranging sensors are sufficient to reconstruct the position, or the entire state vector, of a vehicle navigating through a structured environment, only when some conditions hold true. To support this statement, which is crucial for the further development of this thesis, we report here a simple example showing that when some conditions are not met, a robot cannot reconstruct its position in the environment.

Example 1.1. With reference to Figure 1.1, consider the example of the well-known *trilateration* problem: a vehicle measures its distances ρ_A, ρ_B and ρ_C from the three fixed markers A, B and C, respectively, and, based on these pieces of information, tries to reconstruct its position P on the plane. Figure 1.1(a) shows a successful trilateration scenario, where the point P is univocally defined as the unique intersection between the three circles representing the measurements. Indeed, point $\overline{P}$ has distances ρ_A from A and ρ_B from B, but it has a distance $\overline{\rho_C} \neq \rho_C$ from C. On the contrary, in Figure 1.1(b), both points P_1 and P_2 have distances ρ_A, ρ_B and ρ_C from the three sensors, and thus the vehicle cannot distinguish whether its current position is P_1 or P_2. However, if

the vehicle can rely on some initial information (e.g. the collinear anchors are mounted on a wall and the side with $y < 0$ is not accessible), this ambiguity can be ruled out (P_2 is no more a valid solution) and the vehicle can reconstruct its position. ⋆

Example 1.1 shows that, even in a simple scenario where the vehicle is not moving, and three sensors are collecting simultaneous measurements, reconstructing the position of a vehicle based on ranging information is possible only under some assumptions. Moreover, it introduces two distinct, yet related, perspectives: *global*, when no a priori information is given, and *local* that relies also on some initial knowledge on the system to draw conclusions. Motivated by this example, and based on the fact that reconstructing the position of the vehicle in the example in Figure 1.1(b) fails from a *global* perspective, while succeeds from a *local* point of view, we introduce the main problems that this thesis addresses.

Problem 1.1 (Global observability)**.** *Find the conditions on:*

- *The number and deployment of the fixed sensors;*
- *The trajectory followed by the vehicles composing the system;*
- *The number of range measurements collected by the vehicle(s) and their distribution among the fixed sensors;*
- *The interactions, i.e. relative measurements and communications between vehicles;*

such that the state of the single– or multi–agent system can be univocally reconstructed, with no a priori information*.*

Problem 1.2 (Local observability)**.** *Find the conditions on:*

- *The number and deployment of the fixed sensors;*
- *The trajectory followed by the vehicles composing the system;*
- *The number of range measurements collected by the vehicle(s) and their distribution among the fixed sensors;*
- *The interactions, i.e. relative measurements and communications between vehicles;*

such that the state of the single– or multi–agent system can be reconstructed, when some a priori information *is available.*

With reference to Example 1.1, let us consider the state vector of the system to include only the Cartesian coordinates of the vehicle. The decisive condition that changes among the two scenarios in Figure 1.1 is the deployment of the sensors. Both the scenarios satisfy the *local* conditions, i.e. Problem 1.2 can be solved in both situations, while Problem 1.1 can be solved only in the scenario (a), when the three sensors are not collinear.

While Problems 1.1 and 1.2 deal with the analysis of a given scenario, in this thesis we also address the problem of *perception–aware trajectory planning*, where the vehicles in the system actively plan their trajectory, based on the information collected over time, to solve Problems 1.1 and 1.2.

Problem 1.3 (Perception–aware planning)**.** *Plan the future manoeuvres performed by the vehicle(s) in the system such that we can reconstruct the state of the system with no* a priori *information. Moreover, when range measurements are corrupted by noise, plan the trajectory of the system to maximise the accuracy of the estimated state.*

In this thesis, we deal with the problems described above in the context where ground vehicles, moving on a plane, are equipped with ranging sensors. Although this setting seems restrictive, we can easily generalise our results to the context of marine or aerial vehicles. Indeed, in underwater environments the use of visual sensors is limited by poor visibility conditions and the most popular solution for exteroceptive sensors is based on ultrasound devices collecting ranging measurements. To cope with the 3D nature of the problem, the underwater vehicle is required to be equipped with a depth sensor, thus reducing the observability problem to a plane where the techniques for ground robots can be applied. In the field of aerial robotics, many alternatives can be implemented as exteroceptive sensors and ranging sensors are not the most common choice. Although results are still applicable to this scenario, provided that the aerial robot is equipped with a sensor measuring its distance to the ground, the practical validity of these results is limited.

1.1 Literature review

Since mobile robots have a large variety of applications, the localisation and positioning problems have attracted the attention of a considerable number of researchers. The localisation and positioning problems have been analysed at different levels, spanning from the technological implementation of the exteroceptive sensors, to the so–called *observability conditions*, i.e. the conditions that allow the vehicle to reconstruct its state, to the design of observers estimating

the state of the system.

1.1.1 Sensor technology

As mentioned in the previous sections, mobile robots are usually equipped with exteroceptive sensors perceiving some features or some devices deployed in the environment. A large variety of sensors have been considered and analysed for vehicle localisation, relying on different technologies and physical principles, and on different requirements on the structure of the environment and on the deployment of active or passive devices.

A popular family of solutions relies on visual information collected by the vehicle moving across the environment. A popular solution for localisation is the use of 2D codes deployed in the environment and sensed by a camera that is mounted on the mobile robot. These 2D codes may be fixed to the ceiling [Dzodzo et al., 2013] or to the floor [Nazemzadeh et al., 2015] and have visual cues, such as arrows and ID codes, that allow the vehicle to reconstruct both its position and its orientation in a fixed reference frame. On the same idea, Nazemzadeh et al. [Nazemzadeh et al., 2017] propose a localisation technique based on data fusion that takes into account uncertainties arising in the perception of QR codes deployed on the floor. More popular solutions for visual–based localisation techniques rely on cameras [Falanga et al., 2018], which show two main advantages with respect to the former solutions: they do not need the environment to be instrumented with an infrastructure, and they collect a larger amount of information, but this solution comes with the cost of an increased computation burden and the limitations associated with brighter or darker environments. A further increase in the amount of information that is collected by the vehicle is allowed by Light Detection and Ranging (LiDAR) sensors, which have become common not only in robotics, but also in autonomous guidance vehicles. A discussion on the use of LiDAR's for robot localisation is proposed by [Gallant and Marshall, 2016], where the authors show that a LiDAR yields a 3D point cloud representing the environment and, based on the collected samples, information on the orientation of the vehicle can be inferred, as if the vehicle were virtually using a *LiDAR compass*. While popular and commonly integrated in autonomous robots, the drawbacks of vision–based systems are associated with the quality of the image retrieved by the sensor, thus being very sensitive to changes in brightness level, especially outdoors, to the detection of features in the environment (e.g. no relevant information is retrieved when the vehicle sees a homogeneous wall), or to unexpected light hitting the sensor, e.g. the vehicles goes almost blind when hit by direct sunlight.

Because of the limitations of vision–based systems or inability to exploit them in challenging scenarios, e.g. underwater [Hung and Pascoal, 2020], ranging sensors, i.e. sensors measuring the distance between a pair of devices, have become increasingly popular [Yan et al., 2013]. Many technologies enable the physical implementation of ranging sensors, with different properties in terms of measurement accuracy, sensing range, or performances. An affordable solution is represented by infrared (IR) sensors [Benet et al., 2002]. As for LiDAR's, an infrared sensor consists of two devices: an *emitter* that generates infrared waves that travel across the environment, are reflected by the target surfaces and are sensed by a *detector*. The distance of the surface is estimated either by measuring the Time of Flight (ToF), i.e. the time elapsed between the emission and the detection of the wave, or by measuring the intensity of the detected light. In the latter case, as for vision–based systems, the performances of IR sensors are sensitive to the illumination of the scene and to the reflectance properties of the surfaces hit by IR rays emitted by the vehicle. Furthermore, many IR sensors are often have to be combined in a single device because of their limited field of view. Other popular solutions rely on devices initially meant for communication, such as Wi-Fi, Ultra Wide–Band (UWB) or Bluetooth technology. These technologies require the vehicle to be equipped with active devices that receive a signal and measure the Received Signal Strength Indicator (RSSI) (e.g. Wi-Fi [Biswas and Veloso, 2010]) or the ToF (e.g. UWB [Cheok et al., 2010], Ultrasound [Shen et al., 2019]). Since autonomous mobile robots are usually equipped with these communication devices to receive and transmit data to other robots or to supervisory control systems, many researchers have analysed their capabilities to collect meaningful information to solve the localisation problem [Chen et al., 2013]. New techniques and algorithms tailored for these applications have been proposed, particularly for Wi-Fi–based sensors [Yu et al., 2020], but easily extendable to other technologies. With similar working principles, Bluetooth and Radio Frequency IDentification (RFID) sensors estimate the distance between two devices by measuring the phase difference between the emitted and the received wave [Shu and Wang, 2023]. This information generates ambiguities in the collected distance since different distances may yield the same phase difference [Motroni et al., 2018]. To cope with this issue, Magnago et al. [Magnago et al., 2019] rework the output equation of an Ultra High Frequency RFID (UHF-RFID) antenna and conclude that the vehicle is virtually measuring the projection of its forward velocity on the line joining the vehicle itself and the passive tag that is deployed in the environment.

Many technologies have been considered and analysed as solutions for the physical implementation of ranging devices, and for their application to the field of mobile robotics. While different localisation algorithms and techniques may

be specifically designed for each of these technologies, results with general validity can be extracted by considering a generic device that measures the distance between a vehicle and a fixed point on the plane, or the distance between two robots, as we consider in the remainder of this thesis.

1.1.2 Observability Analyses

The main part of the sensors described in the previous section enable the vehicle to collect a limited amount of information, not allowing it to measure its complete state vector. However, as shown in Example 1.1, the vehicle can reconstruct its state vector, or a portion of its state, when more than one measurement is considered. The analysis of the conditions that enable the vehicle to reconstruct its state fall in the category of *observability* or *constructibility analyses*. For the sake of clarity, we introduce here the definitions of observability and constructibility. Let us consider a discrete–time dynamical system with state $q \in \mathbb{R}^n$:

$$q_{k+1} = f(q_k, u_k), \qquad z_k = h(q_k), \tag{1.1}$$

where $u_k \in \mathbb{R}^m$ is the control input vector, and $z_k \in \mathbb{R}^p$ is the output vector, i.e. the sensor measurements.

Definition 1.1.1 (Observability)**.** *Given the discrete–time dynamical system* (1.1)*, and a time interval* $K = \{k_0, \dots, k_f\}$ observability *is the ability to reconstruct the state* q_0 *of the system at the* initial *time* $k = k_0$*, given the outputs* z_k *and the control inputs* u_k*,* $k \in K$*.*

Definition 1.1.2 (Constructibility)**.** *Given the discrete–time dynamical system* (1.1)*, and a time interval* $K = \{k_0, \dots, k_f\}$ constructibility *is the ability to reconstruct the state* q_f *of the system at the* final *time* $k = k_f$*, given the outputs* z_k *and the control inputs* u_k*,* $k \in K$*.*

When the considered dynamical system is linear, i.e.

$$q_{k+1} = A_k q_k + B_k u_k, \qquad z_k = H_k q_k, \tag{1.2}$$

$A_k \in \mathbb{R}^{n\times n}$, $B_k \in \mathbb{R}^{n\times m}$, $H_k \in \mathbb{R}^{p\times n}$, observability and constructibility can be checked through the rank of the corresponding Gramians G_O and G_C, reading as:

$$G_O = \sum_{k=k_0}^{k_f} \Phi(k, k_0)^\top H_k^\top H_k \Phi(k, k_0), \qquad G_C = \sum_{k=k_0}^{k_f} \Phi(k, k_f)^\top H_k^\top H_k \Phi(k, k_f),$$

where $\Phi(k, k_0)$ and $\Phi(k, k_f)$ are called *state transition* matrices and only depend

on matrix A_k, $k = k_0, \dots, k_f$ (see [Hespanha, 2018]). Therefore, observability and constructibility, for a linear system, only depend on the structure of the system, i.e. on A_k and H_k, and not on the trajectory of the system state. This property holds true for the abstract case where the sequence of matrices A_k, B_k and H_k are fixed upfront. Often times, linear time–varying systems are obtained as linearisation of nonlinear systems, and thus the matrices describing the linearised dynamics depend on the linearisation point, which, in turn, depends on the trajectory followed by the system, hence on the control input history. Indeed, when nonlinearities are involved, observability and constructibility properties depend on the structure of the system, i.e. on the nonlinear maps $f(\cdot)$ and $g(\cdot)$, but also on the trajectory followed by the system, as shown in Example 1.2.

Example 1.2. Let us consider the following 1D nonlinear system where the sensor has a bounded sensing range:

$$q_{k+1} = q_k, \qquad z_k = \begin{cases} q_k & \text{if } |q_k| < 1 \\ \text{unavailable} & \text{otherwise.} \end{cases}$$

By the structure of the system, $q_k = q_0$, $\forall\, k > k_0$, and the system is observable (and constructible) when $|q_0| < 1$, since it is directly measured by the sensor. On the other hand, when $|q_0| \geq 1$, no measurements are available, and thus the state of the system cannot be recovered, hence the system is unobservable (and unconstructible). ⋆

When dealing with nonlinear systems, observability has been tested with several methods, by extending the definition of the Observability Matrix $\mathcal{O}$ and of the Gramians G_O and G_C, or by relying on geometric considerations and on map invertibility. [Isidori, 2013] introduced the concept of Lie derivatives $L_f(h)(q)$ for a continuous–time autonomous system

$$\dot{q} = f(q), \qquad z = h(q),$$

reading as

$$L_f(h)(q) = \frac{\partial h(q)}{\partial q} f(q),$$

where $L_f(h)(q) \in \mathbb{R}^p$ is the *derivative of* $h(\cdot)$ *along the vector field* $f(\cdot)$ and p is the dimension of the output vector z_k. Lie derivatives can be applied sequentially as

$$L_f^i(h)(q) = \frac{\partial}{\partial q}\left(L_f^{i-1}(h)(q)\right) f(q), \qquad L_f^0(h)(q) = h(q),$$

and are used to build the Observability Matrix $\mathcal{O}$ ([Krener and Ide, 2009]) reading as:

$$\mathcal{O} = \begin{bmatrix} \dfrac{\partial h(q)}{\partial q} \\ \nabla_q L_f(h)(q) \\ \nabla_q L_f^2(h)(q) \\ \vdots \end{bmatrix}.$$

When $\mathcal{O}$ has rank n, where n is the dimension of the state, the system is said to *satisfy the Observability Rank Condition (ORC)*, and thus to be *locally observable*.

Remark 1.1.3 (Number of Lie derivatives)**.** *For a linear system with order n, the number of Lie derivatives that are sufficient and necessary to assess the observability of the system is n, as ensured by the Cayley–Hamilton theorem (see [Hespanha, 2018]), guaranteeing that the rank of $\mathcal{O}$ does not increase by adding Lie derivatives of order greater than n. For nonlinear system, there exist no general rule on the order of Lie derivatives increasing the rank of $\mathcal{O}$. From a practical perspective, people seek for general patterns (e.g. columns with only 0 entries) to draw conclusions on the rank of $\mathcal{O}$, as in Example 1.3.*

An equivalent tool to test the observability of a system is the nonlinear Observability Gramian G_O, which, for the discrete–time nonlinear system (1.1), is defined as

$$G_O = \sum_{k=k_0}^{k_f} \Phi(k, k_0)^\top H_k^\top H_k \Phi(k, k_0),$$

where $H_k = \dfrac{\partial h(q_k)}{\partial q_k}$ and the *sensitivity matrix* $\Phi(k, k_0) = \dfrac{\partial q_k}{\partial q_0}$ is the unique solution to the initial value problem

$$\Phi(k+1, k_0) = \frac{\partial f(q_k, u_k)}{\partial q_k} \Phi(k, k_0), \qquad \Phi(k_0, k_0) = \mathbf{I},$$

where $\mathbf{I}$ is the identity matrix. As for the Observability Matrix, the system is locally observable as soon as G_O has rank n ([Krener and Ide, 2009]). When the sensitivity matrix $\Phi(k, k_0)$ is not available in closed form, the nonlinear observability Gramian cannot be computed analytically. Therefore, the empirical Observability Gramian EOG, presented in [Powel and Morgansen, 2015], should be used. The EOG relies only on the ability to simulate several times the system, and for a continuous–time system is defined as

$$G_O^E = \frac{1}{4\varepsilon^2} \int_0^T \mathcal{Z}^\top \mathcal{Z} \, dt, \qquad \mathcal{Z} = [z^{+1} - z^{-1}, \cdots, z^{+n} - z^{-n}],$$

where z^{+i} is the measurement output history of the system with initial conditions $q_0 + \varepsilon \underline{e_i}$, with $\underline{e_i}$ being the unitary vector aligned with the i-th axis. When $\varepsilon \to 0$, the EOG is proved to converge to the actual OG.

Different approaches have been devised to test observability properties of a nonlinear system. By the definition of observability, a system is observable as soon as the function, which is input–dependent, mapping the initial state q_0 to the set of measurements z_k, $k = k_0, \ldots, k_f$ is invertible. To this aim, the authors of [Hung and Pascoal, 2020] consider the sets of function mapping the initial state to each measurement output and check their linear independence on the time interval when the observations are collected. Linear independence implies that the map from the initial condition q_0 to the measurements z_k is injective, and thus invertible. Similarly, the authors of [Palopoli and Fontanelli, 2020] consider a nonholonomic vehicle with state $q = [x, y, \theta]$ with reference to Figure 1.2, and compute the difference of the successive range measurements along its trajectory, obtaining the linear equations

$$M \begin{bmatrix} \cos\theta_0 \\ \sin\theta_0 \end{bmatrix} = h,$$

where $M \in \mathbb{R}^2 \times 2$ is a known matrix, $h \in \mathbb{R}^2$ is a known vector. Since the initial position (x_0, y_0) can be reconstructed when θ_0 is known, the observability condition boils down to the properties of M: when M is singular, the system is *unobservable*.

Observability and constructibility properties define the ability of a vehicle to localise itself in the environment. Indeed, by the definition of observability, a vehicle can reconstruct its current state based on the past input and output histories, only when the system is constructible. For mobile robots, several research papers have analysed the observability properties with many dynamical models for the vehicles and different sensors deployed in the environment. The outputs of the most common sensors are represented in Figure 1.2, where the orientation θ may be part of the state, while the bearing angle α and the distance ρ from a marker $M = [X, Y]^\top$ read as

$$\alpha = \arctan2(y - Y, x - X), \qquad \rho = \sqrt{(x - X)^2 + (y - Y)^2}.$$

In [Martinelli and Siegwart, 2005], the authors consider a pair of vehicles described by the unicycle kinematic model, whose state consists of its position in the Cartesian reference frame and of its orientation with respect to a given reference axis. An observability analysis of the *follower vehicle* is carried out by means of the ORC, when many sensors, measuring different relative quantities, are considered. The main outcomes, which are common throughout the

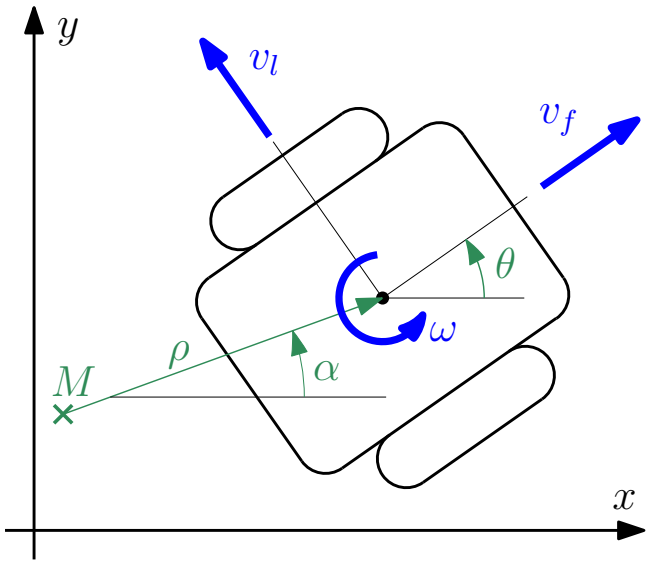

Figure 1.2: Most common sensor outputs and control inputs for a ground vehicle. The landmark M is represented by the green cross, and measures one of the following quantities: orientation θ of the vehicle, distance ρ between the robot and the marker, or bearing α from the marker to the vehicle. When the vehicle is described by a kinematic mode, i.e. dynamics and inertias are neglected, the most common control inputs are the forward velocity v_f, the lateral velocity v_l and the angular velocity ω. While not all the control inputs are usually considered, more complex dynamical models may consider as inputs the accelerations along the same directions.

technical literature, depend on the measured quantity (i.e. on the sensor): (a) when the relative orientation is measured, then the position can never be estimated, (b) when relative distance or one relative bearing is measured, the state of the follower can be reconstructed only when both vehicle move with non–zero velocity, (c) while when both vehicle measure the bearing of the other robot, the motion of one of the two vehicles is sufficient to reconstruct the state of the follower. An extension of this analysis is presented in [Martinelli, 2017], where a disturbance is considered in the same scenario. Focusing on bearing measurements, in [Bicchi et al., 1998] an observability analysis is carried out when a vehicle collects measurements from more than one fixed marker, and aims at reconstructing its state and the position of some fixed targets. Extensions to multiagent systems have also been considered in [Mariottini et al., 2005], where a set of followers measure the bearing of the leader, and in [Belo et al., 2013] where the authors propose a complete observability analysis with a varying number of vehicles and moving sensors based on the ORC. An application–driven extension of these works, both for 2D and 3D environments, is proposed in [Stegagno et al., 2016]. The authors analyse a multiagent system where the vehicles collect relative bearing measurements without sharing their identity,

thus introducing in the system the ambiguities associated with the guessed identity of the sensed vehicles.

With a combination of sensors, e.g. bearing and ranging sensor, a vehicle can measure its position with respect to a fixed marker or to another vehicle. In this scenario, [Hao et al., 2022] analyse a multiagent system, whose state collects the positions of all the agents, based on graph theory. The sensing system being more complex than the one discussed previously, the conclusions that can be drawn are simpler: the system is observable as soon as the graph is connected, and each node has a non–zero out degree, i.e. when there are no detached sub–networks, and each vehicle is sensed by at least another vehicle. On the other hand, when little information is produced by the sensing system, the observability analysis is more convoluted and more restrictive conditions have to be met to ensure observability, as in the case of UHF–RFID sensors [Magnago et al., 2020].

Observability analyses with ranging sensors have been mainly carried out in the field of marine robotics, due to the high cost of deploying more complex sensors (such as short baseline acoustic positioning sensors) and the impossibility to use visual–based sensors in a marine environment. The usual ORC is used in [Arrichiello et al., 2013] to check the observability of an Autonomous Underwater Vehicle (AUV) modelled as a single 3D integrator when a depth and a ranging sensors are used. Moreover, when the system is observable, the authors devise a metric to quantify observability based on the condition number of the Observability matrix. In the particular case when the state of the system consists only in the position of the AUV, the observability metric is maximised when the vehicle follows a circular trajectory centred in the beacon. Similar results on observability are obtained in [Fernando et al., 2021] with the ORC, where a drone is considered that measures its distance from 2 or 3 fixed anchors. The authors show that the unobservable directions, i.e. the portions of the state that the drone cannot reconstruct, depend heavily on the followed trajectory. Interestingly, in [Delaune et al., 2021], the authors consider a scenario where the robot performs Simultaneous Location and Mapping (SLAM), aiming at reconstructing its state and at finding the position of relevant points of the environment. They notice that Visual Inertial Odometry (VIO) is subject to drift, thus not allowing to successfully perform SLAM. Therefore, they propose to add a 1D laser range finder, i.e. a sensor that measures the distance of a visual feature on the forward direction of the robot. This way, despite the simplicity of the added sensor, the vehicle can successfully localise itself and map the environment. Results on observability and localisability of a unicycle mobile robot have been obtained in [Sert et al., 2012] when the ground vehicle measures its heading and its bearing and azimuth angles with respect to a fixed

landmark deployed on the ceiling of a room. With such a sensing system the robot indirectly measures its bearing angle and its distance with respect to the projection of the landmark on the plane where the robot is free to move. In this scenario, the robot is always observable unless it stands still under the landmark, where the bearing angle is not defined, or when the landmark lies on the same plane as the robot, where the azimuth angle is always 0, thus making the sensors useless.

Since the Observability Matrix relies on the linearisation of the dynamics, which is state dependent, the results that are obtained with the ORC have only local validity. With reference to the scenario in Figure 1.1(b), when the vehicle is in position P_1, the ORC is met, although there exists another position (P_2) that yields the same measurements. To overcome this limitation, several researchers (e.g. [De Palma et al., 2017]) augment the state and build the Observability Gramian of the devised linear time varying system. The authors of [Bayat et al., 2015] propose an observability analysis of a system composed of an AUV, modelled as an underactuated nonholonomic vehicle, and a set of fixed targets with unknown positions. They analyse the unobservable directions both in the case where only range is measured, and when also the depth of the AUV is measured. With a different approach, which relies on geometric considerations, the authors of [Palopoli and Fontanelli, 2020] analyse the global observability of a nonholonomic ground vehicle in the presence of fixed ranging sensors. They conclude that: (a) with one sensor the vehicle is never observable, (b) with 2 sensors the vehicle is observable only when it executes a curved trajectory, while (c) with 3 or more sensors the robot is observable when the sensors are not collinear and the vehicle moves with non–zero velocity. Fixed sensors require some properties to the trajectory followed by the observed vehicle, that have to be met. However, when robots are deployed in the environment, they usually have to perform the tasks they are designed for. In these scenarios, many research papers propose to use a set of mobile beacons, i.e. a set of vehicles with known position, which measure their distance from one or more target vehicles. This idea has been increasingly popular for AUV's, since surface vessels can be accurately tracked with a GPS system, and are suitable to host range sensors. The authors of [Rúa et al., 2019] propose to use a range sensor mounted on a manipulator that can perform circular motion. They show that, despite using a single sensor, the AUV can reconstruct its position when the angle of the manipulator, hence the position of the beacon, is known over time. More efficient and versatile solutions rely on range sensors mounted on moving surface vessels with known position (e.g. [Hung and Pascoal, 2020]). The results obtained with this analysis, based on independence and injectivity of functions mapping the initial state to the measurements through the control inputs, have the same

geometrical interpretation as the ones obtained in the previous cases, where a still vehicle is unobservable when a single mobile beacon follows a straight trajectory, or when a pair of trackers move on the same line, while curvature in the trajectories of the trackers guarantee observability.

Observability analyses for mobile robots have also been extended to multiagent systems, where both absolute (from fixed sensors or beacon agents) and relative (between agents) range measurements are collected. The authors of [Araki et al., 2019] propose the analysis of a team of ground vehicles that collect mutual range distances by means of the Observability Matrix, while [Heintzman and Williams, 2020] exploit graph theory and rigidity theory to analyse the case where the vehicles are subject to nonuniform environmental disturbances, which jeopardise observability when not taken into account. From a geometrical standpoint, the results for multiagent systems have the same interpretation as the results on single agents, while their description is more convoluted due to the motion of all the vehicles of the system.

1.1.3 Localisation

Many research papers focus on the *observability* properties of a system, while the recent literature points out that the aim of a system is to reconstruct its *current* state with the *past* history of inputs and outputs, and thus it is associated with the concept of *constructibility* (see [Salaris et al., 2019]). However, for most mobile robotic systems, despite being represented by nonlinear systems, observability implies constructibility since the dynamics of the system can be propagated with the known inputs and known initial condition to obtain the final state of the system. Reconstructing the state q_k of the system is performed by algorithms called *observers* or *estimation filters*, which fuse the sensor measurement z_k and the known control inputs u_k, $k = k_0, \dots, k_f$, and output an estimate $\hat{q}_k$ of the actual state q_k of the system (see [Bernard et al., 2022]). A necessary condition for the existence of an estimation algorithm such that $\hat{q}_k$ converges to q_k is *observability*. In some scenarios, when the system is equipped with many sensors, the state of the system can be directly reconstructed from the measurements collected on a single time step, i.e. when H_k in (1.2) (or $h(\cdot)$ in (1.1)) is invertible and $q_k = H_k^{-1} z_k$. In this case, the system is said to be *statically observable*, and the problem of reconstructing q_k is called *positioning*. On the other hand, in the common setting where the output function is not invertible, the state of the system can still be reconstructed when the system is *dynamically observable*, or simply *observable*. In this more general case, reconstructing the state relies on the dynamics of the system and this problem is

known as *localisation* problem (see [Fontanelli, 2022]).

Example 1.3. Let us consider an example adapted from [Fontanelli, 2022], where an autonomous vehicle is modelled as a 1D single integrator having constant velocity, with two sensors measuring its position and its velocity, respectively. The system is modelled as

$$q_k = \begin{bmatrix} x_k \\ v_k \end{bmatrix}, \qquad q_{k+1} = \begin{bmatrix} x_{k+1} \\ v_{k+1} \end{bmatrix} = \begin{bmatrix} 1 & T_s \\ 0 & 1 \end{bmatrix} q_k = Aq_k$$

where T_s is a sampling time. We have three different measurement models, denoted by the letters a, b, c, reading as

$$z_k = H_i q_k, \quad i = a, b, c,$$

where

$$H_a = \begin{bmatrix} 1 & 0 \\ 0 & 1 \end{bmatrix}, \qquad H_b = \begin{bmatrix} 1 & 0 \end{bmatrix}, \qquad H_c = \begin{bmatrix} 0 & 1 \end{bmatrix}.$$

a) The state q_k is output by the sensors, thus the system is *static observable*. The matrix H_a is invertible, hence the positioning problem can be solved as $q_k = H_a^{-1} z_k = z_k$.

b) Unlike the previous case, the output z_0 is not sufficient to reconstruct q_0, since H_b is not invertible. The outputs z_0 and z_1 of the system can be rewritten as

$$\begin{bmatrix} z_0 \\ z_1 \end{bmatrix} = \begin{bmatrix} H_b q_0 \\ H_b q_1 \end{bmatrix} = \begin{bmatrix} H_b \\ H_b A \end{bmatrix} q_0 = \mathcal{O} q_0.$$

By simple computations, $\mathcal{O}$ is invertible, hence the system is *(dynamically) observable* and the state q_0 can be reconstructed as $q_0 = \mathcal{O}^{-1}[z_0, z_1]^\top$. Intuitively, when only the position is measured, the velocity of the vehicle can be computed through the displacement of the robot.

c) By following the same steps as in the previous case, and extending them to an arbitrarily high number of successive measurements, we obtain

$$\mathcal{O} = \begin{bmatrix} H_c \\ H_c A \\ \vdots \\ H_c A^k \end{bmatrix}.$$

By the structure of H_c and A, the first column of $\mathcal{O}$ has only null entries, thus $\mathcal{O}$ is not invertible and the system is *unobservable*. Intuitively, when only the velocity is measured, the position of the vehicle can never be reconstructed. ⋆

Example 1.3 shows that the same dynamical system subject to a different set of measurements can be *statically observable* (associated with positioning), *dynamically observable* (associated with localisation), or *unobservable*.

Positioning

A well-known problem is finding the position of a fixed target on the plane or in the space based on its distance from a set of fixed sensors with known position in the world reference frame. This is a *positioning* problem, since it does not rely on the motion of the target, and is usually solved by means of multilateration, as in Example 1.1. While trilateration is a fairly old idea, new techniques improving computational efficiency and coping with measurement uncertainties are still being proposed nowadays in the technical literature. As an example, [Thomas and Ros, 2005] presents a novel formulation of the trilateration problem that allow the authors to analyse the effect of possible errors on the accuracy of the estimation of the position of a robot in the space. On the same idea, when the number of sensors is greater than the dimension of the state the robot is located, Zhou [Zhou, 2009] finds the position of the robot as the solution of a minimisation problem, analytically solved by the weighted least square solution, whose cost function is a measure of the uncertainty of the estimate. Similarly, in [Yang et al., 2020] show that better computational performances are obtained when a nonlinear minimisation problem in the position (x, y) of the vehicle is built, where the cost function is based on the difference between the actual collected measurements and the measurements expected with the target in position (x, y). A similar idea is exploited by [Fontanelli et al., 2021] where a virtual multilateration, based on successive measurements, is analytically solved to minimise the uncertainty associated with the estimation of the position of a robot. When the sensors have a bounded sensing range R, i.e. the measurements are available only when the distance between robot and sensor is smaller than R, the authors of [Han et al., 2013] prove that three range sensors are optimally deployed on the plane when they are located at the three vertices of an equilateral triangle with side $\sqrt{3}R$. Based on this result, they propose a trilateration–based trajectory planning algorithm for a mobile beacon, which allows it to minimise the uncertainty of a target when it is detected on a plane. To cope with practical limitations, Filonenko et al. [Filonenko et al., 2013] analyse a scenario where a target on the plane collects 4 range measurements, but can

rely only on the difference between them, i.e. collecting 3 independent measurements. The authors show that solving the positioning problem is still possible with this limited amount of information, and show that the positioning accuracy depends on the deployment of the target, i.e. on its orientation, position and other physical and geometrical parameters. On the same idea, [Yi et al., 2018] consider a trilateration problem with 3 Wi-Fi access points. To compensate for unmodelled and dynamic phenomena, the authors propose to measure online the Received Signal Strength Indicator (RSSI) between pairs of access points, thus decreasing the uncertainty associated with the target distance estimation. In [Cantón Paterna et al., 2017], the authors propose a novel algorithm where the uncertainty associated with the Bluetooth–based distance measurement of three anchors is weighted by considerations on the geometry of the intersections of the circle representing the measurements and on the distance measured by each of the sensors. To cope with the problem that trilateration subject to measurement noise does not yield a single feasible point (i.e. a single intersection among three circles), in [Fang and Chen, 2020] the authors propose an Evolutionary Algorithm that improves the estimation accuracy of a set of fixed targets relying on measurements collected from 3 anchors. When more sensors are considered, the authors of [Diao et al., 2021] propose to dynamically estimate the uncertainty of the measurement yielded by each sensor and use the usual trilateration techniques only on the three sensors with the lowest uncertainty. More recent works, e.g. [Jondhale et al., 2021], propose to improve trilateration for indoor localisation by feeding the range measurements to a Neural Network, thus showing that trilateration is still studied and improved nowadays with new approaches and enhancing phases. Another interesting application of the trilateration technique is offered in [Maxim et al., 2008], where the authors consider a vehicle to be equipped with 3 acoustic transducers. This way, by solving the trilateration problem, the three ranging systems build a device that "measures" the position of the robot with respect to another robot or to a fixed point on the plane.

Localisation

In the scenarios presented above, where the system is *statically observable*, a common assumption is that the environment is sufficiently structured, i.e. a sufficient number of sensors are deployed in the environment, under some conditions. However, as mentioned in the previous sections, static observability is not a necessary condition to reconstruct the state of the system, but *localisation* algorithms can rely on relaxed assumption on the structured environment

(e.g. a smaller number of sensors) and on the manoeuvres executed by the vehicle to reconstruct its state. A significant change in this scenario is associated with the portion of the state that can be reconstructed. Indeed, when the *positioning* is considered, only the position of the vehicle can be reconstructed, while no information can be retrieved about its orientation, which is part of the state in many kinematic or dynamic models, e.g. unicycle kinematic model. Therefore, as a rule of thumb, generally more information can be inferred through localisation despite the smaller number of fixed sensors that are needed [Maurelli et al., 2022].

A research direction that has been deeply explored is associated with the development and design of observers for mobile robots perceiving the environment with different sensors. A survey on localisation techniques and on most common sensors can be found in [O'Mahony et al., 2019] and [Campbell et al., 2020]. In this field, specifically tailored estimation filters have been devised for UHF-RFID sensors [Shamsfakhr et al., 2021], and for bearing measurements through cameras [Jayasuriya et al., 2020], based on the well–known Extended Kalman Filter (EKF), while other works define *ad hoc* filters devised from the bearing output equation [Sert et al., 2011].

When cameras and LiDAR sensors are involved, recent works propose to feed the collected frames to Neural Networks in order to extract relevant features [Barnes and Posner, 2020], or detect and track autonomous vehicles (see e.g. [Mohamed et al., 2020]). Machine–learning–based estimation filters have received a widespread attention in the last years, both in the field of robotic manipulator pose estimation [Miseikis et al., 2018], and for mobile robot localisation. Such estimation algorithms are commonly implemented on robots collecting visual information. As an example, the authors of [Sun et al., 2020] consider the scenario where a vehicle is equipped with a LiDAR and collects synthetic information based on the e Michigan North Campus Long-Term Vision and LiDAR (NCLT) dataset. They use a 2–phase estimation algorithm where the pose of the robot is estimated through a deep neural network processing LiDAR information, and the belief associated with the estimate is updated by means of the Markov process theory. As a result, the time needed by the estimation process is 2 order of magnitude less than a Monte Carlo baseline with a centimetre–level accuracy. Visual information and machine learning algorithms are also used in [Berz et al., 2018] to enhance, through computer vision techniques, the estimate of the position of an idle robot estimated through RFID sensors. Machine learning techniques are also used to estimate the position of a robot in [Islam et al., 2023], where only ranging measurements are collected and trilateration–based positioning is leveraged.

A common drawback coming with visual sensors yielding much information,

e.g. a 360° LiDAR scan of the entire environment, is the notable computational burden that is required to the mobile platform, derived from the common use of machine learning or deep learning methods [Wu et al., 2020].

On a different development idea, as for positioning, the deployment of the sensors in the environment affects heavily the accuracy in the estimation of the state, and thus optimal sensors placement techniques have been considered both for 2D visual cues [Zenatti et al., 2016] and for ranging sensors mounted on a surface vessel for localisation and tracking of UAV's [Moreno-Salinas et al., 2018]. In the same scenario, where a vehicle measures its distance from known points in the environment, many research works propose novel observers to improve the accuracy of the state estimate [Cedervall and Hu, 2007]. A standard Kalman Filter (KF) is used in [Bayat et al., 2015] where the actual nonlinear system is cast to a linear time varying system by means of a state augmentation. The state estimate generated by the devised KF on the augmented system is then recast to the original nonlinear system where, the system being observable, it converges to the actual state of the AUV. A different *rationale* is followed in [Fontanelli et al., 2021], where an *ad hoc* estimation filter is built based on geometric considerations on *global constructibility* properties for a unicycle vehicle subject to range measurements. The authors show that the devised filter has performances comparable with a standard EKF, but it outperforms Kalman–like filters when the process and measurement uncertainties are partly unknown or overestimated.

Similar results have been obtained for range–based cooperative localisation of a team of vehicles. By reworking the output equations based on the known control inputs, in [De Palma et al., 2015a] a KF approach is proposed for a nonlinear system. The authors use a *projection approach* that, together with the linear dynamics and the definition of an equivalent output equation, which, unlike range measurements, is linear in the state, allow them to use the Kalman Filter, which is the Best Linear Unbiased Estimator (BLUE) for linear systems. The direct application of an EKF to the nonlinear multiagent system is discussed in [Huang et al., 2011], where the authors find an inconsistency: when considering only relative measurements, the sensors are insensitive to rigid rotations or translation of the entire system, thus the minimum dimension of the unobservable subspace should be 3, while the error covariance matrix generated by an EKF has a bidimensional null space. To overcome this inconsistency, the authors propose an Observability Constrained EKF, which guarantees that the observability conditions, i.e. the dimension of the unobservable subspace be at least 3, are met. A different variation of the EKF is proposed in [Chakraborty et al., 2020] to cope with scenarios where *local* observability is guaranteed, and checked by means of the Observability Matrix and of the Ob-

servability Gramian, while *global* observability is not. The authors use a Multi–Hypothesis EKF where one EKF is initialised for each of the possible states of the vehicle. As an example, consider Figure 1.1(b), where the positions P_1 and P_2 are compliant with the measurements. Each of the two hypothesis carries its likelihood χ an additional state, where a hypothesis is discarded when χ falls below a predefined threshold.

1.1.4 Active sensing

The main focus of the research papers presented in the previous section is the observability analysis of a system along a trajectory, or the design of suitable observers, based on the dynamics and on the sensing system, estimating the state of the system. In both scenarios, the vehicles navigate the environment along a fixed or given trajectory. In this section, we shift our focus to planning the trajectory of the vehicles in the system to guarantee observability and devise observability metrics to be optimised for. This field, most commonly known under the names of *observability–based* planning, *perception–aware* planning, or *active sensing control*, deals with two different, yet related, problems, which will be referred to as *target localisation* and *self localisation*. The former problem focuses on planning the trajectories of some *tracker* vehicles to optimise for the observability of a moving target and track it along its trajectory, and has had a great impact in the marine robotics field. On the other hand, a widespread interest has been attracted by *self localisation*, where a vehicle (or a team of vehicles) plans its trajectory to optimise for its *own* observability.

Target localisation

The problem of active sensing applied to target localisation and tracking is a conceptual evolution of the optimal sensor placement problem. Indeed, instead of deploying fixed devices in the environment, the aim of this research idea is to plan the trajectory of a mobile sensor. A preliminary solution in a marine environment is proposed in [Rúa et al., 2020] where a ranging sensor is mounted on a manipulator enabling it to a follow a circular motion. While the trajectory of the AUV is given, by means of the Fisher Information Matrix (FIM), the beacon computes the best sequence of actions that improve the estimation accuracy. A remarkable improvement of this idea is proposed in [Hung et al., 2020] where the beacon is mounted on an Autonomous Surface Vehicle (ASV), which plans its trajectory without the circular motion constraint. This approach allows the tracker to localise also a non–cooperative target, with a simple kinematic model,

yielding quasi–steady velocities. Better performances are obtained by extending the same approach to multiple trackers with the aim of *cooperatively* localise on or more ASV targets [Hung et al., 2021]. From a geometric perspective, a common outcome that has been obtained with different observability metrics (e.g. FIM, explicit propagation of the error covariance matrix in an EKF, Observability Matrix, Gramians) is that the optimal tracker path, with ranging sensors, is a circle centred in the position of the target [Mandić et al., 2016], which extends to cycloidal or helical curves when the target moves with known velocities. When the aim of the tracker is not limited to observability, but contains also the tracking objective, i.e. the tracker seeks to reach the target, the authors of [Coleman et al., 2021] show that the optimal trajectories have spiral–like shapes, where the last position reached by the vehicle coincides with the target.

Self localisation

The target localisation problem has received a great attention in the field of marine robotics and ranging sensors, where AUV's are commonly deployed to execute navigation tasks and cannot rely on some classes of sensors, e.g. visual sensors, due to the limitations forced by the underwater environment, while surface vessels offer a cost–effective solution for localisation. On the other hand, the self localisation problem has been considered also for ground or aerial vehicles relying on many classes of sensors. A trajectory planning algorithm for a team of ground vehicles measuring both relative and absolute bearing angles have been proposed in [Sharma, 2014], where the authors maximise the determinant of the Information Matrix computed through an Extended Information Filter (EIF). Bearing measurements are a popular solution for aerial vehicles, where the trajectory planning problem has been extended with the maximisation of observability metrics, commonly associated with the minimisation of the velocity of projection of some control points on the image plane [Falanga et al., 2018], also known as *normalised feature speed* [Wu et al., 2022].

While range–based target localisation is common for marine robotics and underwater vehicles, active sensing techniques have also been devised for ground and aerial vehicles collecting range measurements. Examples of AUV planning their trajectories have been proposed in [De Palma et al., 2015b], where the authors define two different goals. The primary problem consists in reaching a target position, which is solved by a Lyapunov based controller. The secondary task, i.e. the maximisation of the observability of the vehicle measured through the determinant of the FIM, is executed by means of a null

projector, where the devised control law does not affect the success of the primary navigation task. Where only the observability task is considered, based on the *empirical* Observability Gramian, [Quenzer and Morgansen, 2014] proposes optimal control laws, where the optimal trajectory turns to be a circle centred in the beacon collecting the range observations. Based on the Gramians, the authors of [Salaris et al., 2017] propose a general framework, not restricted to a particular class of vehicles or of sensors, where the Observability Gramian is used as an observability metric. Successive extensions of this idea are proposed [Salaris et al., 2019], where the Constructibility Gramian is proved to be more suitable than the Observability Gramian as a metric quantifying the estimation uncertainty. Indeed, the Constructibility Gramian is closely related to the solution to the algebraic Riccati equation and with the error covariance matrix propagated through an EKF without process uncertainties. This result is also shown in a simulation environment where the uncertainty of an OG–optimal trajectory is greater than the uncertainty of a CG–optimal trajectory. These ideas have also been extended to multiagent settings [De Carli et al., 2021] where an approximation of the smallest eigenvalue of the Constructibility Gramian is computed in a distributed fashion, while process noise has been considered in [Napolitano et al., 2021] by introducing the Reachability Gramian along the trajectory. To account for both the tracking and the observability properties, the same ideas have been extended in [Napolitano et al., 2022] for a nonholonomic vehicle subject to range measurements, where an MPC controller is proposed where a feedforward control plans the trajectory to maximise for observability, while a Lyapunov–based feedback controller stabilises the vehicle on the desired trajectory. In the same scenario with a unicycle vehicle subject to range measurements, a completely different approach is followed in [Shamsfakhr et al., 2022], where the vehicle builds an artificial potential field whose contributions are based on a target point to be reached (with an adaptively increasing weight) and on the minimisation of the uncertainty measured by the trace of the error covariance matrix propagated in an EKF. The observability of ground vehicles can be trivially applied to aerial or underwater settings, when the altitude or the depth of the vehicles can be measured. As an example, [Boyinine et al., 2022] propose the analysis of a multiagent system where a set of support vehicles have to localise themselves by collecting range measurements, while they plan their trajectory with the aim of minimising the estimation uncertainty of the leader vehicle executing a predefined task. The problem is solved with a nonlinear Model Predictive Control, whose cost is based on the Observability Matrix. On the same idea, [Chen and Dames, 2020] consider a set of tracking robots that measure their pose with respect to the environment, with respect to other trackers and to

an unknown and time varying number of targets. The authors propose to use the covariance matrix generated by a Probability Hypothesis Density filter as weighing function for a Lloyd–based controller. They then show that the proposed control algorithm guarantees collision avoidance between robots, both between two trackers and between a tracker and a target, and copes also with a remarkable initial uncertainty of the pose of the trackers.

1.2 Thesis contributions and publications

This thesis addresses the constructibility problem for a ground vehicle, or a team of ground vehicles, subject to range measurements. The constructibility problem, which boils down to finding the conditions such that the *localisation* problem can be solved, is addressed on different levels: when no prior information is provided to the system, we analyse the *global constructibility* problem (see Problem 1.1), while the *local constructibility* problem is considered when some *a priori* information is given, such as non–accessible areas of the plane or a sufficiently narrow set containing the initial (or final) state of the system (Problem 1.2). From a different perspective, this thesis also addresses the *active sensing* problem, where a team of vehicles plans its trajectory in order to achieve constructibility (Problem 1.3).

This thesis is divided into three parts, where for Part I and Part II there is a one–to–one correspondence with Problems 1.1 and 1.2, while Part III considers the extension of the concepts to multiagent systems and, in Chapters 7 and 9, addresses Problem 1.3.

1.2.1 Part I – Global constructibility

A motivation for the analysis of global constructibility properties is given in Chapter 2, where we consider the usual environment instrumented with fixed–frame ranging sensors. For this motivation example, we choose to consider an *omnibot*, i.e. a mobile robot with dynamics reading as

$$\dot{q} = \begin{bmatrix} \dot{x} \\ \dot{y} \\ \dot{\theta} \end{bmatrix} = \begin{bmatrix} v_f \cos\theta - v_l \sin\theta \\ v_f \sin\theta + v_l \cos\theta \\ 0 \end{bmatrix},$$

where states and controls are represented in Figure 1.2. For this case, which can be extended to a wider class of vehicles, as shown in Chapter 4, we show that the basic intuition on the trivial extension of the *positioning* concepts to the

localisation problem fails. In particular, we provide a proof of the well–known trilateration problem, showing that three sensors in Example 1.1 are sufficient to reconstruct the position of the vehicle when they collect simultaneous measurements, unless a singular condition occurs. Unlike the *simultaneous trilateration* scenario, when the vehicle moves between successive range measurements, we show that in the general case, three range measurements are not sufficient to reconstruct univocally its position in the world reference frame. This chapter, which is originated by the publication [Riz et al., 2023b], shows that the intuition on the solution of Problem 1.1 may fail, thus justifying the rest of the analysis.

Based on the results in the previous chapter, in Chapter 3, we address a setting similar to the one analysed in [Palopoli and Fontanelli, 2020] and extend the result to sensors with bounded sensing range. This contribution considers a nonholonomic vehicle described by the unicycle kinematic model, reading as

$$\dot{q} = \begin{bmatrix} \dot{x} \\ \dot{y} \\ \dot{\theta} \end{bmatrix} = \begin{bmatrix} v_f \cos\theta \\ v_f \sin\theta \\ \omega \end{bmatrix},$$

as represented in Figure 1.2. In this setting, with the environment instrumented with only two sensors with bounded and non–overlapping sensing range, we provide a sufficient condition on the trajectory of the vehicle that attains global constructibility. At the end of this chapter, which is based on [Riz et al., 2022b], we give some geometrical insights on the sufficient condition, where global constructibility is not achieved when the vehicle follows a straight trajectory under the range of the anchors, or when the two anchors are overlapped.

In Chapter 4 we extend the class of ground vehicles that are analysed, and carry out a global constructibility analysis for intermittent measurements. The ground vehicles that are considered in this analysis have to satisfy the following two properties:

1. Given a state $q_{\bar{t}}$, $t_0 \leq \bar{t} \leq t_f$ and the sequence of control inputs u_t, $t \in [t_0, t_f]$, the state of the system q_t, $t \in [t_0, t_f]$ can be univocally determined;

2. The sequence of positions (x_t, y_t), $t = [t_0, t_f]$ is sufficient to determine the final state q_f.

The kinematic models analysed in the previous chapters meet these conditions, while many mobile robots satisfy the properties provided that some further components of the state are measured. Furthermore, as a reasonable assumption based on the technology employed in the sensors, we consider intermittent measurements. The two listed properties with this last consideration allow us to

consider only a finite number of *measurement* points, instead of considering the trajectory of the state of the system. With this assumption, Chapter 4, which is based on [Riz et al., 2022a], presents a complete global constructibility analysis, where we analyse the effect of the number and deployment of the anchors in the environment, the number of measurement points and their distribution among the anchors on the constructibility properties of the system.

1.2.2 Part II – Local constructibility

Following the global constructibility analysis, a natural development of these concepts is the *local* constructibility analysis. Indeed, as per Example 1.1, often times prior information on the position of the vehicle is available. As presented in the literature overview, local analyses have commonly been carried out by relying on the extension of tools from linear system analysis, such as the Observability Matrix and the Gramians. In Chapter 5, we follow the same procedure as in Chapter 4, restrict our analysis to a unicycle–like vehicle, build the Constructibility Gramian of the system for each distribution of measurements, and test local constructibility. While basic intuition suggests that any constructible setting should be also *locally* constructible, some constructible settings turn out to be weakly unconstructible. This unexpected result, discussed in [Riz et al., 2022a], is presented in Chapter 5 with the help of some geometrical insights and some conclusions on the issues introduced by linearisation are drawn.

With the Constructibility Gramian introduced in Chapter 5, we propose in Chapter 6 a quantitative comparison of the constructibility of different straight trajectories (jeopardising global constructibility) followed by a vehicle in an environment instrumented with two bounded ranging sensors. In this setting, we consider the effect on the smallest eigenvalue of the Constructibility Gramian, chosen as measure of constructibility, of some geometrical parameters of the trajectory, such as the distance between the trajectory and the anchors, the distance between the anchors, or the final position reached by the vehicle. This preliminary analysis, presented in [Riz et al., 2022b] could be beneficial for active sensing problems where these results may be used as a heuristic to plan the optimal trajectory, or a trajectory guaranteeing a given constructibility index.

1.2.3 Part III – Multiagent systems

In this Part, we extend the constructibility results obtained in the previous parts to multiagent systems, and present some solutions for Problem 1.3. Chap-

ter 7, which is originated by [Riz et al., 2023a] presents a trajectory planning algorithm that ensures *global* constructibility for a pair of unicycle vehicles collecting absolute and relative measurements. At the initial time step, the two vehicles are deployed in the environment, each one in sight of a ranging sensor, but with no prior information on its state. Therefore, as an example, the initial manoeuvre planned by the vehicles relies only on its initial distance measured from the anchor, and aims at collecting further informative measurements from the anchor. After collecting this phase, the vehicles move on a circle centred in their reference anchor until they meet, and eventually they plan their last manoeuvres such that the collected measurements ensure global constructibility.

An extension of the constructibility analyses in the previous parts is presented in Chapter 8, where the vehicles in a multiagent system measure their relative distance. While only some necessary conditions form Problem 1.1 have been devised, the local analysis in Problem 1.2 by means of the Constructibility Gramian is generalised for an arbitrarily large number of agents. In this analysis, presented in [Riz et al., 2024b], we provide some geometrical insights on constructible and unconstructible settings on the shape of the trajectories and on the measurements among agents.

Chapter 9, which is based on [Riz et al., 2024a], addresses Problem 1.3 for a tracker–target pair, with a slight difference in the analysed model. Indeed, while unicycle vehicles are still considered, we introduce the simplifying assumption that the orientation θ of the two vehicles can be measured by means of a compass, and thus the portion of the state vector to be reconstructed amounts only to the position of the two vehicles. The system consists of a fixed beacon and of the two vehicles, which are initially unaware of their position, as customary assumption for the global constructibility problem. While no direct interaction exists between the target and the beacon, the tracker collects range measurements from both of them, and plans its trajectory to optimise for a variation of the Constructibility Gramian encompassing the position of the two vehicles. To cope with the lack of prior information, initially the estimation is carried out with a delayed trilateration process, described in Chapter 2, while successively the estimate obtained through an EKF is fed to the Gramian–based planner.

Lastly, in Chapter 10, we draw some final conclusions on constructibility results introduced in the previous chapters, and suggest future research directions that can benefit from the concepts explored in this thesis. While an open problem is still the complete *global constructibility* analysis of a multiagent system, the main challenge is the application of the *global* constructibility analyses to the robotic domain in real–life applications, where the odometry sensors are corrupted by noise, thus affecting the ability of the vehicle to estimate the followed trajectory. While these issues have already been addressed in the tech-

nical literature for the local scenario (see [Napolitano et al., 2021]), addressing this issue from a global perspective is still an open problem. Other interesting challenges deal with multiagent systems with non–collaborative or adversarial agents, which actively avoid measurements and inject false information in the system to not be localised.

Figure 1.3 shows the visual structure of the thesis and points out the mentioned open problems.

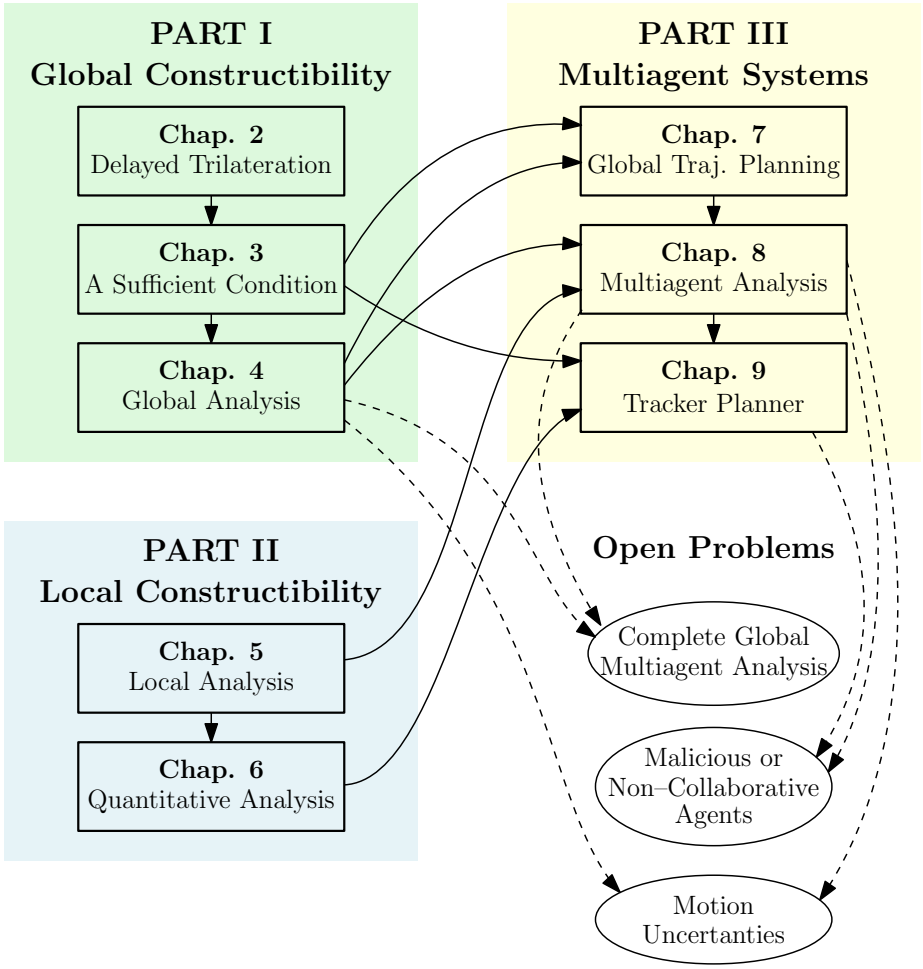

Figure 1.3: Thesis structure with contributions and open problems.

Part I

Global Constructibility Analysis of a Ground Vehicle

Localisation and Positioning: the Delayed Trilateration

2

Contents

Finding the position of a (moving) target in an indoor environment is a problem that has been deeply analysed in the past years. A natural choice for solving the *positioning* problem, i.e. finding the position of a still target, relies on ranging sensors, given the large number of sensors capable of measuring the distance between a number of fixed-frame points and the target. The most common solution relies on the so–called *trilateration* (or multilateration), where 3 (or more) simultaneous range measurements are leveraged to reconstruct the position of the target. In this chapter, we provide an example of the extension of the well–known trilateration problem (referred to as *simultaneous trilateration* for the sake of clarity) to the scenario where the target is not fixed, but it is moving through a planar environment. We notice that the results established in the former case are not directly extendable to the *delayed trilateration* scenario, and basic intuition on this problem fails. Indeed, we show with a counterexample that, when the agent moves through the environment, there are multiple trajectories that are compliant with the motion of the target and with the ranging measurements that have been collected by anchors with known positions. Therefore, we claim here that three measurements are not sufficient to localise a moving target in a given environment even in ideal conditions when no measurements noise or motion uncertainties are considered in the model. In particular, we claim that the classic trilateration problem assumes an additional implicit information besides the three ranging measurements, that is that the three measurements are taken with respect to the same point in space or, in the most general and most probable case of a moving target, simultaneously.

This analysis suggests that there is a structural difference between the *positioning* problem, i.e. finding the position of a fixed target, and the *localisation* problem, i.e. reconstructing the position (or the entire state) of a moving vehicle, and motivates the analyses carried out in the next chapters of this thesis.

Contributions: We consider a target moving through an environment equipped with an infrastructure of three anchors of known position and measuring the distances to the target. Dictated by various actual applications, e.g., limited sensing range, limited bandwidth in the target-beacon communication or scalability issues [Magnago et al., 2019], the measurements are retrieved at different time steps. Contrary to the intuition that a *delayed trilateration* should have the same properties of a *simultaneous trilateration* (i.e., three measurements should be sufficient to localise the target), we show that in this setting we are not able to recover the target location, even if an ideal, perfect knowledge of the manoeuvres performed by the target and of the measurements collected is available. In the developments, we additionally prove that this result roots in an algebraically ill-posed solution of the trilateration.

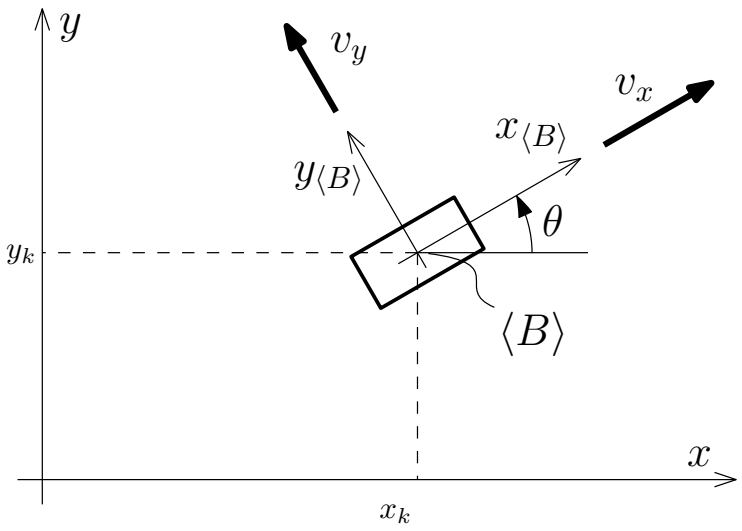

Figure 2.1: Figure with the absolute and the relative reference frame.

2.1 Problem Description

In this section we will present the background knowledge and results that are fundamental to derive the problem we are tackling in this chapter.

2.1.1 Dynamical model – continuous-time dynamics

In a previous work [Farina et al., 2017], Farina et al. presented a dynamical model able to capture the relevant dynamics of the motion of a pedestrian. In the same spirit and for the sake of the problem at hand, we decide to abstract that dynamic model to a pair of integrators in the plane endowed with the orientation θ. Notice that this dynamical system can be leveraged also to model robotic vehicles with a simple kinematic model and these results can be easily extended to unicycle–like vehicles. As depicted in Figure 2.1, we consider the target having two independent inputs v_x and v_y in the target reference frame $\langle B\rangle$, which leads to the following dynamics in the fixed inertial reference frame

$$\dot{x} = v_x \cos\theta - v_y \sin\theta, \qquad \dot{y} = v_x \sin\theta + v_y \cos\theta. \tag{2.1}$$

To simplify the forthcoming analysis, we consider the system to be sampled at discrete time instants with sampling time T_s (dictated by the hardware avail-

able), thus leading to

$$x_{k+1} = x_k + V_x, \qquad y_{k+1} = y_k + V_y, \tag{2.2}$$

where x_k denotes the horizontal position of the target at the time instant $t = kT_s$ and V_x and V_y depend on the system inputs, i.e.

$$V_x = (v_{x,k}\cos\theta - v_{y,k}\sin\theta)T_s, \qquad V_y = (v_{x,k}\sin\theta + v_{y,k}\cos\theta)T_s, \tag{2.3}$$

where $v_{x,k} = v_x(kT_s)$ and $v_{y,k} = v_y(kT_s)$. In the following, we will denote the position of the target at time step k as $P_k = [x_k, y_k]^\top$, and define A_k as the length of the path travelled by the target between steps k and $k+1$, i.e.

$$A_k = \|P_{k+1} - P_k\| = \sqrt{(x_{k+1} - x_k)^2 + (y_{k+1} - y_k)^2}.$$

Notice that we can compute the value of A_k by using the discrete-time dynamics (2.2) of the target, thus yielding

$$A_k = \sqrt{{V_x}^2 + {V_y}^2}, \tag{2.4}$$

which only depends on the relative displacements V_x and V_y in (2.3).

Moreover, we can express the angular increment δ_k described by the segments connecting P_k to P_{k+1}, and P_{k+1} to P_{k+2} as

$$\begin{aligned} \delta_k &= \beta_{k+1} - \beta_k \\ &= \arctan2(v_{y,k+1}, v_{x,k+1}) - \arctan2(v_{y,k}, v_{x,k}), \end{aligned} \tag{2.5}$$

where

$$\begin{aligned} \beta_k &= \arctan2({}^{\langle B\rangle}y_{k+1} - {}^{\langle B\rangle}y_k, {}^{\langle B\rangle}x_{k+1} - {}^{\langle B\rangle}x_k) + \theta \\ &= \arctan2(v_{y,k}, v_{x,k}) + \theta. \end{aligned} \tag{2.6}$$

This way, the target trajectories can be represented by segments connecting P_k and the successive points P_{k+1} by using the length A_k and the inclination β_k, as represented in Figure 2.2.

Remark 2.1.1. *We assume in this chapter that the inputs $v_{x,k}, v_{y,k}$ are known perfectly (i.e., no measurement uncertainty is considered). Nevertheless, without the ranging measurements, since we are not aware of the initial position P_0 of the target and of its inclination θ, given the history of the inputs $v_{x,k}, v_{y,k}$ in any discrete-time interval $[0, 1, \ldots, k_f]$, we are not able to reconstruct the absolute trajectory in the inertial reference frame, but we can only reconstruct the "relative geometrical shape" of the trajectory, i.e. the length of the segments*

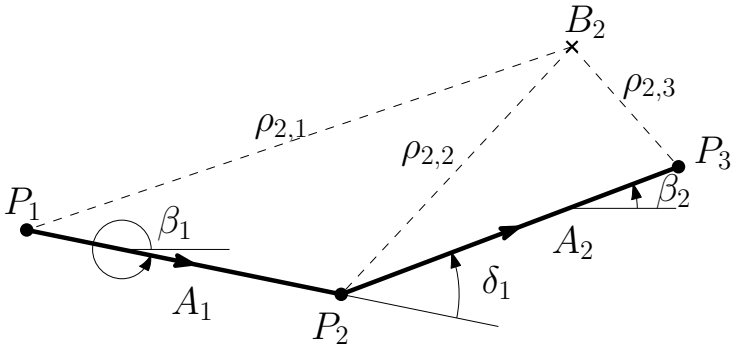

Figure 2.2: Typical trajectories followed by the target. Through the velocity input sequence, we have an immediate description of the segment lengths A_1 and A_2 and their relative orientation δ_1. As an example, the anchor B_2 is represented together with its distances from the target at three consecutive time instants.

A_k, $k \in [0, k_f]$ *and their relative angle* δ_k, $k \in [0, k_f - 1]$. *This is an immediate consequence of the knowledge of relative measurements.*

2.1.2 Sensor model

We assume that the environment is equipped with a set of anchors, e.g., UWB anchors, $B_i = [X_i, Y_i]^\top$, $i = 1, \ldots, n$, retrieving their distance to the target, i.e. the measurement output of the systems at time k are the distances $\rho_{i,k}$, such that

$$\rho_{i,k}^2 = (x_k - X_i)^2 + (y_k - Y_i)^2. \tag{2.7}$$

2.1.3 Problem formulation

It is widely known that the problem of positioning a target on a plane, i.e., to retrieve its coordinates x_k, y_k at a certain time kT_s, is solved by means of *trilateration*, i.e., at time kT_s at least three ranging measurements from non–collinear anchors are available [Palopoli and Fontanelli, 2020]. With respect to (2.7), it amounts to collect $\rho_{i,k}$, for $i = 1, \ldots, 3$, i.e., all the measurements come at the same time instant. In this case, the positioning problem is *statically observable*. When, instead, the measurements from the three anchors come at different time instants, e.g., we have access to $\rho_{1,k}$, $\rho_{2,k+1}$ and $\rho_{3,k+2}$, the positioning problem turns to a *localisation* problem [Fontanelli, 2022], which entails the concept of *dynamic observability*, or simply *observability*. The main idea is that the notion of the motion model compensates for a reduced amount of measurements at time k. In this chapter, we will prove that this is counterintuitively: we analyse both the two different situations: the first is the traditional *simultaneous trilateration*

problem where the three landmarks retrieve the distance measurements at the same time, and then we will analyse the problem of the *delayed trilateration*, where the measurements are retrieved at three different time steps. In the latter case, we will show that three measurements from three different anchors *are not sufficient*: in other words, the standard trilateration does not consider just three measurements, but *four*: the last one is the knowledge of the *simultaneous* measurements. In carrying out the analysis, we are not considering explicitly the role played by the measurement uncertainties. In fact, the results here obtained are applicable also in the *ideal* case, i.e., perfect measurements.

We would like here to stress that the problem we are dealing with is associated with the concept of *observability*, which depends only on the dynamics of the system, on the model of the sensors and on the trajectory followed by the system itself. Therefore, actuation uncertainty and measurement noise play no role at this level [Fontanelli, 2022].

2.2 Trilateration

As aforementioned, the simultaneous trilateration involves three anchors retrieving the distance ideal measurements from the target at the same time. To compact the notation, in the following we will drop the subscript k in (2.7). We introduce here the formal definition of trilateration and its proof.

Proposition 2.2.1 (Simultaneous trilateration)**.** *Let $P = [x, y]^\top \in \mathbb{R}^2$ be the position of the target on the plane and let $B_i = [X_i, Y_i]^\top$, $i = 1, 2, 3$ be the positions of three anchors, each of them measuring their distance ρ_i from P. Whenever the three anchors are not collinear, P is the only point compliant with the three retrieved distances.*

Proof. By taking the differences $\rho_2^2 - \rho_1^2$ and $\rho_3^2 - \rho_1^2$, we come up with two linear equations in the unknown x, y, reading

$$M \begin{bmatrix} x \\ y \end{bmatrix} = h, \qquad \text{with } M = \begin{bmatrix} X_1 - X_2 & Y_1 - Y_2 \\ X_1 - X_3 & Y_1 - Y_3 \end{bmatrix} \tag{2.8}$$

which is invertible as soon as M is nonsingular, i.e. $\det M \neq 0$. The determinant of M can be obtained as the only non–zero element of the cross product between $B_2 - B_1$ and $B_3 - B_1$

$$\begin{bmatrix} 0 \\ 0 \\ \det M \end{bmatrix} = \begin{bmatrix} X_2 - X_1 \\ Y_2 - Y_1 \\ 0 \end{bmatrix} \times \begin{bmatrix} X_3 - X_1 \\ Y_3 - Y_1 \\ 0 \end{bmatrix} = \begin{bmatrix} 0 \\ 0 \\ d_{12} d_{13} \cos \gamma_{213} \end{bmatrix}, \tag{2.9}$$

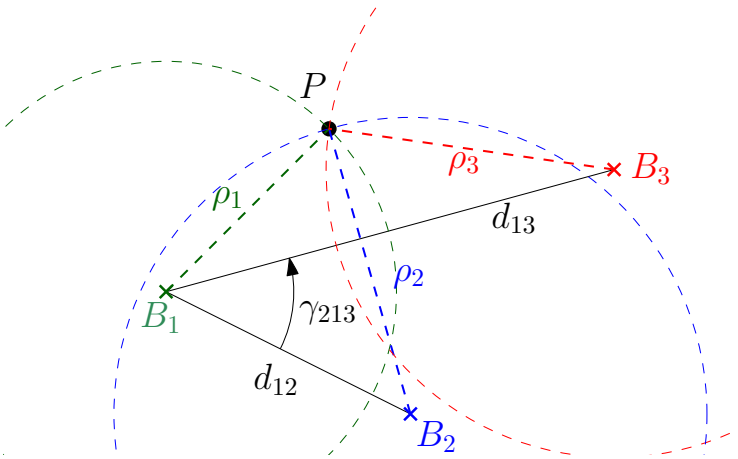

Figure 2.3: Three range sensors measure their distance from the target: whenever the three anchors are not aligned (i.e. $\gamma_{213} \neq h\pi$), we have only one intersection among the three circles, i.e. we know where the target is.

where $\cdot \times \cdot$ denotes the cross product between two vectors, d_{12} and d_{13} are the distances between the anchors B_1 and B_2, and B_1 and B_3, respectively, while γ_{213} is the amplitude of the angle described by the three anchors, with vertex B_1, as represented in Figure 2.3. Whenever $\gamma_{213} = 0$, the three anchors are collinear, and we are not able to uniquely identify the position P of the target. □

The widely known geometric interpretation is the following: for each anchor B_i, we build a circle centred in the anchor itself, with *radius* equal to the retrieved distance ρ_i. The three circles have two intersection points as soon as the three centres are aligned, otherwise they only have one unique intersection.

Remark 2.2.2. *The proof of Proposition 2.2.1 is built upon the differences of the squares of the distances, which ensures that the solution will correspond to the actual target location. However, when the distances are not collected from a real scenario, but the positions of the anchors and their ranges are fixed upfront, we can still find a point* $[x, y]^\top$ *by using* (2.8)*, but it will not be a solution to* (2.7)*.*

Although Remark 2.2.2 seems to account for a situation that is never occurring, it turns out to be fundamental: indeed, a solution to the trilateration problem may be wrongly considered correct even if M is invertible, but the circles do not intersect in a single point. We will explicitly consider this situation in Section 2.2, where we introduce the concept of delayed trilateration, i.e., the ranging measurements are collected at different time instants for a target that is moving, which may lead to the problem discussed in Remark 2.2.2.

Remark 2.2.3. *In the case of simultaneous trilateration, we are able to reconstruct the position P of a still target independently on the orientation angle θ, which has no effect on the measurements retrieved by the three landmarks, since it does not appear in the definition of the distances in* (2.7).

Delayed trilateration

We address now the case of the delayed trilateration. In this scenario, the target is assumed to move according to (2.2) with unknown initial position $P_1 = [x_1, y_1]^\top$ and unknown orientation θ. Assuming that the three measurements in (2.7) are given at time instants $k_1 \neq k_2 \neq k_3$ and by leveraging on our knowledge on the system inputs over time (see Remark 2.1.1), we will try to recover the unknown initial condition P_1 in order to reconstruct the entire trajectory (indeed, the system inputs are assumed to be perfectly known).

In the previous section, we have used the condition of *noncollinearity* among the three anchors B_i, in order to reconstruct the position P of the target. Since in this scenario the target is moving, we will need a different *generalised noncollinearity* condition, as in the following definition.

Definition 2.2.4 (Generalised noncollinearity)**.** *Given three consecutive positions P_k, $k = 1, 2, 3$ of the target and three landmarks B_i, $i = 1, 2, 3$, such that the i-th anchor distance to the target is retrieved at time k_i, the anchors are said to be non-collinear if the following holds:*

$$(\bar{B}_2 - \bar{B}_1) \times (\bar{B}_3 - \bar{B}_1) \neq 0,$$

where the translated anchors $\bar{B}_i$ are defined as

$$\bar{B}_1 = B_1, \quad \bar{B}_2 = B_2 - \begin{bmatrix} V_{x1} \\ V_{y1} \end{bmatrix}, \quad \bar{B}_3 = B_3 - \begin{bmatrix} V_{x1} + V_{x2} \\ V_{y1} + V_{y2} \end{bmatrix}.$$

From a geometric point of view, the condition expressed in Definition 2.2.4 may be interpreted as follows: we move the pair anchor–measurement (i.e. the pair B_i–P_i) such that all the measured points P_i coincide with P_1, to recover a scenario similar to trilateration. The *generalised noncollinearity* holds if the three translated anchors $\bar{B}_i$ are not collinear.

For the sake of simplicity and without loss of generality, we assume that $k_1 = 1$, $k_2 = 2$ and $k_3 = 3$ in (2.7), while we are interested in the initial position $P_1 = [x_1, y_1]^\top$ of the target, together with the inclination θ (see Figure 2.4). In light of Definition 2.2.4, we are ready to prove the following proposition.

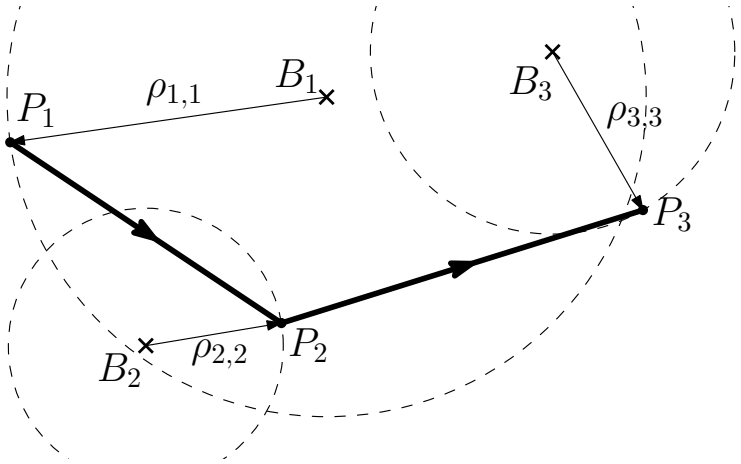

Figure 2.4: Three anchors B_i measure their distance $\rho_{i,i}$ from the target, each of them at time $k_i = i$.

Proposition 2.2.5. *Given the target dynamics* (2.2)*, the system inputs* $v_{x,k}, v_{y,k}$*,* $k = 1, 2$*, the sensor model* (2.7)*, the measurement outputs* $\rho_{1,1}, \rho_{2,2}, \rho_{3,3}$ *and the initial angle* θ*, we can reconstruct the initial position* P_1 *of the target only if the generalised noncollinearity condition holds.*

Proof. For the proof of this proposition, we follow the same *rationale* as in the proof of Proposition 2.2.1, thus we build the differences $\rho_{2,2}^2 - \rho_{1,1}^2$ and $\rho_{3,3}^2 - \rho_{1,1}^2$. By leveraging on Definition 2.2.4, we compute the i-distance as

$$\rho_{i,i} = \|B_i - P_i\| = \|\bar{B}_i - P_1\|.$$

Being P_1 constant and common to all the measurement results, we recover the same structure as in the proof of Proposition 2.2.1

$$\bar{M} \begin{bmatrix} x_1 \\ y_1 \end{bmatrix} = \bar{h}, \qquad \text{with } \bar{M} = \begin{bmatrix} \bar{X}_1 - \bar{X}_2 & \bar{Y}_1 - \bar{Y}_2 \\ \bar{X}_1 - \bar{X}_3 & \bar{Y}_1 - \bar{Y}_3 \end{bmatrix}, \tag{2.10}$$

where $\bar{X}_i$ and $\bar{Y}_i$ are such that $\bar{B}_i = [\bar{X}_i, \bar{Y}_i]^\top$, $i = 1, 2, 3$.

By the same procedure as for (2.8), a unique solution can be found if and only if $\bar{B}_1$, $\bar{B}_2$ and $\bar{B}_3$ make the matrix $\bar{M}$ invertible, thus compliant with the condition of *generalised noncollinearity* of the three anchors B_1, B_2, B_3. □

Proposition 2.2.5 states that there exists *only one* trajectory compliant with the manoeuvres performed by the target, with its initial inclination θ and with the three measurement retrieved by the sensors. However, we can draw a consideration that directly descends from Remark 2.2.2, which is discussed in the following remark and turns out to be fundamental.

Remark 2.2.6. *As in the case of simultaneous trilateration, the proof of Proposition 2.2.5 is based on the differences of the collected distances. However, in this situation, we use the measurement collected by the vehicle moving across the environment, but we fix an arbitrary value of θ, which leads us to find an initial point P_1 according to* (2.10)*, but we have no guarantees that P_1 is also a solution to* (2.7)*. Thus, solutions to* (2.7) *may be found only fixing some specific (unknown) values for the inclination angle θ.*

The main difference with the case of simultaneous trilateration is the dependence on θ of M in (2.10) for the delayed trilateration. Therefore, there may exist multiple solutions having the same sequence of manoeuvres and of measurements, but different values of θ. As a consequence, based on Proposition 2.2.5, we can state that the knowledge of the system inputs, the model and the measurements is not sufficient to reconstruct P_1. Considering Remark 2.2.2 and Remark 2.2.6, we are now ready to introduce the main result of this chapter.

Proposition 2.2.7. *Given a target moving accordingly to* (2.2) *with known velocity inputs $v_{x,k}, v_{y,k}$, $k = 1, 2$, and three fixed-frame anchors B_1, B_2, B_3, measuring their distance from the target at time $k = 1, 2, 3$ respectively, we cannot localise the target in the environment, i.e. we cannot reconstruct its initial position P_1 in the inertial reference frame.*

The main consequence of this proposition is that three ranging measurements are not sufficient for trilateration, but the three measurements should be collected simultaneously to solve the problem, even with the additional perfect knowledge of the model and the system inputs.

2.3 Simulation results

To support our claim, we provide a simulation of the scenario presented in Proposition 2.2.7, with a counterexample that shows that, despite the assumptions in Proposition 2.2.5 hold, there are many trajectories that are compliant with the manoeuvres performed by the target and with the range measurements retrieved by the anchors.

Example 2.1. We assume that the target moves with given inputs (thus we assume to know the relative displacement in (2.3) and the shape of the trajectory) and collects one measurement from each of the three anchors. We further assume the following configuration:

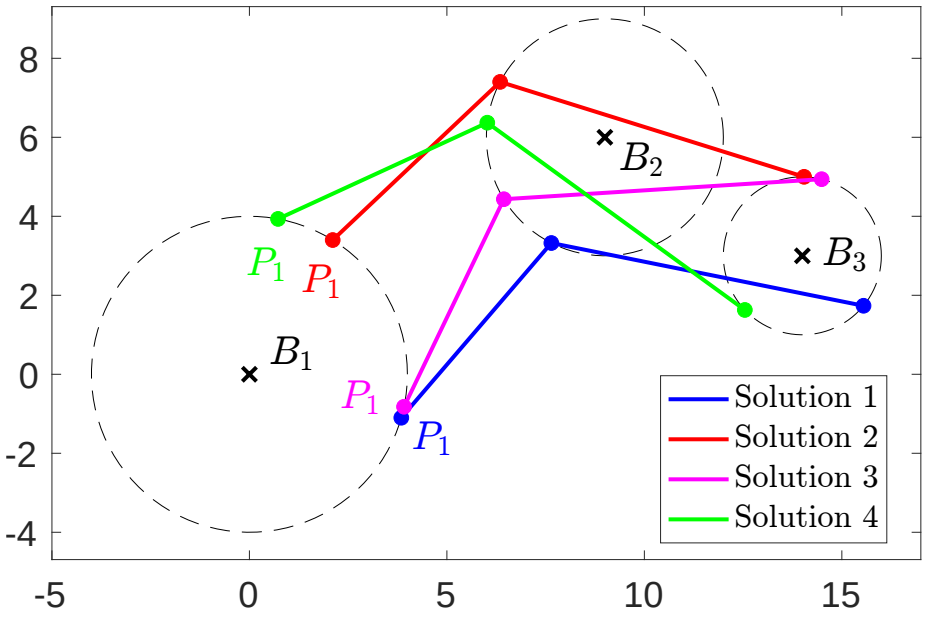

Figure 2.5: Graphical representation of Example 2.1. In this case, despite the *generalised noncollinearity* condition holds, we have (at least) four trajectories that are compliant with the manoeuvres and the measurements retrieved by the three anchors, showing that three range measurements are not sufficient to uniquely identify the trajectory followed by the target.

Sensor positions:

$$B_1 = \begin{bmatrix} 0 \\ 0 \end{bmatrix}, \quad B_2 = \begin{bmatrix} 9 \\ 6 \end{bmatrix}, \quad B_3 = \begin{bmatrix} 14 \\ 3 \end{bmatrix},$$

Sensor readings:

$$\rho_{1,1} = 4, \quad \rho_{2,2} = 3, \quad \rho_{3,3} = 2,$$

Control inputs:

$$v_{x,1} = 5,\ v_{y,1} = 3, \quad v_{x,2} = 7,\ v_{y,2} = -4,$$

with sampling time $T_s = 1\,s$.

Figure 2.5 shows the results obtained in the simulation with the parameters above, i.e. a set of four trajectories that are compliant both with the manoeuvres performed by the target (see Remark 2.1.1) and with the readings of the three range sensors. As reported in Table 2.1, where the results obtained with the four distinct solutions represented in Figure 2.5 are quantified, we can notice that: despite the generalised noncollinearity condition holds (for each trajectory, we can check the generalised noncollinearity condition by building

	Solution 1	Solution 2	Solution 3	Solution 4
P_1	3.85	2.11	3.91	0.73
	−1.10	3.40	−0.82	3.93
P_2	7.64	6.35	6.44	6.02
	3.32	7.40	4.43	6.37
P_3	15.55	14.04	14.49	12.54
	1.74	5.00	4.94	1.63
$\det M$	−2.76	2.54	−20.43	11.87

Table 2.1: Numerical results of the simulation in Example 2.1 and depicted in Figure 2.5. For each solution, we report the position of the points P_k reached by the target at time k and whose distance is measured by the anchor B_k. In the last row we report the determinant of matrix M built as in (2.10).

the matrix M as in (2.10) and computing its determinant $\det M$: the last row of Table 2.1 contains only non-zero values), all the four solutions are compliant with manoeuvres and measurements but are all different: one may simply check by using the obtained numerical results about the positions P_1, P_2 and P_3. ⋆

From the analysis carried out on the simultaneous and delayed trilateration, which are supported by the results obtained in the numerical example, we draw the following consideration: even though the intuition suggests that with three measurements we are able to reconstruct the position of the target on the plane $\mathbb{R}^2$, this is not sufficient whenever we add the dynamics of the system, i.e. whenever the target moves while the measurements are taken. The problem of finding the minimum number of measurements needed to find the position of the target with *three simultaneous* ranging measurements is exhaustively addressed in Proposition 2.2.1, while Example 2.1 and Proposition 2.2.7 state that the minimum number of anchors with *delayed measurements* to reconstruct the target location is still open, and is the base for the analyses in the next chapters of this thesis. From a practical point of view, we are considering a target that is initially unaware of its position and orientation on the plane. These results imply that, when it collects 3 measurements with a delayed trilateration as in Section 2.2, the target can build a set of positions where it could be located. Although the actual position of the vehicle is included in this set, the target cannot retrieve it with only 3 measurements.

With these considerations in mind, we are now ready to state the main claim of this chapter with a clear statement.

Claim 2.3.1. *Whenever we consider a scenario of simultaneous trilateration as in Section 2.2, we are collecting* ***three*** *measurements from the ranging sensors, but we are also relying on one* ***additional*** *information, which is the implicit*

assumption that the target is still.

Notice that this assumption is not explicitly used in the computations and proofs (see proof to Proposition 2.2.1), but it allows us to find the position of the target on the plane. This claim is supported by Section 2.2 and by the numerical simulation in the Example 2.1, where the implicit assumption of simultaneous measurements is explicitly removed, i.e. the target is not still while the measurements are collected, thus leading to reconstruction failure.

2.4 Discussion

In this chapter we have shown how three measurements are not always sufficient to reconstruct the state of the agent, i.e., localise it in the environment, but we have given no hint on the minimum number of measurements and anchors needed to reconstruct the state, i.e. to attain the so-called *global observability*. This counterintuitive result lays the foundations for the analyses that will be carried out in the next chapters of the thesis, where we aim at analysing how the *global observability/constructibility* properties are affected by these three quantities:

- The shape of the trajectory (associated with control inputs and proprioceptive sensors);
- The number and layout of the anchors in a planar environment;
- The number of measurements collected by the vehicle and their distributions among the anchors.

3 A Sufficient Condition for Global Constructibility

Contents

In Chapter 2, we have presented the problem of localising a (moving) target by leveraging range sensors, and we have shown that this problem is not trivial to address, since intuition on the extension of the classic *trilateration* technique fails. In this chapter, we reverse our focus, and rather than analysing an *unconstructible* scenario, i.e. a setting where the state of the system cannot be univocally reconstructed, we look at a condition where the state of the vehicle can be reconstructed. We consider a sparse deployment in which anchors are in a small number and have a finite and non–overlapping sensing range. Under the most extreme conditions (i.e., the robot being in sight of two anchors at different times), we provide a sufficient condition on the manoeuvres that the robot is required to execute within the sensing range of each of the anchors in order to achieve global constructibility. This contribution represents the first step towards a complete analysis of the global constructibility properties of a nonholonomic vehicle moving through a planar environment and collecting range measurements from fixed–frame sensors.

Contributions: In this chapter, we consider a mobile robot, represented by the unicycle kinematic model, travelling across an environment instrumented with a sparse infrastructure of range sensors with non-overlapping ranges. Therefore, the robot can take only one measurement at a time. Moreover, we consider the robot to collect intermittent measurements, modelling discrete–time behaviours of digital components, e.g. finite sampling frequencies. In this setting, we show a particular type of manoeuvres that attain global constructibility. These conditions require the robot to follow curved trajectories and to repeat the same set of manoeuvres under the sensing range of the two anchors.

3.1 Problem Description

We consider discrete-time systems in the state space

$$\begin{aligned} q_{k+1} &= f(q_k, u_k), \\ z_k \quad &= h(q_k) \end{aligned} \tag{3.1}$$

where $q \in \mathbb{R}^n$ is the state, $u \in \mathbb{R}^m$ represents the control inputs and $z \in \mathbb{R}^p$ is the output of the system, i.e. the sensor readings. Specifically, we will focus the kinematic model of a unicycle-like vehicle, given in continuous time by:

$$\begin{aligned} \dot{x}(t) &= v(t)\cos\theta(t), \\ \dot{y}(t) &= v(t)\sin\theta(t), \\ \dot{\theta}(t) &= \omega(t), \end{aligned} \tag{3.2}$$

where $x(t), y(t)$ represent the Cartesian coordinates of the vehicle, while $\theta(t)$ denotes its heading with respect to a reference axis. We make the simplifying assumptions that the control inputs $v(t)$ and $\omega(t)$ be constant over every time interval of fixed duration T_s, as if the system were controlled by a digital system with a finite sampling frequency $1/T_s$, i.e. $v(t) = v_k$, $\forall t \in [kT_s, (k+1)T_s\big)$. By exploiting this simplification, we can explicitly integrate the dynamics over the sampling interval $[kT_s, (k+1)T_s)$ to compute the state $q_{k+1} = q\big((k+1)T_s\big)$. First, we compute the trajectory over time of the heading angle $\theta(t)$, which x_{k+1} and y_{k+1} depend on. To this aim, we compute

$$\theta(t) = \theta_k + \int_{kT_s}^{t} \omega(s)\, ds = \theta_k + \omega_k(t - kT_s).$$

From this, we can compute the next position (x_{k+1}, y_{k+1}) of the vehicle as

$$\begin{aligned} x_{k+1} &= x_k + \int_{kT_s}^{(k+1)T_s} v(s)\cos(\theta(s))\, ds, \\ y_{k+1} &= y_k + \int_{kT_s}^{(k+1)T_s} v(s)\sin(\theta(s))\, ds. \end{aligned}$$

By manipulating these expressions with trigonometric identities, with $v(t) = v_k$ and $\omega(t) = \omega_k$ for $t \in [kT_s, (k+1)T_s\big)$, we get

$$\begin{aligned} x_{k+1} &= x_k + \frac{v_k}{\omega_k}\left(\sin(\theta_k + \omega_k T_s) - \sin\theta_k\right) \\ &= x_k + 2\frac{v_k}{\omega_k}\sin\left(\omega_k\frac{T_s}{2}\right)\cos\left(\theta_k + \omega_k\frac{T_s}{2}\right), \end{aligned}$$

and analogously

$$\begin{aligned} y_{k+1} &= y_k - \frac{v_k}{\omega_k}\left(\cos(\theta_k + \omega_k T_s) - \cos\theta_k\right) \\ &= y_k + 2\frac{v_k}{\omega_k}\sin\left(\omega_k\frac{T_s}{2}\right)\sin\left(\theta_k + \omega_k\frac{T_s}{2}\right). \end{aligned}$$

Therefore, in the rest of this thesis, we will consider the discrete–time counterpart of the well–known continuous–time kinematic model (3.2), reading as

$$\begin{aligned} x_{k+1} &= x_k + A_k C_k, \\ y_{k+1} &= y_k + A_k S_k, \\ \theta_{k+1} &= \theta_k + \omega_k T_s \end{aligned} \tag{3.3}$$

with

$$A_k = \begin{cases} 2\dfrac{v_k}{\omega_k}\sin\left(\dfrac{T_s}{2}\omega_k\right) & \text{if } \omega_k \neq 0, \\ v_k T_s & \text{otherwise,} \end{cases}$$
$$C_k = \cos\left(\theta_k + \frac{T_s}{2}\omega_k\right),$$
$$S_k = \sin\left(\theta_k + \frac{T_s}{2}\omega_k\right),$$

where, in the adopted notation, the subscript k denotes the time $t = kT_s$ for the continuous-time dynamics (for further details the reader is referred to [Palopoli and Fontanelli, 2020]).

The measurement system consists of a set of ranging sensors (henceforth called anchors) yielding their distance from the vehicle, so as the measurement output z_k is defined as

$$z_k = \begin{bmatrix} \rho_1(x_k, y_k) \\ \rho_2(x_k, y_k) \\ \cdots \end{bmatrix} = \begin{bmatrix} \sqrt{(x_k - X_1)^2 + (y_k - Y_1)^2} \\ \sqrt{(x_k - X_2)^2 + (y_k - Y_2)^2} \\ \cdots \end{bmatrix}, \tag{3.4}$$

where ρ_1 and ρ_2 are the measurements collected from the first two anchors B_1 and B_2. We consider the case in which anchors have a bounded range, i.e. a measurement is collected by anchor i only if its distance from the vehicle is smaller than its sensing range $\rho_i^{\max}$.

A common problem arising in the control of dynamical systems is the *estimation problem*, i.e. the reconstruction of the state of the system based on the measurement outputs and on the control inputs, usually performed by the so-called *estimation filters*. If the purpose of the filter is to estimate the initial state, it is required that the trajectories of the system satisfy the *observability* property, i.e., the ability to reconstruct the initial state given an input/output sequence. More recently, the problem of estimating the final state has taken centre [Salaris et al., 2019]. In this case the key property to look at is *constructibility*, as defined below.

Definition 3.1.1 (Constructibility)**.** *Given system* (3.1)*, constructibility is defined as the ability to reconstruct the state q_f of the system at time $k = k_f$, given the outputs $z_k, k = k_0, \ldots, k_f$ and the control inputs $u_k, k = k_0, \ldots, k_f - 1$. Intuitively, constructibility consists in reconstructing the current state q_k given the past history of inputs and outputs.*

Remark 3.1.2. *Unlike linear systems, nonlinear systems are not structurally constructible (or unconstructible), but the concept of constructibility is referred*

to the particular trajectory followed by the system itself.

Given the dynamical system (3.3)-(3.4), moving across an environment instrumented with two fixed–frame ranging sensors with bounded and non–overlapping sensing range, in this chapter we aim at providing a sufficient condition on the set of manoeuvres executed by the vehicle that attain global constructibility.

3.2 Global constructibility analysis

Consider the unicycle model (3.3)-(3.4) moving in an environment equipped with ranging anchors with limited sensing range, i.e., the measurement function $\rho_i(x, y)$ is defined in the region $\Omega_i = \left\{[x, y]^\top | \rho_i(x, y) \leq \rho_i^{\max}\right\}$. For this particular nonlinear system, observability implies constructibility, since from the known initial state q_0, one may apply the known control inputs to the system and reconstruct the entire trajectory, including the final point q_f, hence guaranteeing constructibility.

Given this implication, we can use known results on observability for our constructibility analysis. In our past work, we have shown some observability results, gathered in the following theorem:

Theorem 3.2.1 ([Palopoli and Fontanelli, 2020])**.** *Given the system* (3.3)-(3.4)*, and assuming that the* $p > 0$ *anchors have infinite range, i.e.,* $\Omega_i = \mathbb{R}^2$*,* $\forall i = 1, \ldots, p$*, then:*

1. *If* $p = 1$*, the system state is not globally constructible;*
2. *If either* $p = 2$ *or* $p \geq 3$ *with collinear anchors, and if both* $\exists k$ *such that* $v_k \neq 0$*, and* $\omega_k = 0, \forall\, k$ *(i.e., the robot follows a rectilinear trajectory), the system state is not globally constructible;*
3. *If either* $p = 2$ *or* $p \geq 3$ *with collinear anchors, and if* $\exists k$ *such that* $v_k \neq 0$ *and* $\omega_k \neq 0$ *(i.e., the robot follows a bending trajectory), the system state is globally constructible;*
4. *If* $p \geq 3$ *and the anchors are not collinear, and if* $\exists k$ *such that* $v_k \neq 0$*, the system state is globally constructible.*

We now aim to generalise this result to the case in which the p anchors have finite range and that their sensing ranges are disjoint sets: $\bigcap_{i=1}^{p} \Omega_i = \emptyset$. Specifically, by defining as $\bar{p}_k$ the number of anchors in view at time k, we want to investigate the global constructibility property when $\bar{p}_k = \{0, 1\}$, $\forall k$, and

there exists at least two time instants $k_i'' > k_i'$ such that $[x_k, y_k]^\top \in \Omega_i$, $\forall k \in [k_i', k_i'']$, $\forall i = 1, \dots, p$. Considering disjoint sensing ranges has little practical interest, but this simplifying assumption allows us to state the results that are presented in the following.

Global constructibility for two anchors with finite range

Contrary to the analysis in our previous work, we do not make any claim here of global constructibility for a generic trajectory. On the contrary, we seek specific sequences of controls that allow us to reconstruct the final state in the spirit of active sensing [Salaris et al., 2019]. Specifically, we look for the simplest manoeuvres that allow us to reconstruct the state in the least favourable conditions (i.e., collecting a minimal number of measurements from the minimal number of anchors). To this end, we report the following theorems.

Theorem 3.2.2. *Given the system* (3.3)-(3.4)*, and considering an anchor* $i \in \{1, \dots, p\}$ *and two time instants* $k_i''' > k_i'$ *such that* $[x_k, y_k]^\top \in \Omega_i$, $\forall k \in [k_i', k_i''']$, *the dimension of the unconstructible space reduces to* 2 *when* $k = k_i'$*, i.e. as soon as the first measure is retrieved by the anchor, while it decreases to* 1 *whenever for two consecutive steps* $k_i^\star, k_i^\star + 1$*, such that* $k_i' \leq k_i^\star < k_i''' - 1$, $\omega_{k_i^\star} \neq -\omega_{k_i^\star + 1}$*, i.e. the vehicle curves at least once within the sensing range of the anchor.*

Proof. We divide this proof into two parts, to separately prove the two results.
1) As soon as the first measurement ρ_i' is retrieved, the vehicle must lie on the circle centred on the anchor with radius equal to the collected measurement ρ_i'. Therefore, its position is "constrained" on a unidimensional geometrical variety, while its heading θ is not constrained by the measurement, and thus the unconstructible subspace has dimension 2.
2) Similarly to the proofs in the previous chapter, we write the differences

$$\rho_{k'''}^2 - \rho_{k''}^2 \qquad \text{and} \qquad \rho_{k''}^2 - \rho_{k'}^2,$$

thus obtaining the linear equations

$$M \begin{bmatrix} x_{k'} \\ y_{k'} \end{bmatrix} = h, \qquad \text{with} \qquad \det M = -A_{k'} A_{k''} \sin\left((\omega_{k'} + \omega_{k''}) \frac{T_s}{2} \right).$$

Hence, given $\theta_{k'}$, we can determine the initial position of the vehicle as soon as it turns. However, with only one anchor we will never be able to determine the initial heading of the vehicle ([Palopoli and Fontanelli, 2020, Thm. 1]). □

From Theorem 3.2.2, we can draw two important conclusions. The first

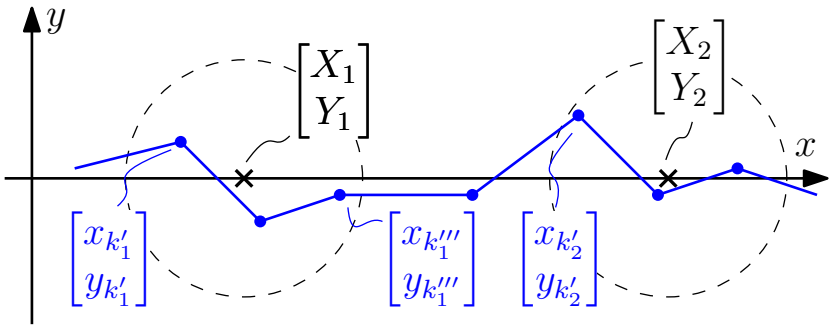

Figure 3.1: Sketch of the trajectory followed by the vehicle to attain global constructibility with two anchors.

(quite obvious) is that we need to collect measurements from at least 2 anchors in order to have constructibility. The second is that by making at least one bend across two measurements the vehicle generates information that can help disambiguate its position. However, repeating this manoeuvre more than once does not produce any benefit for constructibility. In view of these considerations, we can restrict ourselves to a type of trajectory in which the vehicle makes only one bend every time it comes in sight of each anchor. Let us assume for simplicity's sake, but without loss of generality, that the vehicle lies in the sensing range of the i-th anchor only for the three consecutive steps k'_i, k''_i and k'''_i, and consider the following manoeuvres:

1. The robot moves with non-zero translational speed $v_k \neq 0$, $\forall k$;
2. At steps k'_1, k''_1 the vehicle moves with $\omega_{k'_1} \neq -\omega_{k''_1}$;
3. Between steps k'''_1 and $k'_2 - 1$ the robot moves with an arbitrary angular velocity;
4. At step k'_2, the robot comes within the range of anchor 2 and turns with angular velocity $\omega_{k'_2} = \omega_{k'_1} - \sum_{k=k'''_1}^{k'_2-1} \omega_k$ and then with $\omega_{k''_2} = \omega_{k''_1}, \omega_{k'''_2} = \omega_{k'''_1}$.

In other words, the robot turns for two steps, when it is within the range of the first anchors; then it keeps track of the turns it makes before reaching the second anchor.

As soon as the robot reaches the second anchor, it makes a turn to "undo" all the previous manoeuvres, and then it executes the same turns in the range of the second anchor that it made when it was in the range of the first anchor. The trajectory followed by the vehicle is represented in Figure 3.1. Although this manoeuvre is not the easiest from the robot side, it allows us to reconstruct its state, as stated in the following:

Theorem 3.2.3. *Consider the discrete-time unicycle* (3.3) *moving in the scenario described above. If we apply the sequence of manoeuvres in the scenario with* $\omega_{k'_1} T_s \neq 2h_1\pi$ *and* $\omega_{k''_1} T_s \neq 2h_1\pi$ *(with* $h_1 \in \mathbb{N} \setminus \{0\}$*) and* $(\omega_{k'_1} + \omega_{k''_1})T_s \neq 2h_2\pi$ *(with* $h_2 \in \mathbb{N}$*), then the system state is globally constructible.*

Proof. By computing the differences

$$(\rho^2_{k'''_2} - \rho^2_{k''_2}) - (\rho^2_{k'''_1} - \rho^2_{k''_1}) \qquad \text{and} \qquad (\rho^2_{k''_2} - \rho^2_{k'_2}) - (\rho^2_{k''_1} - \rho^2_{k'_1}),$$

we obtain two linear equations

$$M \begin{bmatrix} C_{k'_1} \\ S_{k'_1} \end{bmatrix} = h, \qquad \text{with} \qquad \det M = -A_{k'_1} A_{k''_1} D^2 \sin\left((\omega_{k'_1} - \omega_{k''_1})\tfrac{T_s}{2}\right),$$

and thus the trajectory becomes unconstructible when the two anchors coincide ($D = 0$), when the vehicle does not turn (see Theorem 3.2.2), or when the vehicle retrieves two consecutive measurements in the same position ($A_{k'_1} A_{k''_1} = 0$). The latter may happen due to null velocity $v_{k'} = 0$, or when the vehicle travels along an entire circle between the two time steps ($\sin(\omega_{k'_1} \frac{T_s}{2}) = 0$), thus returning to the same state $q_{k''} = q_{k'}$. □

4 Indistinguishability Analysis for a Nonholonomic Vehicle

Contents

In Chapter 3 we have analysed a particular trajectory followed by a unicycle vehicle in an environment equipped with two ranging sensors with bounded and non–overlapping sensing ranges. We have shown that repeating the same curved trajectory under the sensing ranges of the two anchors represents a sufficient condition for the vehicle to reconstruct its state based only on range information, but no results have been presented on necessary or other sufficient conditions. In this chapter, we shift our focus from the synthesis of a particular trajectory achieving constructibility to the analysis of more general trajectories for a larger class of kinematic models. Therefore, we propose a *global* constructibility analysis for a vehicle moving on a planar surface. Assuming that the vehicle follows a trajectory that can be uniquely identified by the sequence of control inputs and by some intermittent ranging measurements from known points in the environment, we can model the trajectory as a rigid body subject to rotation and translation in the plane. This way, the localisation problem can be reduced to finding the conditions for the existence of a unique roto-translation of the trajectory from a known reference frame to the world reference frame, given the collected measurements. As discussed in this chapter, such conditions can be expressed in terms of the shape of the trajectory, of the layout of the ranging sensors, and of the numbers of measurements collected from each of them.

Contributions: The main part of the technical literature uses the Observability Matrix or the Observability Gramian as tools to quantify the observability of a system. However, since these tools are based on the linearisation of the dynamics of the system or of the output function associated with the measurements collected by the sensors, they produce local results, which are associated with the notion of *weak observability*. By definition, a weakly constructible (or a weakly observable) system can reconstruct its state along its trajectory as long as it is provided with some *a priori* information on its state at a certain time instant, such as a sufficiently narrow set that includes the state itself. In light of this consideration, we analyse the setting where no *a priori* information is given, thus referring to "global observability/constructibility properties". With respect to the results presented in the last chapter, we abstract the dynamics of the system by considering a finite number of points that can be regarded as roto-translations of a given sequence of points in a known reference frame. With this consideration, our aim is to extend the global constructibility analysis (more formally the *u-constructibility analysis*) with intermittent measurements, and provide both sufficient and necessary conditions to achieve global constructibility.

4.1 Problem Description

Let us consider a generic continuous-time nonlinear system in its state space representation

$$\dot{q}(t) = f(q(t), u(t)), \tag{4.1}$$

where $q \in \mathbb{R}^n$ is the state of the system, while $u \in \mathbb{R}^m$ denotes its control inputs. We assume that the nonlinear system represents the dynamics of a vehicle, moving on a planar surface, and thus a portion of the state vector $q(t)$ denotes the Cartesian position $P(t) = [x(t), y(t)]^\top$ of the vehicle in a reference frame $\langle W \rangle$ on the plane $X_w \times Y_w$. We denote by $\langle V \rangle$ a reference frame where the initial conditions $q_V(0)$ of the vehicle are arbitrarily set to 0, i.e. the reference frame is centred on the initial position of the vehicle. In $\langle V \rangle$, the position of the vehicle at time t is represented by $P_V(t) = [x_V(t), y_V(t)]^\top$ and can be reconstructed by using the control input history $u(s)$, $s \in [0, t]$. We will use the following Property 4.1.1, which is directly derived from the definition of the rotation matrix

$$R_\phi = \begin{bmatrix} \cos\phi & -\sin\phi \\ \sin\phi & \cos\phi \end{bmatrix}.$$

Property 4.1.1. *Given the position of the vehicle $P_V(t)$, $\forall t \in [t_0, t_f]$, there exists a unique triplet $(\Delta x, \Delta y, \phi)$ such that*

$$P(t) = R_\phi P_V(t) + \begin{bmatrix} \Delta x \\ \Delta y \end{bmatrix}, \quad \forall t \in [t_0, t_f].$$

From a geometric point of view, Property 1 states that the path followed by the vehicle in any reference frame is a roto-translation of the path travelled in its local reference frame, i.e. the vehicle can reconstruct the "shape" of its own trajectory by dead reckoning. By Property 4.1.1, we may simplify the dynamics (4.1) of the vehicle and consider the path followed by the vehicle as a rigid body on the $X_w \times Y_w$ plane.

The environment is instrumented with a set of sparsely deployed ranging sensors, referred to as *anchors*. The i-th anchor is located at known coordinates $B_i = [X_i, Y_i]^\top$, $i = 1, \ldots, p$, and the vehicle collects the ranging measurement $\|B_i - P(t)\|$.

Assumption 4.1.2 (Intermittent measurements)**.** *Moreover, we consider that measurements are collected at known, but possibly not uniform, sampling instants t_k, with $t_{k+1} > t_k$.*

The output z_k is given by the measurements collected by the anchors, i.e.,

the output equation is the following:

$$z_k = \|P_k - B_{i_k}\|, \tag{4.2}$$

where $P_k = P(t_k)$ is the position of the vehicle at time $t = t_k$, while the index $i_k \in \{1, \dots, p\}$ defines the anchor that the vehicle measures its distance from. For the sake of clarity, the collected distance will be denoted by $\rho_{k,i}$ when the second index i is not clear from the context. Measurements are intermittent; therefore at time t_k, only one ranging measurement $\rho_{k,i}$ is available. The case when multiple measurements can be collected at once has been already solved in [Palopoli and Fontanelli, 2020].

We assume full knowledge of the time instants t_k when the measurements are taken and of the input sequence $u(s)$, $s \in [0, t_k]$, which allows us to reconstruct the sequence of positions $P_V(t_k)$ of the vehicle in $\langle V \rangle$. Therefore, instead of considering the entire paths $P(t)$ and $P_V(t)$, we focus only on the locations where the ranging measurements are collected:

$$\mathcal{P}_k(\Delta x, \Delta y, \phi) = R_\phi P_V(t_k) + \begin{bmatrix} \Delta x \\ \Delta y \end{bmatrix},$$

for $k = 0, \dots, N_m - 1$, with N_m being the total number of measurements. Given two points $\mathcal{P}_l$ and $\mathcal{P}_m$, we define by $\mathcal{S}_{l,m}$ the segment given by their convex combination, with length given by $\|\mathcal{S}_{l,m}\|$. We can now restrict our study to an abstract trajectory $\mathcal{T}$ of the vehicle, defined as the union of all the segments connecting two consecutive positions $\mathcal{P}_k$ of the vehicle, thus

$$\mathcal{T} = \bigcup_{k=0}^{N_m - 1} \mathcal{S}_{k,k+1}, \tag{4.3}$$

which can be regarded as a rigid body.

Remark 4.1.3. *The abstract trajectory $\mathcal{T}$ does not coincide with the actual trajectory $P(t)$, but contains all the features that are needed in the following discussion: the sequence of measurements, the distance and the total change in the orientation between any two measurements.*

In light of the definition of $\mathcal{T}$, we want to find the conditions on the position of the anchors in $\langle W \rangle$ and on the trajectory $\mathcal{T}$ such that it is possible to find a roto-translation such that the points $\mathcal{P}_k$ are compliant with the measurements collected from the anchors. To this aim, we need to introduce the concepts of *constructibility* and *backward indistinguishability* of the states of a nonlinear system. For the sake of generality, in the following definitions, adapted from [Bayat et al., 2015], we consider a plant with a continuous-time dynam-

ics (4.1) and the general version of the discrete-time output equation (4.2), i.e.

$$\dot{q}(t) = f(q(t), u(t)), \qquad z_k = h(q(t_k)). \tag{4.4}$$

We consider the dynamical system to evolve between an initial time instant t_0 (i.e. $k = 0$) and a final time t_f, with $k = k_f$. Given the hybrid nature of (4.4), we will use both k and t to denote the time, with the implicit assumption that by the time instant k we refer to time t_k.

We deal with the notion of *constructibility*, defined as the ability to reconstruct the state q_f of the system at the final time instant t_f. Intuitively, constructibility amounts to reconstructing the current state q_k given the past history of inputs and outputs. In view of Property 4.1.1, the problem of estimating the final state is equivalent to estimating the initial state q_0, which is the well-known concept of *observability*. However, the performance of an estimation filter, i.e. the uncertainty related to the state estimate based on the previous history of motions and measurements, is not directly associated with the concept of observability, but rather to the notion of *constructibility* (for further details, the reader is referred to [Salaris et al., 2019]). To analyse formally the concept of constructibility, both from a local and from a global perspective, we introduce the definition of *backward indistinguishability*, instead of the notion of *indistinguishability* considered for more common observability analyses [Bayat et al., 2015].

Definition 4.1.4. *Given the dynamical system* (4.4)*, a time interval* $T = [t_0, t_f]$*, and an admissible control input function* $u^\star(t)$, $t \in T$*, two final states* q_f *and* $\bar{q}_f$ *are said* $\mathbf{u}^\star$*–**backward indistinguishable** on* T*, if for the input* $u^\star(t)$, $t \in T$*, the output sequences* z_k *and* $\bar{z}_k$, $k = 0, \ldots, k_f$ *of the trajectories satisfying the final conditions* q_f, $\bar{q}_f$*, are identical. Moreover, we define* $\mathcal{I}^{u^\star}_{(b)}(q_f)$ *as the set of all the final conditions that are* $u^\star$*–backward indistinguishable from* q_f *on* T*.*

Since we assume full knowledge of the control input, the shape of the trajectory $\mathcal{T}$ is known in its turn. Hence, we will focus on the concept of u-backward indistinguishability. With a slight abuse of definition, we will refer to *indistinguishable* trajectories as trajectories generated by a known control input and by two *u–backward indistinguishable* final conditions.

Assumption 4.1.5. *We assume that system* (4.4) *with the continuous–time position* $P(t)$ *as output is* constructible*, i.e. we can reconstruct its final state* q_f *given the history of inputs and outputs over a given time interval.*

Remark 4.1.6. *Assumption 4.1.5 holds true for nonholonomic systems modelled through kinematic models (e.g. unicycle–like vehicles and car–trailer vehi-*

cles). Moreover, vehicles represented by dynamical models meet this assumption as soon as they can rely on additional sensors measuring at least *their velocities.*

We can now link the notion of constructibility to the existence of a roto-translation that, when applied to $\mathcal{T}$, produces a set of points compliant with the measurements.

Lemma 4.1.7. *The system is $u^\star$-constructible if there exists a unique roto-translation $(\Delta x, \Delta y, \phi)$ of $\mathcal{T}$ generated by $u^\star$ such that*

$$\|\mathcal{P}_k(\Delta x, \Delta y, \phi) - B_i\| = \rho_{k,i},$$

for each i such that the measurement is available at time k, and for $k = 0, \ldots, k_f$.

Proof. The proof directly follows from Property 4.1.1 and from Assumption 4.1.5. □

Remark 4.1.8. *By Assumption 4.1.5, as soon as a roto-translation is found, we can reconstruct the entire trajectory followed by the vehicle and thus retrieve both the initial condition $q(t_0)$ and the final condition $q(t_f)$. Therefore, the system is observable if and only if it is constructible.*

For the sake of simplicity, we introduce here a new definition to link the number of indistinguishable trajectories to the constructibility properties of the system.

Definition 4.1.9. *Given a trajectory $\mathcal{T}$, if there exist n roto-translations of $\mathcal{T}$ that are indistinguishable from $\mathcal{T}$ itself, we say that $\mathcal{T}$ is* $\mathrm{Ind}(n)$.

Since a trajectory $\mathcal{T}$ is always indistinguishable from itself, it is impossible to have Ind(0). On the other hand, a system is constructible if and only if it is Ind(1). Moreover, in light of Definition 4.1.9, a system is unconstructible when $\mathcal{T}$ is Ind(∞), i.e. when there is an infinite set of roto-translations from $\langle V \rangle$ to $\langle W \rangle$ satisfying (4.2).

Problem Statement

Given a dynamical system such that Property 4.1.1 holds, and the sequence of positions $P_V(t_k)$, $k = 0, \ldots, k_f$, in the vehicle reference frame, we want to find the conditions on $\mathcal{T}$, on the layout of the sensors $B_i = [X_i, Y_i]^\top$, $i = 1, \ldots, p$, in $\langle W \rangle$, and on the distribution of the measurements among the sensors, such that

the system is u-constructible at the final condition q_f. In light of the discussion above, these problems boil down to find whether the equations

$$\|\mathcal{P}_k(\Delta x, \Delta y, \phi) - B_i\| = \rho_{k,i}, \ \ \forall k$$

have a unique solution in the unknowns $\Delta x, \Delta y, \phi$, where the roto-translation of $\mathcal{T}$ from $\langle V \rangle$ to $\langle W \rangle$ is modelled by the translation vector $[\Delta x; \Delta y]^\top$ and by the rotation angle ϕ.

4.2 Global constructibility with a single anchor

We consider the trajectory $\mathcal{T}$ defined in (4.3), and discuss how the readings of a single anchor change depending on roto-translations of $\mathcal{T}$. In our past work [Palopoli and Fontanelli, 2020, Thm. 1], we have restricted our analysis to a unicycle-like vehicle, and we have proved that a single anchor collecting range measurements can never ensure observability of the system state. In simple terms, by Remark 4.1.8, we have proved that u-constructibility as in Definition 4.1.4 can never be achieved with a single anchor. We now want to reformulate this result in terms of the trajectory $\mathcal{T}$ and generalise the analysis of the non-constructible subspaces of the system, depending on the number and on the layout of the measurement points sensed by the anchor.

Without loss of generality, we will consider one anchor located at the origin of the reference frame $\langle W \rangle$, i.e. $B = [0, 0]^\top$, and we will focus on the first three points $\mathcal{P}_0$, $\mathcal{P}_1$ and $\mathcal{P}_2$ of $\mathcal{T}$, where the measurements occur.

Theorem 4.2.1. *Given a vehicle for which Property 4.1.1 holds, its trajectory $\mathcal{T}$ and the set of measurements ρ_k, $k = 0, \ldots, N_m - 1$, collected from an anchor B, a trajectory $\overline{\mathcal{T}}$ is u-indistinguishable from $\mathcal{T}$ if:*

1. *For any N_m, $\overline{\mathcal{T}}$ is a rotation of $\mathcal{T}$ about the anchor;*
2. *For $N_m = 1$ (or $N_m > 1$ coincident points $\mathcal{P}_k$), $\overline{\mathcal{T}}$ is a rotation of $\mathcal{T}$ about the unique measurement point $\mathcal{P}_0$;*
3. *For $N_m = 2$ (or $N_m > 2$ with collinear points $\mathcal{P}_k$), $\overline{\mathcal{T}}$ is symmetric to $\mathcal{T}$ with respect to an axis passing through the anchor.*

Proof. By geometric arguments, any rotation of the trajectory about the anchor does not change the sensor readings, and thus the system sensed with a single anchor is always (at least) Ind(∞). We now analyse scenarios with increasing number of measurements collected by the anchor.

One measurement With one measurement, we identify a point $\mathcal{P}_0$ that is sensed by the anchor, thus constraining the possible roto-translations of $\mathcal{T}$ that satisfy the sensor readings. The measurement point is compliant with the sensor reading only for a position $\mathcal{P}_0 = [\rho_0 \cos\phi, \rho_0 \sin\phi]^\top$, for any $\phi \in [0, 2\pi)$. Therefore, the trajectory is compliant with the measurement for any rotation of the trajectory about the anchor plus any rotation about $\mathcal{P}_0$, i.e. the system is $\mathrm{Ind}(\infty \times \infty)$, unless $\rho_0 = 0$, i.e. $\mathcal{P}_0$ coincides with the anchor.

Two measurements By taking the second measurement in position $\mathcal{P}_1$, provided that the two measurements are not taken in the same point (otherwise the previous case straightforwardly applies), we are adding a constraint on the position and orientation of the trajectory. Indeed, with $\mathcal{P}_0 = R_\phi[\rho_0; 0]^\top$ and $\mathcal{P}_1 = R_\beta[\rho_1; 0]^\top$, and $\|\mathcal{P}_1 - \mathcal{P}_0\| = \|\mathcal{S}_{0,1}\|$, we get an explicit expression of β, which reads as

$$\beta = \phi \pm \arccos\left(\frac{\rho_1^2 - \|\mathcal{S}_{0,1}\|^2 - \rho_0^2}{2\rho_0\|\mathcal{S}_{0,1}\|}\right) \triangleq \phi \pm \delta. \tag{4.5}$$

This result shows that, for any rotation ϕ about the anchor, there are two different points $\mathcal{P}_1^{(a)}$ and $\mathcal{P}_1^{(b)}$, that are compliant with the manoeuvres executed by the vehicle (i.e. $\|\mathcal{S}_{0,1}\|$) and the measurements collected by the anchor (i.e. ρ_0 and ρ_1), hence this setting leads to a $\mathrm{Ind}(2 \times \infty)$ system.

The geometric interpretation of (4.5) is a reflection about an axis passing through the anchor B. Indeed, any point of a circle reflected about an axis passing through its centre lies on the circle itself. Moreover, the geometry of the trajectory, which is uniquely identified by the distance $\|\mathcal{S}_{0,1}\|$, is preserved.

Three measurements Let us consider the setting with two measurements presented previously. For each of the two values of β, we can compute explicitly the position of the third measurement point $\mathcal{P}_2^{(a)}$ and $\mathcal{P}_2^{(b)}$, represented in Figure 4.4.

$$\begin{aligned}
\mathcal{P}_2^{(a)} &= \begin{bmatrix} \rho_0 + \|\mathcal{S}_{0,1}\|\cos(\delta) + \|\mathcal{S}_{1,2}\|\cos(\delta + \mu_{0,1}) \\ \|\mathcal{S}_{0,1}\|\sin(\delta) + \|\mathcal{S}_{1,2}\|\sin(\delta + \mu_{0,1}) \end{bmatrix}, \\
\mathcal{P}_2^{(b)} &= \begin{bmatrix} \rho_0 + \|\mathcal{S}_{0,1}\|\cos(-\delta) + \|\mathcal{S}_{1,2}\|\cos(-\delta + \mu_{0,1}) \\ \|\mathcal{S}_{0,1}\|\sin(-\delta) + \|\mathcal{S}_{1,2}\|\sin(-\delta + \mu_{0,1}) \end{bmatrix},
\end{aligned} \tag{4.6}$$

where $\mu_{0,1}$ is the angle between the segments $\mathcal{S}_{0,1}$ and $\mathcal{S}_{1,2}$. For simplicity, but without loss of generality, we have assumed $\phi = 0$ in (4.5). Computing the differences of the distances of $\mathcal{P}_2^{(a)}$ and $\mathcal{P}_2^{(b)}$ from the origin, we have

$$\|\mathcal{P}_2^{(b)}\|^2 - \|\mathcal{P}_2^{(a)}\|^2 = 4\rho_0\|\mathcal{S}_{1,2}\|\sin\mu_{0,1}\sin\delta.$$

We then conclude that the two distances are equal only when $\mu_{0,1} = h\pi$, $h \in \mathbb{Z}$, i.e. when $\mathcal{P}_0$, $\mathcal{P}_1$ and $\mathcal{P}_2$ are collinear, or when $\delta = h\pi$, $h \in \mathbb{Z}$, i.e. the situation described in Remark 4.2.2 occurs, hence $\mathcal{P}_2^{(a)}$ and $\mathcal{P}_2^{(b)}$ coincide. Therefore, only trajectories rotated around the anchor are indistinguishable, hence the problem is $\mathrm{Ind}(\infty)$. □

Remark 4.2.2. *In the particular case when $\rho_1 = \rho_0 \pm \|\mathcal{S}_{0,1}\|$, i.e. the vehicle moves on the diameter of the circle centred on the anchor, we get $\cos\delta = \pm 1$, i.e. a unique feasible value for β in* (4.5)*, hence avoiding the ambiguity associated with the rotation about $\mathcal{P}_0$, i.e.* $\mathrm{Ind}(1 \times \infty) = \mathrm{Ind}(\infty)$.

With three non–collinear measurement points, we reach the maximum amount of information that can be collected by a single anchor, and thus we conclude that any further measurement beyond the third is no more informative (unless all the preceding measurement points are collinear). Therefore, with the analysis of 1, 2 and 3 measurements, we have exhaustively addressed the analysis of a single anchor, whose results depend both on the number of collected measurements and on their layout on the plane. In light of the results in Theorem 4.2.1, we can define the three equivalence classes **C1**, **C2**, and **C3**, by introducing the following notation.

Notation. By a set **C1** of measurements, we denote any number of measurements collected by the same anchor in the same position $\mathcal{P}$ on the plane, provided that $\mathcal{P}$ does not coincide with the anchor;
By a set **C2** of measurements, we denote any number of *collinear* measurements, not lying on the anchor, collected by the same anchor;
By a set **C3** of measurements, we denote any number of measurements collected by an anchor, not falling in one of the two cases above, i.e. distinct and non-collinear measurement points or with a point coinciding with the anchor.

4.3 Global constructibility with more anchors

In this section, we will leverage the results found for a single anchor to extend the analysis of indistinguishable trajectories to the case of multiple anchors. In light of Lemma 4.1.7, the localisation problem can be solved, i.e. the state of the system can be determined, if and only if $\mathcal{T}$ is $\mathrm{Ind}(1)$.

4.3.1 Pathological conditions

While our primary interest is to analyse positive and negative results for constructibility in the cases in which the available information is minimal (i.e., small

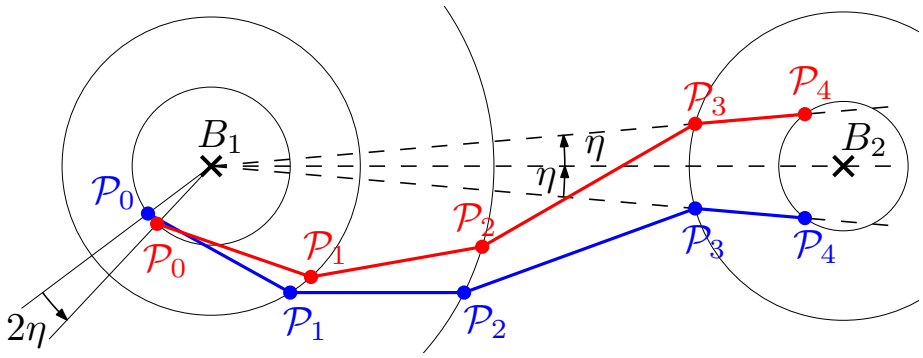

Figure 4.1: Example 4.1. The same trajectory $\mathcal{T}$ rotated about the *pivot* anchor B_1. When $\mathcal{P}_3$, $\mathcal{P}_4$ and B_1 are collinear, we always have two roto-translations of $\mathcal{T}$ that are compliant with the measurements.

number of anchors), it is useful to discuss some negative constructibility results that apply to an arbitrarily large number of anchors and of measurements. This is done in the following examples.

Example 4.1 (Rotation)**.** Consider the scenario shown in Figure 4.1. An anchor B_1 is used to collect a set $\{\mathcal{P}_0, \mathcal{P}_1, \mathcal{P}_2\}$ of **C3** measurements. Consider an additional set $\{\mathcal{P}_3, \mathcal{P}_4\}$ of **C2** measurements from a second anchor B_2 such that $\mathcal{P}_3$ and $\mathcal{P}_4$ are aligned with B_1; let η be the angle between $\mathcal{S}_{3,4}$ and the line $\mathcal{B}_{1,2}$ joining the two anchors. If we rotate the whole set $\mathcal{T}$ by 2η about B_1 neither the new readings for $\{\mathcal{P}_0, \mathcal{P}_1, \mathcal{P}_2\}$ will be affected (Theorem 4.2.1), nor the new readings for $\{\mathcal{P}_3, \mathcal{P}_4\}$ because of the axial symmetry around $\mathcal{B}_{1,2}$. Hence, the blue and red trajectories in Figure 4.1 are indistinguishable. ⋆

Example 4.2 (Translation)**.** Consider the scenario in Figure 4.2. We collect a set $\{\mathcal{P}_0, \mathcal{P}_1\}$ of **C2** measurements from anchor B_1. Let Δ be the distance between B_1 and segment $\mathcal{S}_{0,1}$. By translating the trajectory $\mathcal{T}$ by 2Δ in the direction orthogonal to $\mathcal{S}_{0,1}$, we achieve an axial symmetry, which by Theorem 4.2.1 makes the translated measurements for $\{\mathcal{P}_0, \mathcal{P}_1\}$ indistinguishable from the previous ones. Consider an additional set $\{\mathcal{P}_2, \mathcal{P}_3\}$ of **C2** measurements from an anchor B_2 such that $\mathcal{S}_{2,3}$ is parallel to $\mathcal{S}_{0,1}$, and its distance from B_2 is Δ. By construction, the translation of the trajectory by 2Δ generates an axial symmetry on both the anchors. Therefore, the blue and red trajectories in Figure 4.2 are indistinguishable. ⋆

Remark 4.3.1. *We have presented two examples where each anchor collects a set of* at least **C2** *of measurements. If one or more anchors collect a set* **C1** *of measurements, the condition for indistinguishability simplifies:* $\mathcal{S}_{3,4}$ *should*

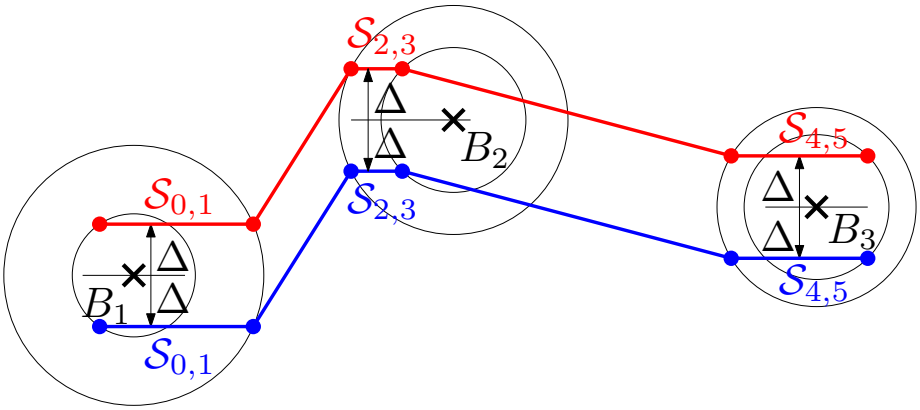

Figure 4.2: Example 4.2. The same trajectory $\mathcal{T}$ translated by 2Δ orthogonally to $\mathcal{S}_{0,1}$. When $\mathcal{S}_{0,1}$, $\mathcal{S}_{2,3}$ and $\mathcal{S}_{4,5}$ are parallel and have the same distance Δ from the anchor collecting the measurements, we always have two translations of $\mathcal{T}$ that are compliant with the measurements.

not be necessarily aligned with B_1 for Example 4.1; likewise $\mathcal{S}_{2,3}$ should not be necessarily parallel to $\mathcal{S}_{0,1}$ for Example 4.2.

The same construction discussed in the previous examples can be iterated for an arbitrary number of anchors, which leads us to the following statement.

Fact 4.3.2. *Given p anchors $B_i = [X_i, Y_i]^\top$, $1, \ldots, p$, deployed on a plane, there always exists at least one abstract trajectory $\mathcal{T}$ for which it is possible to find indistinguishable trajectories.*

This fact is the first main result of this chapter: given any configuration of anchors, there is not a sufficiently high number of measurements and/or anchors such that the system is always constructible. Luckily, this negative result is limited to specific pathological trajectories. As discussed next, in the general case it is possible to overcome this problem.

4.3.2 Conditions for unconstructibility

After discussion some pathological abstract trajectories, which remain indistinguishable no matter the number of anchors and measurements taken, we can now shift our focus to the analysis of *generic trajectories collecting a small number of measurements* from the anchors to determine the conditions for unconstructibility. We will henceforth adopt a special notation to list the number of measurements collected by each anchor: we will use numbers separated by a "+" sign, e.g. $3 + 1$ denotes a **C3** set of measurements collected from the first anchor and a set of **C1** measurements from the second. Our main results on

necessary and sufficient conditions for indistinguishability will be constructed analysing this property for an increasing number of measurements.

$1+1$ scenario:

When two anchors are used to collect one measurement each, *a single* roto-translation from $\langle V \rangle$ to the world frame $\langle W \rangle$ is impossible to construct, which clearly leads to unconstructibility. More precisely, given the two measured points $\mathcal{P}_0^{(0)}$ and $\mathcal{P}_1^{(0)}$, we can always construct an indistinguishable trajectory as follows. First, we rotate $\mathcal{T}$ about B_1 of any angle $\phi \in [0, 2\pi)$ (as in the analysis of the single anchor). Assuming that $\mathcal{P}_0^{(0)}$ has coordinates $[\rho_0, 0]$, its rotated version $\mathcal{P}_0$ will have coordinates $\mathcal{P}_0 = [\rho_0 \cos\phi; \rho_0 \sin\phi]^\top$, and be indistinguishable from $\mathcal{P}_0^{(0)}$. In order for the rotated point $\mathcal{P}_1$ to be indistinguishable from $\mathcal{P}_1^{(0)}$ it is sufficient that it lies the intersection between the circle centred on $\mathcal{P}_0$ of radius $\|\mathcal{S}_{0,1}\|$ and the circle centred on B_2 of radius ρ_1. Therefore, by assuming that $B_1 = [0; 0]^\top$, we can find two possible indistinguishable points

$$\mathcal{P}_1^{(a),(b)} = R_\psi \begin{bmatrix} \|\mathcal{S}_{0,1}\| \\ 0 \end{bmatrix} + R_\phi \begin{bmatrix} \rho_0 \\ 0 \end{bmatrix},$$

where the angle ψ can take one of the following *two* values (one for each intersection between the two aforementioned circles):

$$\psi = \phi + \arctan2\left(D\sin\phi, \rho_0 - D\cos\phi\right) \pm \arccos\left(\frac{\rho_1^2 - \|\mathcal{S}_{0,1}\|^2 - d^2}{2\|\mathcal{S}_{0,1}\| d}\right), \quad (4.7)$$

where $d^2 = D^2 + \rho_0^2 - 2D\rho_0\cos\phi$ is the (unknown) distance between $\mathcal{P}_0$ and B_2, while $D = \|\mathcal{B}_{1,2}\|$ is the distance between the two anchors. Notice that the value of β in (4.5) is a particular case of this value of ψ, when the two anchors coincide, i.e. when $D = 0$. To summarise, *this setting generally leads to* $\mathrm{Ind}(2 \times \infty)$ *trajectories*. For some particular values of ϕ, the two circles become tangent and the two points $\mathcal{P}_1$ coincide. Moreover, since two pairs of points are involved in this analysis (two anchors and two measurement points), the trajectories symmetric with respect to $\mathcal{B}_{1,2}$ are indistinguishable. As a summary we can state the following:

Case 4.3.3. *In the* $1+1$ *case, generic trajectories are* $\mathrm{Ind}(2 \times \infty)$ *(hence, indistinguishable). In the degenerate case when* $\mathcal{S}_{0,1} \subset \mathcal{B}_{1,2}$*, the trajectory is* $\mathrm{Ind}(1)$.

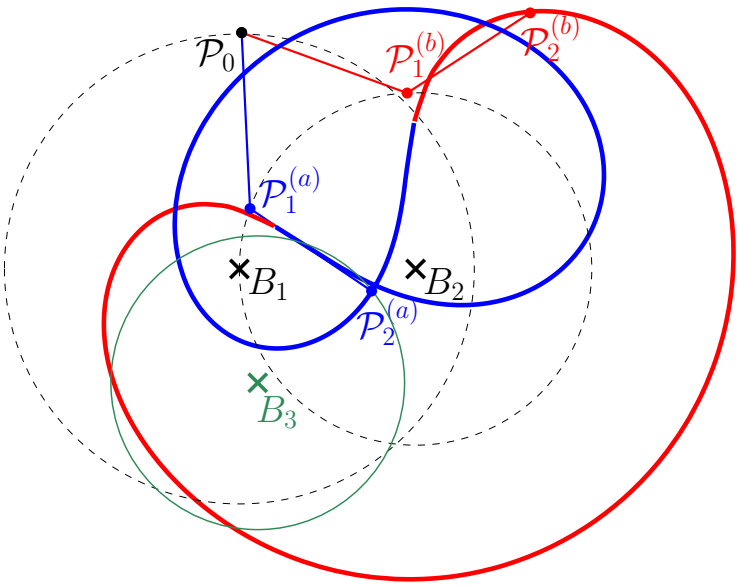

Figure 4.3: Locus where the third measurement point $\mathcal{P}_2$ can lie after the first two measurements ρ_0 and ρ_1 (dashed lines) are collected from the first two anchors. The blue and red colours are associated with the two intersections between the aforementioned circles. The solid green circle represents the third measurement ρ_2 collected by B_3 in a $1+1+1$ setting. After ρ_2, the blue and the red trajectories are no more indistinguishable ($\mathcal{P}_2^{(b)}$ does not lie on the green circle), but there are still 6 intersections of the locus with the green circle, and thus $\mathcal{T}$ is Ind(6).

$1+1+1$ scenario:

We can search for indistinguishable trajectories following the same line of arguments as in the paragraphs above. We start from a trajectory $\mathcal{T}$ characterised by three points $\mathcal{P}_0^{(0)}, \mathcal{P}_1^{(0)}, \mathcal{P}_2^{(0)}$, associated with the measurements ρ_0, ρ_1 and ρ_2. As we did for the $1+1$ case, we rotate the whole trajectory about B_1 of an angle ϕ and come up with two potential points $\mathcal{P}_1^{(a)}, \mathcal{P}_1^{(b)}$, which lie on the intersection between a circle centred on B_2 of radius ρ_1 and a circle centred onto $\mathcal{P}_0$ of radius $\mathcal{S}_{0,1}$ (see (4.7)). The two points $\mathcal{P}_1^{(a)}, \mathcal{P}_1^{(b)}$ uniquely determine the third potential measurements $\mathcal{P}_2^{(a)}, \mathcal{P}_2^{(b)}$. By changing the rotation angle ϕ, the points $\mathcal{P}_2^{(a)}, \mathcal{P}_2^{(b)}$ generate the locus shown in Figure 4.3. The locus is parametrised by the first angle ϕ (and thus its dimension is 1), that it is defined only when $\big|\|\mathcal{S}_{0,1}\| - d\big| < \rho_1 < \|\mathcal{S}_{0,1}\| + d$, and that it is continuous and differentiable on its domain. We have indistinguishability whenever the locus intersects the circle centred on B_3 of radius ρ_2 in more than one point, i.e. when $\mathcal{P}_2^{(a)}$ and $\mathcal{P}_2^{(b)}$ have the same sensor readings.

As a consequence, the indistinguishable third point $\mathcal{P}_2$ has *at most* 8 different locations. Indeed, by defining $C = \cos\phi$ and $S = \sin\phi$, we take the differences

$\rho_2^2 - \rho_0^2$ and $\rho_1^2 - \rho_0^2$ and obtain linear equations in the unknowns C and S, thus yielding a unique solution $(\bar{C}, \bar{S})$. Then we impose the constraints

$$\begin{cases} \bar{C}^2 + \bar{S}^2 = 1 \\ x_0^2 + y_0^2 \ = \rho_0^2 \end{cases},$$

being polynomials with degree 4 and 2 in the unknowns x_0 and y_0, respectively. By Bézout's theorem, the maximum number of real solutions (x_0, y_0) to this set of equations is the product between the degrees of the two polynomials, i.e. 8.

Finally, also for the $1+1+1$ case, we can have a degenerate case, as detailed next.

Case 4.3.4. *In the* $1+1+1$ *case, generic trajectories are* $\mathrm{Ind}(\bar{n})$, $\bar{n} \leq 8$, *and thus indistinguishable. In the degenerate case when the locus is tangent to the circle centred on* B_3 *of radius* ρ_2 *in one point, the trajectory* $\mathcal{T}$ *is* $\mathrm{Ind}(1)$.

$2+1$ scenario:

We address the case $2+1$ following the same procedure as in the previous case. From (4.6) we can compute the distances $d_2^{(a)}$ and $d_2^{(b)}$ of the points $\mathcal{P}_2^{(a)}$ and $\mathcal{P}_2^{(b)}$ from B_1, and the locus in Figure 4.3 degenerates to two circles centred on B_1. Each of the two circles has two intersections as long as $\underline{d} < \|\mathcal{P}_2^\star - B_1\| < \overline{d}$ holds true, where $\underline{d} = |D - \rho_2|$ and $\overline{d} = D + \rho_2$, and $\mathcal{P}_2^\star$ denotes any of the two points $\mathcal{P}_2^{(a)}$ and $\mathcal{P}_2^{(b)}$. Hence, there are *at most* four indistinguishable trajectories. This particular condition allows us to compute the number of indistinguishable trajectories. Moreover, we can introduce a degenerate case for this setting.

Case 4.3.5. *The* $2+1$ *setting is a particular case of the* $1+1+1$ *setting, since the locus in Figure 4.3 is a pair of circles centred on the first anchor. Generic trajectories are* $\mathrm{Ind}(4)$, *while in the degenerate cases when* $\min\{d_2^{(a)}, d_2^{(b)}\} = \|B_2 - B_1\| - \rho_2$ *or* $\max\{d_2^{(a)}, d_2^{(b)}\} = \|B_2 - B_1\| + \rho_2$, *the circles are tangent in a point lying on* $\mathcal{B}_{1,2}$, *and the trajectory is* $\mathrm{Ind}(1)$.

$3+1$ scenario:

With the same *rationale* as in the previous sections, we can reconstruct the distance d_3 between $\mathcal{P}_3$ and B_1. Therefore, $\mathcal{P}_3$ lies on the intersection between the circle centred on B_1 of radius d_3 and the circle centred on B_2 of radius ρ_3, thus yielding two intersections. We can identify the following degenerate case.

Case 4.3.6. *In the* $3{+}1$ *case, generic trajectories are* $\mathrm{Ind}(2)$. *When* $d_3 = D \pm \rho_3$, *the two circles are tangent in a point lying on the line connecting* B_1 *and* B_2.

In this degenerate case, the two intersections, i.e. the two indistinguishable trajectories, collapse on each other, thus achieving Ind(1).

With the definition of these four degenerate cases, keeping in mind that the role of the two anchors can be switched (i.e., $3+1$ is equivalent to $1+3$), and considering that any number N_m of measurements can be at most a **C3** set of measurements, we can now state the following theorem.

Theorem 4.3.7. *Given a trajectory $\mathcal{T}$ with N_m measurement points, the system is unconstructible when two anchors collecting $N_m - 1$ and 1 measurement, respectively, are involved, or when $N_m \leq 3$, unless at least one among the degenerate cases in Case 4.3.3, 4.3.4, 4.3.5 and 4.3.6 occurs.*

We have shown a set of settings where constructibility is never achieved, or it is achieved only for some particular shapes of $\mathcal{T}$ and layouts of the anchors. These setting are summarised in red in Figure 4.5.

4.3.3 Conditions for constructibility

We now consider all the other cases and search for constructibility conditions, keeping in mind that trajectory indistinguishability may arise when pathological trajectories are selected, as stated in Section 4.3.1.

$2+2$ scenario:

For this analysis, we will define a new reference frame, which will simplify the forthcoming discussion. To this aim, we consider Equation (4.6), with $\phi = 0$. This way, we know the position of the first anchor B_1, lying on the origin, and of the two trajectories $\mathcal{T}^{(a)}$ and $\mathcal{T}^{(b)}$, as shown in Figure 4.4. In this particular reference frame, the 4 indistinguishable trajectories arising in the setting $2+1$ correspond to 4 positions of the second anchor B_2. For each pair of indistinguishable trajectories, we want to analyse how a further measurement collected by the second anchor preserves or solves the ambiguity. At first, we notice that ambiguities may arise between two trajectories rotated both about B_1 and about $\mathcal{P}_0$, i.e. $\mathcal{T}^{(a)}$ and $\mathcal{T}^{(b)}$, or between two trajectories only rotated about the anchor B_1, i.e. $\mathcal{T}_1$ and $\mathcal{T}_2$, and thus the analysis will be divided into two parts, one for each pair of trajectories.

Rotation about anchor: Given the two measurement points $\mathcal{P}_2 = [x_2, y_2]^\top$ and $\mathcal{P}_3 = [x_3, y_3]^\top$ about B_2, we want to find the position of the anchor B_2 sat-

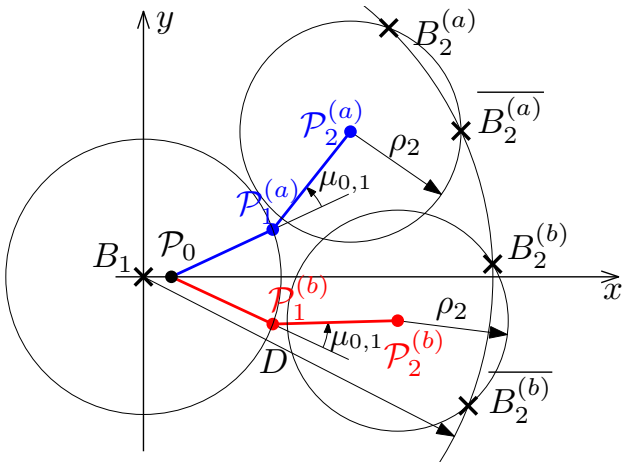

Figure 4.4: New reference frame showing the setting $2+1$. The blue and red lines represent the two trajectories $\mathcal{T}^{(a)}, \mathcal{T}^{(b)}$. Each of them has a circle centred on their last point $\mathcal{P}_2$, hence yielding an overall number of 4 intersections (i.e. possible positions of B_2) with the circle centred on B_1 of radius D.

isfying the following equations:

$$\begin{cases} X_2^2 + Y_2^2 = D^2, \\ (X_2 - x_2)^2 + (Y_2 - y_2)^2 = \rho_2^2, \\ (X_2 - x_3)^2 + (Y_2 - y_3)^2 = \rho_3^2. \end{cases} \tag{4.8}$$

To this end, we take the difference of the last two equations with respect to the first and get to these linear equations in the unknowns X_2, Y_2

$$MB_2 = \begin{bmatrix} x_2 & y_2 \\ x_3 & y_3 \end{bmatrix} \begin{bmatrix} X_2 \\ Y_2 \end{bmatrix} = \frac{1}{2} \begin{bmatrix} D^2 - \rho_2^2 + x_2^2 + y_2^2 \\ D^2 - \rho_3^2 + x_3^2 + y_3^2 \end{bmatrix}. \tag{4.9}$$

To find a unique solution for B_2, we need a nonsingular matrix M, whose determinant is

$$\det M = x_3 y_2 - x_2 y_3. \tag{4.10}$$

Therefore, B_2 has a unique solution, i.e. *there exists no pair of indistinguishable trajectories rotated about the first anchor, if B_1, $\mathcal{P}_2$ and $\mathcal{P}_3$ are not aligned.* Hence, to guarantee Ind(1), $\mathcal{P}_3$ cannot lie on the two lines joining B_1 and $\mathcal{P}_2^{(a)}$, and joining B_1 and $\mathcal{P}_2^{(b)}$, which are available in the reference frame $\langle V \rangle$. From a geometric point of view, we may reformulate the problem as finding the position of B_2 by using three ranging measurements. Indeed, by using trilateration this problem has a unique solution if the three ranging measurement points are non-collinear. This result is perfectly in line with the scenario proposed in Example 4.1 and with the results in Proposition 2.2.1 in Chapter 2.

Rotation about anchor and initial point: Given two points $\mathcal{P}_2^{(a)}$, $\mathcal{P}_3^{(a)}$, we can derive $\mathcal{P}_2^{(b)}$, $\mathcal{P}_3^{(b)}$ as

$$\mathcal{P}_\star^{(b)} = R_\zeta(\mathcal{P}_\star^{(a)} - \mathcal{P}_0) + \mathcal{P}_0,$$

where $\zeta = -2\delta$ and δ defined in (4.5), and the subscript $\star$ is either 2 or 3. With these two pairs, we want to find the positions of two anchors $B_2^{(a)}$, $B_2^{(b)}$ satisfying the set of equations (4.9), for both $\mathcal{T}^{(a)}$ and $\mathcal{T}^{(b)}$. With the same rationale followed previously, we take the differences

$$\begin{aligned} \|\mathcal{P}_2^{(a)} - B_2^{(a)}\|^2 - \|B_2^{(a)}\|^2 &= \|\mathcal{P}_2^{(b)} - B_2^{(b)}\|^2 - \|B_2^{(b)}\|^2 \\ \|\mathcal{P}_3^{(a)} - B_2^{(a)}\|^2 - \|B_2^{(a)}\|^2 &= \|\mathcal{P}_3^{(b)} - B_2^{(b)}\|^2 - \|B_2^{(b)}\|^2 \end{aligned} \tag{4.11}$$

As in the previous case, we get to two linear equations reading as

$$M \begin{bmatrix} X_2^{(a)} \\ Y_2^{(a)} \end{bmatrix} = h,$$

with the same M as in (4.10). In light of this result, given one of the two feasible $B_2^{(b)}$ obtained in the case $2+1$, we find a unique anchor $B_2^{(a)}$ satisfying the differences of the distances, as far as $\mathcal{P}_2^{(a)}$, $\mathcal{P}_3^{(a)}$ and B_1 are not aligned, as before. Since D is the distance from B_1 to B_2 and B_1 is in the origin of the reference frame, we now add the constraint $\|B_2\| = D$, i.e. $\|B_2^{(a)}\| - \|B_2^{(b)}\| = 0$, with $B_2^{(a)}$ obtained as the unique solution of (4.11). Therefore, we have a quadratic equation in the coordinates of $\mathcal{P}_3^{(a)}$ in the form

$$\begin{bmatrix} x_3 & y_3 & 1 \end{bmatrix} Q \begin{bmatrix} x_3 \\ y_3 \\ 1 \end{bmatrix} = 0,$$

where the matrix of the quadratic equation Q, representing a conic section, is

$$Q = \begin{bmatrix} S & b \\ b^\top & c \end{bmatrix},$$

where $S \in \mathbb{R}^{2\times 2}$, $b \in \mathbb{R}^2$ and $c \in \mathbb{R}$, and where its invariants characterise the conic. In particular, the centre of the conic is $O = -S^{-1}b = \mathcal{P}_2^{(a)}$, while $\det Q = 0$, and thus this is a degenerate conic with centre $\mathcal{P}_2^{(a)}$. To identify its shape, we analyse the determinant of the submatrix S, that yields

$$\det S = -\rho_0^2(X_2^{(b)} - \mathcal{X}_2^{(b)})^2(\|\mathcal{P}_2^{(a)}\|^2 - \underline{d}^2)(\overline{d}^2 - \|\mathcal{P}_2^{(a)}\|^2),$$

where $\mathcal{X}_2^{(b)} = X_2^{(b)} \cos\zeta - \rho_0(\cos\zeta - 1) + Y_2^{(b)} \sin\zeta$ is the x coordinate of the point obtained by rotating $B_2^{(b)}$ about $\mathcal{P}_0$ by $-\zeta$. The condition $\underline{d} < \|\mathcal{P}_2\| < \overline{d}$ guarantees that the product of the last two terms is always positive, while the intermediate term is always nonpositive, and it is 0 when the points $\mathcal{P}_0$, $\mathcal{P}_1^{(b)}$ and $B_2^{(b)}$ are collinear. This situation is the mirrored version of the situation analysed above, where the two measurement points collected from B_2 and B_1 were aligned, and thus there exists no points $\mathcal{P}_3^{(a)}$ that can recover Ind(1), as in Example 4.1. In fact, matrix Q is in this case the 0 matrix, i.e. a conic describing the whole $X_w \times Y_w$ motion plane. When this unfortunate situation does not occur, the determinant is negative, hence the conic described by Q is a degenerate hyperbole, i.e. two lines intersecting in $\mathcal{P}_2^{(a)}$ and thus, for each of the two positions $B_2^{(b)}$ arising from the setting $2+1$, we find two critical lines.

In conclusion, *we have two critical directions for $\mathcal{P}_3^{(a)}$ arising from the first situation and four from the second*, and thus there exists 6 lines in $\langle V \rangle$, intersecting in $\mathcal{P}_2^{(a)}$, where $\mathcal{P}_3^{(a)}$ should not lie onto to ensure that the trajectory is Ind(1). The number of critical direction may be geometrically interpreted as follows: in the $2+1$ scenario there are 4 indistinguishable trajectories, and for each of the 6 pairs there is a critical direction that preserves ambiguity among the two.

$2+1+1$ scenario:

With respect to the previous case, we here collect the same number of measurements, but we distribute them among 3 anchors. One can follow the same procedure as before, obtaining more convoluted expressions leading to the same result with a more complex geometrical interpretation. However, as in the previous case, we can conclude that, in the reference frame $\langle V \rangle$ there are at most 6 lines where $\mathcal{P}_3$ should not lie onto to achieve a Ind(1) problem. Indeed, given the (at most) four indistinguishable trajectories arising in the setting $2+1$, we can find the four possible positions of the third anchor in $\langle V \rangle$. We can compute the distances between a given fourth position $\mathcal{P}_{V,3}$ and each of the four "virtual" anchors $B_{V,3}^{(i)}$, $i = 1, \ldots, 4$. Two among these distances coincide, i.e. $\|B_{V,3}^{(i)} - \mathcal{P}_{V,3}\| = \|B_{V,3}^{(j)} - \mathcal{P}_{V,3}\|$, $i \neq j$, if and only if $\mathcal{P}_{V,3}$ lies on the axis of the segment having as vertexes a pair of the "virtual" anchors themselves. If $\mathcal{P}_{V,3}$ lies on one of these 6 critical lines, then the system is Ind(2), while when $\mathcal{P}_{V,3}$ does not lie on any of these lines, $\mathcal{T}$ is Ind(1).

$3 + 2$ scenario:

The analysis carried out in this section is a particular case of the setting $2 + 2$. Indeed, by collecting **C3** measurements from the first anchor, we can discard one of the two indistinguishable trajectories $\mathcal{T}^{(a)}$ and $\mathcal{T}^{(b)}$. Therefore, indistinguishability can be obtained only by rotation about the first anchor, coming up with a set of equations as in (4.8), with the proper modifications on the subscript to account for the additional point sensed by the first anchor. We get to the same conclusion as in (4.10), i.e. that the trajectories are indistinguishable only if B_1, $\mathcal{P}_3$ and $\mathcal{P}_4$ are aligned.

$3 + 1 + 1$ scenario:

With the same *rationale* as in the analysis of the $3 + 2$ setting based on the $2 + 2$ scenario, we can adapt here the analysis of the setting $2 + 1 + 1$. After the first 4 measurements $(3 + 1)$, there exist two indistinguishable trajectories and thus, in the reference frame $\langle V \rangle$, there is a line (obtained with the same procedure presented in the setting $2 + 1 + 1$) where $\mathcal{P}_4$ should not lie to solve this ambiguity.

$1 + 1 + 1 + 1$ scenario:

As discussed in the analysis of the setting $1 + 1 + 1$, after three measurements, there is a finite number $\overline{n} < 8$ of indistinguishable trajectories. As in the previous cases, for each of the (at most) 28 pairs there is a line where $\mathcal{P}_3$ should not lie to achieve a Ind(1) trajectory. Moreover, these lines are known in $\langle V \rangle$, and thus the vehicle can plan its last manoeuvre in order to avoid such lines and reach Ind(1).

With these findings, we can state the following theorem.

Theorem 4.3.8. *Given a trajectory $\mathcal{T}$ and N_m measurement points, the system is constructible when $N_m \geq 4$ and each anchor collects at most $N_m - 2$ measurements, unless the last point of $\mathcal{T}$ lies on one of the indistinguishability line identified in the analysis.*

Using the necessary and sufficient conditions to attain constructibility identified previously, the final taxonomy of Figure 4.5 can be derived, where the area highlighted in red subsumes the results of Theorem 4.3.7, while the part highlighted in green is referred to Theorem 4.3.8.

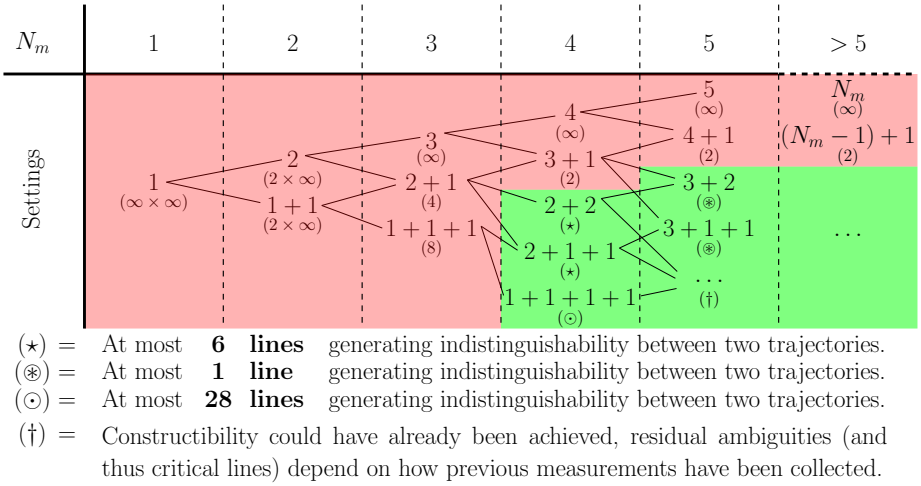

Figure 4.5: Summarising picture subsuming the taxonomy derived in this chapter as a function of the overall number of measurements and of their distribution among the different anchors. The number in brackets denotes the number of indistinguishable trajectories. The red part is referred to Theorem 4.3.7, while the green part is associated with the results obtained in Theorem 4.3.8.

Remark 4.3.9. *Apparently, there is a duality between the conditions for constructibility in Theorem 4.3.7 and 4.3.8. However, from a practical view point, in the latter case, the vehicle can compute numerically in $\langle V \rangle$ the "critical" lines before collecting the last measurement, plan its last manoeuvre to avoid such lines and achieve* $\mathrm{Ind}(1)$. *On the other hand, in the former scenario, the vehicle is not able to plan its trajectory to fall into the degenerate cases 4.3.3, 4.3.4, 4.3.5, 4.3.6, since they are detected once all the measurements are collected.*

Remark 4.3.10. *We now reverse the perspective, by considering the problem of mapping, the dual problem with respect to localisation. In this case, we want to find the position of the anchors $B_i = [X_i; Y_i]^\top$ in the reference frame $\langle V \rangle$, where the trajectory $\mathcal{T}$ of the vehicle is known. Although the two problems are dual, there are remarkable differences in the analysis. Indeed, in the localisation problem, we have used both the shape of the trajectory $\mathcal{T}$ and the layout of the anchors B_i, while here we have no information on the layout of the anchors on the plane. Thus, the overall mapping problem boils down to an independent mapping problem for each anchor, which leads to the classic trilateration problem [Palopoli and Fontanelli, 2020].*

4.4 Discussion

In Part I, we have focused our analysis on the *global constructibility* properties of the system, starting from Chapter 2 where we have shown that extending trilateration techniques to a dynamical system is not trivial.

In the next part, we will focus our attention on *local* properties, i.e. we consider that the vehicle is provided with some *a priori* information on its state, e.g. a sufficiently narrow set that the state of the vehicle belongs to at a given time instant, or a region of the plane (e.g. a room) where the vehicle cannot lie. We will show that some results are inherited from this part, while some others show a counterintuitive behaviour, where local (formally *weak*) constructibility is not achieved while the global property holds.

Part II

Local Constructibility Analysis of a Ground Vehicle

Analysis of Weakly Constructible Trajectories

5

Contents

In Part I we have analysed the problem of *global constructibility*, i.e. the problem of reconstructing the state of a vehicle when no prior information is available. In Part II, starting with this chapter, we analyse the problem from a local perspective by means of the Constructibility Gramian. We will show that the two problems are related, but not trivially and, for example, the natural intuition that any condition sufficient for the global property is sufficient also for *local constructibility* fails. As in Chapter 4, in this chapter we focus on the conditions on the shape of the trajectory and on the history of ranging measurements collected by the vehicle, which make the Constructibility Gramian have full rank. Such conditions can be expressed in terms of the shape of the trajectory, of the layout of the ranging sensors, and of the numbers of measurements collected from each of them.

Contributions: An assumption underlying the design of suitable estimation filters, which have been developed in the technical literature described above, is the *local* (more precisely *weak*) constructibility. Indeed, when the system is not constructible, there exist no estimation algorithm that can reconstruct the pose of the vehicle. On the other hand, *active sensing* planning techniques avoid unconstructibility by design, since, while optimising some chosen matrix metric (a suitable norm of Observability Matrix, Gramians or Fisher Information Matrix), they also make the chosen matrix non–singular [Salaris et al., 2019]. In this chapter, as a particular case of the scenario described in the previous chapter, we analyse the *weak constructibility* properties of a vehicle described by a unicycle kinematic model. We show that a unicycle–like model satisfies the assumptions we leveraged in the previous analyses, and we discuss how similarities and differences from the results in the previous chapter can be geometrically interpreted.

5.1 Problem Description

For the analysis in this chapter, we leverage the unicycle kinematic model, whose state q consists in the (x, y) position of a relevant point of the physical vehicle (usually the barycentre of the vehicle or the centre point of its rear axle) and of its orientation θ with respect to a given reference axis (usually the x–axis of the world reference frame). The state space representation of this system is

$$\dot{q} = \begin{bmatrix} \dot{x} \\ \dot{y} \\ \dot{\theta} \end{bmatrix} = \begin{bmatrix} v\cos\theta \\ v\sin\theta \\ \omega \end{bmatrix}, \tag{5.1}$$

where the control inputs $v(t)$ and $\omega(t)$ represent the forward and angular velocity of the vehicle, respectively. As in the previous chapter, we represent by $P_V(t)$ the Cartesian position of the vehicle a local reference frame $\langle V \rangle$ such that the initial state of the vehicle in $\langle V \rangle$ is $q_V(0) = [0; 0; 0]^\top$.

In the previous chapter, two properties were requested to the dynamic or kinematic model representing the mobile robot. We recall them here and show that a unicycle vehicle satisfies them, since they will be useful to interpret geometrically the results in this chapter.

Property 5.1.1. *Given the position of the vehicle $P_V(t)$, $\forall t \in [t_0, t_f]$, there exists a unique triplet $(\Delta x, \Delta y, \phi)$ such that*

$$P(t) = R_\phi P_V(t) + \begin{bmatrix} \Delta x \\ \Delta y \end{bmatrix}, \quad \forall t \in [t_0, t_f].$$

To show that a unicycle–like vehicle is compliant with this property, we explicitly compute, at a given time t, the positions $P_V(t)$ and $P(t)$ in the local reference frame $\langle V \rangle$ and in the world reference frame $\langle W \rangle$, respectively. By definition the initial state of the vehicle in $\langle V \rangle$ is $[x_V(0); y_V(0); \theta_V(0)]^\top = [0; 0; 0]^\top$, and thus

$$\begin{aligned} x_V(t) &= \int_0^t v(s) \cos\left(\theta_V(s)\right)\, ds, \\ y_V(t) &= \int_0^t v(s) \sin\left(\theta_V(s)\right)\, ds, \\ \theta_V(t) &= \int_0^t \omega(s)\, ds, \end{aligned}$$

while in the world reference frame $\langle W \rangle$, the system starts from the initial condition $q_0 = [x_0; y_0; \theta_0]^\top$. Therefore,

$$\begin{aligned} x(t) &= x_0 + \int_0^t v(s) \cos\left(\theta(s)\right)\, ds, \\ y(t) &= y_0 + \int_0^t v(s) \sin\left(\theta(s)\right)\, ds, \\ \theta(t) &= \theta_0 + \int_0^t \omega(s)\, ds. \end{aligned}$$

Since $\theta(t) = \theta_0 + \theta_V(t)$, the trajectory can be written as

$$\begin{bmatrix} x(t) \\ y(t) \\ \theta(t) \end{bmatrix} = \begin{bmatrix} x_0 \\ y_0 \\ \theta_0 \end{bmatrix} + \begin{bmatrix} \cos\theta_0 & -\sin\theta_0 & 0 \\ \sin\theta_0 & \cos\theta_0 & 0 \\ 0 & 0 & 1 \end{bmatrix} \begin{bmatrix} x_V(t) \\ y_V(t) \\ \theta_V(t) \end{bmatrix},$$

where the position $P(t) = [x(t); y(t)]^\top$ of the vehicle in $\langle W \rangle$, is compliant with Property 5.1.1, with $\Delta x = x_0$, $\Delta y = y_0$, $\phi = \theta_0$.

The second property requested in the previous chapter is the ability of the vehicle to reconstruct its state given the history of its position $P(t)$, proved and reported hereafter as a lemma.

Lemma 5.1.2. *A unicycle vehicle* (5.1) *with the continuous–time position* $P(t)$ *as output is* constructible*, i.e. we can reconstruct its final state* q_f *given the history of inputs and outputs over a given time interval.*

Proof. Proving that this lemma holds true for the unicycle kinematic model is straightforward. Indeed, the output $P(t)$ coincides with the two of position variables $x(t)$ and $y(t)$. At the same time, by the dynamics, we can reconstruct the heading $\theta(t)$ as a function of $\dot{P}(t)$, which is available by assumption. Indeed,

$$\dot{P}(t) = \begin{bmatrix} \dot{x} \\ \dot{y} \end{bmatrix} = \begin{bmatrix} v\cos\theta \\ v\sin\theta \end{bmatrix}, \quad \text{and thus} \quad \theta(t) = \arctan2\left(\frac{\dot{y}}{v}, \frac{\dot{x}}{v}\right).$$

□

The same results can be obtained by proving that the unicycle kinematic model is a *differentially flat system* with the Cartesian position as a *flat output* [Fliess et al., 1995].

In compliance with the previous analyses, we consider here fixed–frame sensors where the vehicle collects intermittent ranging measurements from. The i–th anchor is located at coordinates $B_i = [X_i, Y_i]^\top$, $i = 1, \ldots, p$, and the vehicle collects the measurement $\|B_i - P(t)\|$. Measurements are collected at known sampling instants $t_{k+1} > t_k$. The output z_k is given by the measurements collected by the vehicle, i.e. the output equation reads as

$$z_k = \|P_k - B_{i_k}\|, \tag{5.2}$$

where $P_k = P(t_k)$ is the position of the vehicle at time $t = t_k$, while the index $i_k \in \{1, \ldots, p\}$ defines the anchor that the vehicle measures its distance from. For the sake of clarity, the collected distance will be denoted by $\rho_{k,i}$ when the second index i is not clear from the context. We consider measurements to be intermittent; therefore at time t_k, only one ranging measurement ρ_k is available.

As in the previous chapters, we assume full knowledge of the time instants t_k when the measurements are taken and of the input sequence $u(s)$, $s \in [0, t_k]$, which allows us to reconstruct the sequence of positions $P_V(t_k)$ of the vehicle in $\langle V \rangle$. Therefore, instead of considering the entire paths $P(t)$ and $P_V(t)$, we

focus only on the locations where the ranging measurements are collected:

$$\mathcal{P}_k(\Delta x, \Delta y, \phi) = R_\phi P_V(t_k) + \begin{bmatrix} \Delta x \\ \Delta y \end{bmatrix},$$

for $k = 0, \ldots, N_m - 1$, with N_m being the total number of measurements. Given two points $\mathcal{P}_l$ and $\mathcal{P}_m$, we define by $\mathcal{S}_{l,m}$ the segment given by their convex combination, with length given by $\|\mathcal{S}_{l,m}\|$. We can now restrict our study to an abstract trajectory $\mathcal{T}$ of the vehicle, defined as the union of all the segments connecting two consecutive positions $\mathcal{P}_k$ of the vehicle, thus

$$\mathcal{T} = \bigcup_{k=0}^{N_m-1} \mathcal{S}_{k,k+1}, \tag{5.3}$$

which can be regarded as a rigid body.

Remark 5.1.3. *The abstract trajectory $\mathcal{T}$ does not coincide with the actual trajectory $P(t)$, but contains all the features that are needed in the following discussion: the sequence of measurements, the distance and the total change in the orientation between any two measurements. Indeed, θ_k can be reconstructed by solving*

$$\begin{bmatrix} \int_{t_k}^{t_{k+1}} v(s)\cos(\theta_V(s))\,ds & -\int_{t_k}^{t_{k+1}} v(s)\sin(\theta_V(s))\,ds \\ \int_{t_k}^{t_{k+1}} v(s)\sin(\theta_V(s))\,ds & \int_{t_k}^{t_{k+1}} v(s)\cos(\theta_V(s))\,ds \end{bmatrix} \begin{bmatrix} \cos\theta_k \\ \sin\theta_k \end{bmatrix} = \mathcal{P}_{k+1} - \mathcal{P}_k,$$

where the matrix is known, and it is singular only when $v(t) = 0$, $\forall\, t \in [t_k, t_{k+1})$.

In light of the definition of $\mathcal{T}$, we want to find the conditions on the position of the anchors in $\langle W \rangle$ and on the trajectory $\mathcal{T}$ such that it is possible to find a roto-translation such that the points $\mathcal{P}_k$ are compliant with the measurements collected from the anchors. To this aim, we need to introduce the concepts of *constructibility* and *backward indistinguishability* of the states of a nonlinear system. For the sake of generality, in the following definitions, adapted from [Bayat et al., 2015], we consider a plant with a continuous-time dynamics and a discrete-time output equation, i.e.

$$\begin{aligned} \dot{q}(t) &= f(q(t), u(t)), \\ z_k &= h(q(t_k)). \end{aligned} \tag{5.4}$$

We consider the dynamical system to evolve between an initial time instant t_0 (i.e. $k = 0$) and a final time t_f, with $k = k_f$. Given the hybrid nature of (5.4), we will use both k and t to denote the time, with the implicit assumption that

by the time instant k we refer to time t_k.

We deal with the notion of *constructibility*, defined as the ability to reconstruct the state q_f of the system at the final time instant t_f. Intuitively, constructibility amounts to reconstructing the current state q_k given the past history of inputs and outputs. By Lemma 5.1.2, the problem of estimating the final state is equivalent to estimating the initial state q_0, which is the well-known concept of *observability*. However, the performance of an estimation filter, i.e. the uncertainty related to the state estimate based on the previous history of motions and measurements, is not directly associated with the concept of observability, but rather to the notion of *constructibility* (for further details, the reader is referred to [Salaris et al., 2019]). To analyse formally the concept of constructibility, from a local perspective, we introduce the definition of *backward indistinguishability*, instead of the notion of *indistinguishability* considered for more common observability analyses [Bayat et al., 2015].

Definition 5.1.4. *Given the dynamical system* (5.4)*, a time interval* $T = [t_0, t_f]$*, and an admissible control input function* $u^\star(t)$, $t \in T$*, two final states* q_f *and* $\bar{q}_f$ *are said* $\mathbf{u}^\star$*–**backward indistinguishable** on* T*, if for the input* $u^\star(t)$, $t \in T$*, the output sequences* z_k *and* $\bar{z}_k$, $k = 0, \ldots, k_f$ *of the trajectories satisfying the final conditions* q_f*,* $\bar{q}_f$*, are identical. Moreover, we define* $\mathcal{I}^{u^\star}_{(b)}(q_f)$ *as the set of all the final conditions that are* $u^\star$*–backward indistinguishable from* q_f *on* T*.*

Since we assume full knowledge of the control input, the shape of the trajectory $\mathcal{T}$ is known in its turn. Hence, we will focus on the concept of u-backward indistinguishability. With a slight abuse of definition, we will refer to *indistinguishable* trajectories as trajectories generated by a known control input and by two *u–backward indistinguishable* final conditions.

Definition 5.1.5. *Given the interval* $T = [t_0, t_f]$*, and the control input* $u^\star(t)$, $t \in T$*, the system* (4.4) *is said to be* $\mathbf{u}^\star$*–**weakly constructible at** $\mathbf{q_f}$ *if* q_f *is an isolated point of* $\mathcal{I}^{u^\star}_{(b)}(q_f)$*. Moreover, a system is said to be* $\mathbf{u}^\star$*–**(weakly) constructible** if it is* $u^\star$*–(weakly) constructible at* any q_f*.*

In the local analysis, associated with the concept of *weak constructibility*, we will refer to a *weakly constructible trajectory* as a trajectory, defined by a control sequence $u^\star$, such that the system is *$u^\star$-weakly constructible*. By Definition 5.1.5, the set of *globally constructible* trajectories (analysed in the Chapter 4) is a subset of the *weakly constructible* trajectories, since a unique point in a set is always isolated.

In light of Lemma 5.1.2, we can now state a new relevant result in the following lemma.

Lemma 5.1.6. *Let* $(\overline{\Delta x}, \overline{\Delta y}, \overline{\phi})$ *be such that*

$$\|\mathcal{P}_k(\overline{\Delta x}, \overline{\Delta y}, \overline{\phi}) - B_i\| = \rho_{k,i},$$

for each i *such that the measurement is available at time* k*, and for* $k = 0, \ldots, k_f$*. Then, the system is* $u^\star$*-weakly constructible if*

$$\|\mathcal{P}_k(\Delta x, \Delta y, \phi) - B_i\| \neq \rho_{k,i}, \qquad \forall\, \Delta x \in \mathcal{N}\left(\overline{\Delta x}\right), \Delta y \in \mathcal{N}\left(\overline{\Delta y}\right), \phi \in \mathcal{N}\left(\overline{\phi}\right),$$

where $\mathcal{N}(x)$*,* $x \in \mathbb{R}$ *denotes an arbitrary small subset of* $\mathbb{R}$ *including* x*.*

Proof. The proof directly follows from Lemma 5.1.2. □

Problem Statement

Given the unicycle kinematic model (5.1), and the sequence of positions $P_V(t_k)$, $k = 0, \ldots, k_f$, in the vehicle reference frame, we want to find the conditions on $\mathcal{T}$, on the layout of the sensors $B_i = [X_i, Y_i]^\top$, $i = 1, \ldots, p$, in $\langle W \rangle$, and on the distribution of the measurements among the sensors, such that the system is u-weakly constructible at the final condition q_f.

5.2 Local constructibility

To formally define the relationship between *weak constructibility* properties and rank of the Constructibility Gramian (CG), we report here the following theorem, adapted from [Powel and Morgansen, 2015].

Theorem 5.2.1 ([Powel and Morgansen, 2015])**.** *Given system* (5.4)*, if there exists a sequence of control inputs* $u(t)$*,* $t \in [t_0, t_f]$*, i.e. a shape of* $\mathcal{T}$*, such that* $CG(t_0, t_f)$ *is full rank, then system* (5.4) *is* weakly constructible*.*

5.2.1 Constructibility Gramian

We build the Constructibility Gramian for the unicycle kinematic model (5.1) subject to intermittent ranging measurements (5.2). The CG is an $n \times n$ matrix, where n is the size of the state of the system, that may be used as a tool to check for nonlinear constructibility, i.e. it describes how difficult it is to reconstruct the final state of the system given the controls and the measurements over a time window $[t_0, t_f]$. In particular, the reciprocal of its smallest singular value (or equivalently of its smallest eigenvalue, since the CG is symmetric and

positive semidefinite), quantifies how measurement noise affects the estimate of the final state, and if it is equal to 0, i.e. if the CG is singular, then the system is *weakly unconstructible* (see [Krener and Ide, 2009]). The CG is defined either for continuous- or discrete-time systems, and thus we have to extend its definition to a generic system with continuous-time dynamics and intermittent (discrete-time) measurement output (4.4). For a continuous-time system

$$\dot{q}(t) = f\big(q(t), u(t)\big), \qquad z(t) = h\big(q(t)\big),$$

the Constructibility Gramian $G_C(t_0, t_f)$ is defined as

$$G_C(t_0, t_f) = \int_{t_0}^{t_f} \Phi^\top(\tau, t_f) H^\top(\tau) W_C(\tau) H(\tau) \Phi(\tau, t_f)\, d\tau, \tag{5.5}$$

where $H(t) = \left(\frac{\partial h}{\partial q}\right)\Big|_{q=q(t)}$ is the Jacobian of the measurement evaluated at the current time t, and $W_C(t)$ is a weighing matrix, which accounts for heterogeneous measurement units, different uncertainties among sensors, or for nonlinear effects, such as bounded sensing range. The *sensitivity matrix* $\Phi(t, t_f) = \frac{\partial q(t)}{\partial q_f}$ represents how small perturbations in the final condition of the system affect the state at the current time t, and is the unique solution to the final value problem:

$$\dot{\Phi}(t, t_f) = F(t)\Phi(t, t_f), \qquad \Phi(t_f, t_f) = \mathbf{I}_n,$$

where $F(t) = \left(\frac{\partial f}{\partial q}\right)\Big|_{q=q(t)}$ is the linearised dynamics of the system and $\mathbf{I}_n$ is the $n \times n$ identity matrix. To cope with the discrete-time output z_k in (4.4), we design the weighing matrix W_C such that

$$W_C(t_k) = \begin{cases} \delta_D \operatorname{diag}(\underline{e}_i) & \text{if } B_i \text{ is measured at } t_k, \\ \mathbf{0} & \text{otherwise.} \end{cases}$$

where $\mathbf{0}$ denotes the null matrix, the $\operatorname{diag}(w)$ operator indicates a diagonal matrix having the entries of the vector w as diagonal entries, $\underline{e}_i$ is the unitary vector aligned with the i-th axis, thus assuming that the sensors have homogeneous uncertainty, and δ_D is the Dirac delta. This way, with the same idea as in the previous section, we can disregard the dynamics of the system and the trajectory followed by the vehicle and focus on a finite number of points $\mathcal{P}_k$ where the measurements are collected. However, the definition of the CG explicitly contains the final state q_f and, by computations carried out hereafter, it depends on the final position $\mathcal{P}_f = [x_f, y_f]^\top$, reached by the vehicle at time $t = t_f$. Therefore, the CG in (5.5) may be rewritten in the following simplified

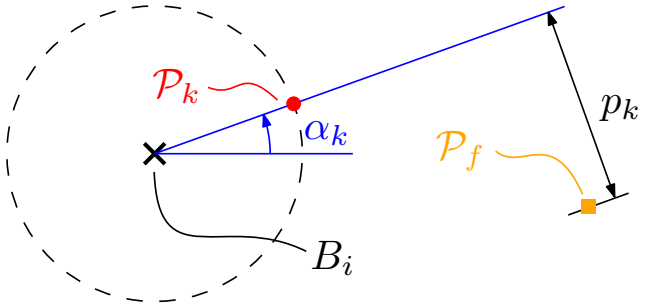

Figure 5.1: The vehicle is located in the point $\mathcal{P}_k$, and it is sensed by the anchor B_i. The quantities affecting the term g_k of the CG only depend on the angle α_k of the measurement and not on the collected distance ρ_k.

expression

$$G_C(t_0, t_f) = \sum_{k=0}^{N_m-1} g(t_k, t_f),$$

where N_m is the overall number of measurements, and the contribution $g(t_k, t_f)$ of the k-th measurement, denoted as g_k in the following, is computed with its definition in (5.5)

$$g_k = \gamma_k \gamma_k^\top, \qquad \gamma_k = [\cos\alpha_k, \sin\alpha_k, p_k]^\top, \tag{5.6}$$

with $\alpha_k = \arctan2(y_k - Y_i, x_k - X_i)$, while p_k is the distance of the final point from the line passing through the measured anchor B_i and having slope α_k, i.e.

$$p_k = \frac{(x_f - x_k)(Y_i - y_k) - (y_f - y_k)(X_i - x_k)}{\sqrt{(x_k - X_i)^2 + (y_k - Y_i)^2}}.$$

Notice that p_k is not dependent on the collected measurement, i.e. the distance ρ_k. Figure 5.1 shows the relevant parameters defining g_k. By construction, g_k is an $n \times n$ matrix with rank 1, whose column space is γ_k. We will leverage considerations on the rank of sum of matrices, relying on alignment among null and column spaces of the contributions g_k. As in Chapter 4, we analyse the settings with increasing number of measurement and anchors.

5.2.2 Single anchor

With a single anchor collecting measurements, the analysis of the CG trivially leads to the same conclusions drawn in Theorem 4.2.1 in the previous chapter, i.e. the trajectory can rotate about the anchor without modifying the sensor readings.

One measurement

When a single measurement is collected, in $\mathcal{P}_0 = [x_0, y_0]^\top$, the Constructibility Gramian is simply computed as $G = \gamma_0 \gamma_0^\top$, where γ_0 is defined in (5.6) and thus, by construction, the CG has rank 1. Its null space, i.e. the unconstructible subspace, is a two-dimensional vector subspace whose basis contains the columns of the matrix

$$\ker(G) = \begin{bmatrix} -(y_f - Y_1) & -(y_f - y_0) \\ x_f - X_1 & x_f - x_0 \\ 1 & 1 \end{bmatrix}.$$

The two vectors defining the unconstructible subspace are tangent to the circle centred on B_1 and passing through P_f, and to the circle centred on $\mathcal{P}_0$ and passing through P_f, respectively. This result is compliant with Theorem 4.2.1, hence highlighting the same constructibility properties.

Two measurements

The second measurement collected by the anchor generates an overall Constructibility Gramian $G = \gamma_0 \gamma_0^\top + \gamma_1 \gamma_1^\top$, having at most rank 2, since it is the sum of two rank 1 matrices. Since the column space of g_0 is γ_0 by construction, we can analytically derive the conditions on $\mathcal{P}_1$ such that the Gramian has still rank 1, by solving $\gamma_1 = \ell \gamma_0$, with $\ell \in \mathbb{R}$, yielding

$$\mathcal{P}_1 = \ell \mathcal{P}_0 + (1 - \ell) B_1,$$

i.e. $\mathcal{P}_0$, $\mathcal{P}_1$ and B_1 are collinear, occurring whenever the vehicle is moving on the diameter of the circle centred on the anchor. From an analytical viewpoint, this result is not surprising, since $\mathcal{P}_0$ and $\mathcal{P}_1$ share the same angle α, and thus $\gamma_0 = \gamma_1$. This result may be interpreted by keeping in mind that we are dealing with local properties, i.e. we are regarding rotations as (small) translations along the tangent of the circle centred on the rotation pole. In this particular scenario, the rotation about B_1 and about $\mathcal{P}_0$ share the same tangent, orthogonal to $\mathcal{S}_{0,1}$, and thus, only in this setting, also a rotation about $\mathcal{P}_0$ is allowed. The two situations with rank 2 and rank 1 are represented in Figure 5.2.

Remark 5.2.2. *This result has a strong connection with the scenario described in Remark 4.2.2, where indistinguishability was avoided, while preventing weak constructibility. In this situation, the angle δ defined in* (4.5) *is equal to* 0 *and the two points $\mathcal{P}_1^{(a)}$ and $\mathcal{P}_1^{(b)}$ collapse on each other.*

Any further measurement collected by the first anchor, beyond the second,

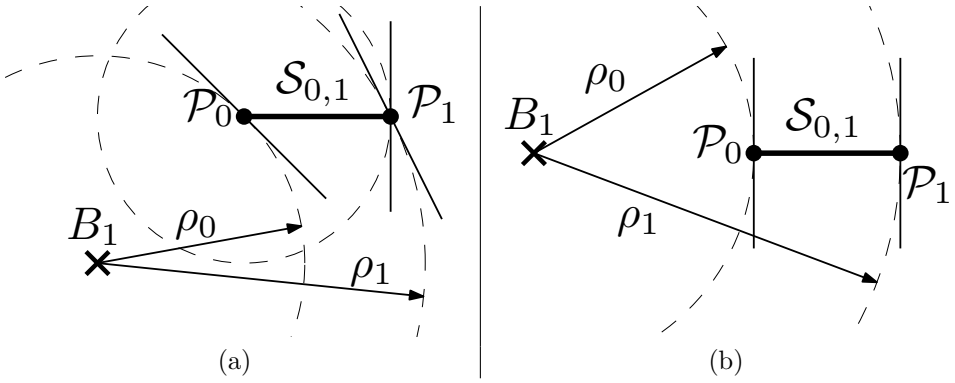

Figure 5.2: A pair of measurements collected by anchor B_1. (a) The three points are not aligned, the rank of the CG is 2 and the two tangents of the circles passing through $\mathcal{P}_1$ are not aligned. (b) The particular situation where B_1, $\mathcal{P}_0$ and $\mathcal{P}_1$ are aligned occurs, the two circles passing through $\mathcal{P}_1$ share the same tangent, hence making the CG rank deficient.

is not informative from a local point of view (provided that the two measurement points are not collinear with the anchor itself). Indeed, the vector $[-(y_f - Y_1); x_f - X_1; 1]^\top$, associated with the rotation of the trajectory about the anchor, does not depend on the sensed measurement point. Hence, a single anchor always generates a singular Gramian, independently on the number of measurements collected.

5.2.3 Two anchors

We now consider a higher number of anchors and an increasing number of measurements distributed among them. Since the maximum number of informative measurements collected by an anchor is 2, we will analyse the settings $1 + 1$, $2 + 1$ and $2 + 2$ hereafter.

$1 + 1$

Since we are summing two rank-1 matrices, we can already state upfront that the CG will be singular. However, with the same rationale of the previous case, we look for the condition on $\mathcal{P}_1$ such that the Gramian has rank 1, i.e. when $\gamma_1 = \ell\gamma_0$, thus getting from the first two equations

$$\mathcal{P}_1 = \ell(\mathcal{P}_0 - B_1) + B_2. \tag{5.7}$$

By plugging this definition of $\mathcal{P}_1$ into the third equation, which reads as $p_1 = \ell p_0$, we get a linear equation in y_0, yielding

$$y_0 = \frac{Y_1 - Y_2}{X_1 - X_2} x_0 + \frac{X_1 Y_2 - X_2 Y_1}{X_1 - X_2},$$

i.e. $\mathcal{P}_0$, B_1 and B_2 collinear. By plugging this result in (5.7), we get that also $\mathcal{P}_1$ lies on the same line. Thus, as soon as the four points are not collinear, the rank of the Gramian is 2.

Remark 5.2.3. *This condition has already been discussed in the degenerate Case 4.3.3, where the circles passing through $\mathcal{P}_1$ and centred on $\mathcal{P}_0$ and B_2, respectively, share the same tangent. In this situation, two indistinguishable trajectories coincide, thus achieving* Ind(1) *and preventing weak constructibility.*

$2 + 1$

Without loss of generality, let us consider the anchor B_1 collecting two measurements in $\mathcal{P}_0$ and $\mathcal{P}_1$, while the second anchor B_2 collects its only measurement in $\mathcal{P}_2$. By the previous analyses, we know that

$$\ker(\gamma_0 \gamma_0^\top + \gamma_1 \gamma_1^\top) = \begin{bmatrix} -(y_f - Y_1) \\ x_f - X_1 \\ 1 \end{bmatrix},$$

while the column space of $\gamma_2^\top \gamma_2$ is γ_2 itself. Whenever these two vectors are orthogonal, i.e. their inner product $\langle \ker(\gamma_0 \gamma_0^\top + \gamma_1 \gamma_1^\top), \gamma_2 \rangle$ is 0, the CG has rank 2. This condition holds true when

$$X_1 Y_2 - X_2 Y_1 - X_1 y_2 + Y_1 x_2 + X_2 y_2 - Y_2 x_2 = 0,$$

i.e. when B_1, B_2 and $\mathcal{P}_2$ are aligned. To give a geometrical interpretation, we need to refer to the results obtained in the case $2 + 1$ in Section 4.3 (see Figure 4.4, reported here as Figure 5.3). From a local perspective we have some knowledge on the initial state of the system, i.e. we can a priori distinguish whether the vehicle is travelling along the trajectory $\mathcal{T}^{(a)}$ or $\mathcal{T}^{(b)}$ in Figure 5.3, and thus we can compute the distance of $\mathcal{P}_2$ from the anchor B_1. Therefore, we know that $\mathcal{P}_2$ lies on the intersection between two circles centred in B_1 and B_2 respectively. Whenever $\mathcal{P}_2$ lies on the line connecting the two anchors, these two circles intersect in a single point, and therefore they share the same tangent direction, with the same conclusions as in the $1 + 1$ setting, described in Figure 5.2. Notice that, in this case, we do not have a perfect duality with

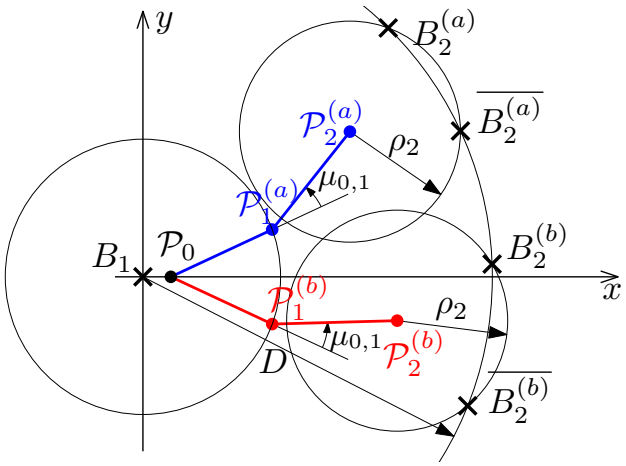

Figure 5.3: Setting $2+1$. The blue and red lines represent two trajectories $\mathcal{T}^{(a)}$, $\mathcal{T}^{(b)}$. If $\mathcal{T}^{(a)}$ is selected based on *a priori* information, the CG is singular when the circle centred in $P_2^{(a)}$ is tangent to the circle centred in B_1.

the degenerated case 4.3.5, since we can discard a priori one of the two circles in Figure 5.3.

$2+2$

We consider two pairs of measurement points being not collinear with the anchor collecting their distance. In this scenario, the CG is singular as long as the 1-dimensional null spaces of the Gramians G_1, G_2, associated with each anchor, are aligned. The condition $\ker(G_2) = \ell \ker(G_1)$ reads

$$-y_f + Y_2 = -\ell y_f + \ell Y_1, \qquad x_f - X_2 = \ell x_f - \ell X_1, \qquad 1 = \ell,$$

hence yielding $B_1 = B_2$, which is impossible by assumption of distinct anchors. Therefore, when two anchors collect a pair of measurements each, the system is weakly constructible as far as the pair of measurement points and the anchor collecting their distances are not collinear.

5.2.4 Three anchors

With three anchors, we only consider the scenario $1+1+1$, which is expected to yield results similar to the case $2+1$. We build the column spaces γ_k, $k = 0, 1, 2$, of the three contributions to the CG. The overall Gramian is full rank as soon as the three column spaces are linearly independent, and this conditions may be checked by computing the determinant of $W = [\gamma_0, \gamma_1, \gamma_2]$,

yielding $\det W = ax_2 + by_2 + c$, where a, b, c are three parameters depending on the coordinates of the three anchors B_1, B_2, B_3, and of the two measurement points $\mathcal{P}_0$ and $\mathcal{P}_1$. Hence, $\det W = 0$ describes a line on the $X_w \times Y_w$ plane, where the coefficients are such that this line passes through the anchor B_3 itself. Therefore, the Gramian is singular as soon as $\mathcal{P}_2$ lies on a line, with known analytical form, passing through B_3. From a geometric point of view, this line has a similar interpretation to the one obtained in the scenario $2 + 1$. Indeed, by combining the rotation of $\mathcal{P}_1$ about B_1 and of $\mathcal{P}_2$ about B_2 such that $\mathcal{S}_{1,2}$ maintains the same length, the (tangent to the) resulting motion of the third point $\mathcal{P}_3$ is tangent to the circle centred on B_3 and passing through $\mathcal{P}_3$ itself. From a global perspective, in this situation two intersections between two 1D geometrical varieties coincide (see Remarks 4.2.2 and 5.2.2), but there are guarantees on the uniqueness of these intersections.

Theorem 5.2.4. *Given at least three measurements, distributed among at least* 2 *anchors, the trajectory* $\mathcal{T}$ *is weakly constructible, unless the last point of* $\mathcal{T}$ *lies on one of the critical lines identified in the analysis.*

6 Measuring Constructibility for a Unicycle Vehicle

Contents

In Chapter 5 we have shown a binary classification of trajectories based on the rank of the Constructibility Gramian. However, when the system is *weakly constructible*, finding the current state requires the inversion of the Gramian. Common problems arise in this setting when the matrix to be inverted is "close" to singular, which can be measured by its smallest singular value. Being the Constructibility Gramian a symmetric and positive (semi)definite matrix, an equivalent metric is represented by its smallest eigenvalue. Motivated by this consideration, unlike the previous chapter, in this chapter we quantify *local* Constructibility and give some geometrical insights on the results. We propose a *local* Constructibility analysis for a nonholonomic vehicle moving across an environment equipped with two ranging sensors. The vehicle travels along a straight line parallel to the line joining the two anchors. By the analysis in the previous chapters, the system is *globally unconstructible*, while its *local* Constructibility can be quantified through the smallest eigenvalue of the Constructibility Gramian (CG). The main contribution of this chapter is to show how this metric changes according to the geometric parameters of the linear trajectory with respect to the position of the anchors and their sensing range.

Contributions: We consider a mobile robot travelling across an environment instrumented with a sparse infrastructure of range sensors with non-overlapping ranges. Therefore, the robot can take only one measurement at a time. When the robot moves along a straight line, weak constructibility is achieved, with a level of performance that can be tied to the minimum eigenvalue of the Constructibility Gramian (CG). In this chapter, we also show the configuration of the anchors and the linear manoeuvres that optimise this metric.

6.1 Problem Description

We consider discrete-time systems in the state space

$$\begin{aligned} q_{k+1} &= f(q_k, u_k), \\ z_k &= h(q_k), \end{aligned} \tag{6.1}$$

where $q \in \mathbb{R}^n$ is the state, $u \in \mathbb{R}^m$ represents the control inputs and $z \in \mathbb{R}^p$ is the output of the system, i.e. the sensor readings. Specifically, we will focus the kinematic model of a unicycle-like vehicle, given in continuous time by:

$$\begin{bmatrix} \dot{x}(t) \\ \dot{y}(t) \\ \dot{\theta}(t) \end{bmatrix} = \begin{bmatrix} v(t)\cos\theta(t) \\ v(t)\sin\theta(t) \\ \omega(t) \end{bmatrix}, \tag{6.2}$$

where $x(t), y(t)$ represent the Cartesian coordinates of the vehicle, while $\theta(t)$ denotes its heading with respect to a reference axis. As in Chapter 5, we make the simplifying assumptions that the control inputs $v(t)$ and $\omega(t)$ be constant over every time interval of fixed duration T_s, as if the system were controlled by a digital system with a finite sampling frequency $1/T_s$, i.e. $v(t) = v_k$, $\forall t \in [kT_s, (k+1)T_s)$. By exploiting this simplification, the kinematic model (6.2) can be exactly integrated over each time interval, yielding the following discrete-time dynamics

$$\begin{bmatrix} x_{k+1} \\ y_{k+1} \\ \theta_{k+1} \end{bmatrix} = \begin{bmatrix} x_k + A_k C_k \\ y_k + A_k S_k \\ \theta_k + \omega_k T_s \end{bmatrix} \tag{6.3}$$

with

$$A_k = 2\frac{v_k}{\omega_k} \sin\left(\frac{T_s}{2}\omega_k\right) \text{ and } \lim_{\omega_k \to 0} A_k = v_k T_s,$$
$$C_k = \cos\left(\theta_k + \frac{T_s}{2}\omega_k\right), \quad S_k = \sin\left(\theta_k + \frac{T_s}{2}\omega_k\right),$$

where, in the adopted notation, the subscript k denotes the time $t = kT_s$ for the continuous-time dynamics (see Chapter 3). The measurement system consists of a set of ranging sensors (henceforth called anchors) yielding their distance from the vehicle, so as the measurement output z_k is defined as

$$z_k = \begin{bmatrix} \rho_1(x_k, y_k) \\ \rho_2(x_k, y_k) \\ \cdots \end{bmatrix} = \begin{bmatrix} \sqrt{(X_1 - x_k)^2 + (Y_1 - y_k)^2} \\ \sqrt{(X_2 - x_k)^2 + (Y_2 - y_k)^2} \\ \cdots \end{bmatrix}, \tag{6.4}$$

where ρ_1 and ρ_2 are the measurements collected from the first two anchors B_1 and B_2. We consider the case in which anchors have a bounded range, i.e. a measurement is collected by anchor i only if its distance from the vehicle is smaller than its sensing range $\rho_i^{\max}$.

The *constructibility* properties of a nonlinear system, unlike for linear systems, depend not only on the structure of the system itself, i.e. on the dynamical model and on the sensors, but also on the trajectory followed by the system itself. Trivially, in our scenario, the system cannot be constructible when the vehicle never enters the sensing ranges of the sensors. For the sake of completeness, we report here an intuitive definition of Constructibility, which has been formally defined in the previous chapter.

Definition 6.1.1 (Constructibility)**.** *Given system* (6.1)*, constructibility is defined as the ability to reconstruct the state q_f of the system at time $k = k_f$, given the outputs $z_k, k = k_0, \ldots, k_f$ and the control inputs $u_k, k = k_0, \ldots, k_f - 1$. In-*

tuitively, constructibility consists in reconstructing the current state q_k given the past history of inputs and outputs.

Given the dynamical system (6.3)-(6.4), this chapter aims at investigating how different geometric parameters of the trajectory followed by the vehicle, such as the position of the anchors, the distance between anchors and vehicle when the measurements occur and the final position reached by the vehicle, affect the constructibility of its trajectory. Specifically, we focus on the effect of these geometric parameters of the trajectory on the smallest eigenvalue of the Constructibility Gramian, defined in the next section.

6.2 Local Constructibility Analysis

When global observability cannot be ensured (e.g., for linear trajectories), we can maximise the local constructibility of some given trajectories given their geometric parameters. To this aim, we introduce the *Constructibility Gramian*. With respect to the analysis in Chapter 5, we derive here the expression of the Constructibility Gramian by considering the discrete–time version (6.3) of the unicycle dynamics. With respect to the previous case, since the same assumption on the intermittence of the measurements is considered, a different procedure will lead to the same output, i.e. to the same Constructibility Gramian.

6.2.1 Constructibility Gramian

The Constructibility Gramian (CG) $G_C(k_0, k_f)$ for the nonlinear system (6.1) is defined as

$$G_C(k_0, k_f) = \sum_{\kappa=k_0}^{k_f-1} \Phi^\top(\kappa, k_f) H_\kappa^\top W_\kappa H_\kappa \Phi(\kappa, k_f), \tag{6.5}$$

where $H_k = \left(\frac{\partial h(q)}{\partial q}\right)\Big|_{q=q_k}$ is the Jacobian of the measurement output evaluated at the current time step and W_k is a diagonal weighing matrix accounting for heterogeneous units of measurement, measurement uncertainty and finite sensing range. To model the finite sensing range of the anchors, we set the i-th diagonal entry of W_k to 0 whenever the vehicle is outside the sensing range (i.e. no measure is retrieved by the i-th anchor), while we set it to 1, without loss of generality, when the vehicle is within the sensing range. The matrix $\Phi(k, k_f) = \frac{\partial q_k}{\partial q_f}$ is called *sensitivity matrix* and is the solution to the following

final value problem

$$\begin{aligned}\Phi(k+1,k_f) &= F_k\,\Phi(k,k_f),\\ \Phi(k_f,k_f) &= \mathbf{I}_n,\end{aligned}$$

where $\mathbf{I}_n$ is the $n \times n$ identity matrix and $F_k = \left(\frac{\partial f(q,u)}{\partial q}\right)\Big|_{q=q_k}$ represents the linearised dynamics of the system. Notice that the CG embeds the linearised dynamics of the nonlinear system and the linearised version of the nonlinear output equation, and thus results achieved with it have local validity.

For the discrete-time unicycle system (6.3), the sensitivity matrix $\Phi(k,k_f)$ is available in closed form, and thus we can write explicitly the contributions $g_i(k,k_f)$ given by each measure to the CG, which can be expressed as

$$G_C(k_0,k_f) = \sum_{i=1}^{N_m} g_i(k,k_f),$$

where N_m is the total number of retrieved measurements. Let us consider the anchor B_1 retrieving the i-th measurement, associated with the i-th row $H_{[i]}(k)$ of the sensitivity matrix H_k:

$$g_i(k,k_f) = \Phi^\top(k,k_f)H_{[i]}^\top(k)H_{[i]}(k)\Phi(k,k_f), \tag{6.6}$$

and thus

$$g_i^{(1)}(k,k_f) = \gamma\gamma^\top, \quad \gamma = \begin{bmatrix}\cos\alpha_i^{(1)} & \sin\alpha_i^{(1)} & p_i^{(1)}\end{bmatrix}^\top, \tag{6.7}$$

where the superscript (1) refers to the anchor B_1, $\alpha_i^{(1)} = \operatorname{arctan2}\left(y_i - Y_1, x_i - X_1\right)$ and $p_i^{(1)}$ is the distance (with sign) of the final position $[x_f, y_f]^\top$ from the line centred on anchor B_1 with slope $\alpha_i^{(1)}$, computed as

$$p_i^{(1)} = \frac{(x_f - x_i)(Y_1 - y_i) - (y_f - y_i)(X_1 - x_i)}{\sqrt{(x_i - X_1)^2 + (y_i - Y_1)^2}},$$

which is only dependent on the angle $\alpha_i^{(1)}$ and on $[x_f, y_f]^\top$, not on the distance from the anchor, as Figure 6.1 shows.

Remark 6.2.1. *The Constructibility Gramian obtained in the previous Chapter* (5.6) *and its expression in* (6.7) *are equal. Indeed, the two systems have the same dynamics (where one is the discretisation of the other), and the same sensor model, relying on the assumption of intermittent measurements.*

As pointed out in [Salaris et al., 2019, §2], the CG is associated with the inverse of the optimal covariance matrix P, hence maximising some norm of the CG allows the robot to travel on the trajectory resulting in the minimum estimation uncertainty on the final state. Moreover, the CG is not dependent

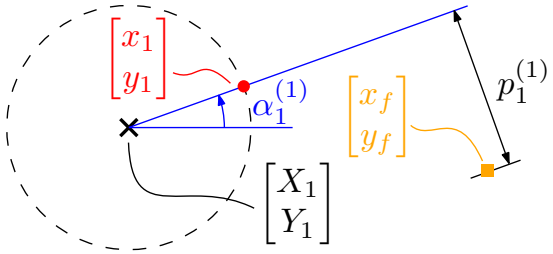

Figure 6.1: Geometrical interpretation of the parameters affecting $g_i^{(1)}(k, k_f)$. The superscript (1) indicates that the measure is collected by anchor B_1, the angle α_1 only depends on the measurement, i.e. the relative position of the anchor and of the measured point, while p_1 depends both on the measurement and on the position of the final position $[x_f, y_f]^\top$.

on the observer that is employed to estimate the state of the system and thus the results obtaining by maximising its norm have general validity.

With the same interpretation as the *Observability Gramian*, which has been much more analysed than the CG, we employ some norm of the CG as a Constructibility metric (see [Krener and Ide, 2009]). Possible choices of norms of the CG (which is symmetric and positive definite by construction) may be found among the so-called *optimality criteria* (see [Gichuki et al., 2020, §4] and references therein). In our analysis, we consider the most critical direction (in the state space) for constructibility, which is captured by the **E**-optimality criterion, i.e., the smallest eigenvalue, whose eigenvector is aligned with the least constructible direction in the state space.

6.2.2 Trace-based lower bound

The smallest eigenvalue of a square matrix is generally not available for a high-dimensional state or for multiagent systems, where the size of the CG grows rapidly. Therefore, we detail hereafter a trace-based lower bound that will simplify the analysis of the constructibility metric and will yield closed form solutions for some simple scenarios.

Theorem 6.2.2 (Lower bound)**.** *Let $M \in \mathbb{R}^{n\times n}$ be a symmetric and positive definite matrix,* $\mathrm{Tr}(M)$ *its trace and* $\lambda_{\min}(M)$ *its smallest eigenvalue. Then the following holds*

$$\lambda_{\min}(M) \geq T, \quad \textit{with} \quad T = \frac{1}{\mathrm{Tr}(M^{-1})}.$$

The proof is based on the definition of the first order "generalised Newton shift" ([Aishima et al., 2010], [Yamamoto, 2017]) and it is skipped for brevity.

Corollary 6.2.3. *By using the definition of $g_i^{(1)}(k, k_f)$ in* (6.7)*, we come up*

with the following expression for T

$$T = \frac{\sum\limits_{(k_1,k_2,k_3)\in\mathcal{K}} \left(p_{k_1}S_{k_2k_3} + p_{k_2}S_{k_3k_1} + p_{k_3}S_{k_1k_2}\right)^2}{\sum\limits_{i=1}^{N}\sum\limits_{j=i+1}^{N} S_{ij}^2 + (N-1)\sum\limits_{i=1}^{N} p_i^2 - 2\left(\sum\limits_{i=1}^{N}\sum\limits_{j=i+1}^{N} p_i p_j C_{ij}\right)},$$

where C_{ij} *and* S_{ij} *are shortened notations of* $\cos(\alpha_i - \alpha_j)$ *and* $\sin(\alpha_i - \alpha_j)$ *respectively, while* $\mathcal{K}$ *is the set of all the combinations of the* N_m *measurements taken* 3 *at a time, regardless of the order, thus* $\mathcal{K}$ *contains* $\binom{N_m}{3}$ *elements.*[1]

6.2.3 Analysis of relevant effects

Before entering into the details of how to derive closed-form solutions for the lower bound T introduced above, we point out that, given its definition, the CG is only affected by the sensor readings and by their relative position with respect to $[x_f, y_f]^\top$, and thus it is independent of the trajectory followed by the vehicle between two successive measurements. As a matter of fact, only a finite set of points (i.e., anchors, measurements and final vehicle positions) are of interest for this analysis, since the measurements order, the starting vehicle position and the system dynamics are already considered in the expression of the CG. Therefore, without loss of generality, we consider the minimum number of two anchors aligned horizontally, i.e., $Y_1 = Y_2$, a pair of measurements from each anchor and that the 4 retrieved measurements and $[x_f, y_f]^\top$ all lie on the x-axis. Figure 6.2 shows the considered motion and identifies the parameters characterising the trajectory of the vehicle: the lateral offset a, the horizontal position of the final point x_f, and the distance between the anchors, determined by X_1 and X_2.

Lateral offset

To analyse the effect of the lateral offset a in Figure 6.2, we consider as given the 4 measurement points, $[x_f, y_f]^\top$ and both X_1 and X_2, while $Y_1 = Y_2 = -a$. This way, $a = \delta \tan\alpha$, where $\delta = X_1 - x_1$ is a parameter common to all the measurements. The simplifying assumption on δ reduces the number of parameters and allows us to find the compact closed-form optimal offset given in (6.8). Moreover, we immediately notice, by symmetry, that the same result is expected for the pair a and $-a$, thus allowing us to analyse settings with only $a \geq 0$.

[1] In combinatorics, $\mathcal{K}$ is defined as the set of all the 3-combinations of the set $\{1, 2, \ldots N_m\}$.

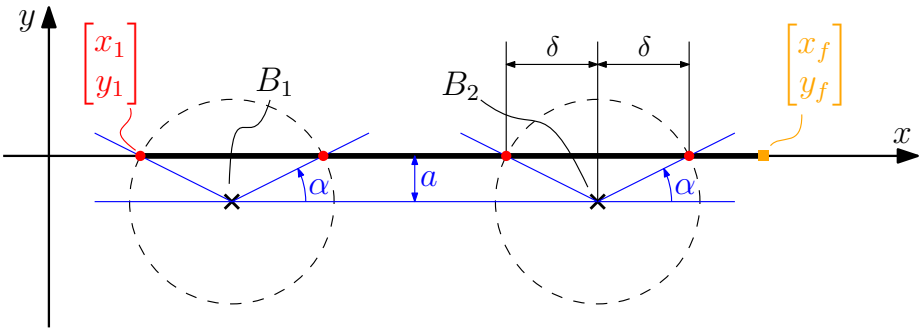

Figure 6.2: General sketch of the scenarios that have been analysed. In the general case we will always consider $y_f = y_1 = 0$ and the relevant parameters are the lateral offset a, the final position x_f and the position of the two anchors B_1 and B_2. The vehicle is travelling on the x-axis, starting from the point $[x_1, y_1]^\top$ with $\theta = 0$ (thicker black line). The four red dots represent the measurements from the anchors. The dashed-dotted green line represents a globally constructible trajectory under the assumptions in Theorem 3.2.3, with the heading constraint.

The smallest eigenvalue of the CG, depicted in Figure 6.3 as a function of a along with its lower bound, shows two different behaviours. The first, visible for small values of offset a, comes from the loss of observability when the vehicle moves along the line connecting the two anchors. In this case, the measurements contributions to $g_i(k, k_f)$ become linearly dependent and small perturbations of the initial state could generate an unobservable trajectory that is symmetric with respect to the line connecting the two anchors and that generates the same measurements sequence (same result as in [De Palma et al., 2017, §5.1]). The second effect becomes visible for large values of a, with angle α approaching $\pi/2$. In this limiting case, the measurements collected from the two anchors collapse into each other making the CG rank deficient. These different effects can be appreciated considering the evolution of the two smallest eigenvalues λ_1 and λ_2. For small values of a, λ_1, whose eigenvector is approximatively parallel to the y axis and which can be associated with the first effect, is lower and its effect is dominant. Conversely, for large values of a, λ_2, associated with an eigenvector approximatively parallel to the x axis and with the second effect, becomes the dominant one. In Figure 6.3, we report a numeric example, with the dashed blue line representing the second smallest eigenvalue of the CG. The lower bound T follows closely this pattern. From its analytic form, it is possible to estimate the lateral offset maximising T, which is $\bar{a} = \delta \tan \bar{\alpha}$, with $\bar{\alpha}$ defined as

$$\bar{\alpha} = \arcsin\left(\sqrt{\frac{2(X_1^2 + X_2^2 + 2) - \sqrt{2}\sqrt{X_1^2 + X_2^2 + 2}\sqrt{(X_1 - X_2)^2 + 4\delta^2}}{(X_1 + X_2)^2 - 4\delta^2 + 4}}\right) \tag{6.8}$$

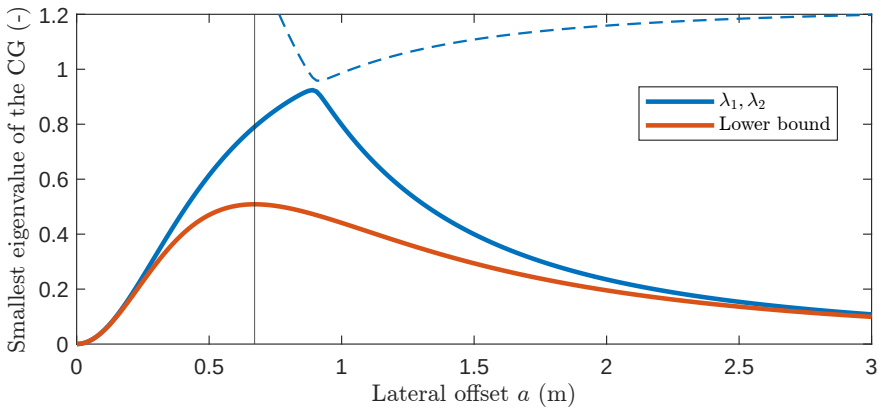

Figure 6.3: Effect of the lateral offset on the smallest eigenvalue of the CG (solid blue line) and on its lower bound T (red line). The offset optimising T, vertical black line, is close to the value of a maximising the smallest eigenvalue. In order to clarify the two prominent effects, the dashed blue line represents the second smallest eigenvalue of the CG.

if $\delta \neq \sqrt{1 + \frac{(X_1+X_2)^2}{4}}$, while, by continuity, $\bar{\alpha} = \frac{\pi}{4}$ otherwise.

Final point

We consider now the effect of the final point x_f of the trajectory on the CG. Figure 6.4(a) shows the smallest eigenvalue of the CG and its lower bound T as a function of the final horizontal coordinate x_f. As in the previous analysis, we are able to write an explicit expression of the lower bound T, and therefore compute an estimate of the optimal final position x_f. Interestingly, this value is given by

$$\overline{x_f} = \frac{X_1 + X_2}{2},$$

i.e., the optimum is in the middle point between the two anchors. In order to cast some light on the practical meaning of this result, we have considered a simulation scenario in which a unicycle-like vehicle (6.2) localises itself using and Extended Kalman Filter (EKF), with a ranging measurement variance of 10^{-6} (i.e., an uncertainty around the millimetre). We suppose that the vehicle collects the four measurements (as depicted in Figure 6.2) and then moves along the x axis using dead-reckoning and stops in the point of minimum uncertainty. By computing the eigenvalues of the covariance matrix P (as the CG is associated with P^{-1} as stated in [Salaris et al., 2019, Sec. II]) of the EKF, it turns out that this point is exactly $\overline{x_f}$ (see the largest eigenvalue in Figure 6.4(b)). This effect is far from obvious: according to the dead-reckoning effects and its unavoidable uncertainty growth, one would expect that the robot should stop

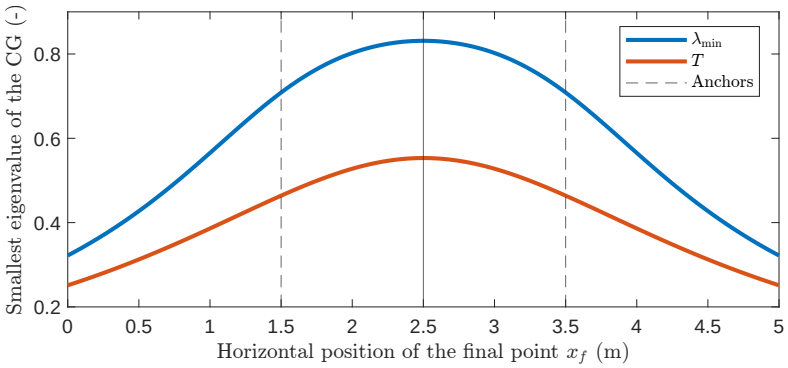

(a)

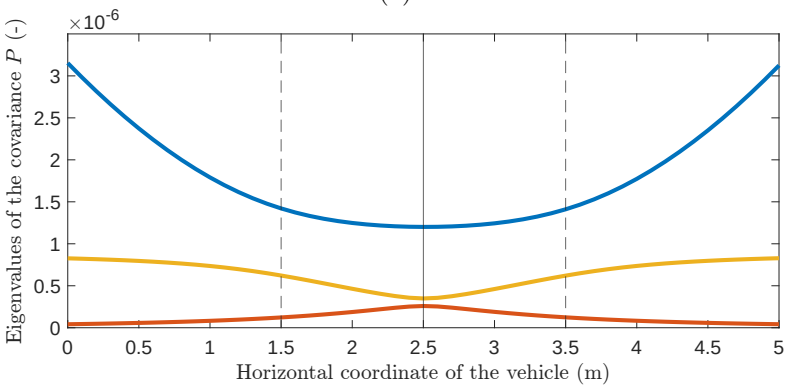

(b)

Figure 6.4: Effect of the final position of the vehicle. (a) Effect of the horizontal coordinate of the final point x_f on the smallest eigenvalue of the CG (blue line) and on its lower bound T (red line). The horizontal position of the two anchors is represented by the two dashed vertical lines, while the solid line represents the position optimising both T and the smallest eigenvalue of the CG. (b) Eigenvalues of the covariance matrix P in dead-reckoning phase, after having retrieved the four measurements. The blue line represents the greatest eigenvalue of P. The two vertical dashed lines denote the position of the two anchors, while the solid line represents the position optimising uncertainty.

right after collecting the second measurement from the second anchor. Indeed, this expectation is verified for all possible motions other than moving backward along the same direction previously followed by the robot up until it reaches $\overline{x_f}$. This anomaly deserves future investigations.

Distance between the anchors

Finally, we analyse the effect of the distance between the anchors on local constructibility. In order not to take into account unwanted contributions due to the position of the final point x_f, in this analysis we fix $x_f = 0$, and consider the two

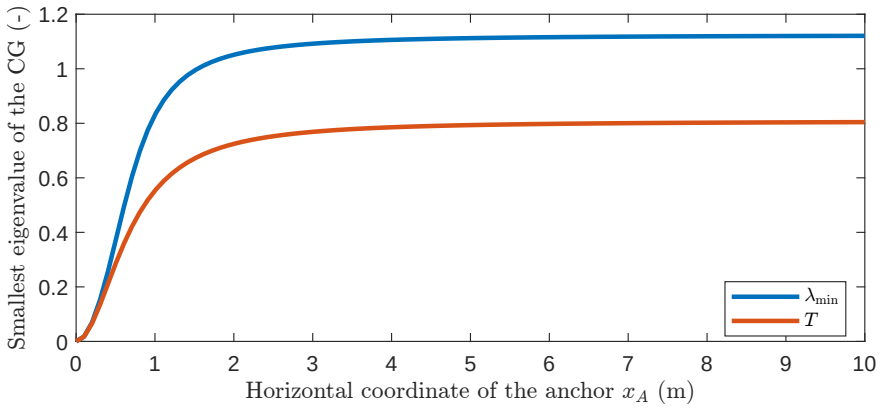

Figure 6.5: Effect of the horizontal coordinate of the anchor X_1 on the smallest eigenvalue of the CG (blue line) and on its lower bound T (red line). The horizontal position of the anchor B_2 is opposite in sign with respect to X_1, while the final point lies in the origin, i.e. $x_f = 0$.

anchors to be symmetric with respect to the y-axis, i.e., $X_2 = -X_1$. Figure 6.5 shows the results obtained with this analysis. As expected for $X_1 = X_2 = 0$, the CG is singular since the two anchors coincide, and we only have 2 independent measurements. This effect vanishes as the two anchors move further apart and both T and $\lambda_{\min}(G_C)$ reach an asymptotic value that depends on the other geometric parameters of the trajectory.

6.3 Discussion

Quantifying local constructibility and interpret its effects from a geometric point of view has not been thoroughly addressed in this chapter, but further investigations on these effects could be beneficial in finding metrics, equivalent to the smallest eigenvalue of the Constructibility Gramian, to optimise for in a trajectory planning algorithm.

Part III

Extension to Multiagent Systems

7 A Trajectory Planning Example for a Pair of Vehicles

Contents

In Parts I and II, we have focused on a single agent travelling across an environment equipped with fixed–frame sensors. We have analysed its Constructibility properties, both from a global and a local perspective. In this part, starting with this chapter, we extend some results to multi–agent systems, where the vehicles rely on both absolute and relative range measurements in order to reconstruct their state. In this chapter we present a trajectory planning algorithm, based on the *global Constructibility analysis* carried out in Part I. The tools developed in Chapter 3 will be used to plan the trajectory of a pair of vehicles, allowing them to achieve global constructibility. We consider two "kidnapped" unicycle vehicles released in an unknown environment. Initially, each vehicle is in sight of a ranging sensor (called anchor with a clear reference to UltraWide–Band technology) and has to choose a trajectory that enables it to localise itself relying only on its anchor measurements, on its odometry and on the information (state and mutual distance) that it can exchange with the other vehicle when they are sufficiently close. We propose a motion planning algorithm that, at each time step, is based on the limited amount of information available to the vehicle, and that solves the simultaneous localisation problem in this challenging scenario.

Contributions: We consider an environment equipped with 2 fixed-frame range sensors, where 2 unicycle vehicles are free to move. Each vehicle is completely unaware of its initial position and orientation and has to plan its trajectory to reconstruct its state only relying on the measurements from its "reference" anchor, on the manoeuvres executed, and on the mutual measurements and information exchanged with the other vehicle, available only when they come sufficiently close to each other. We propose a control strategy, based on three phases, allowing the two vehicles to avoid indistinguishability. In the first phase the robots execute some manoeuvres to extract the maximum information from the anchors. In the second phase, they follow circular trajectories, which (under appropriate assumptions) enable them to meet. The third phase consists of a sequence of manoeuvres that enables the vehicles to rule out the remaining ambiguity.

7.1 Problem Description

We consider a pair of vehicles, denoted by the superscripts a and b, described by the unicycle kinematic model, whose state consists of their coordinates x, y in the world reference frame $\langle W \rangle$, and of their heading θ with respect to a reference

axis. As in the Chapter 6, we use their discrete–time dynamics model

$$\begin{aligned} x_{k+1} &= x_k + A_k C_k, \\ y_{k+1} &= y_k + A_k S_k, \\ \theta_{k+1} &= \theta_k + \omega_k T_s, \end{aligned} \tag{7.1a}$$

with

$$A_k = 2\frac{v_k}{\omega_k}\sin\left(\frac{T_s}{2}\omega_k\right), \quad \lim_{\omega_k \to 0} A_k = v_k T_s,$$
$$C_k = \cos\left(\theta_k + \frac{T_s}{2}\omega_k\right) \qquad S_k = \sin\left(\theta_k + \frac{T_s}{2}\omega_k\right).$$

The control inputs v_k and ω_k represent the forward and angular velocity respectively, while the subscript k denotes the k-th time instant kT_s, while T_s is the sampling period. Each vehicle is equipped with a range sensor with sensing range S, measuring its distance from its reference fixed-frame beacon $B_i = [X_i, Y_i]^\top$, $i = 1, 2$. Without loss of generality, we consider $B_1 = [0; 0]^\top$, and $B_2 = [D; 0]^\top$, with $D > 0$. Moreover, the vehicles can measure their relative distance whenever they come sufficiently close (within S) to each other. Therefore, the measurement model for the robots is

$$\begin{aligned} z_k^a &= \begin{bmatrix} {\rho_k^a}^2 \\ {\rho_k}^2 \end{bmatrix} = \begin{bmatrix} (x_k^a - X_1)^2 + (y_k^a - Y_1)^2 \\ (x_k^a - x_k^b)^2 + (y_k^a - y_k^b)^2 \end{bmatrix}, \\ z_k^b &= \begin{bmatrix} {\rho_k^b}^2 \\ {\rho_k}^2 \end{bmatrix} = \begin{bmatrix} (x_k^b - X_2)^2 + (y_k^b - Y_2)^2 \\ (x_k^a - x_k^b)^2 + (y_k^a - y_k^b)^2 \end{bmatrix}, \end{aligned} \tag{7.1b}$$

with the understanding that the measurements are available only when $\rho_k \leq S$, where S is the sensing range of the devices. For the sake of clarity, we introduce here a new notation to denote the reference frame that will be used in the forthcoming.

Notation: We denote the position of the vehicle a in the world reference frame $\langle W \rangle$ as $Q_k^a = [x_k^a, y_k^a]^\top$ and its position sequence $\mathcal{Q}^a = \{Q_k^a\}$. Furthermore, we define by $\langle a(B_1) \rangle$ the reference frame centred in B_1 and with the x-axis aligned with one point of the trajectory followed by vehicle a that will be specified from time to time; the state of the vehicle a in $\langle a(B_1) \rangle$ will be denoted by P_k^a. The same definitions apply to vehicle b.

Remark 7.1.1. *The knowledge of two positions $Q_{k_1}^a$ and $Q_{k_2}^a$, $k_1 < k_2$, and the knowledge of v_k and ω_k, $\forall k \in [k_1, k_2]$ together with the discrete dynamics* (7.1) *determine uniquely θ_k^a, $\forall k \in [k_1, k_2]$, as discussed in Chapter 5. Hence, the localisation problem can be recast into the reconstruction of two positions $Q_{k_1}^a$*

and $Q^a_{k_2}$.

7.1.1 Theoretical background

We deal with the localisation of the vehicles in the world reference frame $\langle W \rangle$, by relying on the control inputs v_k, ω_k and on the measurement outputs z^a_k, z^b_k over a given time interval $[k_0, k_f]$. This task is associated with the concept of *u-indistinguishability*, introduced in the following definition.

Definition 7.1.2. *Given a nonlinear discrete-time system*

$$\begin{aligned} q_{k+1} &= f(q_k, u_k), \\ z_k &= h(q_k), \end{aligned}$$

a time interval $K = [k_0, k_f]$*, and an admissible control input history* $u^\star_k$, $k \in K$*, two states* q_0 *and* $\bar{q}_0$ *are said to be* $\mathbf{u}^\star$***-indistinguishable*** *if the output histories* z_k *and* $\bar{z}_k$, $k \in K$ *of the trajectories satisfying the initial conditions* q_0 *and* $\bar{q}_0$ *respectively, are identical.*

As in the previous chapters, to compact the notation, we will refer to *indistinguishable trajectories* as trajectories having u-indistinguishable initial conditions. The indistinguishability properties of the trajectories followed by a vehicle depend on the number of measurements that are collected, on their distribution among different fixed-frame landmarks, and on the manoeuvres executed by the vehicle itself (see Chapter 4). We recall here the analysis of indistinguishability of some trajectories followed by a vehicle with respect to an anchor, which will prove useful in the following analyses.

Single anchor

In Chapter 4, we have analysed the situation with a vehicle sensed by a single anchor, whose results are summarised in the following proposition:

Proposition 7.1.3. *Given the vehicle a, its position sequence* $\mathcal{Q}^a = \{Q^a_k\}$, $k = 0, \ldots, N-1$*, and the set of measurements* ρ^a_k *collected from anchor* B_1*, a position sequence* $\bar{\mathcal{Q}}^a$ *is u-indistinguishable from* $\mathcal{Q}^a$ *if: (1) For any* N*,* $\bar{\mathcal{Q}}^a$ *is a rotation of* $\mathcal{Q}^a$ *about the anchor; (2) For* $N = 2$ *(or for* $N > 2$ *collinear measurement points),* $\bar{\mathcal{Q}}^a$ *is symmetric to* $\mathcal{Q}^a$ *with respect to an axis passing through the anchor.*

By the analysis in 4, Proposition 7.1.3 collects the *sufficient and necessary* conditions for the case $N \geq 2$. In light of it, any measurement beyond the

third, provided that the measurement points are noncollinear, adds no further information to the state of the vehicle. Indeed, the vehicle is aware of its distance from the anchor and of its orientation with respect to the line joining the anchor with the vehicle itself. Therefore, we consider this to be the condition where the vehicle has extracted the *maximum amount of information* from one anchor. On the other hand, when only 2 measurements are collected, the vehicle can compute a distance-orientation pair for each one of the two axial symmetric trajectories. This result will prove useful in the analysis with more anchors, presented hereafter.

More anchors

To compact the notation, we list the number of measurements collected from each anchor, divided by a "+" sign. With a $3+1$ setting, i.e. 3 measurements from one anchor and 1 from another, the vehicle a is aware of its distance from the first anchor at any time. Thus, Q_3^a, related to the second anchor, lies on an intersection between the circles centred in the two anchors, hence defining two indistinguishable sequences $\bar{\mathcal{Q}}^a$ and $\mathcal{Q}^a$. With the same rationale, 2 measurements from the first anchor yield 2 potential distances from it, and thus a $2+1$ setting yields a maximum number of 4 indistinguishable trajectories. When the indistinguishable trajectories are known, the vehicle can explicitly design a further manoeuvre to obtain a measurement ruling out the ambiguities. This procedure will be detailed out more in our specific case at the end of Section 7.2.

7.1.2 Problem statement

Given the position of the two anchors B_1 and B_2 in $\langle W \rangle$, we aim at designing the manoeuvres of the two vehicles that solve the localisation problem. Furthermore, we will use the measurements collected along the trajectories and the sequence of manoeuvres executed by the vehicles to reconstruct their trajectories in $\langle W \rangle$.

7.2 Trajectory planning Algorithm

The two vehicles a and b start from unknown initial positions Q_0^a and Q_0^b in the range of the respective anchor. Then, each vehicle implements its perception-aware trajectory planning algorithm to meet the other agent and share the

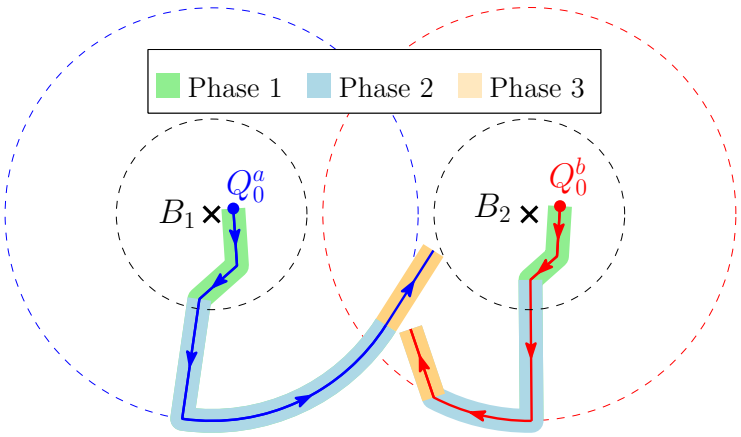

Figure 7.1: Trajectory planning algorithm: the paths of the two vehicles are represented in blue and red respectively, while the three phases are highlighted with different colours. The black dashed lines represent the sensing range of the anchors, while coloured dashed lines represent the "orbiting" distance of the two vehicles, which will be defined in phase 2.

collected information in order to simultaneously localise the agents. The planning algorithm comprises three main phases: (1) collecting the largest amount of information by the reference anchor, (2) meeting the other vehicle by "orbiting" about the anchors, (3) designing the last manoeuvres to avoid indistinguishability. The three phases are presented in Figure 7.1, and are described separately in the next sections.

7.2.1 Phase 1: Fixed-frame marker

In this phase, highlighted in green in Figure 7.1, the vehicles are far away from each other and cannot communicate or exchange information, thus they have to plan their trajectory separately. Without loss of generality, we will analyse vehicle a, dropping the superscript a for readability. At the initial time, the vehicle collects its distance ρ_0 from the anchor and has to determine v_0 and ω_0 to the second measurement point. To cope with a potential measurement noise, making two near points be sensed as a unique point, we plan the first manoeuvre to maximise the distance between Q_0 and Q_1, by maximising A_0 in (7.1), i.e., $v_0 = v_{\max}$ and $\omega_0 = 0$. Since the vehicle is not aware of its position in $\langle W \rangle$, it may or may not collect ρ_1 at $k = 1$. The two cases are treated separately.

ρ_1 is collected after the first manoeuvre

If the vehicle remains in the sensing range of the anchor and collects the measurement ρ_1, it can now build two position sequences, $\mathcal{Q}$ and $\bar{\mathcal{Q}}$, compliant with the measurements and with the manoeuvres in its local reference frame $\langle a(B_1)\rangle$: $P_0 = [\rho_0, 0]^\top$, and $P_1 = [\rho_0 + A_0\cos\alpha, \pm A_0 \sin\alpha]^\top$, with

$$\alpha = \arccos\left(\frac{\rho_1^2 - \rho_0^2 - A_0^2}{2\rho_0 A_0}\right), \tag{7.2}$$

yielding $\|P_0 - P_1\| = A_0$, and $\|P_1 - B_1\| = \rho_1$. From P_1, the vehicle has to plan the next manoeuvre (v_1, ω_1). By the definition of P_1 and by applying the controls, we can compute the distance from the anchor the robot will reach in P_2, i.e.

$$d^2 = \Delta^2 + 2\rho_0 A_1 \cos(\pm\alpha + \delta_1), \tag{7.3}$$

where $\delta_1 = \omega_1 \frac{T_s}{2}$ and

$$\Delta^2 = \rho_0^2 + A_0^2 + A_1^2 + 2A_0A_1\cos\delta_1 + 2\rho_0 A_0 \cos\alpha,$$

which yields two solutions, say d_+ and d_-. By Proposition 7.1.3, any pair (v_1, ω_1), such that $v_1 \neq 0$, $\omega_1 \neq j\pi$, $j \in \mathbb{Z}$, is suitable to get the maximum amount of information. We design the pair (v_1, ω_1) maximising the difference

$$\left|d_+^2 - d_-^2\right| = 8\rho_0 \sin\alpha \frac{v_1}{\omega_1}\sin^2\left(\frac{T_s}{2}\omega_1\right).$$

This way, we maximise the intensity of a potential measurement noise that is necessary to "confuse" the two predicted distances with each other, thus increasing the robustness of this process to measurement noise. More precisely, we define

$$\max_{v_1,\omega_1} \frac{v_1}{\omega_1}\sin^2\left(\frac{T_s}{2}\omega_1\right), \text{ s.t. } |v_1| \leq v_{\max},\ |\omega_1| \leq \omega_{\max}, \tag{7.4}$$

thus the optimal value of ω_1 can be found by computing the partial derivative of the cost function with respect to ω_1 and setting it to 0. This procedure yields

$$\cos(T_s\omega_1) + T_s\omega_1\sin(T_s\omega_1) - 1 = 0,$$

whose solution cannot be found in closed form, but numerically yields $\omega_1 = 2.3311/T_s$. Since the optimisation problem in (7.4) is constrained, the optimal value for ω_1 is $\min\{2.3311/T_s, \omega_{\max}\}$. Although the forward velocity solving (7.4) is $v_1 = v_{\max}$, we have no guarantee that at least one of the two measurement points will fall in the sensing range of the anchor. However, by

using (7.3), we can enforce that $\min\{d_+, d_-\}^2 \leq S^2$ by choosing v_1 as

$$v_1 = \frac{\omega_1}{2\sin\left(\frac{T_s}{2}\omega_1\right)} \left[\sqrt{S^2 - \left(\rho_0 \sin(\alpha + \tfrac{T_s}{2}\,\omega_1) + A_0 \sin(\tfrac{T_s}{2}\,\omega_1)\right)^2} - \rho_0 \cos\left(\alpha + \tfrac{T_s}{2}\omega_1\right) - A_0 \cos\left(\tfrac{T_s}{2}\omega_1\right)\right].$$

Hence, if the vehicle falls outside the sensing range, i.e., no measurement is collected, a *virtual measurement* $\rho_2 = \max\{d_-, d_+\}$ is collected. Therefore, by Proposition 7.1.3, with three non-collinear measurement points, the vehicle collects the largest amount of information from its reference anchor.

ρ_1 is not collected after the first manoeuvre

To collect the second measurement, the vehicle turns on the spot by $\pi/2$, i.e., $v_1 = 0$ and $\omega_1 = \frac{\pi}{2T_s}$, and starts moving on a circle with centre Q_0 and radius A_0, i.e., $v_k/\omega_k = A_0$, with $k = 2, \ldots, k_\rho - 1$, where k_ρ is the time instant when the measurement is collected. Since Q_0 is within the sensing range of the anchor and $A_0 < S$, an arc of the circular trajectory of the vehicle, with amplitude $2\pi - 2\eta$, will be inside the sensing range, leading the vehicle to collect the measurement ρ_1, as in Figure 7.2(a), where

$$\eta = \arccos\left(\frac{S^2 - \rho_0^2 - A_0^2}{2A_0\rho_0}\right).$$

However, since measurements occur only at sampling times kT_s, the vehicle travels an arc of maximum amplitude $2\pi - 2\eta$ during T_s, hence upper-bounding its velocity to $\omega_k = \min\{\omega_{\max}, \frac{2\pi-2\eta}{T_s}, \frac{v_{\max}}{A_0}\}$ and leading to the forward velocity $v_k = \omega_k A_0$. After N_l manoeuvres, the vehicle enters the sensing range of the anchor, collects ρ_1, and computes α by using (7.2): this way, the vehicle can find two trajectories $\mathcal{Q}$ and $\bar{\mathcal{Q}}$ (associated with $\pm\alpha$ as in the previous case), that are compliant with the measurements and the manoeuvres, hence indistinguishable. In the reference frame $\langle a(B_1)\rangle$, the vehicle can compute the coordinates, and consequently the distance d_l, of each point P_l in $\mathcal{Q}$ and $\bar{\mathcal{Q}}$

$$d_l^2 = \rho_0^2 + A_0^2 + 2\rho_0 A_0 \cos(\pm\alpha - l\omega_k), \quad l = 1, \ldots, N_l.$$

If one of these distances $d_l \leq S$, the corresponding trajectory is disregarded, thus collecting the largest amount of information from one anchor with only two measurements (see Figure 7.3(b)). Should this situation not happen, i.e.,

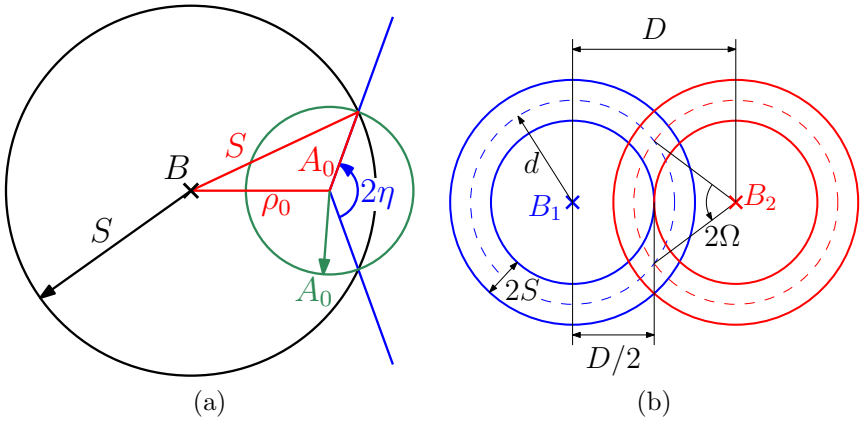

Figure 7.2: (a) Phase 1, ρ_1 not collected after the first manoeuvre: Circular path followed by the vehicle after the first (straight) motion. (b) Phase 2: orbiting paths with the definitions of the angle Ω.

$d_l > S, \forall l = 1, \dots, N_l$, the vehicle can follow the same procedure as before to collect the third measurement ρ_2, with the proper modifications accounting for its orientation.

7.2.2 Phase 2: Meeting the other vehicle

By Proposition 7.1.3, after the first phase, the two vehicles can now estimate their position P_k and determine their orientation μ with respect to the line joining the anchor and the vehicle itself in their reference frame $\langle a(B_1)\rangle$ and $\langle b(B_2)\rangle$, with

$$\mu = \begin{cases} \omega_2 T_s & +\alpha - \arctan2(y,x), \quad \text{with 3 measurements} \\ \dfrac{\pi}{2} & +\alpha - \arctan2(y,x), \quad \text{with 2 measurements} \end{cases},$$

where the x and y coordinates are known in the local $\langle a(B_1)\rangle$ and $\langle b(B_2)\rangle$ reference frames, and depend on the procedure followed in the first phase. Moreover, the distance from the anchor is known from the last measurement. To reach any prescribed distance from its anchor, the vehicle can turn by $-\mu$ on the spot (i.e. $v = 0, \omega = -\mu/T_s$), to align to the diameter of the circle centred in the reference anchor, and travel on a straight path, i.e. $\omega = 0$. The vehicles are aware of their radial coordinates with respect to their reference anchor and of the distance D between the two anchors themselves, and have to plan their trajectories in order to reduce their relative distance below the sensing range S. To this aim, the two vehicles travel on a circular trajectory, centred in their reference anchor, with prescribed radius d, as reported in Figure 7.1, highlighted

in light blue. To determine the optimal radius d, we consider the situation represented in Figure 7.2(b) where the vehicles and the anchors are aligned on the x-axis of $\langle W \rangle$, with horizontal coordinates $X_1 = 0, x_a = d, x_b = D - d, X_2 = D$, where we want the two vehicles to have distance S, and $x_a > x_b$, and thus $d = \frac{D+S}{2}$. We then define $\Omega = \arccos\left(\frac{D}{D+S}\right)$ as half of the angle described by the two segments connecting one of the anchors with the two intersections of the trajectories, giving an estimate of the arc where the measurement between the two vehicles can occur. To meet, the vehicles rotate in opposite directions, choosing their velocities such that while a travels over a circle, b travels an arc with amplitude 2Ω,

$$\begin{aligned} \omega_a &= \min\left\{\omega_{\max}, \frac{2v_{\max}}{D+S}\right\}, & v_a &= \omega_a \frac{D+S}{2}, \\ \omega_b &= -\frac{\Omega}{\pi}\omega_a, & v_b &= -\omega_b \frac{D+S}{2}. \end{aligned} \tag{7.5}$$

With this choice of the control inputs, we can estimate an upper bound $T_{\max}$ to the time needed by the two vehicles to meet, based on the time needed by b to travel over the entire circle, travelling twice on the 2Ω arc, yielding

$$T_{\max} = \frac{2\pi + 2\Omega}{|\omega_b|} = 2\pi\left(\frac{\pi}{\Omega} + 1\right)\max\left\{\frac{1}{\omega_{\max}}, \frac{D+S}{2v_{\max}}\right\}.$$

7.2.3 Phase 3: Designing the last manoeuvres

As soon as the two vehicles meet and collect the first mutual measurement $\rho_{1,m}$, they are aware of their sequence $\mathcal{Q}$ in their local reference frame, of their distance, and of the distance D between the two anchors. Let P_1^a and P_1^b be the positions of the vehicles when the $\rho_{1,m}$ is collected. We define the local reference frame $\langle a(B_1) \rangle$ such that $B_1 = [0,0]^\top$ and $P_1^a = [\frac{D+S}{2}, 0]^\top$. With the same procedure, in $\langle b(B_2) \rangle$, $B_2 = [0,0]^\top$ and $P_1^b = [\frac{D+S}{2}, 0]^\top$, while the heading of the two vehicles with respect to their x-axis is $\pm\pi/2$ since they are travelling on the circle centred in their reference anchor. In $\langle b(B_2) \rangle$, we can regard B_2 and P_1^b as fixed-frame anchors, and thus the two distances D and $\rho_{1,m}$ generate a $1+1$ setting (see Section 7.1) for the vehicle a.

Second mutual measurement With the same rationale, we can treat the next position P_2^b of vehicle b as an additional anchor in $\langle b(B_2) \rangle$. Therefore, by collecting an additional measurement, we add no further information if the two vehicles do not move, while we have a $2+1$ if one of the two stays still, and a $1+1+1$ if both vehicles move. By the analysis in 4, a $2+1$ setting should be preferred, since it yields a number $N_{IT}^{[2+1]} \leq 4$ of indistinguishable trajectories

that can be computed by checking a condition that will be detailed out later, while a setting $1+1+1$ yields $N_{IT}^{[1+1+1]} \leq 8$ indistinguishable trajectories, where $N_{IT}^{[1+1+1]}$ cannot be computed. Therefore, vehicle b stops as soon as it collects the first measurement (i.e. $P_2^b = P_1^b$), while vehicle a follows the same procedure as in the first phase to collect a second mutual measurement, i.e. moving straight and possibly travelling on a circle centred in its previous position. With these manoeuvres, we can update the reference frame $\langle a(B_1)\rangle$, by adding the known position $P_2^a = P_1^a + [\delta x, \delta y]^\top$, and define γ as the angle described by the two branches of $\mathcal{Q}_a$ intersecting in P_1^a as $\gamma = \pi - \arctan2(\delta y, \delta x)$. To compute the number of indistinguishable trajectories arising in this $2+1$ setting, we build a reference frame where P_1^b lies on the origin, while P_1^a lies on the x–axis, i.e. $\langle a(P_1^b)\rangle$, which will allow us to compute the distance $\|B_1 - P_1^b\|$. In this frame, $P_1^a = [\rho_{1,m}, 0]^\top$, $P_2^a = P_1^a + A_1[\cos\alpha, \pm\sin\alpha]^\top$ and

$$B_1 = P_1^a + \frac{D+S}{2}\left[\cos(\pm\alpha+\gamma);\ \sin(\pm\alpha+\gamma)\right]^\top,$$

and thus, we conclude that

$$\|B_1 - P_1^b\|^2 = \left(\frac{D+S}{2}\right)^2 + \rho_{1,m}^2 + \rho_{1,m}(D+S)\cos(\pm\alpha+\gamma).$$

Therefore, in $\langle b(B_2)\rangle$, the landmark B_1 lies at the intersection between one of the two circles centred in P_1^b with radius $\|B_1 - P_1^b\|$ and the circle centred in B_2 with radius D. We can compute the number of intersections between the circles. In particular, each circle centred in B_1 has 2 intersections if $\|B_1 - P_1^b\| \in (|D-S|/2, (3D+S)/2)$, hence fixing the maximum number of indistinguishable trajectories to 4. If the vehicle collects the second mutual measurement after travelling over a circular arc, it may be able to discard either α or $-\alpha$, hence yielding 2 indistinguishable trajectories. We remark that each of these *indistinguishable* sequences $\mathcal{Q}_a$ can be roto-translated from $\langle b(B_2)\rangle$ to $\langle W\rangle$, since the coordinates of all the positions, including B_1, are known.

Third mutual measurement The indistinguishable sequences $\mathcal{Q}^a$ in $\langle b(B_2)\rangle$ can be built by using the solutions $\phi, \Delta x, \Delta y$ of the following set of equations

$$\begin{aligned} \|\ B_2 - (R_\phi B_1 + T)\|^2 &= D^2 \\ \|\ P_1^b - (R_\phi P_1^a + T)\|^2 &= \rho_{1,m}^2 \\ \|\ P_1^b - (R_\phi P_2^a + T)\|^2 &= \rho_{2,m}^2, \end{aligned} \tag{7.6}$$

where $R_\phi = \begin{bmatrix} \cos\phi & -\sin\phi \\ \sin\phi & \cos\phi \end{bmatrix}$ is a rotation matrix, $T = [\Delta x, \Delta y]^\top$ is a translation vector, B_1, P_1^a and P_2^a are expressed in $\langle a(B_1)\rangle$, while B_2, P_1^b and P_2^b in

$\langle b(B_2)\rangle$. To this end, it is convenient to subtract the first equation from the others, yielding two linear equations in Δx and Δy, substitute the result into the first equation, thus having a nonlinear equation in ϕ with a known number of solutions. Once the $N \leq 4$ solutions to (7.6) are found, vehicle b is aware of the possible positions $P^a_{2,i}$, $i = 1, .., N$ in $\langle b(B_2)\rangle$. For simplicity's sake, a stops as soon as it collects $\rho_{2,m}$. Vehicle b plans (v_2, ω_2) and moves to the next point P^b_2, whose distance d from vehicle a is one of the N possible $d_i = \|P^a_{2,i} - P^b_2\|$. As in the previous analysis, to cope with measurement noise, b plans its manoeuvre such that the predicted measurements d_i are as far as possible from each other, thus defining the optimisation problem

$$\max_{v_2,\omega_2} J, \qquad \text{s. t.} \qquad |v_2| \leq v_{\max},\ |\omega_2| \leq \omega_{\max}, \tag{7.7}$$

where $J = \min_{(i,j)} |d_i - d_j|$ is linear in v_2, indeed with $v_2 = 0$ the vehicles collect the same measurement $\rho_{2,m}$, and thus we select $v_2 = v_{\max}$. For each pair of possible positions of vehicle a in $\langle b(B_2)\rangle$, we can compute the difference of the distances as a function of ω_2. However, the cost J is defined piecewise, due to the $\min(\cdot)$ operator, and thus a closed-form solution cannot be found. Therefore, we deal with this problem by enumeration: we select a sufficiently high number of values for ω_2 and, for each of them, we determine and choose the smallest difference of distances, which gives us the value of ω_2 corresponding to the maximum value of the cost function J obtained through this procedure. Once v_2 and ω_2 are selected, vehicle b moves and collects the last mutual measurement, which rules out the ambiguity between the N possible positions P^a_2. The global localisation problem is thus solved using the planned trajectories.

7.3 Simulation examples

We present here two different examples, with the same parameters $S = 3$ m, $D = 10$ m, $T_s = 1$ s, $v_{\max} = 1$ m/s and $\omega_{\max} = \pi$ rad/s, with different initial conditions. Different initial states will lead the vehicles to take different decisions, thus covering all the described cases. We remark that the representation of the trajectories will consist in a line connecting the successive positions of the vehicles, while the path followed by the vehicles (see discretisation in (7.1a)), consists of straight lines and arcs of circles. Figures 7.3 and 7.4, showing the simulation results, are reported at the end of this chapter.

First simulation

In the first simulation example, in Figure 7.3, we choose the initial conditions as $Q_0^a = [2.4, -1.2, 4.8]^\top$, $Q_0^b = [11.3, -0.4, 3.6]^\top$. Figure 7.3(a) shows the position sequences $\mathcal{Q}_a$ in blue and $\mathcal{Q}_b$ in red, during the whole simulation. Phase 1 of vehicle a is described in Figure 7.3(b), where the vehicle moves straight falling outside the sensing range of B_1, represented by the solid black line, travels on a circle and eventually collects the second measurement. These two measurements are sufficient to collect the maximum amount of information from the anchor, since the dotted trajectory, associated with $-\alpha$, has points inside the sensing range that should have been sensed by the anchor, thus allowing vehicle a to avoid the potential ambiguity $\pm\alpha$. The same outcome is obtained by b by collecting three measurements from B_2. During phase 2, the two vehicles reach their orbiting distance, dashed red and blue lines in Figure 7.3(a), until they meet. A screenshot of the first mutual measurement is reported in Figure 7.3(d1), where b stops, while a proceeds straight, i.e. on the tangent of its orbiting circle, as depicted in Figure 7.3(d2). After the second mutual measurement, vehicle a stops, while b finds the 4 potential trajectories followed by a in $\langle b(B_2)\rangle$, getting to the setting in Figure 7.3(c), thus finding the optimal value for ω_2, maximising the smallest difference of the distances, generating the motion in Figure 7.3(d3). Despite the natural intuition, vehicle b does not move on the bisector between two axes in Figure 7.3(c), but it seeks for a trade-off between this behaviour and the maximum possible displacement.

Second simulation

For the second simulation example, presented in Figure 7.4, we choose the initial conditions $Q_0^a = [-1.5, -1.7, 2.6]^\top$, $Q_0^b = [10, -0.1, 6]^\top$. In phase 1 the two vehicles collect 3 measurements each from their reference anchors, then reach the prescribed orbiting distance (phase 2). The noteworthy difference with the previous example occurs in phase 3. Indeed, by following a straight path, vehicle a falls outside the sensing range of b, travels over a circle, and eventually falls inside the sensing range of b, ruling out the ambiguity $\pm\alpha$ in (7.3), thus decreasing to 2 the number of indistinguishable trajectories. Vehicle b plans its last manoeuvre in the same way as before, maximising the only difference of the two distances, as in Figure 7.4(b).

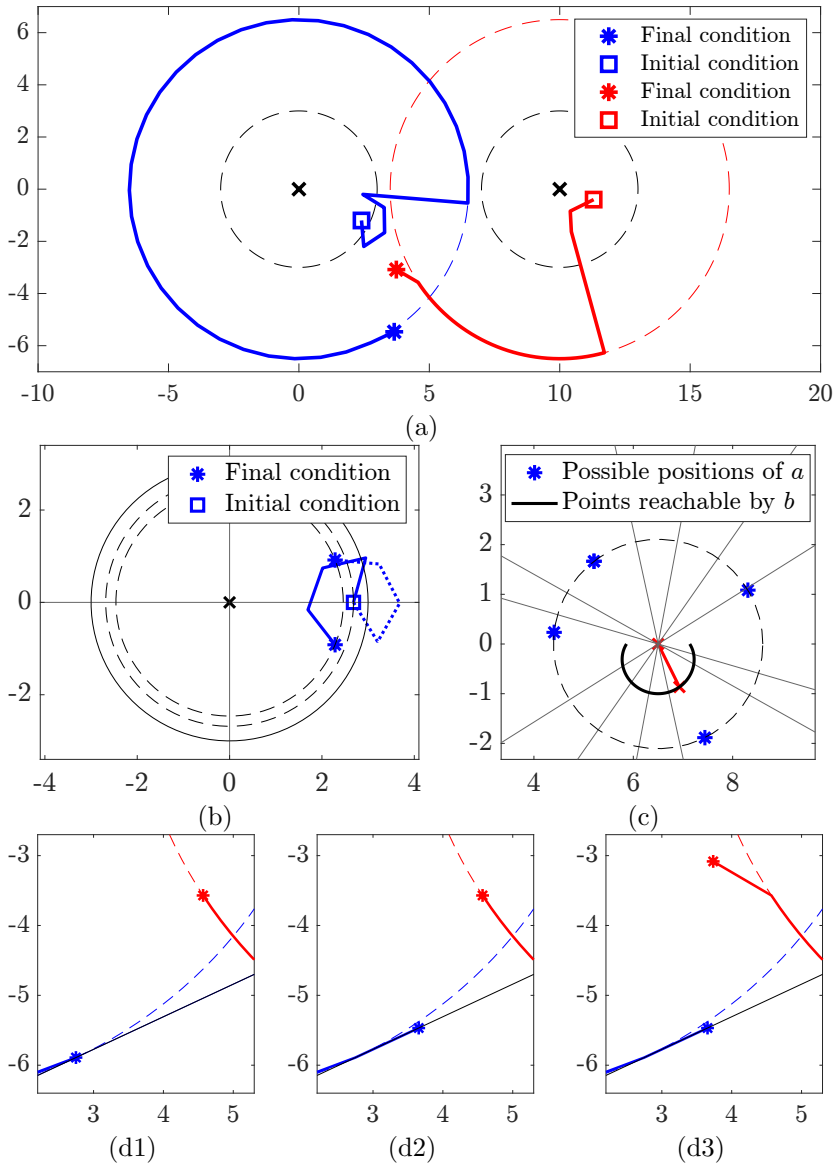

Figure 7.3: First simulation example. (a) Path followed by vehicle a in blue, and by b in red. The black crosses the position of the two landmarks B_1, B_2, with sensing range S (black dashed line), whereas the dashed lines represent the orbiting distances. (b) Phase 1: $\langle a(B_1)\rangle$, two trajectories $\pm\alpha$ of vehicle a, where the solid line represents the sensing range S, the dashed lines represent the measurements ρ_0 (outer) and ρ_1 (inner). The dotted trajectory is discarded, since some of its points are inside the sensing range. (c) Phase 3: $\langle b(B_2)\rangle$ after the second mutual measurement. The black solid line represents the points reachable by b with $v_2 = v_{\max}$, the red line and the red crosses denote the best choice for ω_2, the blue dots are the four potential positions of the vehicle a, with distance ρ_2 denoted by the black dashed line, while the thin black lines represent the axes of the segments with a pair of blue dots as endpoints. (d) Phase 3, zoom from (a): the vehicles collect their first mutual measurement (d1), a moves on the tangent (black solid line) of the dashed circle (d2), and eventually b moves according to the control inputs described in (c), i.e. turning slightly left.

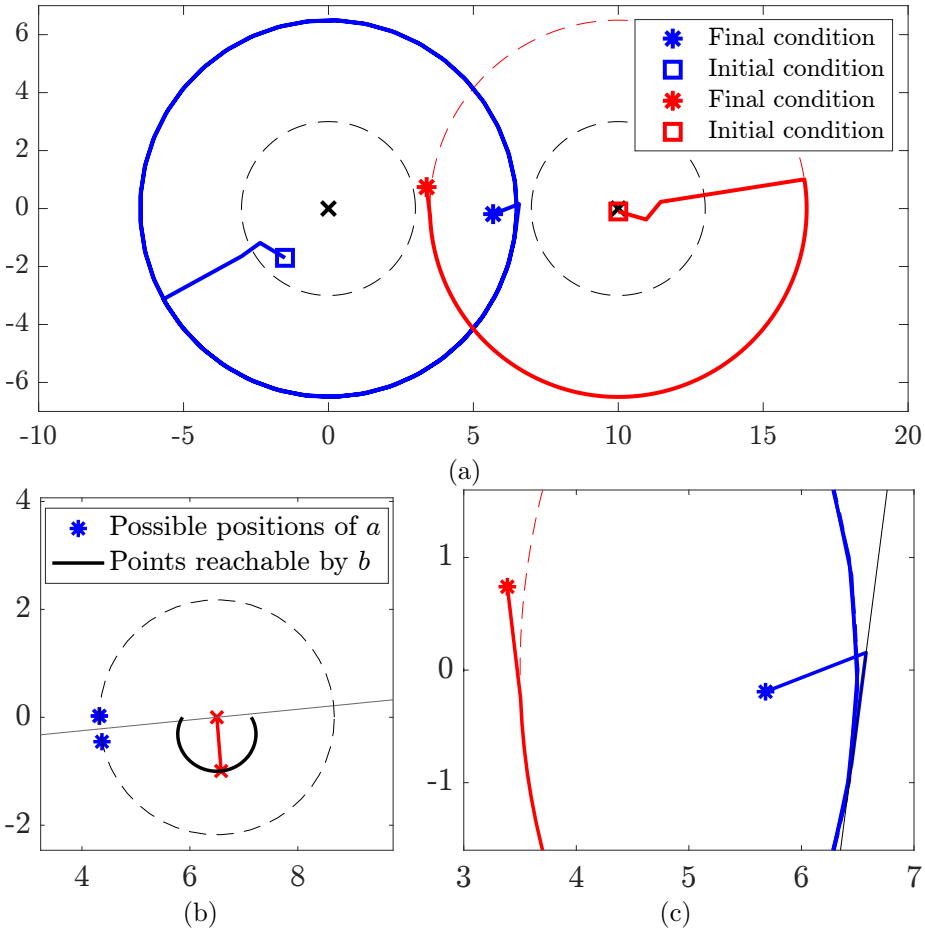

Figure 7.4: Second simulation example. (a) Paths followed by the two vehicles. (b) Phase 3: Situation seen by vehicle b while planning its last manoeuvre, with the same conventions as in Figure 7.3. The possible positions of vehicle a are reduced to 2, since it has followed a curved trajectory outside the sensing range of b (similar to the one in Figure 7.3(a)), thus ruling out the ambiguity between the two trajectories. (c) Phase 3: zoom on the last points reached by the two vehicles.

Constructibility Analysis for a Team of Vehicles

8

Contents

In Chapter 7, we have proposed a trajectory planning algorithm for a pair of vehicles with absolute and relative range measurements. For the given scenario with two fixed ranging sensors and two vehicles moving without prior information on their state, the algorithm we have proposed is sufficient to guarantee global constructibility, while no analysis has been presented on the necessary conditions to attain local or global constructibility properties. In this chapter, following the same *rationale* as in Parts I and Part II, we analyse the constructibility properties of a multiagent system composed of unicycle–like vehicles collecting relative range measurements. The results of the global analysis in Chapter 4 are extended to the multiagent scenario, but, as stated in Chapter 1, a complete global constructibility analysis has not been carried out in this chapter, but only a limited amount of results is presented on the global problem.

Contributions: In this analysis, we introduce some simplifications, in line with the assumptions in the previous chapters, that allow us to consider the position sequences of the vehicles and obtain some simpler geometrical insights on the results devised analytically. Moreover, we address *relative* localisation, with respect to an *anchor* vehicle. First, we analyse the constructibility problem from a global perspective and propose some necessary conditions on the trajectory and measurements of each vehicle when a constructible subsystem can be identified. Second, we analyse the local constructibility properties for a 3–agent system by means of the Constructibility Gramian for the whole system, and lastly, we extend this results for multiagent systems with a generic number N of vehicles.

8.1 Problem Description

Let us consider a multiagent system composed of $N \geq 2$ vehicles. Each vehicle is described in the global reference frame $\langle W \rangle$ by its state vector ${}^{W}q^{[i]} = [{}^{W}x^{[i]}; {}^{W}y^{[i]}; {}^{W}\theta^{[i]}]^{\top}$ composed of its Cartesian position and its orientation with respect to a given reference axis. For each vehicle $V^{[i]}$, $i = 0, \ldots, N-1$, we define a local reference frame $\langle V^{[i]} \rangle$, whose origin lies on the initial position ${}^{W}P^{[i]}(0) = [{}^{W}x^{[i]}(0); {}^{W}y^{[i]}(0)]$ of the vehicle and whose x-axis is aligned with the initial heading ${}^{W}\theta^{[i]}(0)$ of the vehicle. In $\langle V^{[i]} \rangle$, and analogously in $\langle W \rangle$, the time evolution of the i-th vehicle state $q^{[i]} = [x^{[i]}; y^{[i]}; \theta^{[i]}]^{\top}$ is governed by the following equations:

$$\dot{x}^{[i]} = v^{[i]} \cos\theta^{[i]}, \qquad \dot{y}^{[i]} = v^{[i]} \sin\theta^{[i]}, \qquad \dot{\theta}^{[i]} = \omega^{[i]}, \tag{8.1}$$

where $v^{[i]}$ and $\omega^{[i]}$ are the control inputs, representing the forward and angular velocities of the vehicle, respectively. By propagating the system dynamics (8.1) with the control input history $v^{[i]}(\tau), \omega^{[i]}(\tau)$, which is assumed known for $\tau \in [0, t]$, we can reconstruct the position $P^{[i]}(t)$ of the vehicle in $\langle V^{[i]} \rangle$ at any time $t \geq 0$. We assume that the vehicles are equipped with ranging sensors measuring the relative distance between two agents; we also assume that a vehicle can collect the distances from more than one vehicle simultaneously. Moreover, we consider the sensors to collect measurements only at known time instants, to model finite sensing range or finite sampling frequency of the sensors. We denote by $t_k^{[i,j]}$, $k \in \mathbb{N}$, a time instant when two vehicles $V^{[i]}$ and $V^{[j]}$ collect their relative distance, while elements $t_k^{[i]} \in \Theta^{[i]}$ are defined as the time instant when $V^{[i]}$ collects a measurement, independently on the other vehicle involved in the measurements. For $V^{[i]}$, the output equation reads as

$$z_k^{[i]} = \left\{ \rho^{[i,j]}(t_k^{[i]}),\, \forall\, j \in \mathcal{N}^{[i]}(t_k^{[i]}) \right\}, \tag{8.2}$$

where $\rho^{[i,j]}(t_k^{[i]}) := \| {}^W P^{[i]}(t_k^{[i,j]}) - {}^W P^{[j]}(t_k^{[i,j]}) \|$, ${}^W P^{[i]}(t_k^{[i,j]})$ is the position of the i-th agent at time $t_k^{[i,j]}$ in the world reference frame $\langle W \rangle$, while $\mathcal{N}^{[i]}(t_k^{[i]})$ is the set of neighbours of the i-th agent at time t_k, i.e. the set of vehicles measuring their distance from $V^{[i]}$ at time $t_k^{[i]}$.

Notation. To simplify the notation, we denote by the subscript k the time instant $t_k^{[i]}$, when the index i is clear from the context, e.g. $\mathcal{N}_k^{[i]}$ is the short notation for $\mathcal{N}^{[i]}(t_k^{[i]})$, and $\rho_k^{[i,j]}$ is short for $\rho^{[i,j]}(t_k^{[i]})$.

We notice that, by (8.2), only the position of the vehicles is involved in the measurements, and thus we can focus on the sequence of positions $\mathcal{Q}^{[i]}$

$$\mathcal{Q}^{[i]} = \left\{ P_k^{[i]},\, \forall\, k : t_k^{[i]} \in \Theta^{[i]} \right\}, \tag{8.3}$$

expressed in the local reference frame $\langle V^{[i]} \rangle$, which is known by the previous considerations. By the dynamics (8.1), we can express the sequence of points reached by a vehicle in the world reference frame, denoted by ${}^W\mathcal{Q}^{[i]}$, through the rigid transformation $[{}^W R^{[i]}, {}^W T^{[i]}]$ of $\mathcal{Q}^{[i]}$ as

$${}^W P_k^{[i]} = {}^W R^{[i]} P_k^{[i]} + {}^W T^{[i]}, \tag{8.4}$$

where ${}^W R^{[i]} = \begin{bmatrix} \cos\phi^{[i]} & -\sin\phi^{[i]} \\ \sin\phi^{[i]} & \cos\phi^{[i]} \end{bmatrix}$ is a rotation matrix, while ${}^W T^{[i]} = [\Delta x^{[i]}; \Delta y^{[i]}]^\top$ is the translation vector. While the actual rigid transformation $[{}^W R^{[i]}, {}^W T^{[i]}]$ is unknown, we define for each vehicle the sequence of points $\tilde{\mathcal{Q}}^{[i]}$ as

$$\tilde{\mathcal{Q}}^{[i]} = \left\{ \tilde{P}_k^{[i]} = \tilde{R}^{[i]} P_k^{[i]} + \tilde{T}^{[i]},\, \forall\, t_k^{[i]} \in \Theta^{[i]} \right\}, \tag{8.5}$$

with $\tilde{R}^{[i]}$ and $\tilde{T}^{[i]}$ *arbitrary* rotation and translation.

Definition 8.1.1. *A trajectory of the multiagent system is said to be* compliant with the measurements *when* $\tilde{R}^{[i]}$ *and* $\tilde{T}^{[i]}$, $i = 0, \dots, N-1$ *are such that*

$$\|\tilde{P}_k^{[i]} - \tilde{P}^{[j]}(t_k^{[i]})\| = \rho_k^{[i,j]}, \tag{8.6}$$

with $\tilde{P}_k^{[i]} \in \tilde{\mathcal{Q}}^{[i]}$, $j \in \mathcal{N}_k^{[i]}$, $t_k^{[i]} \in \Theta^{[i]}$.

Trivially, by Definition 8.1.1, when $\tilde{R}^{[i]} = {}^{W}R^{[i]}$ and $\tilde{T}^{[i]} = {}^{W}T^{[i]}$, $i = 0, \dots, N-1$, i.e. when we pick the *actual* rigid transformation, the trajectory is compliant with the measurements, but there may exist other compliant rigid transformation.

For the multiagent system, we build an overall state vector ${}^{W}q(t) \in \mathbb{R}^{3N}$ by stacking the state vectors of the N vehicles, expressing their *unknown* coordinates and orientations in the world reference frame $\langle W \rangle$. We aim at analysing the necessary and sufficient conditions to reconstruct the state ${}^{W}q(t)$, based on the measurements and on the control input history associated with each vehicle. To this aim, we give some definitions on the system obtained, with continuous-time dynamics and discrete-time output, having the shape

$$\dot{q}(t) = f\left(q(t), u(t)\right), \qquad z_k = h\left(q(t_k)\right). \tag{8.7}$$

To account for both continuous and discrete time, we associate with $k = 0$ the initial time $t = t_0$, while $k = k_f$ corresponds to the final time t_f, where the absence of superscripts refers to the whole multi–agent system.

Definition 8.1.2 (u-backward indistinguishability)**.** *Given the system* (8.7) *and a time interval* $T = [t_0, t_f]$*, two final states* q_f *and* $\bar{q}_f$ *are said to be* u-backward indistinguishable *if, for the given input history* $u(t)$, $t \in T$*, the output histories* z_k *and* $\bar{z}_k$, $k = 0, \dots, k_f$ *of the trajectories satisfying the final conditions* q_f *and* $\bar{q}_f$*, respectively, are identical. Moreover, we define* $\mathcal{I}^u(q_f)$ *as the set of final states that are backward indistinguishable from* q_f*.*

While backward indistinguishability is a property of the final state reached by the system, we can also assess the constructibility properties of the system itself.

Definition 8.1.3 (u-(weak) constructibility)**.** *Given a time interval* $T = [t_0, t_f]$ *and a control input history* $u(t)$, $t \in T$*, the system* (8.7) *is said to be* u-constructible at q_f on T *if* $\mathcal{I}^u(q_f) = \{q_f\}$*, while it is said to be* u-weakly constructible at q_f on T *if* q_f *is an isolated point of* $\mathcal{I}^u(q_f)$*.*

As in the previous chapters of this thesis, with a slight abuse of notation, we will refer to a *(weakly) constructible system* as a system that is (weakly)

constructible at its final state q_f over a time interval $T = [t_0, t_f]$ where the measurements are collected, while we will refer to *indistinguishable trajectories* as trajectories having u-indistinguishable final conditions. In the remainder of the chapter, without loss of generality, we assume the reference frame $\langle V^{[0]} \rangle$ to coincide with the world reference frame, and we will refer to the vehicle $V^{[0]}$ as to *anchor vehicle*, to underline that its position sequence $\mathcal{Q}^{[0]}$ is known in $\langle W \rangle$.

To give a practical interpretation of Definitions 8.1.2 and 8.1.3 for our multiagent system, we provide two facts, which rely on the following proposition:

Proposition 8.1.4. *The state $q(t) = [x(t), y(t), \theta(t)]^\top$ of a unicycle vehicle with dynamics* (8.1) *can be reconstructed from a finite number of time derivatives of its position $P(t) = [x(t), y(t)]^\top$.*

Proof. The proof descends from the fact that the unicycle kinematic model is *differentially flat*, with its position as flat output [Fliess et al., 1995]. □

By Proposition 8.1.4, reconstructing the state of a vehicle boils down to finding a rigid transformation $[\tilde{R}^{[i]}, \tilde{T}^{[i]}]$ from the reference frame $\langle V^{[i]} \rangle$ of the vehicle to the world reference frame $\langle W \rangle$.

Fact 8.1.5 (Global Constructibility)**.** *A multiagent system is* constructible *if there is a unique set of rigid transformation $\{[\tilde{R}^{[i]}, \tilde{T}^{[i]}],\ i = 1, \dots, N-1\}$ such that* (8.6) *holds true, i.e. when there exist a* unique *trajectory of the multiagent system which is* compliant with the measurements*, as for Definition 8.1.1.*

Fact 8.1.6 (Local Constructibility)**.** *A multiagent system is* weakly constructible *if, given a solution $\tilde{\phi}^{[i]}$, $\Delta\tilde{x}^{[i]}$ and $\Delta\tilde{y}^{[i]}$ of* (8.6)*, there exist neighbourhoods $\mathcal{S}(\tilde{\phi}^{[i]})$, $\mathcal{S}(\Delta\tilde{x}^{[i]})$ and $\mathcal{S}(\Delta\tilde{y}^{[i]})$ of non–null size such that $\forall\hat{\phi}^{[i]} \in \mathcal{S}(\tilde{\phi}^{[i]})$, $\forall\Delta\hat{x}^{[i]} \in \mathcal{S}(\Delta\tilde{x}^{[i]})$ and $\forall\Delta\hat{y}^{[i]} \in \mathcal{S}(\Delta\tilde{y}^{[i]})$,* (8.6) *does not hold true.*

Fact 8.1.6 presents considerations with only *local* validity, hence the name local constructibility, since it excludes the existence of other compliant rigid transformation $\tilde{R}^{[i]}, \tilde{T}^{[i]}$ *only* in the neighbourhood of the given solution. The *global* result is presented in Fact 8.1.5.

8.1.1 Problem Statement

As a natural extension of the analysis in Chapter 4 to multiagent systems, we analyse how the conditions on the trajectories followed by the vehicles, their number and their relative measurements affect the constructibility of the system.

Problem 8.1. *Given N agents, whose trajectories in their local reference frames $\langle V^{[i]} \rangle$ are represented by the sequences of positions $\mathcal{Q}^{[i]}$, $i = 0, \dots, N-1$, find the*

conditions on the trajectories $\mathcal{Q}^{[i]}$ *and on the measurements* $z_k^{[i]}$, $i = 0, \dots, N-1$, *such that the system is (weakly) constructible. In light of Facts 8.1.5 and 8.1.6, this problem is equivalent to finding the conditions such that* (8.6) *has a unique or a finite number of solutions* $[\tilde{R}^{[i]}, \tilde{T}^{[i]}]$ *representing rigid transformation from* $\langle V^{[i]} \rangle$ *to* $\langle V^{[0]} \rangle$, $i = 1, \dots, N-1$.

8.1.2 Preliminary Results

In Chapter 4, we have analysed the setting where a vehicle collects non–simultaneous measurements from fixed sensors ("anchors") deployed in the environment. In this section we report and extend the devised necessary conditions to settings where simultaneous measurements are collected. Indeed, in Chapter 7, we have shown that simultaneous measurements have peculiar structural properties, which are clearly different from the case in which measurements are collected at distinct times. This extension is instrumental to the constructibility analysis of multiagent systems, modelling a vehicle that does not change position between to successive measurements or being in sight of two or more agents at the same time instant. The two following theorems, with reference to Facts 8.1.5 and 8.1.6, describe global and local constructibility results and consider the setting where a vehicle is aware of its position sequence $\mathcal{Q}$ in its reference frame $\langle V \rangle$, while the environment is instrumented with fixed sensors with known position B_j, $j = 0, \dots, N_B - 1$ in $\langle W \rangle$.

Theorem 8.1.7 (Global Constructibility)**.** *Given a sequence of points* $\mathcal{Q}$ *with* N_m *measurement points,* necessary conditions *for the system to be* globally constructible *are:* $N_m \geq 4$, *the vehicle collects at most* $N_m - 2$ *range measurements from each anchor* B_j, *and at most* $N_m - 2$ *measurements from each position* $P_k \in \mathcal{Q}$.

Theorem 8.1.8 (Local Constructibility)**.** *Given a sequence of points* $\mathcal{Q}$ *with* N_m *measurement points,* necessary conditions *for the system to be* locally constructible *are:* $N_m \geq 3$, *the vehicle collects at most* $N_m - 1$ *range measurements from each anchor* B_j, *and at most* $N_m - 1$ *measurements from each position* $P_k \in \mathcal{Q}$.

Remark 8.1.9. *In Chapter 4 we have proved a variation of these theorems with the demanding assumption that all the positions* $P_k \in \mathcal{Q}$ *are distinct. The proof is based on finding a rigid transformation* $[{}^W R, {}^W T]$ *from* $\langle V \rangle$ *to* $\langle W \rangle$ *such that* (8.6) *holds true.*

Proof. Since the proofs of Theorem 8.1.7 and Theorem 8.1.8 rely on the same idea, they are presented here together. Starting from Chapter 4, we relax the

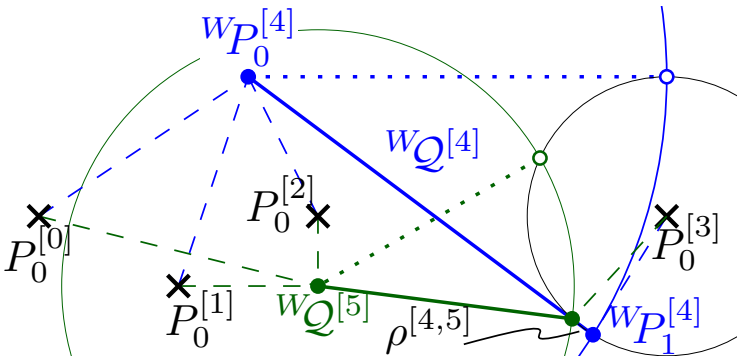

Figure 8.1: Example: the four idle anchor vehicles $V^{[j]}$, $j = 0, \ldots, 3$ are represented by black crosses, and collect their relative distance from the blue $V^{[4]}$ and green $V^{[5]}$ vehicles, which also measure their relative distance $\rho^{[4,5]}$ at their last position. The actual sequence of the vehicles positions are depicted in solid lines, while their *alias* sequences are dotted. When only one target vehicle is considered (system $\mathbb{S}^{-}$), the system is *weakly constructible*, while when both vehicles are considered, the system is *globally constructible*.

condition of non–coincident points and allow for simultaneous measurements, or equivalently, for coincident positions P_k of the vehicle. To show that the last condition in the two theorems is necessary, we follow a symmetric procedure with respect to the proof in Chapter 4, by seeking for a rigid transformation $[{}^{V}R, {}^{V}T]$ from $\langle W \rangle$ to $\langle V \rangle$ such that (8.6) holds true. By symmetry, and since ${}^{W}R = {}^{V}R^{\top}$, and ${}^{W}T = -{}^{V}R^{\top}\,{}^{V}T$, the procedure and the results are equivalent, hence concluding the proof. □

Example 8.1. To visualise the conditions in Theorem 8.1.7 and Theorem 8.1.8, let us consider the scenario in Figure 8.1. The vehicle $V^{[4]}$ (in blue) collects 4 measurements from 4 distinct anchors in position $P_0^{[j]}$, $j = 0, \ldots, 3$, but it collects 3 measurements in its first position ${}^{W}P_0^{[4]}$ and only one from its last position ${}^{W}P_1^{[4]}$. Therefore, it meets the necessary conditions for *local*, but not for *global* constructibility, i.e., in a neighbourhood of the initial vehicle orientation $\theta^{[4]}(0)$ we can distinguish between the solid and the dotted blue lines representing the possible sequences of robot positions stemming from ${}^{W}P_0^{[4]}$. ⋆

Fact 8.1.10. *The analysis in Chapter 4 also reports the* sufficient *conditions for local and global constructibility, where some more properties are required to the relative position of the measurement points and of the fixed sensors, e.g. non–collinearity.*

8.2 Global Constructibility Analysis

In the previous section, we have recalled and proposed some results where the environment is assumed to be equipped with fixed sensors. In this section we shift our focus to multiagent systems measuring their mutual distance, hence dealing with the problem of *relative localisation*. As a first simplification, let us consider the scenario where a set of *anchor vehicles* are deployed in the environment and do not move, i.e. they act as sensors with positions $P^{[i]}(t) = B^{[i]}, \forall\, t$, known in $\langle W \rangle$, and a vehicle V is localising itself with respect to these positions. The extension of the results in Theorem 8.1.7 and Theorem 8.1.8 to this scenario is trivial. As a natural follow–up of this scenario, we consider some anchor vehicles to be *moving* across the environment, while a target vehicle V is localising itself with respect to them. We formalise the problem as follows.

Let us consider a constructible multiagent system, denoted by $\mathbb{S}^-$, composed of N vehicles, whose position sequences ${}^{W}\mathcal{Q}^{[i]}$, $i = 0, \ldots, N-1$, are known in the world reference frame $\langle W \rangle$. By relying on the results stated in the previous sections, we want to find the conditions on the trajectory and measurements collected by an additional vehicle V, such that the new system, denoted by $\mathbb{S}$, achieves local/global constructibility. To analyse this problem, we cast it to a similar problem involving a set of fixed-frame sensors, where results in Theorem 8.1.7 and Theorem 8.1.8 are applicable. Indeed, for any time instant $t_k^{[N]} \in T^{[N]}$, the position $P_k^{[N]}$ of V are known in its local reference frame, and so are the positions ${}^{W}P^{[j]}(t_k^{[N]})$ of the anchor vehicles in $\langle W \rangle$. Therefore, we build the set $\mathcal{B}$

$$\mathcal{B} = \bigcup_{t_k^{[N]} \in T^{[N]}} \mathcal{B}_k, \text{ with } \mathcal{B}_k = \left\{ {}^{W}P^{[j]}(t_k^{[N]}) : j \in \mathcal{N}_k^{[N]} \right\},$$

containing the position of the vehicles (acting as anchors) collecting measurements from the N-th agent. This equivalent single–agent system is locally or globally constructible as long as the conditions in Theorems 8.1.7 and 8.1.8 hold true. Moreover, by the definition of $\mathbb{S}^-$ and $\mathbb{S}$, whenever this single-agent system is (weakly) constructible, so is $\mathbb{S}$. An example is shown in Figure 8.2, where a vehicle added to a constructible system $\mathbb{S}^-$ satisfies the local conditions. When no constructible system $\mathbb{S}^-$ exists, the overall system $\mathbb{S}$ may still be globally constructible, as reported in Example 8.2. However, the analysis of this scenario is still an open problem.

Example 8.2. With reference to Figure 8.1, let $\mathbb{S}^-$ include the anchor vehicles $V^{[j]}$, $j = 0, \ldots, 3$, and the vehicle $V^{[4]}$ (blue). By Theorem 8.1.7, there are two

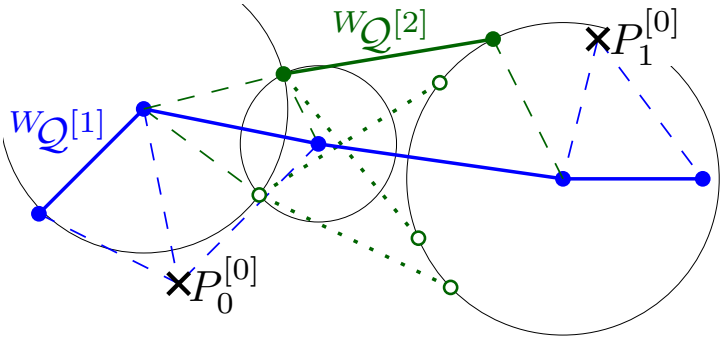

Figure 8.2: Systems $\mathbb{S}^-$ and $\mathbb{S}$. The crosses represent the positions of the anchor vehicle, while the dashed lines represent the measurements collected. The system $\mathbb{S}^-$, with $V^{[1]}$ in blue, is constructible, since the position sequence ${}^{W}\mathcal{Q}^{[1]}$ satisfies the sufficient conditions. The second vehicle with position sequence ${}^{W}\mathcal{Q}^{[2]}$ (solid green line), does not meet the necessary conditions in Theorem 8.1.7, and different rigid transformation of $\mathcal{Q}^{[2]}$ compliant with the measurements from $V^{[1]}$ (black circles) are depicted in dotted lines with the hollow circles. However, system $\mathbb{S}$ is weakly constructible, since small rigid transformations of ${}^{W}\mathcal{Q}^{[2]}$ change the sensor readings.

indistinguishable trajectories, hence $\mathbb{S}^-$ is *weakly constructible*. The system $\mathbb{S}$, where $V^{[5]}$ (green) collects ranging measurements from the anchor vehicles and its distance $\rho^{[4,5]}$ from $V^{[4]}$ at their last time step, is *constructible* because only for the actual trajectories in Figure 8.1 the distance between the last positions of the vehicles is $\rho^{[4,5]}$. Similarly, the same conclusions are drawn when $\mathbb{S}^-$ includes $V^{[5]}$ instead of $V^{[4]}$. ⋆

The main result of this section is a sufficient, but not necessary condition for *global constructibility*, stated in the following fact.

Fact 8.2.1. *When a* globally constructible *subsystem* $\mathbb{S}^-$ *can be identified,* sufficient *conditions for the system* $\mathbb{S}$ *with an added vehicle* V *to be* globally constructible *are given in Theorem 8.1.7 and in Fact 8.1.10, while conditions for* local constructibility *are given in Theorem 8.1.8 and in Fact 8.1.10.*

8.3 Weak Constructibility Analysis

We have considered previously a particular case of multiagent system, where a new vehicle is added to an already constructible system, and we have analysed the properties of the trajectory $\mathcal{Q}^{[N]}$ of the new vehicle and of the measurements collected, while we have shown in Example 8.2 that a system $\mathbb{S}$ may be constructible even though there exist no constructible subsystem $\mathbb{S}^-$. In this section, we analyse the *weak* constructibility properties of a general multiagent

system, which is a remarkable generalisation of what proposed in Chapter 7, where just two agents and fixed anchors were considered. To this aim, we build the Constructibility Gramian of the system and analyse when the contributions given by the measurements are linearly dependent. Since the state of the *anchor vehicle* $V^{[0]}$ is known, we estimate the state $q \in \mathbb{R}^{3(N-1)}$ of the vehicles $V^{[i]}$, $i = 1, \dots, N$. Therefore, when the vehicles in the system collect at least $3(N-1)$ linearly independent measurements, where N is the number of agents and 3 is the dimension of the state of each vehicle, the Constructibility Gramian has full rank, hence the system is *weakly constructible*. At the end of the section, we also propose some geometrical insights, for a 3–agent system, on the results obtained analytically.

8.3.1 Constructibility Gramian

We build the Constructibility Gramian of the multiagent system with state ${}^{W}q(t) \in \mathbb{R}^{3N}$, dynamics (8.1) and intermittent ranging measurements (8.2). Let N_m be the total number of measurements collected by the vehicles, i.e. $N_m = \frac{1}{2}\sum_{i=0}^{N-1} N_m^{[i]}$, where $N_m^{[i]}$ is the number of measurements collected by $V^{[i]}$, while the division by 2 accounts for each measurement involving two vehicles. As in Chapter 4, for a system (8.7) with continuous-time dynamics and discrete-time output, the Constructibility Gramian can be defined as

$$G_C = \sum_{l=1}^{N_m} \gamma_l \gamma_l^\top, \quad \text{with} \quad \gamma_l^\top = \left.\frac{\partial h}{\partial q}\right|_{t=t_l} \Phi(t_l, t_f), \tag{8.8}$$

with t_l denoting the time instant when the l-th measurement is collected. The *sensitivity matrix* $\Phi(t_l, t_f)$ is the unique solution to the final value problem

$$\dot{\Phi}(t_l, t_f) = \left.\frac{\partial f}{\partial q}\right|_{t=t_l} \Phi(t_l, t_f), \qquad \Phi(t_f, t_f) = \mathbf{I}_n.$$

Fact 8.3.1. *For a team of unicycle vehicles* (8.1)*, we compute* $\Phi(t, t_f)$ *in closed form as*

$$\Phi(t, t_f) = \operatorname*{diag}_i \left\{ \begin{bmatrix} 1 & 0 & -\left(y^{[i]}(t) - y^{[i]}(t_f)\right) \\ 0 & 1 & x^{[i]}(t) - x^{[i]}(t_f) \\ 0 & 0 & 1 \end{bmatrix} \right\}, \tag{8.9}$$

where $\operatorname{diag}_i\{M_i\}$ *is a block diagonal matrix with blocks* M_i*.*

From (8.9) we can compute explicitly the expression of the contributions γ_l to the Constructibility Gramian. Let us consider the measurement represented in Figure 8.3. The slope of the line joining the two vehicles is $\alpha_k^{[i,j]} =$

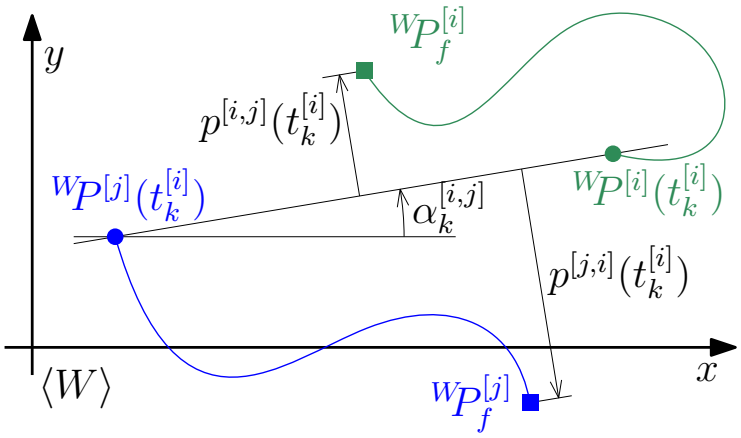

Figure 8.3: Quantities that affect the vector $\gamma_k^{[i,j]}$ of a measurement between vehicles $V^{[i]}$ and $V^{[j]}$. The two circles represent the position $P^{[i]}$ and $P^{[j]}$ of the two vehicles at the current time instant $t_k^{[i]}$, while the two squares denote their final positions P_f. The quantities that define the vector $\gamma_k^{[i,j]}$ are $\alpha_k^{[i,j]}$, $p_k^{[i,j]}$ and $p^{[j,i]}(t_k^{[i]})$.

$\arctan2\left({}^{W}P_k^{[i]} - {}^{W}P^{[j]}(t_k^{[i]})\right)$. By this definition, $\alpha^{[j,i]}(t_k^{[i]}) = \pi + \alpha_k^{[i,j]}$. The *signed* distances of the final points from the line joining the two vehicles are

$$p_k^{[i,j]} = \frac{1}{\rho_k^{[i,j]}} \det\left[{}^{W}P_f^{[i]} - {}^{W}P_k^{[i]},\quad {}^{W}P^{[j]}(t_k^{[i]}) - {}^{W}P_k^{[i]}\right],$$
$$p^{[j,i]}(t_k^{[i]}) = \frac{-1}{\rho_k^{[i,j]}} \det\left[{}^{W}P_f^{[j]} - {}^{W}P^{[j]}(t_k^{[i]}),\ {}^{W}P_k^{[i]} - {}^{W}P^{[j]}(t_k^{[i]})\right]$$

A measurement $\rho_k^{[i,j]}$, as represented in Figure 8.3, gives the Constructibility Gramian a contribution $\gamma_k^{[i,j]}$

$$\gamma_k^{[i,j]} = \underline{e}_i^{\top} \odot \begin{bmatrix} \cos\alpha_k^{[i,j]} \\ \sin\alpha_k^{[i,j]} \\ p_k^{[i,j]} \end{bmatrix} - \underline{e}_j^{\top} \odot \begin{bmatrix} \cos\alpha_k^{[i,j]} \\ \sin\alpha_k^{[i,j]} \\ p^{[j,i]}(t_k^{[i]}) \end{bmatrix}, \tag{8.10}$$

where $\odot$ denotes the Kronecker product and $\underline{e}_i$ is the unitary row vector aligned with the i-th axis of $\mathbb{R}^{N-1}$ and $\underline{e}_0 = \mathbf{0}$. To build the Constructibility Gramian, we take the sum of these contributions, with the constraint $j < i$ to avoid mutual measurements be considered twice and to include the measurements collected from the reference vehicle $V^{[0]}$. Therefore,

$$G_C = \sum_{i=1}^{N-1} \sum_{t_k^{[i]} \in \Theta^{[i]}} \sum_{\substack{j \in \mathcal{N}_k^{[i]} \\ j<i}} \gamma_k^{[i,j]} \gamma_k^{[i,j]\top}, \tag{8.11}$$

where each term $\gamma_k^{[i,j]}{\gamma_k^{[i,j]}}^\top$ is a $3(N-1) \times 3(N-1)$ matrix with rank 1. We want to find the conditions on the measurements collected by the vehicles such that the Gramian has full rank, thus guaranteeing weak constructibility.

8.3.2 Three-agent System

For the sake of simplicity, let us consider a system composed of three vehicles $V^{[i]}$, $i = 0, 1, 2$, where the world reference frame $\langle W \rangle$ coincides with the reference frame $\langle V^{[0]} \rangle$ of the first vehicle. We seek sufficient conditions on the measurements to achieve a full–rank Gramian. To this aim, we analyse the contributions given by all the measurements and draw some considerations on their linear dependence. By using (8.10), we compute the two contributions $\gamma^{[1,0]}$ and $\gamma^{[2,0]}$ given by measurements involving the vehicle $V^{[0]}$, and the contribution $\gamma^{[1,2]}$ given by the relative measurement between $V^{[1]}$ and $V^{[2]}$, where the subscript k is dropped for brevity.

$$
\begin{aligned}
\gamma^{[1,0]} &= [\, C^{[1,0]} \,;\, S^{[1,0]} \,;\, p^{[1,0]} \,;\quad 0 \quad ;\quad 0 \quad ;\quad 0 \quad]^\top, \\
\gamma^{[2,0]} &= [\quad 0 \quad ;\quad 0 \quad ;\quad 0 \quad ;\quad C^{[2,0]} \,;\quad S^{[2,0]} \,;\quad p^{[2,0]} \,]^\top, \\
\gamma^{[1,2]} &= [\, C^{[1,2]} \,;\, S^{[1,2]} \,;\, p^{[1,2]} \,;\, -C^{[1,2]} \,;\, -S^{[1,2]} \,;\, -p^{[2,1]} \,]^\top,
\end{aligned}
$$

where $C^{[i,j]}$ and $S^{[i,j]}$ are short notations for $\cos\alpha^{[i,j]}$ and $\sin\alpha^{[i,j]}$, respectively. By definition, each contribution $\gamma^{[i,j]}{\gamma^{[i,j]}}^\top$ is a matrix with rank 1, and thus 6 measurements are needed to have a full rank Gramian, provided that their contributions $\gamma^{[i,j]}$ are linearly independent, as stated in the following Lemma.

Lemma 8.3.2. *Let $\mu_k \in \mathbb{R}^n$, $k = 1, \ldots, N_\mu$, be a set of vectors. The matrix $\overline{M}$ having the vectors μ_k as columns has the same rank as the matrix $M = \sum_{k=1}^{N_\mu} \mu_k \mu_k^\top$.*

Proof. We prove this result by showing that the null spaces of the matrices $\overline{M}^\top$ and M coincide. Let $w \in \mathbb{R}^n$ belong to the null space of $\overline{M}^\top$, i.e. $\overline{M}^\top w = 0$. By the definition of $\overline{M}$, w is such that $\mu_k^\top w = 0, \forall\, k$, and thus $Mw = \sum_{k=1}^{N} \mu_k \mu_k^\top w = 0$, hence w belongs to the null space of M. Let $w \in \mathbb{R}^n$ be a vector of the null space of M. Then, by definition of M, $\sum_{k=1}^{N} w^\top \mu_k \mu_k^\top w = 0$. Matrices $\mu_k \mu_k^\top$ are symmetric and positive semidefinite, therefore all the terms $w^\top \mu_k \mu_k^\top w$ are non–negative. Thus, the summation is 0 if and only if $w^\top \mu_k \mu_k^\top w = 0, \forall\, k = 1, \ldots, N_\mu$. Therefore, w must belong to the null space of $\overline{M}^\top$, hence concluding the proof. □

In light of Lemma 8.3.2, we can get results on the rank of the Constructibility Gramian by analysing the terms $\gamma_k^{[i,j]}$ and their linear dependence. To this

aim, we first analyse the conditions when measurements between the same pair of agents generate linearly dependent column spaces $\gamma_k^{[i,j]}$. For each measurement, we define a line with slope $\alpha_k^{[i,j]}$ joining the two points involved in the measurement.

Lemma 8.3.3 (Same pair of vehicles)**.** *Given two vehicles collecting N_m measurements of their mutual distance, the maximum rank achieved by the Constructibility Gramian is* 3*. Moreover, (1) For any N_m, the Gramian has rank* 1 *when the $2N_m$ points involved in the measurements are aligned; (2) for any $N_m \geq 3$, the Gramian has rank* 2 *when the lines associated with each measurement have a common intersection, or are parallel.*

Proof. For the sake of simplicity, we will consider the pair $V^{[1]}$–$V^{[0]}$. Each measurement generates a contribution $\gamma_k^{[1,0]}{\gamma_k^{[1,0]}}^\top$ with rank 1 and only 3 non–zero entries, hence the maximum rank of the Gramian is 3.

With two measurements, dependence is achieved when $\gamma_1^{[1,0]} = \ell\gamma_2^{[1,0]}$, $\ell \in \mathbb{R}$. Two terms constrain the two lines to have the same slope, while the third one imposes that the (signed) distance $p^{[1,0]}$ between the final position and these lines be the same, hence the two lines must coincide. This result can be extended to any number of measurements where all the involved points are aligned.

With three non-collinear measurements, by Lemma 8.3.2, we build the matrix Γ having the first three entries of $\gamma_1^{[1,0]}$, $\gamma_2^{[1,0]}$ and $\gamma_3^{[1,0]}$ as columns, and compute its determinant. $\det\Gamma = m_1(\delta_3 - \delta_2) + m_2(\delta_1 - \delta_3) + m_3(\delta_2 - \delta_1)$, where $m_k = \tan\alpha_k^{[1,0]}$ is the slope of the k-th line and $\delta_k = {}^W y_k^{[1]} - m_k {}^W x_k^{[1]}$ is its y-intercept. The determinant is 0 as long as these three lines have one common intersection, or are parallel. The proof can be extended to any number of measurements with similar arguments. □

This result includes one of the conditions in Theorem 8.1.8. Indeed, when a vehicle collects 3 or more measurement from an idle anchor vehicle, all the lines associated with the measurements intersect in the position of the anchor vehicle, while when a still vehicle collects 3 or more measurements, all the lines associated with the measurements intersect in the location of the robot.

Besides linear dependence between measurements collected by the same pair of vehicles, dependence may occur also when different pairs of vehicles are taken into account. By the structures of the terms $\gamma_k^{[i,j]}$, we need to involve all the 3 pairs of vehicles in a 3–agent system. To analyse this scenario, we introduce the definition of *agent–wise linear independence.*

Definition 8.3.4 (Agent–wise linear independence)**.** *Let us consider a set of ranging measurements $\rho_k^{[i,j]}$ involving the i-th agent. The measurements are said to be* linearly independent with respect to vehicle $V^{[i]}$ *if the entries of*

the vectors $\gamma_k^{[i,j]}$ *corresponding to the agent* $V^{[i]}$*, i.e.* $\gamma_k^{[i]} = (\underline{e}_i \odot \mathbf{I}_3)\,\gamma_k^{[i,j]}$*, are linearly independent.*

With a slight abuse of notation, we will refer to a *measurement agent–wise dependent with respect to agent* $V^{[i]}$ as to a measurement that does not provide any constructibility contribution given the set of measurements previously collected by $V^{[i]}$.

For the sake of simplicity, we initially consider the particular case where one of the 3 pairs arising in a 3–agent system collects its first measurement. This way we analyse the conditions when linear dependence arises among distinct pairs of agents.

Lemma 8.3.5 (Different pairs of vehicles)**.** *Let us consider a* 3*–agent system, whose* 3 *pairs have collected* n_1*,* n_2*, and* 0 *linearly independent measurements, respectively, i.e. the rank of the Constructibility Gramian is* $n_1 + n_2$*, with* $n_1, n_2 \leq 3$*. A measurement collected by the pair that has collected* 0 *measurements increases by* 1 *the rank of the Constructibility Gramian, unless it is agent–wise linearly dependent with respect to both the agents involved in the measurement.*

Proof. Without loss of generality, consider this scenario: the pair $V^{[0]}$–$V^{[1]}$ has collected 3 linearly independent measurements (i.e. the system $\mathbb{S}^-$ consisting of this pair is weakly constructible), while the pair $V^{[0]}$–$V^{[2]}$ has collected n_2 measurements. The pair $V^{[1]}$–$V^{[2]}$ collects its first measurement. By Lemma 8.3.2, the Constructibility Gramian has the same rank as a matrix Γ having the vectors $\gamma_k^{[i,j]} \in \mathbb{R}^6$ as columns, with

$$\Gamma = \left[\begin{array}{c|ccc|c} \Gamma^{[1,0]} & \multicolumn{3}{c|}{0} & \begin{matrix} C_3^{[1,2]} \\ S_3^{[1,2]} \\ p_3^{[1,2]} \end{matrix} \\ \hline 0 & \begin{matrix} C_0^{[2,0]} \\ S_0^{[2,0]} \\ p_0^{[2,0]} \end{matrix} & \begin{matrix} C_1^{[2,0]} \\ S_1^{[2,0]} \\ p_1^{[2,0]} \end{matrix} & \begin{matrix} C_2^{[2,0]} \\ S_2^{[2,0]} \\ p_2^{[2,0]} \end{matrix} & \begin{matrix} -C_3^{[1,2]} \\ -S_3^{[1,2]} \\ -p_3^{[2,1]} \end{matrix} \end{array}\right], \tag{8.12}$$

where the first three columns gather the terms $\gamma_k^{[1,0]}$ and $\Gamma^{[1,0]}$ is a 3×3 non–singular matrix by assumption. We now consider an increasing number of columns in the second block, associated with the measurements $\rho_k^{[2,0]}$, which is equal to n_2. We remark that, since $\Gamma^{[1,0]}$ is full rank, any contribution $\gamma_3^{[1,2]}$ will be agent–wise linearly dependent with respect to $V^{[1]}$.

$\mathbf{n_2 = 0}$: The last column, i.e. $\gamma_3^{[1,2]}$, is the first measurement involving $V^{[2]}$, and thus it is clearly agent–wise independent with respect to $V^{[2]}$ itself. Since the last three entries are non–zero, $\gamma_3^{[1,2]}$ increases by 1 the rank of Γ.

$\mathbf{n_2 = 1}$ **or** $\mathbf{n_2 = 2}$: We exploit the block structure of Γ, and look at the last three rows. When considering the role of the measurement $\rho_3^{[1,2]}$, the same conditions as in Lemma 8.3.3 apply, i.e. $\rho_3^{[1,2]}$ does not increase the rank if it is collected on the same line as the only measurement $\rho_1^{[2,0]}$ ($n_2 = 1$), or when the three lines associated with the three measurements intersect in a single point ($n_2 = 2$).

$\mathbf{n_2 = 3}$: The Gramian is full rank, and the contribution $\gamma_3^{[1,2]}$ is agent–wise dependent with both $V^{[1]}$ and $V^{[2]}$.

We can adapt the same procedure to the cases with lower values of n_1, where the agent–wise dependence conditions must hold true for both $V^{[1]}$ and $V^{[2]}$ simultaneously, hence concluding the proof. □

Since there is no explicit time dependence, Lemmas 8.3.3 and 8.3.5 cover all the cases where one pair has collected three independent measurements. Since a system with 6 independent measurements is already constructible, only one situation is left to analyse: two pairs have collected 2 independent measurements, while the last pair is collecting its second measurement.

Lemma 8.3.6 (Same and different pairs of vehicles)**.** *Let us consider a* 3*–agent system, whose* 3 *pairs of vehicles have collected* 2*,* 2 *and* 1 *agent–wise* linearly independent *measurements, respectively, i.e. the rank of the Constructibility Gramian is* 5*. A further measurement* $\rho_k^{[i,j]}$*, collected by the pair that has collected only* 1 *measurement, increases to* 6 *the rank of the Constructibility Gramian unless* ${}^{W}P^{[j]}(t_k^{[i]})$ *lies on the line passing through* ${}^{W}P_k^{[i]}$ *having a slope that depends on the other* 5 *measurements and on* ${}^{W}P_k^{[i]}$ *itself.*

Proof. Without loss of generality, let us consider the pair $V^{[1]}$–$V^{[2]}$ to collect the last measurement $\rho_k^{[1,2]}$ with the position ${}^{W}P_k^{[1]}$ fixed on the plane, while ${}^{W}P_k^{[2]} = [{}^{W}x_k^{[2]}, {}^{W}y_k^{[2]}]^\top$. As in (8.12), we build the matrix Γ having as columns the 6 vectors $\gamma_k^{[i,j]}$. Matrix Γ is singular whenever $\det\Gamma = a\,{}^{W}x_k^{[2]} + b\,{}^{W}y_k^{[2]} + c = 0$, where the coefficients a, b and c depend on the other measurements and are such that $a\,{}^{W}x_k^{[1]} + b\,{}^{W}y_k^{[1]} + c = 0$, i.e. describing a line passing through the position ${}^{W}P_k^{[1]}$. If ${}^{W}P_k^{[2]}$ lies on this line, then, by Lemma 8.3.2, the Constructibility Gramian is singular, and thus the system is *unconstructible.* □

In light of the results in Lemmas 8.3.3, 8.3.5 and 8.3.6, we can state the main result of this analysis.

Proposition 8.3.7 (3–agent system)**.** *A* 3*–agent system is weakly constructible if: (1) a number of* $N_m \geq 6$ *measurements is collected, (2) each pair collects at most* $N_m - 3$ *measurements, (3) each vehicle satisfies the conditions in Theorem 8.1.8 (i.e. the critical cases in Lemmas 8.3.3 and 8.3.5 do not occur).*

Moreover, if each pair of agents collects 2 *measurements, then the conditions in Lemma 8.3.6 need to be satisfied.*

By Proposition 8.3.7, 6 measurements can be sufficient for *weak* constructibility in a 3–agent system. Since constructibility properties do not change with the reference frame, we can split the 6 measurements among the 3 pairs of vehicles in 3 ways: 3–3–0, 3–2–1, and 2–2–2, where, without loss of generality, we list in order the three pairs $V^{[0]}$–$V^{[1]}$, $V^{[0]}$–$V^{[2]}$, and $V^{[1]}$–$V^{[2]}$. In the 3–3–0 scenario, both $V^{[1]}$ and $V^{[2]}$ collect three measurements from $V^{[0]}$, without interacting with each other. They independently fulfil the conditions in Theorem 8.1.8, thus achieving weak constructibility. The same conclusion is drawn for the pair $V^{[0]}$–$V^{[1]}$ in the 3–2–1 setting, thus generating a weakly constructible subsystem $\mathbb{S}^-$, as described in Figure 8.2. Vehicle $V^{[2]}$ collects 3 measurements from $\mathbb{S}^-$, satisfying the conditions in Theorems 8.1.8, and thus the system $\mathbb{S}$ is weakly constructible. In the case 2–2–2, the system cannot be decomposed into weakly constructible subsystems as in the previous situations, but all the agents are needed to achieve weak constructibility of the whole system, as in Lemma 8.3.6.

8.3.3 Geometry of Constructibility

From a geometrical perspective, we consider the sets of points $\mathcal{Q}^{[1]}$ and $\mathcal{Q}^{[2]}$ as rigid bodies, whose positions and orientations are constrained by the collected measurements. Figure 8.4 shows a scenario where two vehicles $V^{[1]}$ and $V^{[2]}$ collect two measurements from $V^{[0]}$ each, and a mutual measurement. With the measurements in ${}^{W}P_0^{[1]}$ and ${}^{W}P_1^{[1]}$, the pair $V^{[0]}$–$V^{[1]}$ does not change its sensor readings when $\mathcal{Q}^{[1]}$ slightly rotates about J_1; indeed the circles centred in J_1 and in ${}^{W}P_0^{[0]}$ share the same tangent in ${}^{W}P_0^{[1]}$, and analogously for ${}^{W}P_1^{[1]}$. Therefore, any *allowed* motion of $\mathcal{Q}^{[1]}$, i.e. different choice of $[\tilde{R}^{[1]}, \tilde{T}^{[1]}]$ such that (8.6) still holds true, makes the point ${}^{W}P_2^{[1]}$ *locally* move on the tangent of the circle centred in J_1. The same applies to $V^{[2]}$ with respect to J_2. Since the measurement $\rho_2^{[1,2]}$ is collected on the line joining J_1 and J_2, i.e. the degenerate case in Lemma 8.3.5 occurs, the tangents to the circles centred on J_1 and J_2 passing through ${}^{W}P_2^{[1]}$ are aligned, and thus any *allowed* motion of $\mathcal{Q}^{[1]}$ and $\mathcal{Q}^{[2]}$ generates no *local* changes in the term $\gamma_2^{[1,2]}$. Therefore, in this particular configuration of the system, the measurement $\gamma_2^{[1,2]}$ does not add further information to the system, and the number of *informative* measurements, i.e., the rank of the Constructibility Gramian remains 4.

In general, we can interpret a measurement $\rho_k^{[i,j]}$ as a physical constraint between two different rigid bodies that are described by the sequences of positions $\mathcal{Q}^{[i]}$ and $\mathcal{Q}^{[j]}$. As a consequence, a measurement $\rho_k^{[i,j]}$ increases the information

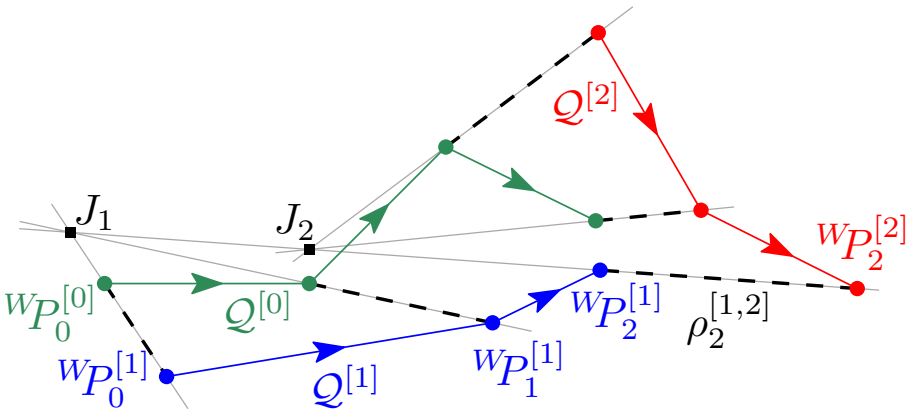

Figure 8.4: A 2–2–1 scenario. The three vehicles (with position sequences $\mathcal{Q}^{[i]}$, $i = 0, 1, 2$ represented by coloured dots and connected by solid lines) collect ranging 5 measurements (dashed black lines), each of them defining a line (grey thin line). The measurements associated with $V^{[1]}$ intersect in J_1, while the ones related to $V^{[2]}$ intersect in J_2. The line associated with the measurement $\rho_2^{[1,2]}$ passes through J_1 and J_2, thus not increasing the rank of the Constructibility Gramian, by Proposition 8.3.7.

in the system (quantified through the rank of the Constructibility Gramian), as soon as it introduces a *non–redundant* constraint in the system itself. By nature of the constraint $\rho_k^{[i,j]}$, the measurement is *redundant* as soon as its associated line is both orthogonal to translations of ${}^{W}P_k^{[i]}$ generated by *allowed* motions of $\mathcal{Q}^{[i]}$ and orthogonal to translations of ${}^{W}P^{[j]}(t_k^{[i]})$ generated by *allowed* motions of $\mathcal{Q}^{[j]}$.

8.3.4 The Case with $N > 3$ Agents

We leverage the results obtained for a 3–agent system to extend the analysis to an arbitrarily high number N of agents in the system. Unlike Lemma 8.3.3, the results in Lemma 8.3.5 have to be adapted to the increased number of agents in the network. To this aim, we consider three vehicles $V^{[i]}$, $V^{[l]}$ and $V^{[j]}$ and the measurements $\rho_k^{[l,i]}$ and $\rho_k^{[l,j]}$. These measurements generate *virtual* measurements $\overline{\rho}_k^{[i,j]}$ associated with the contributions $\overline{\gamma}_k^{[i,j]}$.

Lemma 8.3.8 (Virtual measurements)**.** *Let us consider three vehicles $V^{[i]}$, $V^{[j]}$ and $V^{[l]}$ such that the independent measurements $\rho_k^{[l,i]}$, $k = 0, \dots, n^{[l,i]} - 1$ and $\rho_k^{[l,j]}$, $k = 0, \dots, n^{[l,j]} - 1$ are collected. For each of the $n^{[l,j]}$ contributions $\gamma_k^{[l,j]}$ that are* agent–wise linearly dependent *on the terms $\gamma_k^{[l,i]}$, $k = 0, \dots, n^{[l,i]} - 1$* with respect to $V^{[l]}$*, we can build the linearly independent* virtual contributions

$\overline{\gamma}_k^{[i,j]}$, $k = 0, \ldots, \overline{n}^{[i,j]} - 1$,

$$\overline{\gamma}_k^{[i,j]} = \gamma_k^{[l,j]} - \sum_{\kappa=0}^{n^{[l,i]}-1} \beta_\kappa \gamma_\kappa^{[l,i]},$$

where the coefficients β_κ *are such that*

$$\left(\underline{e_l} \odot \mathbf{I}_3\right) \left(\gamma_k^{[l,j]} - \sum_{\kappa=0}^{n^{[l,i]}-1} \beta_\kappa \gamma_\kappa^{[l,i]} \right) = 0.$$

Proof. By construction, the vectors $\overline{\gamma}_k^{[i,j]}$ have non–zero values only in the entries associated with $V^{[i]}$ and $V^{[j]}$. Moreover, since the terms $\gamma_k^{[l,j]}$ are independent by assumption, so are the virtual contributions $\overline{\gamma}_k^{[i,j]}$. □

In light of the considerations in Section 8.3.3, the measurements $\rho_k^{[1,0]}$ and $\rho_k^{[2,0]}$ in Figure 8.4, generate virtual measurements $\overline{\rho}^{[1,2]}$. Indeed, the sequence of points $\mathcal{Q}^{[1]}$ is allowed to rotate about the point J_1, while $\mathcal{Q}^{[2]}$ is allowed to rotate about J_2, and thus, when $V^{[1]}$ and $V^{[2]}$ lie on the line joining J_1 and J_2, their distance is constrained even though no measurements are collected between them, as if they were *virtually constrained* by a measurement $\overline{\rho}^{[1,2]}$.

Intuitively, by Lemma 8.3.5, a measurement $\rho_k^{[i,j]}$ that is agent–wise linearly dependent on both $V^{[i]}$ and $V^{[j]}$ is not increasing the rank of the Constructibility Gramian, and thus its carried information is already available in the system. Therefore, there is no structural difference between actual measurements collected by the pair $V^{[i]}$–$V^{[j]}$ and measurements collected by the two agents from an intermediate vehicle $V^{[l]}$.

Remark 8.3.9. *The procedure in Lemma 8.3.8 does not account for actual measurements collected by the pair* $V^{[i]}$–$V^{[j]}$*, but the results in Lemma 8.3.6 hold true for this situation.*

The results in Lemma 8.3.8, with Remark 8.3.9, hold true for any sequence of *intermediate* agents $V^{[i_w]}$, $w = 0, \ldots, n$, with $i_0 = i$ and $i_n = j$, where each iteration of the procedure removes an agent from the sequence, until reaching the same situation detailed out above.

Corollary 8.3.10. *In a sequence of vehicles* $V^{[i_w]}$, $w = 0, \ldots, m$, *the maximum dimension of the subspace spanned by the virtual contributions* $\overline{\gamma}_k^{[i_0,i_m]}$ *is equal to the smallest dimension of the subspace spanned by the vectors* $\gamma_k^{[i_w,i_{w+1}]}$, $w = 0, \ldots, m-1$.

Proof. By Lemma 8.3.8, $n^{[i_0,i_m]} \leq \min\{n^{[i_0,i_1]}, n^{[i_1,i_m]}\}$, and recursively $n^{[i_0,i_m]} \leq \min_{w\in[0,m-1]} n^{[i_w,i_{w+1}]}$. □

With Lemma 8.3.8, Corollary 8.3.10 and Lemma 8.3.6, each vehicle $V^{[i]}$ computes its set of measurements (both actual and virtual) collected from the reference vehicle $V^{[0]}$. Therefore, any incoming measurement $\rho^{[i,j]}$ can be checked for linear dependence against the *previous* contributions $\gamma_k^{[i,0]}$, $\gamma_k^{[j,0]}$ and $\gamma_k^{[i,j]}$. If the new measurement is dependent on the previous ones, then it adds no further information to the system and can be neglected; otherwise, each vehicle updates its set $\rho_k^{[i,0]}$ given the additional measurement that has been collected. This procedure guarantees that, as soon as $3N$ measurements are considered, the system is *weakly constructible*, i.e. the Constructibility Gramian is full rank. Proposition 8.3.11 sums up the results discussed and obtained in this section.

Proposition 8.3.11. *Given an N-agent system, the system is weakly constructible if the vehicles collect a number $N_m \geq 3(N-1)$ of measurements that is* linearly independent *on the measurements previously collected, where* linear independence *is checked with the procedure described in Lemma 8.3.3, Lemma 8.3.6 and Lemma 8.3.8.*

9 A Multiagent Trajectory Planning Scenario

Contents

In Chapter 7 we have proposed a trajectory planning scenario for a pair of unicycle–like vehicles to achieve global constructibility, where each manoeuvre is planned based only on the current knowledge on the state acquired along the trajectory. This planning algorithm is based on the demanding and unrealistic assumption that the measurements are not corrupted by noise, thus making the algorithm not directly applicable to real–life robotic scenarios. In this chapter, we move the first steps towards the application of trajectory planning techniques without prior state information to the robotic domain by including the effect of sensor noises in the planning algorithm. As a common practice in marine robotics, we consider the vehicles to be equipped with a ranging sensor, a depth sensor and a compass, or an equivalent sensor, measuring the orientation of the vehicles with low uncertainty. These assumptions allow us to simplify the analysis, by dealing with a planar problem, and come up with some closed–form solutions.

Contributions: We consider a system composed of a tracker and a target vehicle, modelled as unicycle robots. The tracker measures its distance from a fixed sensor and its distance from the target that broadcasts its future manoeuvres. The tracker, without *a priori* information, aims at minimising simultaneously the estimation uncertainty on its position and on the position of the target. The trajectory planning algorithm consists in two phases: in the initial phase, the tracker estimates the positions of the beacon and of the target in its reference frame by means of trilateration and, by translation, estimates its position and the position of the target in the beacon's reference frame, with the associated uncertainty. In the second phase, the tracker plans its manoeuvres, in an MPC–like framework, to maximise the smallest eigenvalue of the Position Gramian, a variation of the Constructibility Gramian, associated with the estimation uncertainty. We show with examples that the second phase is not sufficient to guarantee the convergence of an Extended Kalman Filter, especially when the initial estimate of the position of the tracker is rough. Moreover, we show that the approach is robust to actuation uncertainties, although they are not explicitly considered in the planning algorithm.

9.1 Problem Description

9.1.1 System model

We consider a tracker and a target vehicle, denoted by the subscripts P and Q, respectively. Both are described by the discrete–time unicycle kinematic model,

whose state consists of the x, y coordinates of the vehicle and of its orientation θ with respect to the world reference frame $\langle W \rangle$. The model can be written as

$$x_{k+1} = x_k + A_k C_k, \quad y_{k+1} = y_k + A_k S_k, \quad \theta_{k+1} = \theta_k + \omega T_s, \tag{9.1}$$

$$A_k = 2\frac{v_k}{\omega_k} \sin\left(\omega_k \frac{T_s}{2}\right), \quad \lim_{\omega_k \to 0} A_k = v_k T_s,$$
$$C_k = \cos(\phi_k), \quad S_k = \sin(\phi_k), \quad \phi_k = \theta_k + \omega_k \frac{T_s}{2},$$

where T_s is the duration of the sampling interval where the forward velocity v_k and the angular velocity ω_k of the vehicle are constant. We build the state of the whole system q_k by stacking the state vectors of the two vehicles, thus $q_k = [x_{P,k}, y_{P,k}, \theta_{P,k}, x_{Q,k}, y_{Q,k}, \theta_{Q,k}]^\top$.

9.1.2 Sensor model

Each vehicle is provided with a compass measuring its heading θ_k. Moreover, the tracker is equipped with two ranging sensors, one measuring its distance from a fixed–frame beacon $B = [X; Y]^\top$ with known coordinates, and the other measuring the distance between the tracker and the target. We assume the compasses to be more accurate than the ranging sensors, and thus we consider the vehicles to be aware of their (almost) exact heading θ_k at any time instant k. Therefore, we build as subset of the measurement output vector of the system, reading as

$$z_k = \begin{bmatrix} \|P_k - B\|; & \|P_k - Q_k\| \end{bmatrix}^\top, \tag{9.2}$$

where $\|\cdot\|$ denotes the Euclidean norm, while $P_k = [x_{P,k}, y_{P,k}]^\top$ and $Q_k = [x_{Q,k}, y_{Q,k}]^\top$ represent the positions of the tracker and of the target, respectively, at time k. Furthermore, the range measurements given by each of the two ranging sensors are corrupted by a white Gaussian noise with covariance matrix $\eta \mathbf{I}_2$, where $\mathbf{I}_2$ is the 2×2 identity matrix.

Remark 9.1.1. *Unlike the scenarios analysed in the previous chapters, the presence of the sensors measuring θ_k for both vehicles makes the system observable also when the vehicle is sensed by a single ranging sensor.*

9.1.3 Problem statement

Given a fixed beacon, a target vehicle and a tracker vehicle described by the models (9.1) and (9.2), we want to plan the trajectory of the tracker vehicle such

that it can simultaneously localise itself and the target vehicle, i.e. to estimate the state vector q_k of the whole system, with the smallest uncertainty.

To tackle the problem, we need a metric to quantify the amount of information (and in turn, the residual uncertainty) that is collected by the tracker along its trajectory. To this end, we introduce a variation of the standard Constructibility Gramian [Krener and Ide, 2009].

9.2 Position Gramian

In light of the different levels of measurement noise of the two kinds of sensors, we define a variation of the Constructibility Gramian (or, with the same results, of the Observability Gramian). Our version is restricted to the position coordinates P_k, Q_k, instead of the state q_k of the whole system, and thus it is referred to as *Position Gramian* (PG). The PG, devised from the Constructibility Gramian, is defined as

$$G_P = \Pi_0^{-1} + \frac{1}{\eta}\sum_{k=1}^{k_f} \gamma_k \gamma_k^\top, \quad \gamma_k^\top = \left[\frac{\partial z_k}{\partial P_k}\frac{\partial P_k}{\partial P_f}; \quad \frac{\partial z_k}{\partial Q_k}\frac{\partial Q_k}{\partial Q_f}\right], \tag{9.3}$$

where P_f and Q_f represent the positions of the two vehicles at the final time instant k_f, while Π_0 is the error covariance matrix associated with the initial estimate of the *positions* of the two vehicles. In the following, we will refer to the *running* part of the PG as $G = G_P - \Pi_0^{-1}$. By the dynamics of the system, the *sensitivity matrices* $\partial P_k/\partial P_f$ and $\partial Q_k/\partial Q_f$ are equal to the identity matrix[1], and thus γ_k can be computed explicitly as

$$\gamma_k^\top = \begin{bmatrix} \cos\alpha_{B,k} & \sin\alpha_{B,k} & 0 & 0 \\ \cos\alpha_{Q,k} & \sin\alpha_{Q,k} & -\cos\alpha_{Q,k} & -\sin\alpha_{Q,k} \end{bmatrix}, \tag{9.4}$$

where $\alpha_{B,k} = \arctan2(P_k - B)$ and $\alpha_{Q,k} = \arctan2(P_k - Q_k)$.

Therefore, the *running* part of the PG is

$$G = \left[\begin{array}{c|c} A+M & -M \\ \hline -M & M \end{array}\right], \tag{9.5}$$

[1]The Observability Gramian involves the sensitivity with respect to the initial positions P_0 and Q_0. The sensitivity matrices $\partial P_k/\partial P_0$ and $\partial Q_k/\partial Q_0$ are equal to the identity, and thus the derivation through the two Gramians leads to the same PG.

where $A \in \eta^{2\times 2}$ refers to the absolute ranging measurements, and is defined as

$$A = \frac{1}{\eta}\begin{bmatrix} \sum_{k=1}^{k_f} C_{B,k}^2 & \sum_{k=1}^{k_f} C_{B,k}S_{B,k} \\ \sum_{k=1}^{k_f} C_{B,k}S_{B,k} & \sum_{k=1}^{k_f} S_{B,k}^2 \end{bmatrix}, \tag{9.6}$$

where $C_{B,k}$ and $S_{B,k}$ are short notations for $\cos\alpha_{B,k}$ and $\sin\alpha_{B,k}$, respectively, while M is defined analogously with $\alpha_{Q,k}$ in place of $\alpha_{B,k}$.

Since the PG is related to the inverse of the error covariance matrix of an optimal estimator [Salaris et al., 2019], we want to find the trajectory of the tracker vehicle that maximises the smallest eigenvalue of the PG in (9.5) (**E**–optimality criterion).

9.2.1 Analysis of a single vehicle

In the simplified scenario with only one vehicle (be it a vehicle localising itself or a tracker vehicle localising a fixed/moving target), the running part of the PG coincides with matrix A, with $N = k_f - 1$ the number of measurements collected. We present here a known result for this scenario.

Proposition 9.2.1. *Let us consider a system with a single vehicle. Its PG, defined as* $G_P = \Pi_0^{-1} + A$, *(*A *as in* (9.6)*) is* optimal, *i.e. its smallest eigenvalue is maximum, when*

$$G_P = \frac{1}{2}\left(Tr\left(\Pi_0^{-1}\right) + \frac{N}{\eta}\right)\mathbf{I}_2,$$

where $Tr(\cdot)$ *denotes the trace of a matrix.*

Proof. Let the initial error covariance matrix Π_0 be such that

$$\Pi_0^{-1} = \begin{bmatrix} a & b \\ b & c \end{bmatrix}.$$

Since G_P is a 2×2 matrix, we can extract the explicit expression of its smallest eigenvalue $\lambda_1(G_P)$ as

$$\lambda_1(G_P) = \frac{1}{2}\Bigg(a + c + \frac{N}{\eta} - \left(\left(a + \frac{\sum_{k=1}^{k_f}\cos^2\alpha_{B,k}}{\eta} - c - \frac{\sum_{k=1}^{k_f}\sin^2\alpha_{B,k}}{\eta}\right)^2 + 4\left(b + \frac{\sum_{k=1}^{k_f}\sin\alpha_{B,k}\cos\alpha_{B,k}}{\eta}\right)^2\right)^{\frac{1}{2}}\Bigg) \tag{9.7}$$

By (9.7), $\lambda_1(G_P)$ is maximum when

$$2bR + \sum_{k=1}^{k_f} \sin(2\alpha_{B,k}) = 0, \quad (a-c)\eta + \sum_{k=1}^{k_f} \cos(2\alpha_{B,k}) = 0. \tag{9.8}$$

The first condition generates 0 off–diagonal terms, and the second condition forces the two terms on the diagonal to be equal. By the definition of A in (9.6), the trace of the resulting PG is $\mathrm{Tr}\,(G_P) = \mathrm{Tr}\left(\Pi_0^{-1}\right) + \frac{N}{\eta}$. As a consequence, the optimal PG has half of this quantity as diagonal terms, thus concluding the proof. □

Remark 9.2.2. *One popular (but not necessarily the only) optimal trajectory, when the initial covariance matrix Π_0 is a multiple of the identity, is represented by a circle centred on the beacon (see [Hung and Pascoal, 2020]).*

This result proves useful in the following section, where we analyse the PG of the entire system, as defined in (9.5).

9.2.2 Analysis of the tracker–target pair

In the general scenario, the PG has the block structure described in (9.5). For simplicity's sake, we consider only its running part. The extension to the complete PG accounting for the *a priori* information can be obtained following the same arguments as in Proposition 9.2.1. We introduce the two real positive number N_A and N_M interpreted as the *weighted* number of measurements collected from the beacon and from the target, respectively. N_A is defined as the number of observations collected from the beacon divided by the noise variance (i.e. $\frac{N}{\eta}$ in the previous analysis) of the sensor and N_M is defined analogously. They allow us to account for a different level of sensor noise or for a different number of measurements collected from the beacon and from the target. We introduce here the first main result of this paper.

Theorem 9.2.3. *Let us consider the PG defined in* (9.5)*. When the trajectory is optimal, i.e. the smallest eigenvalue of the PG is maximum, both A and M are optimal, i.e.*

$$A = \frac{N_A}{2}\mathbf{I}_2, \qquad M = \frac{N_M}{2}\mathbf{I}_2.$$

9.2.3 Proof of Theorem 9.2.3

This proof is divided into two sections: first, we find the eigenvector associated with the smallest eigenvalue of the *optimal* PG, then we leverage this result to

prove that the PG is optimal when both A and M are optimal.

Eigenvector associated with the smallest eigenvalue

Let $w = [w_1, w_2, w_3, w_4]^\top$ be a unitary vector, i.e. $w^\top w = 1$. Then, by symmetry of G, $\min_w(\lambda) = \lambda_1(G)$, where $\lambda = w^\top G w$ is the cost function, and $\lambda_1(G)$ is the smallest eigenvalue of the PG (Rayleigh quotient with unitary vector w). To solve the minimisation problem, we build the Lagrangian function $\mathcal{L} = w^\top G v + \mu(w^\top w - 1)$, where μ is the Lagrangian multiplier associated with the constrained norm of w. The candidate solution for w is

$$w = \frac{1}{\sqrt{1+\ell^2}} \left[\cos\beta, \quad \sin\beta, \quad \ell\cos\beta, \quad \ell\sin\beta\right]^\top,$$

where

$$\ell = \frac{N_A}{2N_M} + \frac{\sqrt{N_A^2 + 4N_M^2}}{2N_M},\ \ell^\dagger = \frac{N_A}{2N_M} - \frac{\sqrt{N_A^2 + 4N_M^2}}{2N_M}, \tag{9.9}$$

and $\beta \in [0, 2\pi)$ is a generic angle. The gradient of the Lagrangian function evaluated at w is 0 (for both ℓ and $\ell^\dagger$), thus satisfying the first order optimality condition. By plugging w in λ, we get

$$\lambda^\star = \frac{\left(N_A + (\ell-1)^2 N_M\right)}{2(1+\ell^2)} = \frac{N_A}{4} + \frac{N_M}{2} - \frac{\sqrt{N_A^2 + 4N_M^2}}{4},$$

which is the smallest eigenvalue of the optimal PG. The same vector w with $\ell^\dagger$ in place of ℓ is associated with the maximum value of λ. By its structure, G has two eigenvalues with multiplicity 2. Therefore, no more cases are left to inspect.

PG is optimal when its blocks are optimal

Based on the shape of w, we show hereafter that for any choice G different from the optimal PG (i.e. at least one between A and M is not optimal), we can find a unitary vector $\overline{w}$ such that $\overline{w}^\top G \overline{w} < \lambda^\star$, i.e. the smallest eigenvalue of G is smaller than the smallest eigenvalue of the optimal PG.

Let us define the two vectors

$$\overline{w}_i = \frac{1}{\sqrt{1+\ell^2}} \left[\cos\beta_i,\ \sin\beta_i,\ \ell\cos\beta_i,\ \ell\sin\beta_i\right]^\top,\ i = A, M,$$

such that $[\cos\beta_i, \sin\beta_i]^\top$ is the eigenvector associated with the smallest eigenvalue of matrix i, yielding the cost functions $\lambda_i = \overline{w}_i^\top G \overline{w}_i$, $i = A, M$. To prove our point, we show that $\lambda^{\star 2} > \lambda_A \lambda_M$, which is sufficient for at least one between

λ_A and λ_M to be smaller than $\lambda^\star$,

$$\lambda^{\star 2} - \lambda_A \lambda_M \geq \left(\frac{(\ell-1)^2 \sigma_M - \sigma_A}{1+\ell^2} \right)^2 \geq 0,$$

where $\sigma_A = \frac{N_A}{2} - \lambda_1(A)$ represents the difference between the *optimal eigenvalue* (half of the trace) and the actual smallest eigenvalue of A, and analogously for σ_M. In the chain of weak inequalities, the equality $\lambda^{\star 2} - \lambda_A \lambda_M = 0$ holds only when two conditions are met: $\sigma_A = (\ell-1)^2 \sigma_M$ (second equality), and when the eigenvector of A associated with its *smallest* eigenvalue coincides with the eigenvector of M associated with its *greatest* eigenvalue, and vice versa (first equality). In this unfortunate situation, where $\lambda_M = \lambda_A = \lambda^\star$, let us consider $\lambda_l = \overline{w}_l^\top G \overline{w}_l$, with

$$\overline{w}_l = \tfrac{1}{\sqrt{1+l^2}} \left[\cos\beta,\, \sin\beta,\, l\cos\beta,\, l\sin\beta\right]^\top.$$

Its derivative $\frac{d}{dl}\lambda_l\big|_{l=\ell}$ is 0 only for $\ell = 1$, which is infeasible because $N_A, N_M > 0$ in (9.9). Therefore, there exists at least one $l \neq \ell$ such that $\lambda_l < \lambda^\star$, thus concluding the proof. □

Theorem 9.2.3 accounts only for the *running part* G of the PG. The extension of the result to the scenario where an initial covariance P_0 is given, requires the following property. We will prove in the following that for the system at stake Property 9.2.4 holds true.

Property 9.2.4. *The initial covariance matrix* Π_0 *has the following block structure*

$$\Pi_0 = \left[\begin{array}{c|c} \Pi_B & \Pi_B \\ \hline \Pi_B & \Pi_B + \Pi_Q \end{array}\right], \qquad \Pi_B, \Pi_Q \in \mathbb{R}^{2\times 2},$$

whose inverse (appearing in the definition of G_P *in* (9.3)*) is*

$$\Pi_0^{-1} = \left[\begin{array}{c|c} \Pi_B^{-1} + \Pi_Q^{-1} & -\Pi_Q^{-1} \\ \hline -\Pi_Q^{-1} & \Pi_Q^{-1} \end{array}\right]. \tag{9.10}$$

Corollary 9.2.5. *When Property 9.2.4 holds true, the* global maximum *of the smallest eigenvalue of* G_P *in* (9.3) *coincides with the* global minimum *of the*

following function:

$$J_\Sigma = \left((a_B - c_B)\eta + \sum_{k=1}^{k_f} \cos(2\alpha_{B,k})\right)^2 + \left(2b_B\eta + \sum_{k=1}^{k_f} \sin(2\alpha_{B,k})\right)^2 + \left((a_Q - c_Q)\eta + \sum_{k=1}^{k_f} \cos(2\alpha_{Q,k})\right)^2 + \left(2b_Q\eta + \sum_{k=1}^{k_f} \sin(2\alpha_{Q,k})\right)^2, \quad (9.11)$$

where $\Pi_B^{-1} = \left[\begin{smallmatrix} a_B & b_B \\ b_B & c_B \end{smallmatrix}\right]$ *and* $\Pi_Q^{-1} = \left[\begin{smallmatrix} a_Q & b_Q \\ b_Q & c_Q \end{smallmatrix}\right]$.

Proof. The proof is similar to the proof of Theorem 9.2.3 and hinges on the optimality of A and M in Proposition 9.2.1. □

9.2.4 Optimal Control Problem

In light of the results in Theorem 9.2.3 and in Corollary 9.2.5, we state the Optimal Control Problem (OCP) that can be solved by the tracker to plan its optimal trajectory.

Problem 9.1. *The OCP is stated as*

$$\min_{v_{P,k}, \omega_{P,k}} J \quad \textit{subject to} \quad \begin{cases} v_{P,\min} \leq v_{P,k} \leq v_{P,\max}, \\ \omega_{P,\min} \leq \omega_{P,k} \leq \omega_{P,\max}, \end{cases}$$

where $J = -\lambda_1(G_P)$*, or* $J = J_\Sigma$ *in* (9.11).

We compare the solutions of the OCP in Problem 9.1 with the two different versions of the cost function with $N_A = N_M = N$, $\Pi_0 = \mathbf{I}_4$ and $\eta = 0.1$, hence satisfying Property 9.2.4. To this aim, we show in Table 9.1 the average performances over 30 simulations, with the two different cost functions. While the two cost functions have the same global optimum point, the numerical optimisation of the two may yield different results due to the high nonlinearity and nonconvexity of the problem. Results are shown in terms of time taken for the optimisation, and smallest eigenvalue of the PG. The simulations have been performed in a MATLAB® environment with CasADi [Andersson et al., 2019], running on an Apple® M1 chip. In each set of simulations (each row of Table 9.1), we observe a reduction in the optimisation metric $\lambda_1(G)$ (block of columns on the right), which shows that choosing J_Σ over J generates a disadvantage. On the other hand, we observe a greater reduction in the time needed by numerical algorithm to yield the result to Problem 9.1. Therefore, J_Σ should be preferred for the formulation of the OCP when solved online, as we show in Section 9.3.

Table 9.1: Comparison between $J = \lambda_1(G)$ and J_Σ in (9.11).

N	Time (s)			Eigenvalue		
	J	J_Σ	Reduction	J	J_Σ	Reduction
5	0.21	0.16	−22%	1.25	1.20	−4%
10	0.92	0.59	−37%	2.51	2.18	−13%
40	4.56	2.63	−42%	8.60	8.48	−1%
100	25.38	17.81	−30%	20.10	20.10	0%

Condition 9.1. *To solve the OCP at each time step, Property 9.2.4 must always hold true.*

While Condition 9.1 seems demanding, we prove in Fact 9.3.1 and in Fact 9.3.2 that it holds true for the analysed system subject to the trajectory planning algorithm described in the next section.

9.3 Trajectory Planning

The previous section addresses the problem of defining a suitable cost function, which the tracker uses to plan its optimal trajectory. To effectively implement this theoretical result in a real–world scenario, we need to take into account some limitations, e.g. the tracker's and target's positions P_k and Q_k are not known in advance, and their motions are restricted by the kinematic model (9.1) and may be affected by some process noise. To overcome these limitations and design an effective control algorithm, we propose a scheme that executes online two tasks: (i) update the estimate of the positions of the vehicles, which is based on the new ranging information collected by the tracker, and performed via an Extended Kalman Filter, and (ii) plan the trajectory of the tracker via a Model Predictive Control (MPC) algorithm to optimise for the cost function J_Σ in (9.11) based on the updated information and on the manoeuvres planned and communicated by the target. Before the online estimation scheme, to provide a sufficiently accurate initial estimate of the state of the system, we propose an initialisation phase, based on trilateration, where the tracker collects 3 ranging measurements from the target and from the beacon. A block diagram of the complete control and estimation scheme is represented in Figure 9.1.

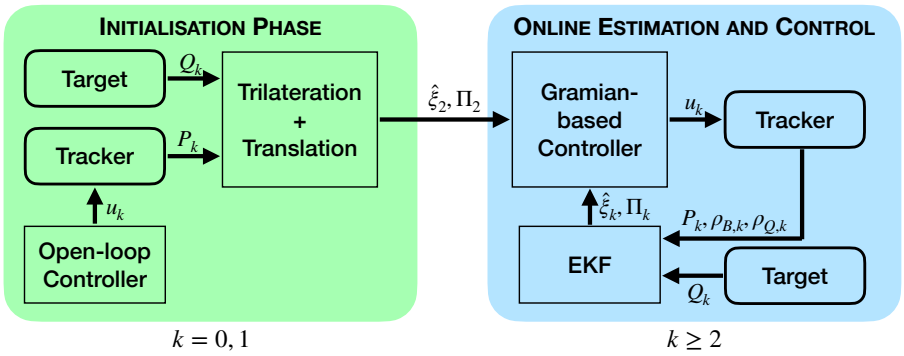

Figure 9.1: Block diagram of the complete scheme responsible for estimation and control.

9.3.1 Online Estimation and Control Scheme

Estimation Filter

Before presenting the Gramian–based planning algorithm, we draw some considerations on the outputs of an estimation filter for the state q_k with (almost) perfect measurements of the headings $\theta_{P,k}$ and $\theta_{Q,k}$ of the two vehicles, and the ranging sensor model in (9.2) corrupted by a zero–mean white Gaussian noise with covariance $\eta \mathbf{I}_2$. Therefore, the overall output vector ζ_k is defined as

$$\zeta_k = [z_k; \theta_{P,k}; \theta_{Q,k}]^\top,$$

with covariance matrix $Z_k = \text{diag}(\eta, \eta, \varepsilon, \varepsilon)$, $\varepsilon \ll \eta$. As an estimation filter, we choose the Extended Kalman Filter (EKF). At each time step k, it yields an estimate $\hat{q}_k$ of the state q_k and its error covariance matrix Ψ_k, based on the estimate $\hat{q}_{k-1}$ and covariance Ψ_{k-1} at the previous time step, on the expected motion of the robots (control inputs and model), and on the collected measurements ζ_k. The current covariance matrix Ψ_k is computed as

$$\Psi_k = (\mathbf{I}_6 - K_k H_k)\Psi_{k|k-1},$$

where $H_k = \frac{\partial \zeta_k}{\partial q_k}$ is the observation matrix, while $\Psi_{k|k-1}$ is the covariance of the prediction, accounting for the propagation of the uncertainty due to the dynamics and to possible actuation uncertainties. The Kalman gain K_k is defined as

$$K_k = \Psi_{k|k-1} H_k^\top (H_k \Psi_{k|k-1} H_k^\top + Z_k)^{-1}.$$

One may check from these definitions that, for any $\Psi_{k|k-1} \in \mathbb{R}^{6\times 6}$, the entries of the covariance matrix $\Psi_k$in the rows and columns associated with the headings (i.e. third and sixth) are much smaller than the others. Therefore, without loss of generality, we can focus on the reduced state $\xi_k = [P_k; Q_k]^\top \in \mathbb{R}^4$ with covariance matrix $\Pi_k \in \mathbb{R}^{4\times 4}$, propagated with the usual EKF equations with model (9.1) and output z_k as in (9.2).

Fact 9.3.1. *When Property 9.2.4 holds true for Π_k, Property 9.2.4 holds true also for the next covariance matrix Π_{k+1} obtained with the EKF equations, thus recursively satisfying Condition 9.1.*

This fact descends from the propagation of the covariance matrix in the EKF equation. Equivalently, it can be inferred from the definition of G_P in (9.3), the shape of its running part G in (9.5) and shape of Π_0^{-1} in (9.10), hence $\Pi_{k+1} = (\Pi_k^{-1} + G)^{-1}$ has the block structure required in Property 9.2.4.

Gramian–Based Trajectory Planning

After the estimation phase, the planner is fed with the position estimates $\hat{\xi}_k$ and the covariance matrix Π_k. Based on the provided information, the PG and the cost function J_Σ on the next N steps (i.e. $k+1, k+2, \ldots, k+N$) is predicted using the system and sensor models (9.1) and (9.2). The tracker solves a variation of the OCP in Problem 9.1 with the predicted cost function $\hat{J}_\Sigma$ based on the estimated positions $\hat{\xi}_k$ and the associated covariance Π_k, as an approximation of the unknown J_Σ. Since the result of the OCP depends on the estimate $\hat{\xi}$, which is updated at each time instant k, the optimal trajectory has to be replanned at each time step, thus justifying our choice of an MPC approach to the problem.

After the planning phase, the controller applies $v_{P,k}$ and $\omega_{P,k}$ to the tracker, and once the next measurements ζ_{k+1} are collected, the EKF estimates $\hat{\xi}_{k+1}$ and Π_{k+1} that are provided again to the planner.

In the description of this approach, each phase of the algorithm recursively relies on the previous step. The usual EKF approach relies on initial data $\hat{\xi}_0$ and Π_0 set by the user, whose choice affects sensibly the performances of the estimation algorithm. Therefore, we propose an initialisation phase that allows the tracker to estimate the zero and first order moments of the *probability density function (pdf)* describing the initial positions P_0 and Q_0.

9.3.2 Initialisation phase

In the initial phase of the trajectory, the tracker collects range measurements to estimate the position vector ξ_0. Since no prior information are available (i.e. the angles α_k cannot be estimated), the vehicle cannot plan its manoeuvres according to the OCP in Problem 9.1. Therefore, we propose a different set of manoeuvres, based on geometric considerations, which allow the vehicle to collect *informative* measurements.

The initial phase faces a trade–off: increasing its duration allows the vehicle to collect more information, and thus to estimate more accurately the positions ξ_k, but at the same time, it delays the Gramian–based trajectory planning algorithm. Therefore, in our solution, the tracker plans 2 manoeuvres, thus collecting 3 pair of measurements, and uses trilateration.

Trilateration

We define a local reference frame with the origin lying in the initial position P_0 of the tracker with the axes parallel to the axes of the world reference frame. To denote the positions in this reference frame, we add the subscript v, thus the positions of the tracker are

$$P_{v,0} = \begin{bmatrix} x_{v,0} \\ y_{v,0} \end{bmatrix} = \begin{bmatrix} 0 \\ 0 \end{bmatrix}, \; P_{v,1} = \begin{bmatrix} A_0 C_0 \\ A_0 S_0 \end{bmatrix}, \; P_{v,2} = P_{v,1} + \begin{bmatrix} A_1 C_1 \\ A_1 S_1 \end{bmatrix},$$

where A_k, C_k, S_k, $k = 0, 1$, are known via planning. To plan the manoeuvres of the tracker, we draw some considerations on the *pdf* describing the position B_v of the beacon.

Without measurements, B_v is described by a *uniform pdf* on $\mathbb{R}^2$. The tracker aims at reducing this *pdf* to a *unimodal* distribution. This problem boils down to an *observability* problem: the distribution is *multimodal* as long as the nominal system (i.e. without actuation uncertainties and measurement noises) is *unobservable*, i.e. when more than one point B_v is compliant with the measurements $\rho_{B,k}$ collected by the tracker (see Chapter 4). Following the same *rationale* as in Chapter 7, to cope with measurement noise making two near points be sensed as a unique point, the tracker plans its first manoeuvre to travel the longest distance, i.e. $v_{P,0} = v_{\max}$, $\omega_{P,0} = 0$. With two measurements collected, the nominal system is still *unobservable*, since there exist two points that have distances $\rho_{B,0}$ from $P_{v,0}$ and $\rho_{B,1}$ from $P_{v,1}$, and they are mirrored with respect to the segment connecting $P_{v,0}$ and $P_{v,1}$. Therefore, the *pdf* describing B_v is *bimodal*, whose two peaks are mirrored with respect to the segment connecting

$P_{v,0}$ and $P_{v,1}$. To minimise the likelihood of one of these two peaks, i.e. to approach a *unimodal pdf*, the second manoeuvre is planned with $v_{P,1} = v_{\max}$ and $\omega_{P,1} = \pm\min\{2.3311/T_s, \omega_{\max}\}$.

We want to estimate separately the position of the anchor $\hat{B}_v = [\hat{X}_v, \hat{Y}_v]^\top$ and of the target $\hat{Q}_v = [\hat{x}_{Q,v}, \hat{y}_{Q,v}]^\top$, together with their covariance matrices Π_B and Π_Q, while relying on the ranging measurements z_k, $k = 0, 1, 2$. To compact the notation, we denote the distances collected from the anchor and from the target with $\rho_{B,k}$ and $\rho_{Q,k}$, $k = 0, 1, 2$, respectively.

Beacon By the analysis in [Fontanelli et al., 2021], we estimate the position B_v of the beacon and its covariance matrix Π_B as

$$\hat{B}_v = \begin{bmatrix} \hat{x}_{B,v} \\ \hat{y}_{B,v} \end{bmatrix} = \frac{1}{2}\Sigma_B^{-1} h_B, \quad \Pi_B = \Sigma_B^{-1} N_B \left(\Sigma_B^{-1}\right)^\top, \tag{9.12}$$

with

$$N_B = \eta \begin{bmatrix} \rho_{B,0}^2 + \rho_{B,1}^2 & \rho_{B,0}^2 \\ \rho_{B,0}^2 & \rho_{B,0}^2 + \rho_{B,2}^2 \end{bmatrix},$$

$$\Sigma_B = \begin{bmatrix} x_{v,1} - x_{v,0} & y_{v,1} - y_{v,0} \\ x_{v,2} - x_{v,0} & y_{v,2} - y_{v,0} \end{bmatrix},$$

$$h_B = \begin{bmatrix} \rho_{B,0}^2 - \rho_{B,1}^2 - x_{v,0}^2 - y_{v,0}^2 + x_{v,1}^2 + y_{v,1}^2 \\ \rho_{B,0}^2 - \rho_{B,2}^2 - x_{v,0}^2 - y_{v,0}^2 + x_{v,2}^2 + y_{v,2}^2 \end{bmatrix}.$$

Target The extension to the target is not trivial, since the tracker should take into account the (known) manoeuvres executed by the target itself. Therefore, the tracker performs a *delayed trilateration* (see Chapter 7), i.e. generates a new reference frame where each pair of positions $(P_{v,k}, Q_{v,k})$, $k = 0, 1$, is translated such that $Q_{v,k}$ coincides with $Q_{v,2}$. As a result, the *virtual target* is still, while the motion of the *virtual tracker* is the combination of the motions of the two vehicles, and thus matrices Σ_Q and h_Q are computed with these substitutions:

$$P_{v,0} \to P_{v,0} - (Q_{v,0} - Q_{v,2}), \qquad P_{v,1} \to P_{v,1} - (Q_{v,1} - Q_{v,2}),$$

where $Q_{v,k} - Q_{v,2}$, $k = 0, 1$, can be explicitly computed since $A_{Q,k}$ and $\phi_{Q,k}$ in the dynamics (9.1) are known.

With these procedures, (9.12) yields the estimates of the positions $\hat{B}_v$ and $\hat{Q}_{v,2}$ in the tracker's reference frame, with the associated covariance matrices Π_B and Π_Q.

Translation

We now translate the estimates to the world reference frame. This operation boils down to a translation of the origin of the reference frame by the *random variable* $-\hat{B}_v$. Hence, the propagation of the *pdf* estimating the positions of the vehicles (i.e. ξ_2) is not trivial. We define

$$\xi_2 = \begin{bmatrix} P_2 \\ Q_2 \end{bmatrix} = \begin{bmatrix} P_{v,2} - B_v \\ Q_{v,2} - B_v \end{bmatrix}, \qquad \hat{\xi}_2 = \begin{bmatrix} \hat{P}_2 \\ \hat{Q}_2 \end{bmatrix} = \begin{bmatrix} P_{v,2} - \hat{B}_v \\ \hat{Q}_{v,2} - \hat{B}_v \end{bmatrix},$$

with expected value $\mathrm{E}\left\{\hat{\xi}_2\right\} = \xi_2$. Furthermore, we define $\delta B_v = \hat{B}_v - B_v$ and $\delta Q_{v,2} = \hat{Q}_{v,2} - Q_{v,2}$, with expected value $\mathrm{E}\left\{\delta B_v\right\} = \mathrm{E}\left\{\delta Q_{v,2}\right\} = 0$ and first moment $\mathrm{E}\left\{\delta B_v\, \delta B_v^\top\right\} = \Pi_B$ and $\mathrm{E}\left\{\delta Q_{v,2}\, \delta Q_{v,2}^\top\right\} = \Pi_Q$, respectively, by (9.12). By the first order Taylor expansion, we express $\hat{\xi}_2$ as

$$\hat{\xi}_2 \simeq \mathrm{E}\left\{\hat{\xi}_2\right\} + \delta\hat{\xi}_2, \qquad \delta\hat{\xi}_2 = J_B\, \delta B_v + J_Q\, \delta Q_{v,2},$$

where $J_B = -[\mathbf{I}_2; \mathbf{I}_2]^\top$ and $J_Q = [\mathbf{0}_2; \mathbf{I}_2]^\top$ are the Jacobians of ξ_2 with respect to B_v and $Q_{v,2}$, respectively. Therefore, the error covariance matrix Π_2 associated with the estimated positions $\hat{\xi}_2$ is computed as

$$\Pi_2 = \mathrm{E}\left\{\delta\hat{\xi}_2\, \delta\hat{\xi}_2^\top\right\} = \left[\begin{array}{c|c} \Pi_B & \Pi_B \\ \hline \Pi_B & \Pi_B + \Pi_Q \end{array}\right].$$

Fact 9.3.2. *Property 9.2.4 holds true for the initial covariance matrix Π_2 when the first Gramian–based OCP is solved, hence satisfying Condition 9.1.*

Remark 9.3.3. *Matrix Σ_Q may be singular even though the positions P_k and Q_k, $k = 0, 1, 2$, are not so. Should this unfortunate situation occur, the tracker can simply choose the opposite sign for $\omega_{P,1}$, thus making Σ_Q invertible.*

Once the estimate $\hat{\xi}_2$ and its error covariance matrix Π_2 are computed, they are fed to the Gramian–based planner and used to initialise the trajectory planning algorithm.

9.4 Simulation Examples

In this section, we simulate 2 scenarios described in Section 9.3. For both the simulations, we consider a planning horizon of $N = 5$ steps, with a sampling time of 0.5 s, and a final discrete time $k_f = 40$, corresponding to 20 s, *after* the 3–step initialisation phase. In all the scenarios, the control inputs are bounded

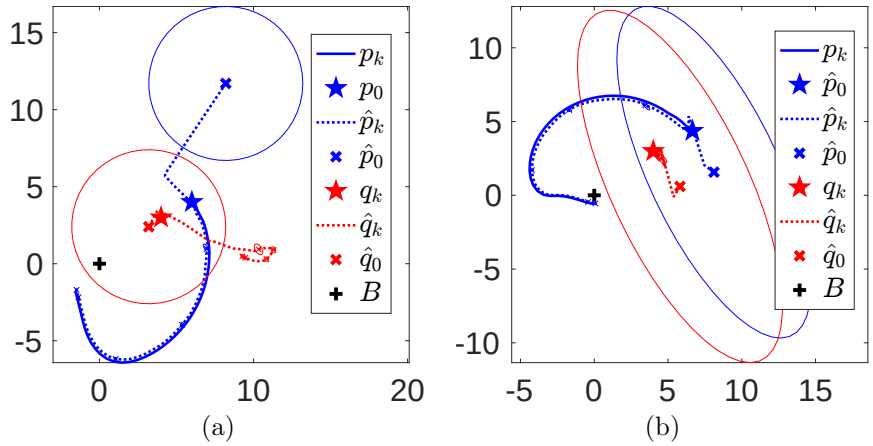

Figure 9.2: First simulation example. Blue lines refer to the tracker, red lines refer to the target. Ellipses represent the diagonal blocks of the covariance matrix Π_k, $k = 0, 10, 20, 30, 40$, while dotted lines denote the estimates of the positions of the vehicle. (a) *Without* the initial estimation phase, the estimate $\hat{P}_k$ of the position of the tracker eventually converges to the actual position P_k, while the estimate $\hat{Q}_k$ of the position of the target drifts apart. (b) *With* the initial estimation phase, both estimates $\hat{P}_k$ and $\hat{Q}_k$ converge to the actual positions of the vehicles.

with 0 m/s $\leq v_{P,k} \leq 1$ m/s, and $-\frac{\pi}{2}$ rad/s $\leq \omega_{P,k} \leq \frac{\pi}{2}$ rad/s. As for the previous simulations, whose results are presented in Table 9.1, the optimisations have been carried out with CasADi [Andersson et al., 2019], a framework for optimisation and optimal control.

9.4.1 With or without initialisation phase

In the first simulation example, we compare the performances of the Gramian–based planning algorithm *with* and *without* the initialisation phase. We consider *perfect* actuation (no actuation uncertainty) and show that an imperfect, but still reasonable, choice of the initial estimates jeopardises the convergence of the EKF estimates to the ground–truth, thus showing, in Figure 9.2, that the initialisation phase is beneficial.

For both the simulations, the initial state of the system is $q_0 = [6; 4; 0; 4; 3; 0]^\top$, while in the first scenario, the initial estimate is $\hat{q}_0 = [8.2; 11.7; 0; 3.2; 2.4; 0]^\top$, with covariance $\Pi_0 = \text{diag}(25, 25, 0, 25, 25, 0)$. Figure 9.2 shows two notable results: (1) although the estimate $\hat{Q}_0$ in the first simulation is close to the actual target position, $\hat{Q}_k$ drifts due to the initial rough approximations of the position P_k of the tracker, and (2) despite the greater initial covariance in the second simulation, both estimates are close to actual initial positions, and thus they converge fast to the actual positions.

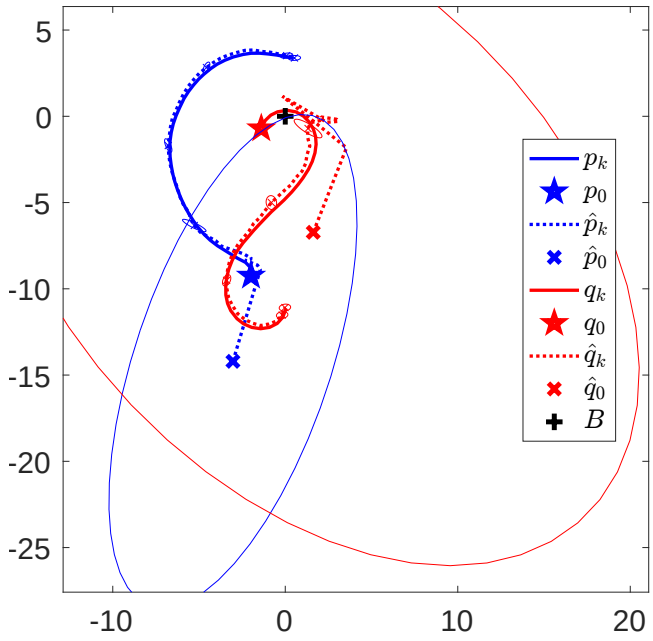

Figure 9.3: Second simulation example. Blue lines refer to the tracker, red lines refer to the target. Ellipses represent the diagonal blocks of the covariance matrix Π_k, $k = 0, 10, 20, 30, 40$, while dotted lines denote the estimates of the positions of the vehicle. Both estimates yielded by the EKF converge to the actual value.

9.4.2 With actuation uncertainties

The second simulation example considers the general setting with a moving and collaborative target, where the Gramian–based planning relies on the initial estimation phase. To highlight the robustness of our method, we simulate *imperfect* actuation. The nominal control inputs v and ω for both vehicles are corrupted by am uncorrelated white Gaussian noise with covariance matrix $\mathrm{diag}(0.1\,\mathrm{m/s}, 0.08\,\mathrm{rad/s})$ as estimated in [Fontanelli et al., 2021] for a standard unicycle–like vehicle. Figure 9.3 shows that, despite the presence of the actuation uncertainty, which is not explicitly accounted for in either the initial estimation phase or in the Gramian–based planning algorithm, both the initial estimates based on trilateration and the EKF estimates are close to the actual positions of the vehicles.

Conclusions and Future Perspectives

10

Contents

In this thesis, we have addressed various problems concerning the *constructibility* properties of a system composed of ground vehicles relying on ranging sensors, motivated by a large part of the technical literature dealing with these problems but showing a deep focus on local constructibility properties. With the same procedures, both global and local results have been presented, and have been implemented for an application–driven scenario where the vehicles in the system actively plan their trajectory. The path towards the real–life application of these ideas still needs to solve some practical problems, which will be detailed out in the section dedicated to future perspectives. This final chapter draws some conclusions on the contributions presented in this thesis and discusses some future research directions based on some problems left open in this thesis.

10.1 Summary of the Thesis Contributions

In Part I we have analysed the constructibility problem from a *global* perspective. We have presented in Chapter 2 an example showing that the solutions to the well–known *positioning* problem cannot be trivially extended to the *localisation* problem. Indeed, when the *generalised noncollinearity condition* holds, there are still indistinguishable trajectories of the vehicle. Motivated by this result, in Chapter 3 we have shown a sufficient condition on the trajectory of the vehicle for constructibility, in the setting where the environment is instrumented with only 2 anchors with non–overlapping sensing range. As a natural development, in Chapter 4 we have carried out a global constructibility analysis for a ground vehicle collecting various numbers of measurements distributed among a variable number of anchors, where no simultaneous measurements are collected and the vehicle moves between successive measurement collections. As a result, there no sufficient condition on the number or distribution of observations, but constructibility depends also on the geometry of the trajectory followed by the vehicle and on the deployment of sensors in the environment.

We have addressed the *local* constructibility problem in Part II, where the analysis is carried out by means of the Constructibility Gramian. In Chapter 5 we analyse the rank of the Constructibility Gramian to determine whether the system is constructible, with the same procedure as in the previous analysis. Surprisingly, some constructible settings turn out to yield a singular Gramian, thus showing the limitations of linearisation–based techniques on nonlinear systems. This counterintuitive result has been discussed in comparison with the global analysis in Chapter 4. The smallest eigenvalue of the Constructibility Gramian has been introduced in Chapter 6 as a constructibility metric. With an approximation of the devised metric, we have analysed straight trajectories

parallel to the line joining the two sensors the environment is instrumented with. We have analysed the effect of some geometrical parameters of the trajectory on the constructibility metric, and we have discussed the results giving some geometrical insights.

Finally, in Part III, we have extended the results obtained in the previous analyses to multiagent systems. In Chapter 7 we have presented a trajectory planning algorithm for a pair of vehicles collecting absolute and mutual ranging measurements. This algorithm is articulated into three phases where the vehicles (a) collect measurements from one anchor, (b) they travel until they come sufficiently close to each other, and eventually (c) they plan their last manoeuvres to rule out residual ambiguities and indistinguishabilities. A different extension of the results in Parts I and II has been addressed in Chapter 8, where the *local* analysis, based on the Constructibility Gramian, has been carried out, while only sufficient conditions have been presented for *global* constructibility. A variation of the Constructibility Gramian has been leveraged in Chapter 9, where a vehicle (tracker) plans its trajectory to simultaneously localise itself and a collaborative target based on relative and absolute measurements. To plan its trajectory the tracker initially relies on manoeuvres based on delayed trilateration, while the main part of the controller relies on the Constructibility Gramian, hence merging the results presented in the previous parts of this thesis.

10.2 A Real–world Application

In this section, we discuss a possible application of the techniques and results devised in this thesis, driven by practical and real–world problems, showing how the constructibility results devised in this thesis may impact the robotics research.

Recently, the field of agricultural robotics has attracted significant interest from researchers, largely due to the substantial dependence on human-guided machinery and manual labour throughout the processes involved in transporting fruit from the tree to the consumer. One of the challenges arising in this domain is the outdoor localisation of mobile robots navigating orchards and vineyards. Although visual sensors represent a popular solution for this problem (see [Shalal et al., 2015]), they have inherent limitations due to changing luminance conditions, due to season and daily changes, and due to the growth and alteration of the tree aspect from which visual features are extracted. A sensor fusion approach that combines cameras and laser range sensor has been explored in [Lepej and Rakun, 2016] for the application in outdoor unstructured

environments, where similar issues due to changes in the environment arise.

A different approach is suggested by the results devised in this thesis, where the robot localises itself by measuring its distance to a set of devices deployed in the environment. Although ranging measurements require the environment to be instrumented, unlike visual sensors, this type of sensors enjoys some properties such as robustness with respect to direct sunlight and with respect to environmental alterations. An example of deployment of sensors in a vineyard is shown in Figure 10.1.

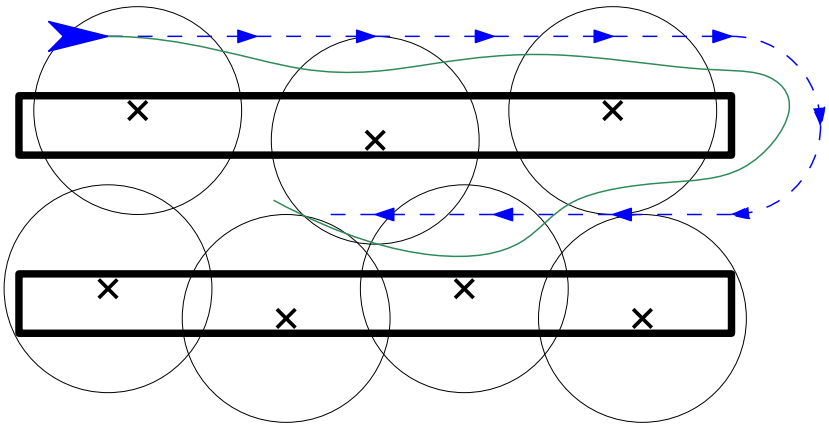

Figure 10.1: An example of practical application. The vineyard, whose 2 rows are depicted as boxes, is instrumented with some beacons represented by crosses, deployed in known positions and with a small sensing range represented by a circle. A usual path followed by a robot to execute predefined tasks (e.g. harvesting) is represented in a blue dashed, while the green path shows a better behaviour for localisation.

From a purely theoretical perspective, the vehicle may collect 4 measurements from the first two beacons in a $2 + 2$ setting, and achieve global constructibility, thus allowing it to solve the localisation problem. But additional challenges arise in this scenario when non–idealities are taken into account: the vehicle has to execute some tasks, measurements are affected by noise, and the motion of the vehicle is affected by uncertainties due to the non–ideal contact between the wheels and the ground. To cope with these issues, one may suggest the following solutions:

1. Multiple tasks:

    - Set time–dependent or uncertainty–dependent weights to the localisation task and to the other tasks (e.g. harvesting). The main challenge to be addressed here is avoiding that the harvesting task has poor efficiency in the areas where the vehicle has less accurate estimates of its state. A suggested approach to this aim is based on

null–space projectors of the control actions, where a secondary objective may be achieved without affecting the efficiency in executing the primary task (see [De Palma et al., 2015b]).

2. Measurement noise:

   - As in Chapter 9, the vehicle should plan its trajectory to collect informative measurements (in a constructibility perspective), but also to reduce the impact of measurement noise. The solution proposed in Chapter 9 is based on two phases where global constructibility is achieved in the initialisation phase based on trilateration, while local constructibility, which is associated with the inverse of the estimation uncertainty, is maximised by means of the Position Gramian.

3. Actuation uncertainties:

   - This problem has been neglected in the results obtained in this thesis to simplify the analysis by introducing a deterministic position sequence. A thorough and careful analysis of the actuation noise must be carried out to apply to a real—life scenario the results devised in this thesis. Indeed, the manoeuvres executed by the vehicle affect the estimation uncertainty in many ways, e.g. the smallest eigenvalue of the Constructibility Gramian is influenced by the final position reached by the vehicle and by the geometrical properties of the position where measurements are collected (see Chapter 6). On the other hand, the manoeuvres performed by the vehicle introduce different levels of uncertainty. As an example, consider a tracked vehicle where the uncertainty introduced by slippage phenomena increases with the curvature of the path.

This example shows a practical application that could benefit from the results devised in this thesis. Indeed, the concept of *global constructibility*, and the conditions to achieve it, lay the foundation for localising the vehicle when no prior information is available, or when the uncertainty associated with the state estimate is high. When global constructibility is achieved in these uncertain conditions, the vehicle could benefit from the local analysis, whose *a priori* information is an approximation (estimation) of the state of the system, and the robot may plan its trajectory to increase the sensitivity of the measurements with respect to the final state of the system, i.e. maximising some norm of the Constructibility Gramian or of an equivalent local constructibility metric.

With a similar formulation, an equivalent problem may be stated for the navigation and localisation of a mobile robot across indoor intelligent environ-

ments, e.g. an automated warehouse, where the ranging information may be used together with visual sensors.

10.3 Suggestions for Future Research

In this section, we show some suggestions for future research directions, which deal with problems left open in this thesis, or with developments based on the results presented in this thesis. While many research directions can be identified as a follow–up of this thesis, we present here some future perspectives with some intuitions on the complexity of the problems and possibly some hints on how to tackle them.

10.3.1 Complete global analysis for multiagent systems

In Chapter 4, we have presented a thorough global constructibility analysis for a single vehicle, while in Chapter 8, we have extended the concepts to the particular case of multiagent setting where a constructible subsystem exists. The general problem can be formalised as in Chapter 8, where we want to find the conditions on the trajectories of the vehicles and on the relative measurements such that there exists a unique set of rototranslations $(R^{[i]}, T^{[i]})$, $i = 1, \dots, N-1$, to the reference frame of the vehicle $V^{[0]}$. Based on the results presented in this thesis, we can intuitively state some *necessary* conditions that each vehicle has to satisfy:

Condition 10.1 (Necessary)**.** *Let $V^{[i]}$ collect $N_m^{[i]}$ measurements in positions $P_k^{[i]}$, $k = 0, \dots, N_m^{[i]} - 1$, where some positions $P_k^{[i]}$ might coincide. Moreover, let the position of the other vehicle involved in the measurements be $P_k^{[j_k]}$, where the index j_k denotes the vehicle collecting a relative measurement from $V^{[i]}$ at time k. The following necessary conditions must hold true:*

1. *$V^{[i]}$ must collect at least 4 measurements ($N_m^{[i]} \geq 4$);*
2. *At most $N_m^{[i]} - 2$ positions $P_k^{[j_k]}$ of the other vehicles involved in the measurements can coincide;*
3. *At most $N_m^{[i]} - 2$ positions $P_k^{[i]}$ can coincide.*

Conditions 1 and 2 are an intuitive, yet not proved, consequence of the analysis in Chapter 4, where the minimum number of non—simultaneous measurements is proved to be 4, provided that the measurements are collected by at least 2 anchors. Condition 3 is intuitively derived from the analysis in Chapter 8, on simultaneous measurements. However, drawing conclusions on the

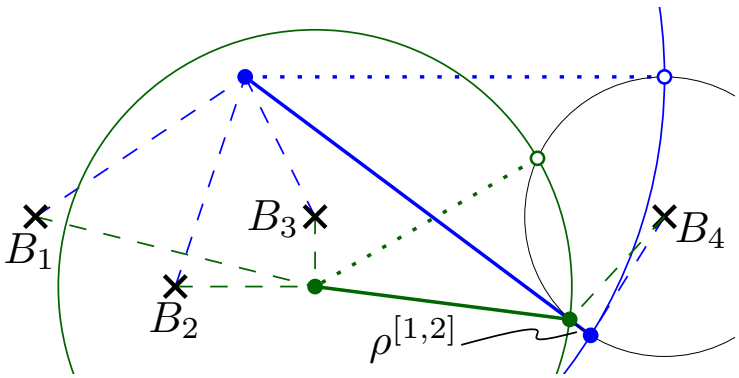

Figure 10.2: Example: the two vehicles collect 3 measurements from the beacons in their position $P_0^{[i]}$, $i = 1, 2$, one measurement from B_4 and a relative measurement in $P_1^{[i]}$. The system is only *locally* constructible when $\rho^{[1,2]}$ is *not* collected, while it is *globally constructible* when also the relative distance is measured.

sufficient and necessary conditions for global constructibility on such a multi-agent system is not a straightforward extension of the procedures followed in Chapter 4. To show the complexity of the problem, let us consider the example proposed in Chapter 8, and reported in Figure 10.2. The final position P_1^i of the vehicles must satisfy the constraints arising from the measurements and the constraint deriving from the dynamics, i.e. the distance from the initial point be $A_0^{[i]}$. The positions $P_1^{[i]} = [x_1^{[i]}; y_1^{[i]}]^\top$ are the solution to the following set of nonlinear equations:

$$\begin{aligned}
\| P_1^{[1]} - P_0^{[1]} \|^2 &= {A_0^{[1]}}^2 \\
\| P_1^{[2]} - P_0^{[2]} \|^2 &= {A_0^{[2]}}^2 \\
\| P_1^{[1]} - B_4 \|^2 &= {\rho_4^{[1]}}^2 \\
\| P_1^{[2]} - B_4 \|^2 &= {\rho_4^{[2]}}^2 \\
\| P_1^{[1]} - P_1^{[2]} \|^2 &= {\rho^{[1,2]}}^2
\end{aligned}$$

As in Chapter 3, we can take the differences between pairs of equations to have linear equations in some unknowns, solve them and substitute in the following equations. As a result, we obtain an equation with only $x_1^{[2]}$ as a variable (or equivalently one of the others unknowns). The equation has a fourth–order numerator, which may have up to 4 solutions, while it is clear from Figure 10.2 that it only has one real solution in the depicted setting. Analysing this problem for a generic number of vehicles and interactions between them seems unfeasible with these arguments. A more promising solution leverages graph theory, as shown in [Hao et al., 2022], where each node (representing the vehicle) should be "rigidly connected" to $V^{[0]}$. Intuitively, two vehicles $V^{[i]}$ and $V^{[j]}$ are "rigidly connected" when the sequence of positions of $V^{[i]}$ is known in the reference frame $\langle V^{[j]} \rangle$ and vice versa, but the concept of "rigid connection"

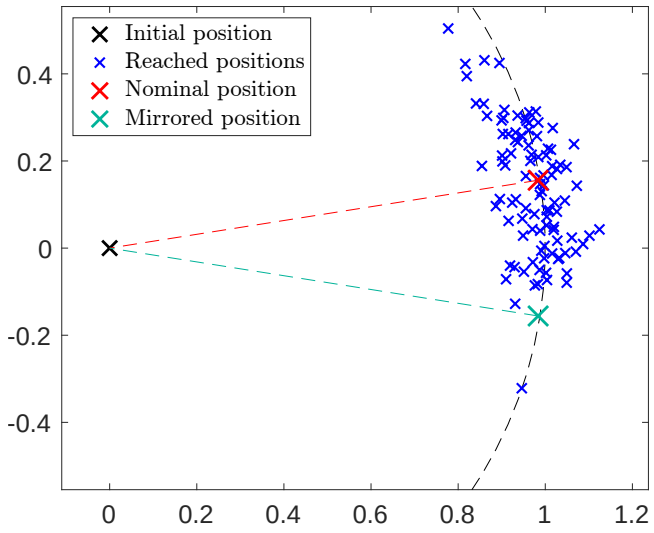

Figure 10.3: Example with actuation noise: 100 realisations of the path of the vehicle with actuation noise (blue crosses). The nominal position predicted by the vehicle with the nominal controls is represented in red, while its mirrored position, reached with the sign of the nominal angular velocity ω reversed is depicted in green.

should be formally stated and analysed.

10.3.2 Motion uncertainties

This thesis, both in the parts presenting constructibility analysis and synthesis, does not take into account possible uncertainties that may arise in the actuation. From a *local* perspective, actuation noise has been considered in the literature, e.g. in [Napolitano et al., 2021] where the authors propose a cost function for an MPC controller that has both the contribution of the Constructibility Gramian, associated with the amount of information that can be collected through exteroceptive sensors, and of the Reachability Gramian, which minimises the uncertainty on the state vector generated by actuation noise (otherwise modelled as noise in the proprioceptive sensors). When looking at the problem from a *global* perspective, there are some limitations that have to be taken into account. Let us consider the following example:

Example 10.1. Let us consider a unicycle vehicle lying in the origin of the world reference frame, aware of its initial state. The setting is represented in Figure 10.3. The vehicle executes a manoeuvre with control inputs

$$v_0 = 1 + 0.05\sigma_1, \qquad \omega_0 = \frac{\pi}{10} + 0.3\sigma_2,$$

where σ_1 and σ_2 are two independent random variables from a zero–mean normal

distribution with covariance equal to 1. When the vehicle reaches its second position, it measures its distance from the origin. While the predicted position is represented in red in Figure 10.3, when actuation noise is involved, the vehicle may reach a position which is closer to the *mirrored position* in green. Therefore, in some settings, actuation noise may induce the vehicle to pick one trajectory (in this example the red), while it is travelling along a different trajectory, thus jeopardising the validity of the analyses carried out in this thesis. ⋆

Example 10.1 shows that actuation noise deserves a deeper analysis, which is associated with the concepts of *reachability*. In particular, we should devise a metric to quantify the *global constructibility* of a trajectory, measuring "how indistinguishable" two or more trajectories are. When the position of the vehicle is found by solving a linear equation

$$M \begin{bmatrix} x \\ y \end{bmatrix} = h,$$

a metric could be the smallest eigenvalue of the matrix M, but some settings in Chapter 4 do not rely on the inversion of a matrix M. This metric may also be used in trajectory planning algorithms, e.g. to minimise for the likelihood of one or more hypothesis in a Multi–Hypothesis Extended Kalman Filter or of a Generalised Pseudo Bayesian algorithm.

10.3.3 Malicious or non–collaborative agents

The extension of constructibility analyses to multiagent systems opens many further research directions, which can rely on the tools devised and presented in this thesis. In particular, extensions with heterogeneous agents can be trivially performed when each of them meets the usual conditions on its trajectory, i.e. the sequence of positions is sufficient to reconstruct the state, and the path followed by the vehicle has a shape that only depends on the control inputs. An interesting extension involves malicious and non–collaborative agents, which actively avoid measurements or broadcast wrong information on their actual state due to faulty sensors, unmodelled dynamics or malicious intentions. Let us consider some scenarios, of increasing complexity, where constructibility is jeopardised by limited or false information.

Example 10.2. Let us consider a still target with unknown position $P = [x; y]^\top$, measuring its distance from a tracker vehicle that is aware of its state and plans its successive positions. The tracker aims at making the target localise itself in a different position $\overline{P}$, and to do this, it seeks for a set of positions

$P_k = [x_k, y_k]^\top$, $k = 1, 2, 3$ to communicate to the target, which is aware of the three measured distances ρ_k, $k = 1, 2, 3$. Therefore, in the usual trilateration equation

$$\begin{bmatrix} \tilde{x}_0 - \tilde{x}_1 & \tilde{y}_0 - \tilde{y}_1 \\ \tilde{x}_0 - \tilde{x}_2 & \tilde{y}_0 - \tilde{y}_2 \end{bmatrix} \begin{bmatrix} \tilde{x} \\ \tilde{y} \end{bmatrix} = \frac{1}{2} \begin{bmatrix} -\rho_0^2 + \rho_1^2 + \tilde{x}_0^2 - \tilde{x}_1^2 + \tilde{y}_0^2 - \tilde{y}_1^2 \\ -\rho_0^2 + \rho_2^2 + \tilde{x}_0^2 - \tilde{x}_2^2 + \tilde{y}_0^2 - \tilde{y}_2^2 \end{bmatrix},$$

the trackers, given ρ_k, $k = 1, 2, 3$, aims at finding the positions $\tilde{P}_k$ such that $\tilde{P} = \overline{P}$.

A trivial solution to this problem is $\tilde{P}_k = P_k + \tilde{P} - P$, infinitely many solutions for this problem can be found. ⋆

While Example 10.2 shows a scenario that does seem to be uncommon in real–life settings, it represents a starting point to devise a set of behaviours for a malicious agent to not be localised.

Example 10.3. Let us consider a target–tracker scenario, where the target is non–collaborative (see [Hung et al., 2020]). When the target has a complex or byzantine behaviour, game theory should be involved, while less sophisticated methods may be leveraged with some simplifying assumption, e.g. when the target moves with constant but unknown velocities. In this scenario, the target may be modelled as a double integrator system reading as

$$q = \begin{bmatrix} x \\ y \\ v_x \\ v_y \end{bmatrix}, \qquad \dot{q} = \begin{bmatrix} 0 & 0 & 1 & 0 \\ 0 & 0 & 0 & 1 \\ 0 & 0 & 0 & 0 \\ 0 & 0 & 0 & 0 \end{bmatrix} q.$$

The problem may be addressed with the same machinery as in Chapter 9, where the results are expected to have the same shape, i.e. the optimal trajectory has a Gramian with diagonal blocks, but an analytical proof has to be provided. ⋆

Example 10.4. As a last example, let us consider a more complex scenario where a team of vehicles is patrolling a room. A byzantine agent, part of the patrolling team, aims at leaving an area of the room unmonitored, or at creating a path for an intruder to move across the room without been seen by the patrolling team. To successfully execute this task, the malicious agent should inject false information in the system to make the team localise it in the wrong position, which is the position where the intruder can lie without being seen. ⋆

While the problem in Example 10.4 is evidently more complex than the examples shown before, it inherently requires disrupting *global* constructibility, and thus it can rely on the concepts devised in this thesis.

10.3.4 Other types of sensors

In the analysis of a unicycle–like vehicle, ranging sensors measure a quantity that only depends on a part of the state (in the case the x and y coordinates), while the orientation θ is reconstructed by relying on the dynamics and manoeuvres executed by the vehicle. Similar results, which may be obtained with a geometric analysis, are expected with other classes of sensors where only a part of the state is involved. Some insights may come from the local observability analysis for a unicycle vehicle has already been presented in [Martinelli and Siegwart, 2005], where, for instance, *local* constructibility can never be achieved with orientation measurements, since any final position $P_f = [x_f; y_f]^\top$ yields the same output history when the executed manoeuvres and the final orientation θ_f are the given.

Bearing sensors have been deeply analysed in the technical literature from a local perspective, and they present many remarkable differences with respect to the ranging sensors. Indeed, let us consider a vehicle moving on a straight line, perceived by a single sensors in the origin, i.e. $[X; Y]^\top = [0; 0]^\top$, with

$$q_0 = \begin{bmatrix} 0 \\ 2 \\ 0 \end{bmatrix}, \quad q_1 = \begin{bmatrix} 1 \\ 2 \\ 0 \end{bmatrix}, \quad q_2 = \begin{bmatrix} 2 \\ 2 \\ 0 \end{bmatrix},$$

and $h(q_k) = \text{arctan2}(y_k - Y, x_k - X)$. Unlike ranging sensors, in this scenario where *absolute bearing* is measured, the vehicle is constructible, i.e. there is a unique solution to the set of equations

$$\begin{aligned}
&\text{arctan2}(\,\tilde{y_0} &&, \tilde{x_0} &&) = \text{arctan2}(\,y_0 &&, x_0 &&) \\
&\text{arctan2}(\,\tilde{y_0} + \sin\tilde{\theta_0} &&, \tilde{x_0} + \cos\tilde{\theta_0} &&) = \text{arctan2}(\,y_0 + \sin\theta_0 &&, x_0 + \cos\theta_0 &&), \\
&\text{arctan2}(\,\tilde{y_0} + 2\sin\tilde{\theta_0} &&, \tilde{x_0} + 2\cos\tilde{\theta_0} &&) = \text{arctan2}(\,y_0 + 2\sin\theta_0 &&, x_0 + 2\cos\theta_0 &&)
\end{aligned}$$

which is $\tilde{q}_0 = q_0$. Instead, different results are achieved when the *relative bearing* is measured, i.e. the slope of the line joining the vehicle to the beacon with respect to the orientation of the vehicle itself, reading as

$$h(q_k) = \text{arctan2}(y_k - Y, x_k - X) - \theta_k.$$

Indeed, when computing the Constructibility Gramian with a single sensor deployed in the environment, we always obtain a null space, i.e. an unconstructible direction, with dimension 1, reading as $[-y_f + Y, x_f - X, 1]^\top$, hence associated with the rotation of the trajectory about the beacon, as for the ranging scenario. Theoretically, similar results are expected for sensors measuring the distance between the vehicle and a line (instead of the range between the vehicle and

a device), which could be represented by a wall. Intuitively, when the vehicle measures its distance from a single wall or from a set of parallel walls, it cannot reconstruct its coordinate parallel to the wall itself.

Finally, extending the techniques and procedures utilized in this thesis to the case of RFID sensors presents its own challenges. Indeed, since RFID measurements rely on the phase difference of a backscattered signal, the problem of periodicity arises, i.e. any distance $D + n\lambda$, $n \in \mathbb{Z}$, where λ is the wavelength of the signal, yields the same measurement. This problem has been tackled in [Magnago et al., 2020] by using the derivative of the measurement, which represents the projection of the velocity of the vehicle on the line joining the beacon and the vehicle itself. Addressing this problem from a *global* perspective with the same arguments as in the ranging scenario, introduces one further limitation: when the vehicle collects two simultaneous measurements from two distinct tags, the positions compliant with the measurements, i.e. the indistinguishable positions, are more than two, as shown in Figure 10.4. From geometric intuitions, the set of indistinguishable positions with range sensors is a subset of the indistinguishable positions with RFID tags. Therefore, the analysis of ranging system may be beneficial in drawing conclusions on the RFID scenario.

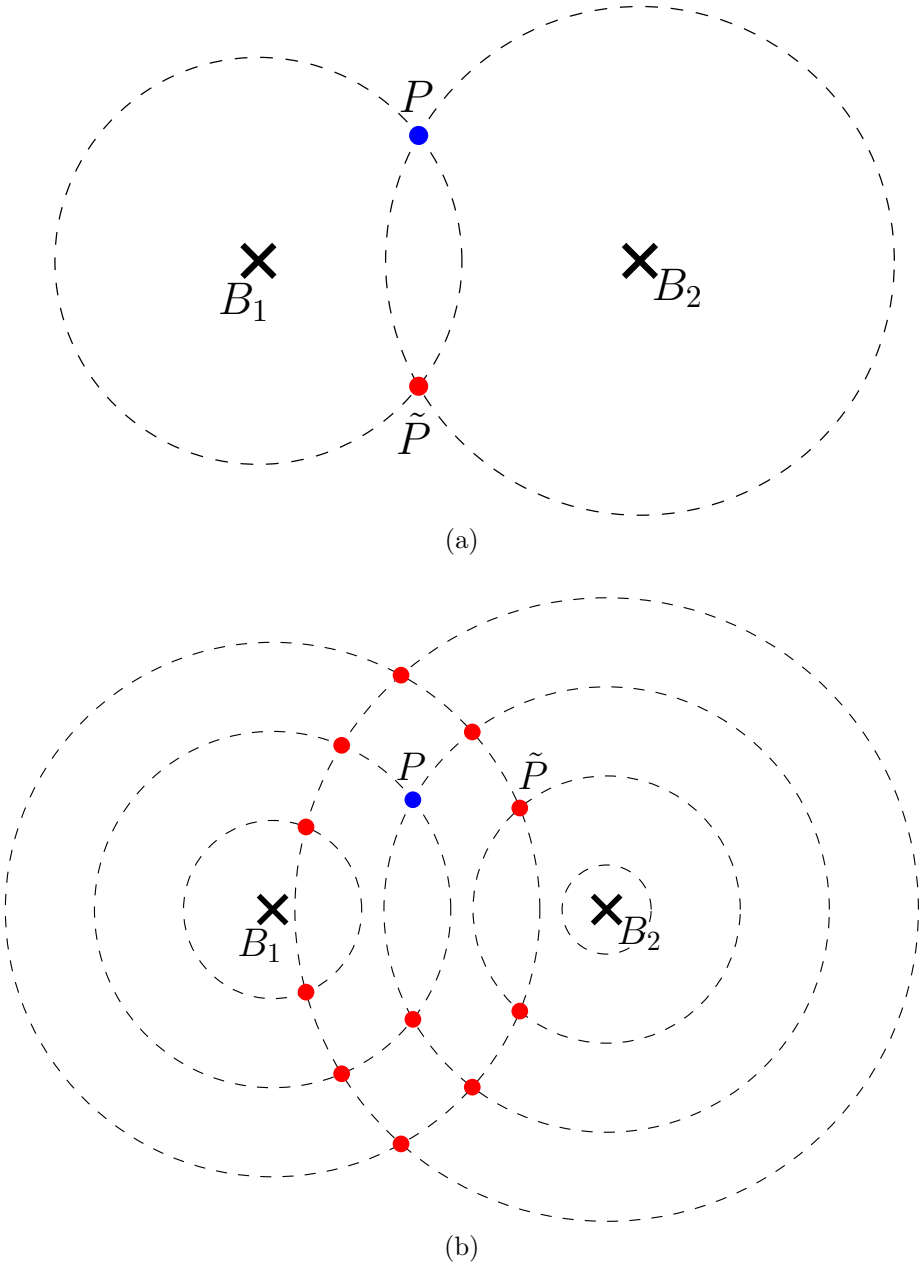

Figure 10.4: Comparison between ranging sensors and RFID sensors with the same position P of the vehicle (blue) and of the devices (black crosses) deployed in the environment. The red positions $\tilde{P}$ represent the alias positions, i.e. positions different from P that are compliant with the measurements. (a) With ranging systems, there exists only one alias position, which is mirrored with respect to the line joining the two devices. (b) When RFID tags are deployed in the environment, more than one circle is compliant with the measurement from each tag, thus increasing the number of alias positions.

Bibliography

[Aishima et al., 2010] Aishima, K., Matsuo, T., Murota, K., and Sugihara, M. (2010). A survey on convergence theorems of the dqds algorithm for computing singular values. *J. Math-for-Ind*, 2:1–11.

[Andersson et al., 2019] Andersson, J. A. E., Gillis, J., Horn, G., Rawlings, J. B., and Diehl, M. (2019). CasADi – A software framework for nonlinear optimization and optimal control. *Mathematical Programming Computation*, 11(1):1–36.

[Araki et al., 2019] Araki, B., Gilitschenski, I., Ogata, T., Wallar, A., Schwarting, W., Choudhury, Z., Karaman, S., and Rus, D. (2019). Range-based cooperative localization with nonlinear observability analysis. In *2019 IEEE Intelligent Transportation Systems Conference (ITSC)*, pages 1864–1870. IEEE.

[Arrichiello et al., 2013] Arrichiello, F., Antonelli, G., Aguiar, A. P., and Pascoal, A. (2013). An observability metric for underwater vehicle localization using range measurements. *Sensors*, 13(12):16191–16215.

[Barnes and Posner, 2020] Barnes, D. and Posner, I. (2020). Under the Radar: Learning to Predict Robust Keypoints for Odometry Estimation and Metric Localisation in Radar. In *2020 IEEE International Conference on Robotics and Automation (ICRA)*, pages 9484–9490.

[Bayat et al., 2015] Bayat, M., Crasta, N., Aguiar, A. P., and Pascoal, A. M. (2015). Range-based underwater vehicle localization in the presence of unknown ocean currents: Theory and experiments. *IEEE Transactions on Control Systems Technology (TCST)*, 24(1):122–139.

[Belo et al., 2013] Belo, F. A., Salaris, P., Fontanelli, D., and Bicchi, A. (2013). A complete observability analysis of the planar bearing localization and mapping for visual servoing with known camera velocities. *International Journal of Advanced Robotic Systems*, 10(4):197.

[Benet et al., 2002] Benet, G., Blanes, F., Simó, J. E., and Pérez, P. (2002). Using infrared sensors for distance measurement in mobile robots. *Robotics and Autonomous Systems*, 40(4):255–266.

[Bernard et al., 2022] Bernard, P., Andrieu, V., and Astolfi, D. (2022). Observer design for continuous-time dynamical systems. *Annual Reviews in Control*, 53:224–248.

[Berz et al., 2018] Berz, E. L., Tesch, D. A., and Hessel, F. P. (2018). Machine-learning-based system for multi-sensor 3D localisation of stationary objects. *IET Cyber-Physical Systems: Theory & Applications*, 3(2):81–88.

[Bicchi et al., 1998] Bicchi, A., Prattichizzo, D., Marigo, A., and Balestrino, A. (1998). On the observability of mobile vehicle localization. In *Theory and Practice of Control and Systems*, pages 142–147. World Scientific.

[Biswas and Veloso, 2010] Biswas, J. and Veloso, M. (2010). WiFi localization and navigation for autonomous indoor mobile robots. In *2010 IEEE International Conference on Robotics and Automation*, pages 4379–4384. IEEE.

[Boldrer et al., 2022] Boldrer, M., Antonucci, A., Bevilacqua, P., Palopoli, L., and Fontanelli, D. (2022). Multi-agent navigation in human-shared environments: A safe and socially-aware approach. *Robotics and Autonomous Systems*, 149:103979.

[Boyinine et al., 2022] Boyinine, R., Sharma, R., and Brink, K. (2022). Observability based path planning for multi-agent systems to aid relative pose estimation. In *2022 International Conference on Unmanned Aircraft Systems (ICUAS)*, pages 912–921. IEEE.

[Campbell et al., 2020] Campbell, S., O'Mahony, N., Carvalho, A., Krpalkova, L., Riordan, D., and Walsh, J. (2020). Where am I? Localization techniques for mobile robots a review. In *2020 6th International Conference on Mechatronics and Robotics Engineering (ICMRE)*, pages 43–47. IEEE.

[Cantón Paterna et al., 2017] Cantón Paterna, V., Calveras Auge, A., Paradells Aspas, J., and Perez Bullones, M. A. (2017). A Bluetooth low energy indoor positioning system with channel diversity, weighted trilateration and Kalman filtering. *Sensors*, 17(12):2927.

[Cedervall and Hu, 2007] Cedervall, S. and Hu, X. (2007). Nonlinear observers for unicycle robots with range sensors. *IEEE Transactions on Automatic Control*, 52(7):1325–1329.

[Chakraborty et al., 2020] Chakraborty, A., Brink, K. M., and Sharma, R. (2020). Cooperative relative localization using range measurements without a priori information. *IEEE Access*, 8:205669–205684.

[Chen and Dames, 2020] Chen, J. and Dames, P. (2020). Collision-free distributed multi-target tracking using teams of mobile robots with localization uncertainty. In *2020 IEEE/RSJ International Conference on Intelligent Robots and Systems (IROS)*, pages 6968–6974. IEEE.

[Chen et al., 2013] Chen, P., Xu, Y. B., Chen, L., and Deng, Z. A. (2013). Survey of WLAN fingerprinting positioning system. In *Applied Mechanics and Materials*, volume 380, pages 2499–2505. Trans Tech Publ.

[Cheok et al., 2010] Cheok, K. C., Radovnikovich, M., Vempaty, P., Hudas, G. R., Overholt, J. L., and Fleck, P. (2010). UWB tracking of mobile robots. In *21st Annual IEEE International Symposium on Personal, Indoor and Mobile Radio Communications*, pages 2615–2620. IEEE.

[Coleman et al., 2021] Coleman, D., Bopardikar, S. D., and Tan, X. (2021). Observability-aware target tracking with range only measurement. In *2021 American Control Conference (ACC)*, pages 4217–4224. IEEE.

[De Carli et al., 2021] De Carli, N., Salaris, P., and Giordano, P. R. (2021). Online decentralized perception-aware path planning for multi-robot systems. In *2021 International Symposium on Multi-Robot and Multi-Agent Systems (MRS)*, pages 128–136. IEEE.

[De Palma et al., 2017] De Palma, D., Arrichiello, F., Parlangeli, G., and Indiveri, G. (2017). Underwater localization using single beacon measurements: Observability analysis for a double integrator system. *Ocean Engineering*, 142:650–665.

[De Palma et al., 2015a] De Palma, D., Indiveri, G., and Parlangeli, G. (2015a). Multi-vehicle relative localization based on single range measurements. *IFAC-PapersOnLine*, 48(5):17–22.

[De Palma et al., 2015b] De Palma, D., Indiveri, G., and Pascoal, A. M. (2015b). A null-space-based behavioral approach to single range underwater positioning. *IFAC-PapersOnLine*, 48(16):55–60.

[Delaune et al., 2021] Delaune, J., Bayard, D. S., and Brockers, R. (2021). Range-visual-inertial odometry: Scale observability without excitation. *IEEE Robotics and Automation Letters*, 6(2):2421–2428.

[Diao et al., 2021] Diao, S., Luo, Q., Wang, C., and Ding, J. (2021). Enhancing trilateration localization by adaptive selecting distances. In *2021 IEEE 5th Advanced Information Technology, Electronic and Automation Control Conference (IAEAC)*, volume 5, pages 357–363. IEEE.

[Dzodzo et al., 2013] Dzodzo, B., Han, L., Chen, X., Qian, H., and Xu, Y. (2013). Realtime 2D code based localization for indoor robot navigation. In *2013 IEEE International Conference on Robotics and Biomimetics (ROBIO)*, pages 486–492. IEEE.

[Falanga et al., 2018] Falanga, D., Foehn, P., Lu, P., and Scaramuzza, D. (2018). PAMPC: Perception-aware model predictive control for quadrotors. In *2018 IEEE/RSJ International Conference on Intelligent Robots and Systems (IROS)*, pages 1–8. IEEE.

[Fang and Chen, 2020] Fang, X. and Chen, L. (2020). An optimal multi-channel trilateration localization algorithm by radio-multipath multi-objective evolution in RSS-ranging-based wireless sensor networks. *Sensors*, 20(6):1798.

[Farina et al., 2017] Farina, F., Fontanelli, D., Garulli, A., Giannitrapani, A., and Prattichizzo, D. (2017). Walking Ahead: The Headed Social Force Model. *PLOS ONE*, 12(1):1–23.

[Fernando et al., 2021] Fernando, E., De Silva, O., Mann, G. K., and Gosine, R. (2021). Toward Developing an Indoor Localization System for MAVs Using Two or Three RF Range Anchors: An Observability Based Approach. *IEEE Sensors Journal*, 22(6):5173–5187.

[Filonenko et al., 2013] Filonenko, V., Cullen, C., and Carswell, J. D. (2013). Indoor positioning for smartphones using asynchronous ultrasound trilateration. *ISPRS International Journal of Geo-Information*, 2(3):598–620.

[Fliess et al., 1995] Fliess, M., Lévine, J., Martin, P., and Rouchon, P. (1995). Flatness and defect of non-linear systems: introductory theory and examples. *International journal of control*, 61(6):1327–1361.

[Fontanelli, 2022] Fontanelli, D. (2022). Perception for autonomous systems: A measurement perspective on localization and positioning. *IEEE Instrumentation & Measurement Magazine*, 25(4):4–9.

[Fontanelli et al., 2021] Fontanelli, D., Shamsfakhr, F., Macii, D., and Palopoli, L. (2021). An Uncertainty-driven and Observability-based State Estimator for Nonholonomic Robots. *IEEE Trans. on Instrumentation and Measurement*, 70:1–12.

[Gallant and Marshall, 2016] Gallant, M. J. and Marshall, J. A. (2016). Two-dimensional axis mapping using LiDAR. *IEEE Transactions on Robotics*, 32(1):150–160.

[Gichuki et al., 2020] Gichuki, K. T., Joseph, K., and John, M. (2020). The D-, A-, E-and T-optimal values of a second order rotatable design in four dimension constructed using balanced incomplete block designs. *American Journal of Applied Mathematics*, 8(3):83–88.

[Han et al., 2013] Han, G., Xu, H., Jiang, J., Shu, L., Hara, T., and Nishio, S. (2013). Path planning using a mobile anchor node based on trilateration in wireless sensor networks. *Wireless Communications and Mobile Computing*, 13(14):1324–1336.

[Hao et al., 2022] Hao, N., He, F., Hou, Y., and Yao, Y. (2022). Graph-based observability analysis for mutual localization in multi-robot systems. *Systems & Control Letters*, 161:105152.

[Heintzman and Williams, 2020] Heintzman, L. and Williams, R. K. (2020). Nonlinear observability of unicycle multi-robot teams subject to nonuniform environmental disturbances. *Autonomous Robots*, 44(7):1149–1166.

[Hespanha, 2018] Hespanha, J. P. (2018). *Linear systems theory*. Princeton University Press.

[Huang et al., 2011] Huang, G. P., Trawny, N., Mourikis, A. I., and Roumeliotis, S. I. (2011). Observability-based consistent EKF estimators for multi-robot cooperative localization. *Autonomous Robots*, 30(1):99–122.

[Hung et al., 2020] Hung, N. T., Crasta, N., Moreno-Salinas, D., Pascoal, A. M., and Johansen, T. A. (2020). Range-based target localization and pursuit with autonomous vehicles: An approach using posterior CRLB and model predictive control. *Robotics and Autonomous Systems*, 132:103608.

[Hung and Pascoal, 2020] Hung, N. T. and Pascoal, A. M. (2020). Range-based navigation and target localization: Observability analysis and guidelines for motion planning. *IFAC-PapersOnLine*, 53(2):14620–14627.

[Hung et al., 2021] Hung, N. T., Rego, F. F., and Pascoal, A. M. (2021). Cooperative distributed estimation and control of multiple autonomous vehicles for range-based underwater target localization and pursuit. *IEEE Transactions on Control Systems Technology*, 30(4):1433–1447.

[Isidori, 2013] Isidori, A. (2013). *Nonlinear control systems*. Springer Science & Business Media.

[Islam et al., 2023] Islam, K. Z., Murray, D., Diepeveen, D., Jones, M. G., and Sohel, F. (2023). Machine learning-based LoRa localisation using multiple received signal features. *IET Wireless Sensor Systems*, 13(4):133–150.

[Jayasuriya et al., 2020] Jayasuriya, M., Ranasinghe, R., and Dissanayake, G. (2020). Active perception for outdoor localisation with an omnidirectional camera. In *2020 IEEE/RSJ International Conference on Intelligent Robots and Systems (IROS)*, pages 4567–4574. IEEE.

[Jondhale et al., 2021] Jondhale, S. R., Jondhale, A. S., Deshpande, P. S., and Lloret, J. (2021). Improved trilateration for indoor localization: Neural network and centroid-based approach. *International Journal of Distributed Sensor Networks*, 17(11):15501477211053997.

[Krener and Ide, 2009] Krener, A. J. and Ide, K. (2009). Measures of unobservability. In *48th IEEE Conference on Decision and Control (CDC) held jointly with 28th Chinese Control Conference (CCC)*, pages 6401–6406. IEEE.

[Lepej and Rakun, 2016] Lepej, P. and Rakun, J. (2016). Simultaneous localisation and mapping in a complex field environment. *Biosystems engineering*, 150:160–169.

[Magnago et al., 2019] Magnago, V., Corbalán, P., Picco, G., Palopoli, L., and Fontanelli, D. (2019). Robot Localization via Odometry-assisted Ultrawideband Ranging with Stochastic Guarantees. In *Proc. IEEE/RSJ International Conference on Intelligent Robots and System (IROS)*, pages 1607–1613, Macao, China. IEEE.

[Magnago et al., 2020] Magnago, V., Palopoli, L., Buffi, A., Tellini, B., Motroni, A., Nepa, P., Macii, D., and Fontanelli, D. (2020). Ranging-free UHF-RFID Robot Positioning through Phase Measurements of Passive Tags. *IEEE Trans. on Instrumentation and Measurement*, 69(5):2408–2418.

[Mandić et al., 2016] Mandić, F., Mišković, N., Palomeras, N., Carreras, M., and Vallicrosa, G. (2016). Mobile beacon control algorithm that ensures observability in single range navigation. *IFAC-PapersOnLine*, 49(23):48–53.

[Mariottini et al., 2005] Mariottini, G. L., Pappas, G., Prattichizzo, D., and Daniilidis, K. (2005). Vision-based localization of leader-follower formations. In *Proceedings of the 44th IEEE Conference on Decision and Control*, pages 635–640. IEEE.

[Martinelli, 2017] Martinelli, A. (2017). The unicycle in presence of a single disturbance: Observability properties. In *2017 Proceedings of the Conference on Control and its Applications*, pages 62–69. SIAM.

[Martinelli and Siegwart, 2005] Martinelli, A. and Siegwart, R. (2005). Observability analysis for mobile robot localization. In *2005 IEEE/RSJ International Conference on Intelligent Robots and Systems*, pages 1471–1476. IEEE.

[Maurelli et al., 2022] Maurelli, F., Krupiński, S., Xiang, X., and Petillot, Y. (2022). AUV localisation: a review of passive and active techniques. *International Journal of Intelligent Robotics and Applications*, 6(2):246–269.

[Maxim et al., 2008] Maxim, P. M., Hettiarachchi, S., Spears, W. M., Spears, D. F., Hamann, J. C., Kunkel, T., and Speiser, C. (2008). Trilateration localization for multi-robot teams. In *ICINCO-RA (2)*, pages 301–307. Citeseer.

[Miseikis et al., 2018] Miseikis, J., Brijacak, I., Yahyanejad, S., Glette, K., Elle, O. J., and Torresen, J. (2018). Multi-objective convolutional neural networks for robot localisation and 3D position estimation in 2D camera images. In *2018 15th International Conference on Ubiquitous Robots (UR)*, pages 597–603. IEEE.

[Mohamed et al., 2020] Mohamed, I. S., Capitanelli, A., Mastrogiovanni, F., Rovetta, S., and Zaccaria, R. (2020). Detection, localisation and tracking of pallets using machine learning techniques and 2D range data. *Neural Computing and Applications*, 32:8811–8828.

[Moreno-Salinas et al., 2018] Moreno-Salinas, D., Crasta, N., Pascoal, A., and Aranda, J. (2018). Optimal multiple underwater target localization and tracking using two surface acoustic ranging sensors. *IFAC-PapersOnLine*, 51(29):177–182.

[Motroni et al., 2018] Motroni, A., Nepa, P., Magnago, V., Buffi, A., Tellini, B., Fontanelli, D., and Macii, D. (2018). SAR-based indoor localization of UHF-RFID tags via mobile robot. In *2018 International Conference on Indoor Positioning and Indoor Navigation (IPIN)*, pages 1–8. IEEE.

[Napolitano et al., 2021] Napolitano, O., Fontanelli, D., Pallottino, L., and Salaris, P. (2021). Gramian-based optimal active sensing control under intermittent measurements. In *Proc. IEEE International Conference on Robotics and Automation (ICRA)*, pages 9680–9686, Xian, China. IEEE.

[Napolitano et al., 2022] Napolitano, O., Fontanelli, D., Pallottino, L., and Salaris, P. (2022). Information-aware Lyapunov-based MPC in a feedback-feedforward control strategy for autonomous robots. *IEEE Robotics and Automation Letters*, 7(2):4765–4772.

[Nazemzadeh et al., 2017] Nazemzadeh, P., Fontanelli, D., Macii, D., and Palopoli, L. (2017). Indoor localization of mobile robots through QR code detection and dead reckoning data fusion. *IEEE/ASME Transactions On Mechatronics*, 22(6):2588–2599.

[Nazemzadeh et al., 2015] Nazemzadeh, P., Moro, F., Fontanelli, D., Macii, D., and Palopoli, L. (2015). Indoor Positioning of a Robotic Walking Assistant for Large Public Environments. *IEEE Trans. on Instrumentation and Measurement*, 64(11):2965–2976.

[O'Mahony et al., 2019] O'Mahony, N., Campbell, S., Carvalho, A., Harapanahalli, S., Velasco-Hernández, G. A., Riordan, D., and Walsh, J. (2019). Adaptive multimodal localisation techniques for mobile robots in unstructured environments: A review. In *2019 IEEE 5th World Forum on Internet of Things (WF-IoT)*, pages 799–804. IEEE.

[Palopoli and Fontanelli, 2020] Palopoli, L. and Fontanelli, D. (2020). Global observability analysis of a nonholonomic robot using range sensors. In *2020 European Control Conference (ECC)*, pages 1300–1305. IEEE.

[Powel and Morgansen, 2015] Powel, N. D. and Morgansen, K. A. (2015). Empirical observability gramian rank condition for weak observability of nonlinear systems with control. In *2015 54th IEEE Conference on Decision and Control (CDC)*, pages 6342–6348. IEEE.

[Quenzer and Morgansen, 2014] Quenzer, J. D. and Morgansen, K. A. (2014). Observability based control in range-only underwater vehicle localization. In *2014 American control conference*, pages 4702–4707. IEEE.

[Raibert and Brown Jr, 1984] Raibert, M. H. and Brown Jr, H. B. (1984). Experiments in balance with a 2D one-legged hopping machine.

[Riz et al., 2024a] Riz, F., Dorigoni, D., Palopoli, L., Fontanelli, D., and Pascoal, A. M. (2024a). Range–Based Simultaneous Localisation of a Tracker–Target Pair with a Single Beacon. Manuscript in preparation for submission to Elsevier Robotics & Autonomous Systems.

[Riz et al., 2022a] Riz, F., Palopoli, L., and Fontanelli, D. (2022a). Analysis of indistinguishable trajectories of a nonholonomic vehicle subject to range measurements. arXiv preprint arXiv:2209.00567, 2022.

[Riz et al., 2022b] Riz, F., Palopoli, L., and Fontanelli, D. (2022b). On Local/Global Constructibility for Mobile Robots using Bounded Range Measurements. *IEEE Control Systems Letters*, 6:3038–3043. ©2024 IEEE.

[Riz et al., 2023a] Riz, F., Palopoli, L., and Fontanelli, D. (2023a). Perception-aware Trajectory Planning for a Pair of Unicycle-like Robots with Absolute and Relative Ranging Measurements. *IEEE Control Systems Letters*. ©2024 IEEE.

[Riz et al., 2023b] Riz, F., Palopoli, L., and Fontanelli, D. (2023b). Why Three Measurements are not Enough for Trilateration–based Localisation. In *2023 IEEE International Instrumentation and Measurement Technology Conference (I2MTC)*, pages 01–06. IEEE. ©2024 IEEE.

[Riz et al., 2024b] Riz, F., Palopoli, L., and Fontanelli, D. (2024b). Constructibility Analysis of a Team of Nonholomic Vehicles Using Mutual Range Measurements. Manuscript submitted for publication to Elsevier Automatica.

[Rúa et al., 2019] Rúa, S., Crasta, N., Vásquez, R. E., Betancur, M. J., and Pascoal, A. M. (2019). Cooperative range-based navigation using a beacon with circular motion installed on board the support platform. *IFAC-PapersOnLine*, 52(21):390–395.

[Rúa et al., 2020] Rúa, S., Crasta, N., Vásquez, R. E., and Pascoal, A. M. (2020). Enhanced cooperative single-range underwater navigation based on optimal trajectories. *IFAC-PapersOnLine*, 53(2):14668–14673.

[Salaris et al., 2019] Salaris, P., Cognetti, M., Spica, R., and Giordano, P. R. (2019). Online optimal perception-aware trajectory generation. *IEEE Transactions on Robotics*, 35(6):1307–1322.

[Salaris et al., 2017] Salaris, P., Spica, R., Giordano, P. R., and Rives, P. (2017). Online optimal active sensing control. In *2017 IEEE International Conference on Robotics and Automation (ICRA)*, pages 672–678. IEEE.

[Sert et al., 2011] Sert, H., Kökösy, A., and Perruquetti, W. (2011). A single landmark based localization algorithm for non-holonomic mobile robots. In *2011 IEEE International Conference on Robotics and Automation*, pages 293–298. IEEE.

[Sert et al., 2012] Sert, H., Perruquetti, W., Kokosy, A., Jin, X., and Palos, J. (2012). Localizability of unicycle mobiles robots: An algebraic point of view. In *2012 IEEE/RSJ International Conference on Intelligent Robots and Systems*, pages 223–228. IEEE.

[Shalal et al., 2015] Shalal, N., Low, T., McCarthy, C., and Hancock, N. (2015). Orchard mapping and mobile robot localisation using on-board camera and laser scanner data fusion–part b: Mapping and localisation. *Computers and Electronics in Agriculture*, 119:267–278.

[Shamsfakhr et al., 2022] Shamsfakhr, F., Antonucci, A., Palopoli, L., Macii, D., and Fontanelli, D. (2022). Indoor Localisation Uncertainty Control based on Wireless Ranging for Robots Path Planning. *IEEE Trans. on Instrumentation and Measurement*, 71:1–11.

[Shamsfakhr et al., 2021] Shamsfakhr, F., Motroni, A., Palopoli, L., Buffi, A., Nepa, P., and Fontanelli, D. (2021). Robot Localisation using UHF-RFID Tags: A Kalman Smoother approach. *Sensors*, 21(3):1–19.

[Sharma, 2014] Sharma, R. (2014). Observability based control for cooperative localization. In *2014 International Conference on Unmanned Aircraft Systems (ICUAS)*, pages 134–139. IEEE.

[Shen et al., 2019] Shen, M., Wang, Y., Jiang, Y., Ji, H., Wang, B., and Huang, Z. (2019). A new positioning method based on multiple ultrasonic sensors for autonomous mobile robot. *Sensors*, 20(1):17.

[Shu and Wang, 2023] Shu, W. and Wang, S. (2023). A Study of Bluetooth Range-Based Trilateral Localisation by DA14695 Device. *Authorea Preprints*.

[Stegagno et al., 2016] Stegagno, P., Cognetti, M., Oriolo, G., Bülthoff, H. H., and Franchi, A. (2016). Ground and aerial mutual localization using anonymous relative-bearing measurements. *IEEE Transactions on Robotics*, 32(5):1133–1151.

[Sun et al., 2020] Sun, L., Adolfsson, D., Magnusson, M., Andreasson, H., Posner, I., and Duckett, T. (2020). Localising Faster: Efficient and precise LiDAR-based robot localisation in large-scale environments. In *2020 IEEE international conference on robotics and automation (ICRA)*, pages 4386–4392. IEEE.

[Thomas and Ros, 2005] Thomas, F. and Ros, L. (2005). Revisiting trilateration for robot localization. *IEEE Transactions on robotics*, 21(1):93–101.

[Vicentini, 2021] Vicentini, F. (2021). Collaborative robotics: a survey. *Journal of Mechanical Design*, 143(4):040802.

[Wu et al., 2022] Wu, X., Chen, S., Sreenath, K., and Mueller, M. W. (2022). Perception-aware receding horizon trajectory planning for multicopters with visual-inertial odometry. *IEEE Access*, 10:87911–87922.

[Wu et al., 2020] Wu, Y., Li, Y., Li, W., Li, H., and Lu, R. (2020). Robust LiDAR-based localization scheme for unmanned ground vehicle via multisensor fusion. *IEEE Transactions on Neural Networks and Learning Systems*, 32(12):5633–5643.

[Yamamoto, 2017] Yamamoto, Y. (2017). On the optimality and sharpness of Laguerre's lower bound on the smallest eigenvalue of a symmetric positive definite matrix. *Applications of Mathematics*, 62(4):319–331.

[Yan et al., 2013] Yan, J., Tiberius, C. C., Janssen, G. J., Teunissen, P. J., and Bellusci, G. (2013). Review of range-based positioning algorithms. *IEEE Aerospace and Electronic Systems Magazine*, 28(8):2–27.

[Yang et al., 2020] Yang, B., Guo, L., Guo, R., Zhao, M., and Zhao, T. (2020). A novel trilateration algorithm for RSSI-based indoor localization. *IEEE Sensors Journal*, 20(14):8164–8172.

[Yi et al., 2018] Yi, G. H., bin Djaswadi, G. W., bin Md Khir, M. H., and Ramli, N. (2018). An adaptive Wi-Fi trilateration-based indoor localization. In *2018 International Conference on Intelligent and Advanced System (ICIAS)*, pages 1–6. IEEE.

[Yu et al., 2020] Yu, Y., Chen, R., Liu, Z., Guo, G., Ye, F., and Chen, L. (2020). Wi-Fi fine time measurement: Data analysis and processing for indoor localisation. *The Journal of Navigation*, 73(5):1106–1128.

[Zenatti et al., 2016] Zenatti, F., Fontanelli, D., Palopoli, L., Macii, D., and Nazemzadeh, P. (2016). Optimal placement of passive sensors for robot localisation. In *2016 IEEE/RSJ International Conference on Intelligent Robots and Systems (IROS)*, pages 4586–4593. IEEE.

[Zhou, 2009] Zhou, Y. (2009). An efficient least-squares trilateration algorithm for mobile robot localization. In *2009 IEEE/RSJ International Conference on Intelligent Robots and Systems*, pages 3474–3479. IEEE.